

# NASA CONTRACTOR REPORT

NASA CR-2602



NASA CR-2

0061511



TECH LIBRARY KAFB, NM

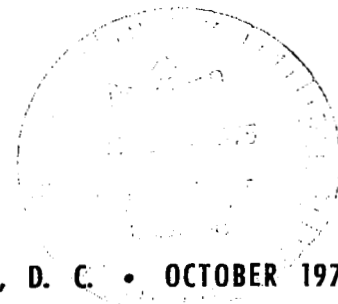
LOAN COPY: RETURN TO  
AFWL TECHNICAL LIBRARY  
KIRTLAND AFB, N. M.

## PREDICTION OF SPAN LOADING OF STRAIGHT-WING/PROPELLER COMBINATIONS UP TO STALL

*M. A. McVeigh, L. Gray, and E. Kisielowski*

*Prepared by*  
UNITED TECHNOLOGY, INC.  
Blue Bell, Pa. 19422  
*for Langley Research Center*

NATIONAL AERONAUTICS AND SPACE ADMINISTRATION • WASHINGTON, D. C. • OCTOBER 1975

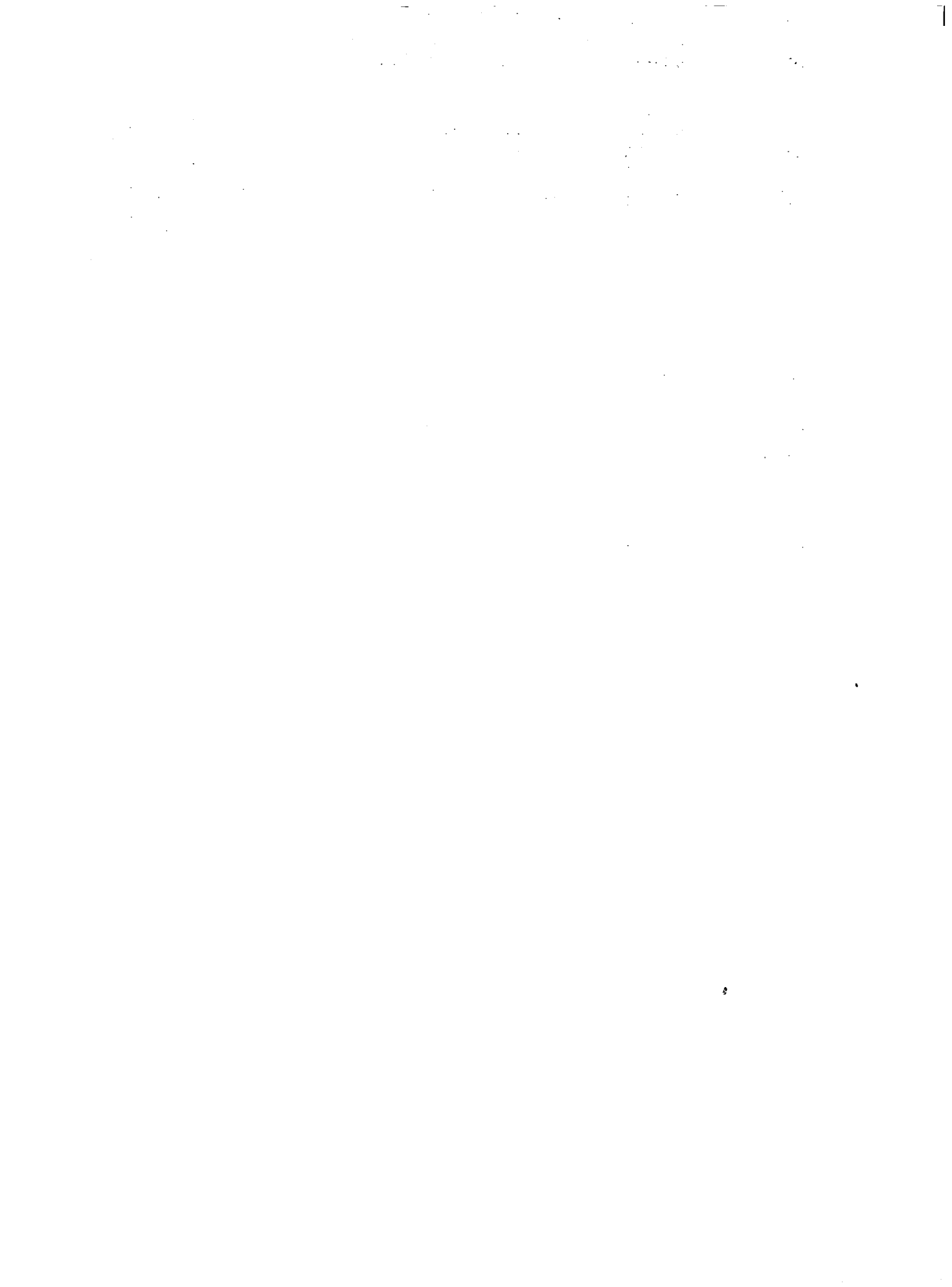




0061511

October 1975

1. Report No. NASA CR-2602		2. Government Accession No.	
4. Title and Subtitle Prediction of span loading of straight-wing/propeller combinations up to stall		6. Performing Organization Code	
7. Author(s) M. A. McVeigh L. Gray E. Kisielowski		8. Performing Organization Report No. UTR-004	
9. Performing Organization Name and Address United Technology, Inc. 1777 Walton Road Blue Bell, Pa. 19422		10. Work Unit No.	
12. Sponsoring Agency Name and Address National Aeronautics and Space Administration Washington, D.C. 20546		11. Contract or Grant No. NAS1-12238	
15. Supplementary Notes The NASA technical representatives were Mr. Robert T. Taylor and Mr. Louis P. Tosti. The contributions of the NASA technical personnel to this work are gratefully acknowledged. FINAL REPORT		13. Type of Report and Period Covered	
16. Abstract A method is presented for calculating the spanwise lift distribution on straight-wing/propeller combinations. The method combines a modified form of the Prandtl wing theory with a realistic representation of the propeller slipstream distribution. The slipstream analysis permits calculations of the non-uniform axial and rotational slipstream velocity field of propeller/nacelle combinations. This non-uniform field is then used to calculate the wing lift distribution by means of the modified Prandtl wing theory. The method utilizes non-linear aerodynamic section data for both the wing and the propeller blade airfoil sections and is applicable up to stall. The theory is developed for any number of non-overlapping propellers, on a wing with partial or full-span flaps, and is applicable throughout the aspect ratio range from 2.0 and higher. The analysis is programmed for use on the CDC 6600 series digital computer. The computer program is used to calculate slipstream characteristics and wing span load distributions for a number of configurations for which experimental data are available. Favorable comparisons are demonstrated between the theoretical predictions and the existing data.		14. Sponsoring Agency Code	
17. Key Words (Suggested by Author(s)) Propeller      Load distribution Wing            Angle of attack Aircraft      Twist Stall            Taper ratio		18. Distribution Statement Distribution unlimited  Subject Category 01	
19. Security Classif. (of this report) Unclassified	20. Security Classif. (of this page) Unclassified	21. No. of Pages 208	22. Price* \$7.25



## SUMMARY

A method is presented for calculating the spanwise lift distribution on straight-wing/propeller combinations. The method combines a modified form of the Prandtl wing theory with a realistic representation of the propeller slipstream distribution. The slipstream analysis permits calculations of the non-uniform axial and rotational slipstream velocity field of propeller/nacelle combinations. This non-uniform field is then used to calculate the wing lift distribution by means of the modified Prandtl wing theory.

The method utilizes non-linear aerodynamic section data for both the wing and the propeller blade airfoil sections and is applicable up to stall. The theory is developed for any number of non-overlapping propellers, on a wing with partial or full-span flaps, and is applicable throughout the aspect ratio range from 2.0 and higher.

The analysis is programmed for use on the CDC 6600 series digital computer. The computer program is used to calculate slipstream characteristics and wing span load distributions for a number of configurations for which experimental data are available. Favorable comparisons are demonstrated between the theoretical predictions and the existing data.



## CONTENTS

	<u>Page</u>
SUMMARY.....	iii
LIST OF ILLUSTRATIONS.....	viii
LIST OF TABLES.....	xi
LIST OF SYMBOLS.....	xii
SECTION 1 INTRODUCTION.....	1
SECTION 2 GENERAL REVIEW OF THE ANALYTICAL METHODS.....	3
2.1 STATEMENT OF THE PROBLEM.....	3
2.2 REVIEW OF EXISTING SOLUTIONS.....	4
2.3 BASIS FOR THE PRESENT ANALYSIS.....	6
SECTION 3 THEORETICAL ANALYSIS.....	8
3.1 PROPELLER SLIPSTREAM ANALYSIS.....	8
3.1.1 General Propeller Solution.....	8
3.1.2 Initial Calculation of Inflow Angle....	13
3.1.3 Convergence of the Iterative Propeller Solution.....	15
3.1.4 Analysis for Slipstream Velocity Distributions .....	18
3.2 WING-IN-SLIPSTREAM ANALYSIS.....	21
3.2.1 Analysis for a Wing With no Flaps or With Full-Span Deflected Flaps.....	21
3.2.2 Analysis for a Wing With Part-Span Deflected Flaps.....	29
3.2.3 Extension of the Wing Analysis to Small Aspect Ratios.....	39
SECTION 4 DIGITAL COMPUTER PROGRAM.....	42
4.1 PROPELLER SLIP-STREAM COMPUTATIONS.....	42
4.1.1 Computational Procedures for Propeller Slipstream Velocity Distributions .....	42

4.1.2	Propeller Blade Section Characteristics.....	48
4.1.3	Table Look-Up Procedures for Propeller Airfoil Characteristics.....	52
4.2	WING-IN-SLIPSTREAM COMPUTATIONS.....	54
4.2.1	Computational Procedures for Spanwise Loading on a Wing With no Flaps or with Full-Span Deflected Flaps...	54
4.2.2	Computational Procedures for Spanwise Loading on a Wing With Part-Span Deflected Flaps.....	57
4.2.3	Wing Section Characteristics.....	61
4.2.4	Table Look-Up Procedures for Wing Section Characteristics.....	61
4.3	DESCRIPTION OF THE COMPUTER PROGRAM LOGIC.....	61
4.4	SAMPLE OUTPUT.....	65
SECTION 5	VERIFICATION OF THE DEVELOPED THEORY	68
5.1	CORRELATIONS FOR AN ISOLATED PROPELLER.....	68
5.2	CORRELATIONS FOR WING-IN-SLIPSTREAM	77
5.2.1	Correlations for Low Aspect Ratio Wings.....	78
5.2.2	Correlation for Centrally-Mounted Propellers and Jets.....	80
5.2.3	Correlation for Twin Propeller Configurations.....	84
5.2.4	Effect of Propeller Rotation.....	88
5.2.5	Effect of Flap Deflection.....	96
SECTION 6	CONCLUSIONS AND RECOMMENDATIONS.....	98
SECTION 7	REFERENCES.....	99

APPENDIX A	PROPELLER TIP LOSS CORRECTION TABLES	104
APPENDIX B	PROPELLER AIRFOIL TABLES.....	108
APPENDIX C	PROGRAM USER INSTRUCTIONS.....	121
APPENDIX D	INTERNAL LISTING OF THE COMPUTER PROGRAM.....	146



## LIST OF ILLUSTRATIONS

		<u>Page</u>
Figure 1	Notation for a Propeller Operating in the Presence of a Wing.....	9
2	Blade Element Velocity Diagram....	12
3	Analytical Model for Slipstream Contraction.....	20
4	Notation for Wing-In-Slipstream Model.....	24
5	Mathematical Representation of Flap Discontinuity.....	30
6	Method for Superposition of Solutions.....	35
7	Computer Program Flow Diagram.....	62
8	Logic Diagram for Propeller Slipstream Subroutine.....	64
9	Correlation Between Predicted and Measured Elemental Thrust and Torque Loadings at 75 Percent Radius.....	69
10	Correlation Between Predicted and Measured Elemental Thrust and Torque Loadings at 52 Percent Radius.....	70
11	Correlation Between Predicted and Measured Elemental Thrust and Torque Loadings at 25 Percent Radius.....	71
12	Comparison Between Predicted and Measured Distributions of Slipstream Axial Velocity and Swirl Angle for the P-2 Propeller of Reference 17, at $J = 0.12$ .....	73

		<u>Page</u>
Figure 13	Comparison Between Predicted and Measured Distributions of Slipstream Axial Velocity and Swirl Angle for the P-1 Propeller of Reference 17, at $J = 0.26$ .....	74
14	Comparison Between Predicted and Measured Distributions of Slipstream Swirl Angle for Typical Test Conditions of Reference 42.....	76
15	Verification of Low Aspect Ratio Analysis.....	79
16	Comparison Between Predicted Spanwise Loading and Measurements of Reference 6 for a Rectangular Wing With End Plates Subjected to a Uniform Jet; $V_S/V_O = 1.36$ .....	81
17	Predicted Versus Measured Spanwise Loadings for the Rectangular Wing of Reference 29 With a Centrally-Mounted Propeller; $AR = 6$ .....	82
18	Predicted Versus Measured Spanwise Loadings for the Rectangular Wing of Reference 29 With a Centrally-Mounted Propeller; $AR = 3$ .....	83
19	Predicted Versus Measured Spanwise Loadings for the Twin-Propeller Configuration of Reference 42; $AR = 3.0, C_{TS} = 0$ .....	85
20	Predicted Versus Measured Spanwise Loadings for the Twin-Propeller Configuration of Reference 42; $AR = 3.0, C_{TS} = 0.36, \beta_{75} = 25^\circ$ ..	86
21	Predicted Versus Measured Spanwise Loadings for the Twin-Propeller Configuration of Reference 42; $AR = 3.0, C_{TS} = 0.64, \beta_{75} = 25^\circ$ ..	87

		<u>Page</u>
Figure 22	Predicted Versus Measured Spanwise Loadings for the Twin-Propeller Configuration of Reference 44; AR = 4.7, $C_{TS} = 0$ .....	89
23	Predicted Versus Measured Spanwise Loadings for the Twin-Propeller Configuration of Reference 44; AR = 3.26, $C_{TS} = 0$ .....	90
24	Predicted Versus Measured Spanwise Loadings for the Twin-Propeller Configuration of Reference 44; AR = 2.28, $C_{TS} = 0$ .....	91
25	Predicted Versus Measured Spanwise Loadings for the Twin-Propeller Configuration of Reference 44; AR = 4.7, $C_{TS} = 0.4$ .....	92
26	Predicted Versus Measured Spanwise Loadings for the Twin-Propeller Configuration of Reference 44; AR = 3.26, $C_{TS} = 0.4$ .....	93
27	Predicted Versus Measured Spanwise Loadings for the Twin-Propeller Configuration of Reference 44; AR = 2.28, $C_{TS} = 0.4$ .....	94
28	Effect of Propeller Rotation on Span Loading for the Configuration of Reference 42; AR = 3.0, $C_{TS} = 0.64$ , $\alpha = 10$ Degrees.....	95
29	Predicted Spanwise Loadings for the Twin-Propeller Configuration of Reference 44 to Show the Effect of Flap Deflection; AR = 4.7, $\alpha = 10$ Degrees.....	97
30	Assembly of Computer Program Input Data Card Deck.....	123

LIST OF TABLES

		<u>Page</u>
Table	I	Typical Propeller Blade Sections.. 49
	II	Summary of Propeller Airfoil Sections Tabulated for use in the Computer Program..... 51
	III	Sample Output for Lift Distribution on a Wing-In-Slipstream..... 66
	IV	Sample Output for Propeller Velocity Distribution..... 67
	V	Card Format for Wing Section Airfoil Tables..... 130

## LIST OF SYMBOLS

AR	wing aspect ratio
a	lift curve slope for finite aspect ratio, per degree
$a_s$	speed of sound, m/sec
$a_o$	section lift curve slope, per degree
B	number of blades per propeller
$B_n$	coefficients in trigonometric series
b	wing span, m
$C_D$	total wing drag coefficient
$C_d$	section drag coefficient
$C_L$	total wing lift coefficient
$C_l$	section lift coefficient
$C_Q$	propeller torque coefficient, $Q/\rho n^2 D^5$
$C_T$	propeller thrust coefficient, $T/\rho n^2 D^4$
$C_{TS}$	propeller thrust coefficient, $T/q_s \pi R^2$
c	wing local chord, m
$c_R$	wing root chord, m
D	propeller tip diameter, m
E	edge velocity factor
F	propeller tip loss factor
$i_{TL}$	inclination of the propeller axis to the fuselage centerline, degrees

J	propeller advance ratio, $V_o/nD$
l	wing section lift, per unit span, N
$M_o$	freestream Mach number, $V_o/a_s$
$M_v$	local Mach number for propeller blade element, $V/a_s$
n	rotational speed, rev/sec
Q	propeller shaft torque, N.m.
$q_s$	average slipstream dynamic pressure, $N/m^2$
R	propeller tip radius, $D/2$ , m
$R_e$	Reynolds number
r	local radius in propeller disk plane, m
$r_s$	local radius in slipstream, m
T	propeller thrust, N
u	axial component of velocity induced by a blade element in the propeller disk plane, m/sec.
V	local velocity, m/sec.
$V_a$	component of freestream velocity along the propeller axis, m/sec.
$V_n$	component of local slipstream velocity normal to the zero-lift line, m/sec.
$V_o$	freestream velocity, m/sec.
$V_s$	component of local slipstream velocity parallel to the zero-lift line, m/sec.
$\bar{V}_{sa}$	axial component of local velocity in the fully-developed slipstream, m/sec.

$V_{sa}$	momentum-weighted mean axial velocity in the fully-developed slipstream, m/sec.
$V_{st}$	tangential component of local velocity in the fully-developed slipstream, m/sec.
$V_w$	upwash velocity component acting in the propeller disk plane due to the presence of a lifting wing, m/sec.
$v$	nondimensional change in upwash due to the slipstream
$X_p$	distance of propeller hub forward of wing quarter chord, m
$Y$	spanwise co-ordinate of local wing element, m
$Y^*$	spanwise co-ordinate of flap end, m
$Y_p$	spanwise co-ordinate of propeller axis, m
$\alpha$	angle of attack relative to airfoil section chord-line, degrees
$\alpha_B$	angle of attack relative to fuselage centerline, degrees
$\alpha_c$	corrected section angle of attack, degrees
$\alpha_c$	effective angle of attack of wing section, degrees
$\alpha_g$	geometric angle of attack of wing section, degrees
$\alpha_i$	induced angle of attack of wing section, degrees
$\alpha_{l_0}$	angle of attack of airfoil section at zero lift, degrees
$\alpha_0$	section angle of attack for two-dimensional airfoil, degrees
$\alpha_p$	propeller axis angle of attack, degrees

$\alpha_R$	geometric angle of attack of wing root, degrees
$\alpha_S$	inclination of the slipstream axis to the flight path, degrees
$\beta$	pitch angle for propeller blade element, degrees
$\beta_{mk}$	multiplier for induced angle of attack, degrees
$\delta$	magnitude of discontinuity in absolute and induced angles of attack, degrees
$\epsilon$	geometric twist at any wing section, degrees
$\Gamma$	circulation about any wing section, $m^2/\text{sec}$ .
$\lambda$	wing taper ratio
$\mu$	blade speed ratio for propeller blade element
$\mu_T$	blade tip speed ratio
$\nu$	kinematic viscosity, $m^2/\text{sec}$ .
$\phi$	inflow angle for propeller blade element, degrees
$\phi_0$	inflow angle for propeller blade element, excluding contribution from induced velocity in disk plane, degrees
$\rho$	ambient density, $\text{kg}/m^3$
$\sigma$	solidity for propeller blade element
$\theta$	wing spanwise coordinate, $\cos^{-1}(2y/b)$
$\theta^*$	spanwise co-ordinate for flap end, $\cos^{-1}(2y^*/b)$
$\Omega$	rotational speed, $2\pi n$ radians/sec.
$\omega$	angular velocity induced by a blade element behind the propeller disk plane, radians/sec.
$\omega'$	factor to account for low aspect ratio effects



PREDICTION OF SPAN LOADING OF  
STRAIGHT-WING/PROPELLER COMBINATIONS  
UP TO STALL

by

M. A. McVeigh, L. Gray, and E. Kisielowski

UNITED TECHNOLOGY, INC.

SECTION 1

INTRODUCTION

The propeller slipstream exerts an important influence on wing load distribution, which in turn affects the aircraft stall characteristics. This effect is introduced through an increase in local velocity over the slipstream-immersed portion of the wing and a change of wing local angle of attack due to slipstream rotation. While the increased velocity tends to stabilize the flow over that wing portion, the slipstream rotation may give rise to an asymmetric stall condition due to increased local angles of attack of the wing sections behind the up-going propeller blades, and reduced angles of attack of the wing sections behind the down-going blades.

A review of the available technical literature indicates that there are no reliable theoretical or semi-empirical methods which can adequately predict the effects of a propeller slipstream on the spanwise load distribution of an entire wing. Many of the existing methods are suitable only for computing total wing forces since they are often based on gross simplifying assumptions. Thus, for example, an assumption that the slipstream-immersed portions of the wing can be treated as isolated planforms neglects the strong influence of the slipstream on adjacent wing regions. Other theoretical methods are generally classed as rigorous mathematical approaches which are usually very complex and are frequently not in sufficient agreement with experimental data to warrant their use as a design tool. Furthermore, most of the above theories use linear lift curves and as a result can not be expected to yield satisfactory agreement with test data near wing stall.

The limitation imposed by the use of linear lift curves for the wing has been successfully removed in the work reported in Reference 1. This reference presents a computerized method for predicting spanwise load distributions of straight-wing/fuselage combinations at angles of attack up to stall. This method, which is based on the Prandtl wing or "lifting line" theory as formulated by Sivells in Reference 2, provides a reliable analytical tool for predicting wing stalling characteristics of general aviation type aircraft, but is only applicable to power-off flight conditions, such as might be encountered during landing.

The current investigation extends the analysis of Reference 1 to permit calculations of span loading and stalling characteristics under power-on conditions (e.g. take-off) for wings with or without flaps and having any number of non-overlapping propellers. The present method is based on employing non-linear airfoil section characteristics for both the propeller and the wing. The basic analytical approach of this method is to retain the inherent simplicity of the Prandtl wing theory, modify the theory as required to accept non-uniform slipstream velocities, and effectively combine this modified lifting line theory with a realistic propeller theory to form a unified analytical tool.

A detailed description of this analytical method, together with the specially developed digital computer program is presented in the following pages.

## SECTION 2

### GENERAL REVIEW OF THE ANALYTICAL METHODS

The prime objective of the current development is to provide a practical analytical solution for determining the lift distribution and stalling characteristics of wings partially or totally immersed in a propeller slipstream. In order to depict some of the highlights of the current work relative to other approaches, this section presents a brief review of the existing analytical and experimental investigations that attempt solutions of the wing/propeller problem.

#### 2.1 STATEMENT OF THE PROBLEM

The basic limitation in providing reliable solutions to the wing/propeller problem is related to a lack of complete understanding of the flow field generated by the wing/propeller interaction under practical operating conditions. The problem is further compounded by the difficulty of developing realistic analytical representations of this complex flow field environment so as to account for the major interaction effects acting on a wing/propeller combination. A complete solution to the problem must therefore account for all these effects, which as a minimum should include the following

- (a) Local wing angle-of-attack changes due to the mean inclination and rotation of the slipstream flow.
- (b) Non-uniform spanwise distribution of velocity over those portions of the wing within the slipstream.
- (c) Non-uniform vertical distribution of velocity within the slipstream-immersed regions of the wing.
- (d) Viscous mixing between the slipstream and freestream flow along the slipstream boundary.

In view of the real fluid flow effects involved it is unlikely that every aspect of the problem can be treated adequately, using the established analytical approaches. Historically, the approach has been to introduce a series of simplifying assumptions in order to arrive at a solution. These approaches are discussed below.

## 2.2 REVIEW OF EXISTING SOLUTIONS

The earliest treatment of the propeller slipstream problem is contained in the pioneering work of Koning (Reference 3) who treated the simplified case of a wing centrally immersed in a circular uninclined slipstream of uniform axial velocity without rotation. Koning applied the methods of lifting line theory to obtain a solution when the ratio of free stream velocity to slipstream velocity is close to unity. This work was extended by Glauert (Reference 4) and by Franke and Weinig (Reference 5) to a wider range of forward speeds.

Stuper (Reference 6) conducted a series of experiments to verify the predictions of Koning's theory by measuring the lift distribution on a rectangular wing with end plates under the action of a circular jet. Stuper used a specially designed fan to produce a jet without rotation and with a velocity cross-section which was approximately uniform. While the results of those experiments are somewhat impaired by the particular test arrangement used by Stuper, there is sufficient evidence to show that the Koning theory over-predicts the lift increase due to the jet.

Because of the inability of the lifting line approach, as formulated by Koning, Glauert et. al., to satisfactorily predict experimental measurements, subsequent investigators assumed that the failure of the lifting-line theory was associated with the fact that the portion of the wing immersed in the slipstream was usually of small aspect ratio. Graham, et. al., (Reference 7) therefore approached a solution via slender body theory and the approximate lifting surface theory of Weissinger (Reference 8). Calculations made by Graham showed improved agreement with Stuper's experimental data.

Ribner and Ellis (Reference 9) generalized the Weissinger lifting surface formulation to multiple, uninclined slipstreams. Their results showed reasonable agreement with the experimental data obtained by Brenckmann (Reference 10) for the overall lift increase due to the propeller slipstream.

The test results obtained by Brenckmann represent an improvement over the experimental data of Stuper in that the former experiments utilized an infinite aspect ratio wing, thus avoiding the use of end-plates which introduce uncertain-

ties as to the effective value of wing aspect ratio. Since Brenckmann employed a free propeller yielding a non-uniform slipstream velocity profile, the Ribner-Ellis theory, which assumes uniform velocity distributions, would not be expected to yield adequate predictions of the spanwise lift distributions as compared with Brenckmann's measurements.

Another series of tests of interest are those of Gobetz (Reference 11) and Snedeker (Reference 12) who employed a similar experimental arrangement to that of Stuper, in that a jet of air of approximately uniform velocity profile was used to simulate the propeller slipstream. These tests were designed to determine the basic effects of both wing aspect ratio and wing chord/slipstream diameter. The results were compared with theoretical calculations using the modified lifting-line theory of Rethorst (Reference 13) and it is shown that this theory is at least capable of predicting the trends of the test data.

Goland, et. al., (Reference 14) formulated a mathematical model based on potential theory approach to predict overall performance and stability characteristics of small aspect ratio wing spanning a slipstream of uniform velocity. Although this work effectively combined the R. T. Jones small aspect ratio theory with the potential flow theory to yield good correlation with test data, no attempt was made to predict and correlate the wing spanwise load distributions. This work was extended in References 15 and 16 to provide equations and charts for estimating lift and longitudinal force coefficients of STOL aircraft wings immersed in propeller slipstreams.

George and Kisielowski (Reference 17) modified the work of Reference 16 to account for non-uniformity of the propeller slipstream. In this analysis the propeller slipstream velocity was represented by a number of concentric zones of uniform velocity (staircase functions) with the wing spanning the slipstream. Although satisfactory correlations were obtained between the theoretical and experimental test data for low and moderate wing angles of attack, the theory of Reference 17 did not adequately predict lift distributions close to the wing stall.

In reviewing the above analytical attempts to solve the wing-slipstream problem, it is apparent that none of these

approaches is suitable for direct application to the present problem of predicting the effects of propeller slipstream on the stall characteristics of straight wing airplanes. Either the existing theoretical models are too simplified and disregard effects which are known to be critical, (e.g. Reference 6 and 13), or the analyses are too complex and do not yield practical and reliable solutions (e.g. Reference 9). Therefore, there exists a requirement to develop an improved mathematical model capable of providing practical and reliable analytical solutions to the wing/propeller problem.

The analytical methods developed under the current program potentially represent an answer to this problem. Although this optimism is based on a few isolated correlations with the available test data, sufficient indication of the effectiveness of the developed methodology has already been obtained, as confirmed by comparative results presented later in the text. The basis for this improved mathematical model is described below.

### 2.3 BASIS FOR THE PRESENT ANALYSIS

A common approach of past investigations involves an idealized representation of the propeller slipstream in which the velocity is discontinuous across the slipstream boundary. This model generally requires complex solutions to the boundary conditions associated with the discontinuity.

The basis of the current analysis lies in the observation that in a real slipstream the velocity distribution remains continuous throughout the slipstream boundary.

An examination of experimental data obtained on the velocity distributions in the wakes of propellers shows that there is no sudden jump in velocity across the slipstream boundary. There is, however, a rapid increase in velocity as the boundary is crossed but the continuity of velocity is still preserved. Since the lift distribution must be continuous and the velocity distribution is continuous, then the associated circulation distribution must also be continuous. Therefore, the strength of the shed vorticity may be obtained by differentiating the spanwise distribution of circulation in the usual manner, without the complication of accounting for discontinuities in circulation.

The approach presented in the following pages utilizes a comprehensive propeller analysis to compute the slipstream flow field including swirl components of velocity. The wing-nacelle combination is then introduced into this flow field and the effects of the non-uniform propeller flow field on the wing lift distribution is computed using a modification of lifting line theory which permits the calculation of the low aspect ratio effects associated with the slipstream-immersed positions of the wing.

The validity of the simple lifting line theory utilized herein for treating wings with non-uniform spanwise velocity distributions has been verified by applying it to a problem of linearly varying spanwise velocity gradients treated in a more general and complex manner by Fejer in Reference 18. The implementation of this lifting line theory to practical wing/propeller combinations is presented in Sections 3 and 4 below.

## SECTION 3

### THEORETICAL ANALYSIS

This section presents a summary of the analytical methods developed for predicting the propeller slipstream effects on the spanwise load distribution of wings operating at angles of attack up to stall. The analytical approach presented herein is based upon first determining the velocity distribution in the propeller wake and then calculating its effect on the wing lift distribution. The analysis provides for the use of non-linear lift curves for both the propeller and the wing in order to realistically represent the propeller slipstream distribution and its effect on wing loading at angles of attack up to stall.

Accordingly, the first part of this section deals with the propeller slipstream calculations, and the second part presents the implementation of the slipstream parameters in the modified wing theory.

#### 3.1 PROPELLER SLIPSTREAM ANALYSIS

The first part of the analysis deals with the propeller slipstream representation, including the required iterative solution and convergence procedures.

##### 3.1.1 General Propeller Solution

Consider a propeller operating at an angle of attack  $\alpha_p$  to the remote freestream of velocity  $V_0$ , as shown in Figure 1. The presence of a lifting wing behind the propeller modifies the inflow to the propeller disk through an induced upwash velocity  $V_w$ . As an approximation this upwash velocity is assumed to be uniform across the propeller disk, and to lie within the disk plane. The method used for calculating this upwash velocity is presented in Section 4.2.

For the purpose of analyzing the wing lift distribution it is assumed that the slipstream can be considered as being fully developed. With this assumption the average inclination of the contracted slipstream can be readily calculated using



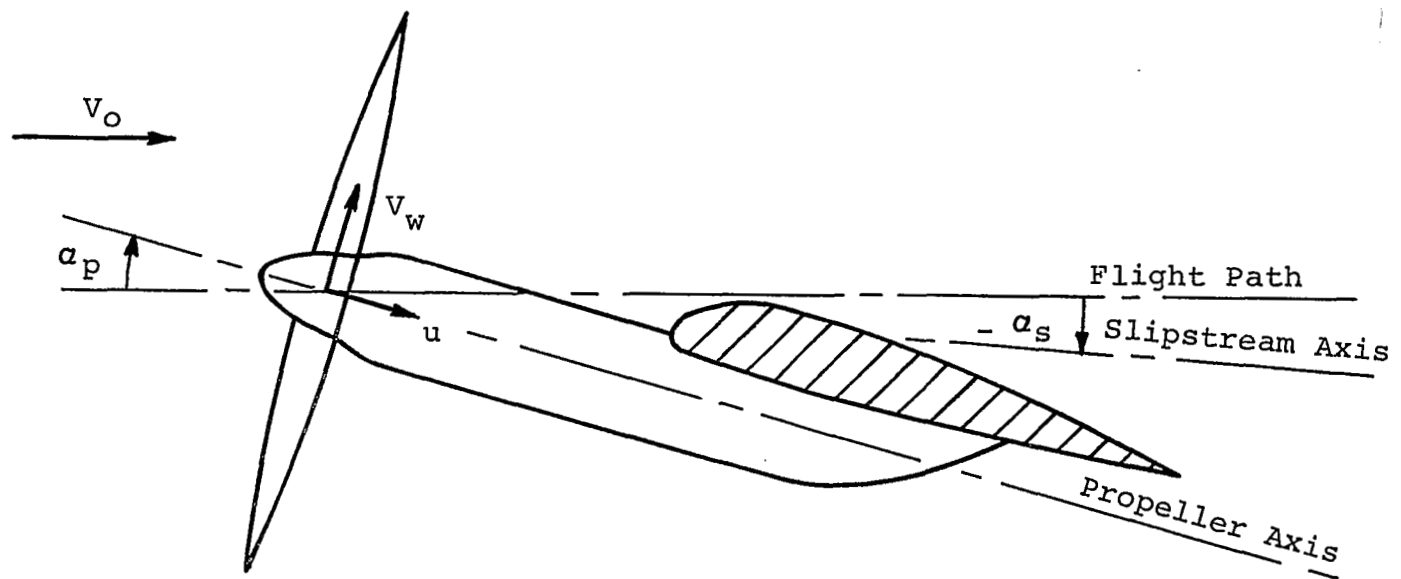


Figure 1. Notation For a Propeller Operating in the Presence of a Wing

simple actuator disk theory (e.g. Reference 19) and, in the notation of Figure 1, is obtained from

$$\tan(\alpha_p + \alpha_s) = \frac{V_0 \sin \alpha_p + V_w}{V_0 \cos \alpha_p + 2u} \quad (1)$$

where  $u$  is the axial induced velocity increment at the propeller disk. From momentum theory,  $u$  is related to propeller thrust,  $T$ , by

$$u^2 = \frac{T}{2\rho \pi R^2 V'} \quad (2)$$

where  $V'$  is the resultant velocity at the disk and is given by

$$V' = \sqrt{(V_0 \cos \alpha_p + u)^2 + (V_0 \sin \alpha_p + V_w)^2} \quad (3)$$

On combining equations (2) and (3) a quartic in  $u$  is obtained and is generally solved by iteration. However, since the present application is to conventional aircraft where  $\alpha_p$  is small and  $V_w \leq V_0$  this quartic may be reduced to a quadratic whose solution is

$$u = \frac{-V_0 \cos \alpha_p}{2} + \sqrt{\left(\frac{V_0 \cos \alpha_p}{2}\right)^2 + \frac{T}{2\rho \pi R^2}} \quad (4)$$

With the above value of  $u$ , equation (1) can be solved to yield the mean slipstream inclination  $\alpha_s$ , relative to the freestream.

To obtain the detailed velocity distribution within the inclined slipstream it is assumed that, to a good approximation, this can be obtained directly from the solution for an isolated propeller operating in axial flow at speed

$$V_a = V_0 \cos \alpha_p \quad (5)$$

The calculation of non-uniform slipstream velocity

distributions behind a propeller of arbitrary geometry is based upon established blade element-momentum theory as presented in Reference 20. While the solution to the general theory is very complex, a relatively simple and practical solution is obtained on the assumptions that the rotational energy in the slipstream is small compared to the axial energy and that the radial variation of static pressure in the slipstream can be neglected.

Standard blade element-momentum theory assumes that the flow is both incompressible and inviscid. Thus the flow in annular stream tube elements is treated in an independent manner. For any annular stream tube element, the slipstream velocities are related to both the induced velocities at the propeller disk and the radius in the fully contracted slipstream.

Following the analysis of Reference 20, the induced axial and rotational velocity components,  $u, 1/2\omega r$ , at any radius,  $r$ , in the propeller disk can be obtained by an iterative solution to the equations

$$\frac{\frac{\omega}{2}}{(\Omega - \frac{\omega}{2})} = \frac{\sigma}{4} \left( \frac{C_l}{\cos \phi} + \frac{C_d}{\sin \phi} \right) \quad (6)$$

and

$$\frac{u}{(\Omega - \frac{\omega}{2})r} = \frac{\sigma}{4} \left( \frac{C_l}{\sin \phi} - \frac{C_d}{\cos \phi} \right) \quad (7)$$

where, from Figure 2, the inflow angle,  $\phi$ , is given by

$$\phi = \tan^{-1} \left[ \frac{V_a + u}{(\Omega - \frac{\omega}{2})r} \right] \quad (8)$$

and the blade section lift and drag coefficients are known in terms of angle of attack,  $\alpha$ , given by

$$\alpha = \beta - \phi \quad (9)$$

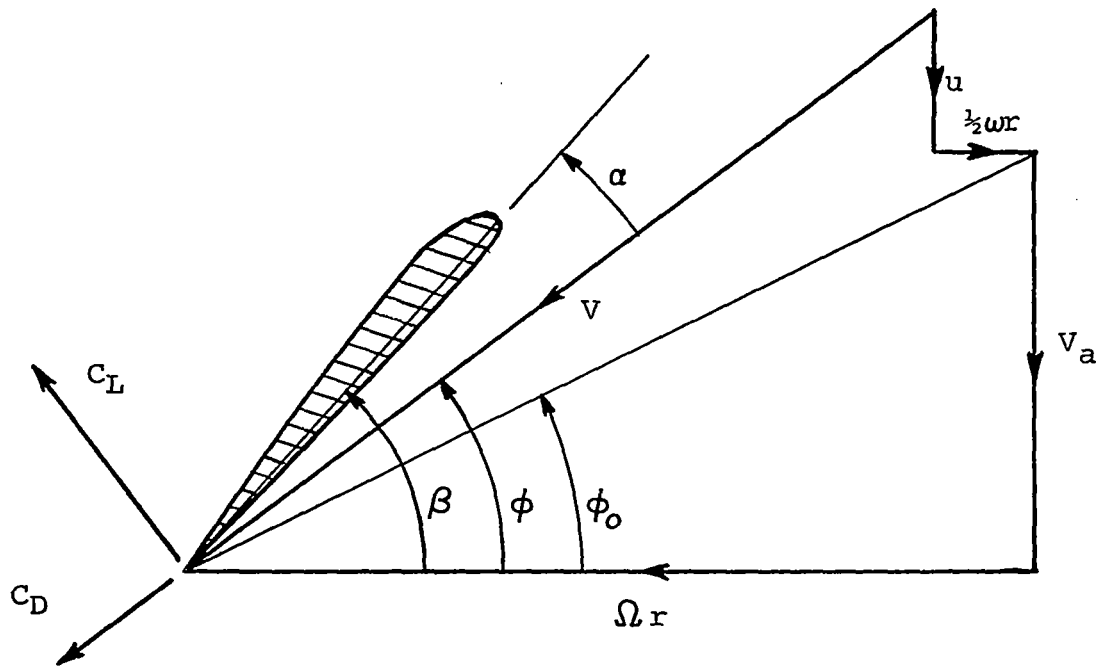


Figure 2. Blade Element Velocity Diagram

To account for the significant and well known loss of lift toward the blade tip equations (6) and (7) are rewritten in the form

$$\frac{\frac{\omega^*}{2}}{\left(\Omega - \frac{\omega^*}{2}\right)} = \frac{\sigma}{4F} \left( \frac{C_l}{\cos \phi} + \frac{C_d}{\sin \phi} \right) \quad (10)$$

and

$$\frac{\frac{u^*}{2}}{\left(\Omega - \frac{\omega^*}{2}\right)_r} = \frac{\sigma}{4F} \left( \frac{C_l}{\sin \phi} - \frac{C_d}{\cos \phi} \right) \quad (11)$$

where  $F$  is the tip-loss correction factor given by Lock in Reference 21 and  $u^*$ ,  $1/2(\omega^*r)$  are modified values of the induced velocity components.

Equations (10) and (11) yield improved values of the inflow angle  $\phi$  and section characteristics  $C_l$  and  $C_d$ , as affected by the tip-loss correction factor  $F$ . These values are then used to obtain a better approximation for slipstream-induced velocity components  $u$  and  $\omega r/2$ , using equations (6) and (7).

### 3.1.2 Initial Calculation of Inflow Angle

The iterative solution for the system of equations (8) through (11) requires that an initial approximate value of  $\phi$  be obtained. Equation (4) can be used if the propeller total thrust is known. However, since the propeller thrust is generally not known in advance, a method that yields a satisfactory starting value for  $\phi$  is developed as follows:

From Figure 2 the inflow angle  $\phi$  can be expressed as

$$\phi = \phi_0 + \frac{u^*}{\Omega r} \quad (12)$$

where the resultant induced velocity increment is assumed to be normal to the local blade velocity.

On making the assumption that  $C_d \leq C_l$  and  $\frac{\omega^*}{2} \leq \Omega$  equation (11) can be written as

$$\frac{u^*}{\Omega r} \left( \frac{V_a + u^*}{\Omega r} \right) = \frac{\sigma V C_\ell}{4 F \Omega r} \quad (13)$$

By solving equation (13) for  $u^*/\Omega r$  and substituting this value in equation (12) an initial value for  $\phi$  is obtained. However, the right hand side of equation (13) must first be reduced to a tractable form. This is accomplished by applying the following relationships:

(a) A linearized expression for the blade section lift curve, given by

$$C_\ell = a_0 (\alpha - \alpha_0) \quad (14)$$

where  $a_0$  is a representative lift slope  
 $\alpha$  is given by equation (9), and  
 $\alpha_0$  is the angle of attack at zero lift.

(b) An expression for  $V$ , obtained from Figure 2 as

$$V = \sqrt{V_a^2 + (\Omega r)^2} \quad (15)$$

(c) Prandtl's expression for the tip loss factor  $F_p$  obtained from Reference 21 as

$$F_p = \frac{2}{\pi} \cos^{-1} \left[ \exp \left\{ -\frac{B}{2} \left( 1 - \frac{r}{R} \right) \sqrt{1 + \left( \frac{\Omega R}{V_a} \right)^2} \right\} \right] \quad (16)$$

where  $B$  is the number of blades

Combining equations (12) through (15) and substituting for the tip loss factor,  $F_p$ , given by equation (16) leads to the following expression:

$$\frac{u^*}{\Omega r} \left( \frac{V_a + u^*}{\Omega r} \right) = \frac{\sigma a_0}{4 F_p} \sqrt{1 + \left( \frac{V_a}{\Omega r} \right)^2} \cdot \left( \beta - \phi_0 - \alpha_0 - \frac{u^*}{\Omega r} \right) \quad (17)$$

from which the solution for  $u^*/\Omega r$  is obtained as

$$\frac{u^*}{\Omega r} = 1/2 \left[ \sqrt{\left(\frac{V_a}{\Omega r} + x\right)^2 + 4x(\beta - \phi_0 - a_0)} - \left(\frac{V_a}{\Omega r} + x\right) \right] \quad (18)$$

where

$$x = \frac{\sigma a_0}{4 F_p} \sqrt{1 + \left(\frac{V_a}{\Omega r}\right)^2}$$

### 3.1.3 Convergence of the Iterative Propeller Solution

The iterative solution to equations (8) through (11) is naturally divergent within the normal range of the blade section lift curves. Therefore, convergence of the solution must be forced by applying a correction to each new computed value of  $\phi$ . A correction procedure which yields rapid convergence is derived by the method presented below

Let the exact solution for inflow angle,  $\phi$ , be expressed as

$$\phi = \phi' + \delta_1 \quad (19)$$

where  $\phi'$  is the value used as input to the  $n^{\text{th}}$  iteration and  $\delta_1$  is a small unknown increment.

In the general iteration procedure,  $\phi'$  is first used in equation (9) to obtain a value of  $\alpha$  from which  $C_l$  and  $C_d$  may be determined knowing the blade airfoil section characteristics. Next, equations (10) and (11) are used to solve for  $u^*$  and  $\omega^*$  and these values are then substituted in equation (8) to obtain a new value of inflow angle, denoted by  $\phi''$ . It is this new value of inflow angle which must be corrected before proceeding to the  $(n+1)^{\text{th}}$  iteration.

Therefore, let the exact solution for inflow angle,  $\phi$ , also be expressed as

$$\phi = \phi'' - \delta_2 \quad (20)$$

where  $\delta_2$  is a second small unknown increment.

Combining equations (19) and (20), to eliminate  $\phi$ , yields

$$\delta_1 + \delta_2 = \phi'' - \phi' \quad (21)$$

Substituting equation (21) into equation (19), there follows:

$$\phi = \phi' + (\phi'' - \phi') \cdot \frac{1}{1 + (\delta_2/\delta_1)} \quad (22)$$

Equation (22) forms the basis of a method for calculating an improved value of inflow angle for input to the next iteration cycle by using the guessed and calculated values from the previous cycle. The ratio,  $\delta_2/\delta_1$ , remains to be determined from an approximate error analysis in the following manner:

From equation (20) the value of  $\tan \phi$  is expressed to first order in  $\delta_2$  by

$$\tan \phi = \tan \phi'' - \delta_2 \sec^2 \phi'' \quad (23)$$

From equations (9) and (19) the exact solution for blade lift coefficient,  $C_L$ , is expressed in terms of the value  $C_L'$  calculated in the  $n^{\text{th}}$  iteration cycle from

$$C_L = C_L' - \alpha_0 \delta_1 \quad (24)$$

where  $\alpha_0$  is a mean value of lift-curve slope.

Equation (10) written in terms of values for the exact



solution but with the assumption that  $C_d \leq C_l$ , reduces to

$$\frac{\frac{\omega^*}{2}}{(\Omega - \frac{\omega^*}{2})} = \frac{\sigma C_l}{4F \cos \phi} = k_x \quad (25)$$

Substituting equations (19) and (24) into equation (25), and retaining only first order terms in  $\delta_1$ , there follows:

$$k_x = k_x' \left[ 1 - \delta_1 \left( \frac{a_0}{C_l} - \tan \phi' \right) \right] \quad (26)$$

where

$$k_x' = \frac{\sigma C_l'}{4F \cos \phi'}$$

and where small changes in the tip loss factor are neglected.

Similarly, equation (11) reduces to

$$\frac{u^*}{(\Omega - \frac{\omega^*}{2})_r} = \frac{\sigma C_l}{4F \sin \phi} = k_y \quad (27)$$

and, using equations (19) and (24), results in the expression

$$k_y = k_y' \left[ 1 - \delta_1 \left( \frac{a_0}{C_l} + \cot \phi \right) \right]$$

where

$$k_y' = \frac{\sigma C_l'}{4F \sin \phi'}$$

Now, using equations (25) and (27), equation (8) can be expressed as

$$\tan \phi = \mu (1 + k_x) + k_y \quad (29)$$

where  $\mu$  is the local forward speed ratio ( $V_0/\Omega r$ ).

Rewriting equation (29) in terms of the values  $k_x^1, k_y^1$  calculated in the  $n^{\text{th}}$  iteration cycle yields

$$\tan \phi'' = \mu (1 + k_x^1) + k_y^1 \quad (30)$$

Combining equations (29) and (30) leads to the following relationship

$$\tan \phi = \tan \phi'' - \mu k_x^1 \left(1 - \frac{k_x^1}{k_x^1}\right) - k_y^1 \left(1 - \frac{k_y^1}{k_y^1}\right) \quad (31)$$

Finally using equations (23), (26), (28) and (31) a solution for the ratio  $\delta_2/\delta_1$  is obtained as follows:

$$\frac{\delta_2}{\delta_1} = \cos^2 \phi'' \left[ \mu k_x^1 \left(\frac{a_0}{C_{\ell}} - \tan \phi^1\right) + k_y^1 \left(\frac{a_0}{C_{\ell}} + \cot \phi^1\right) \right] \quad (32)$$

Equation (32) thus provides the essential relationship by which equation (22) is applied to obtain an improved value of inflow angle for input to the next iteration cycle. In practice, the iteration procedure is terminated when the difference  $(\phi'' - \phi')$  for each successive iteration cycle has converged to within a prescribed margin of error.

#### 3.1.4 Analysis for Slipstream Velocity Distributions

Upon reaching a converged solution for the inflow angle  $\phi$ , the final values of  $\phi$ ,  $C_{\ell}$  and  $C_d$  are then substituted in equation (6) and (7) to solve for the true induced velocity components in the propeller disk plane,  $u$  and  $1/2 \omega r$ .

The local axial velocity component  $V_{s0}$  in the fully developed slipstream is obtained from Figure 1 as

$$V_{s0} = \frac{V_0 \cos \alpha_p + 2u}{\cos(\alpha_p + \alpha_s)} \quad (33)$$

The local rotational velocity component,  $V_{st}$ , in the fully developed slipstream is obtained from conservation of angular momentum and is given by

$$V_{st} = \omega r \left( \frac{r}{r_s} \right) \quad (34)$$

where  $r_s$  is the local radius in the slipstream for the streamtube element which has a local radius  $r$  in the propeller disk plane.

The local radius  $r_s$  for each flow element in the slipstream is derived from a simplified application of the continuity expression to successive streamtube elements. For the  $n^{\text{th}}$  blade element station at radius  $r_n$  the corresponding radius  $r_{s_n}$  in the slipstream is given by

$$r_{s_n}^2 = r_{s_1}^2 + 1/2 \sum_{m=2}^{m=n} (r_m^2 - r_{m-1}^2) \cdot \left( \frac{2V_a + u_m + u_{m-1}}{V_a + u_m + u_{m-1}} \right) \quad (35)$$

where, in the notation of Figure 3,  $r_1$  and  $r_{s_1}$  are the values of hub and nacelle radius, respectively.

The value of  $r_{s_n}$  given by equation (35) is based upon representing the slipstream by a series of concentric annular streamtubes with uniform velocity between each element station. This solution, while approximate, is found to be more than adequate for all reasonable variations between  $u_{n-1}$  and  $u_n$ .

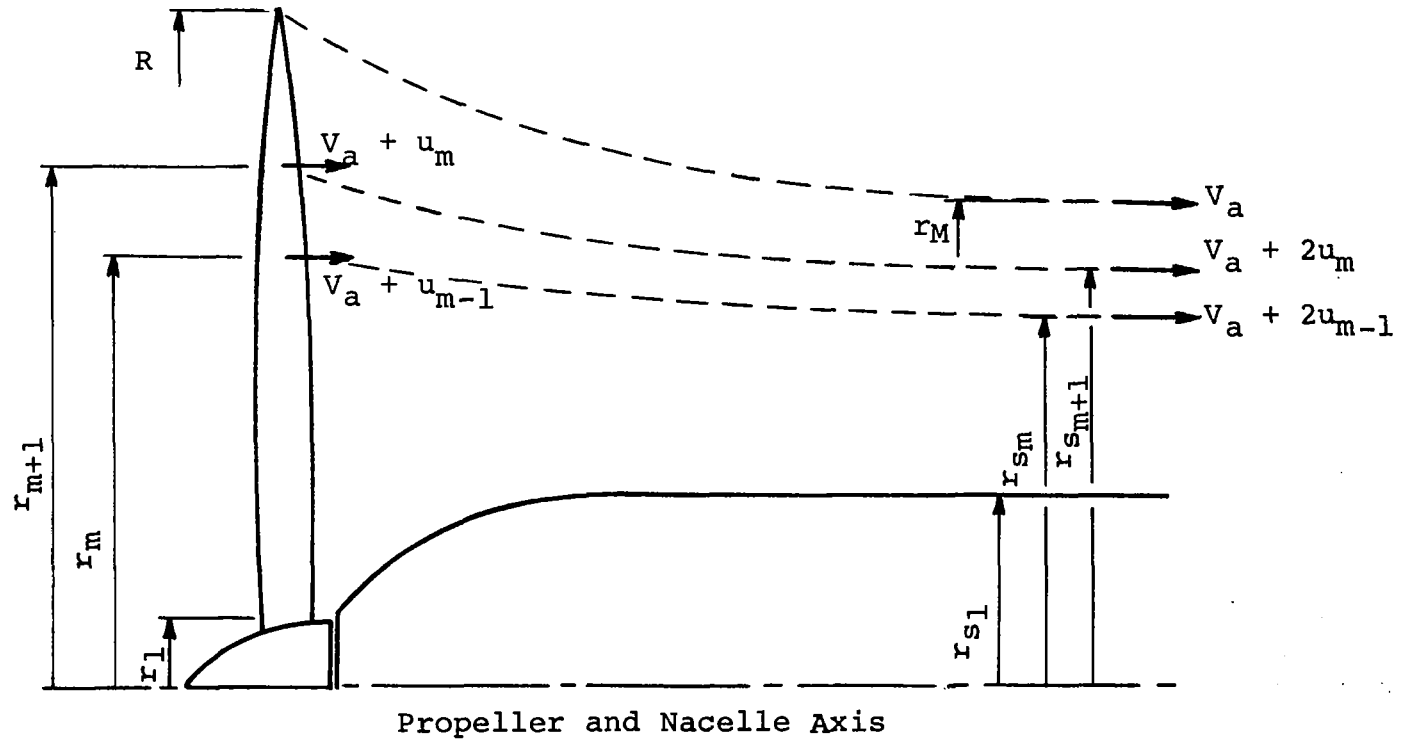


Figure 3. Analytical Model For Slipstream Contraction.

### 3.2 WING-IN-SLIPSTREAM ANALYSIS

In the second part of the analysis a modified form of lifting line theory is presented which uses the nonuniform slipstream velocity distribution, as determined above, to calculate the lift distribution on wings with propellers. The approach presented relies on the use of a simple physical model to obtain a solution for wing-in-slipstream loadings for a wide range of real aircraft propeller-wing combinations.

First the method is presented for an unflapped wing immersed in one or more non-overlapping slipstreams. Following this, the modifications required to include flaps are described. Finally, an extension of the analysis to include low aspect-ratio propeller-wing combinations is discussed.

#### 3.2.1 Analysis for a Wing with no Flaps or with Full-Span Deflected Flaps

Consider the basic case of a wing in a uniform stream of velocity,  $V_0$ . If the local circulation is  $\Gamma_0$ , then the span load distribution at any spanwise station is given by

$$l_0 = \rho V_0 \Gamma_0 \quad (36)$$

The superposition of a propeller slipstream flow gives rise to an increased local velocity  $V_s'$  and an increased circulation  $\Gamma_s'$ , which can be expressed, respectively, as

$$V_s' = V_0 + \Delta V \quad (37)$$

and

$$\Gamma_s' = \Gamma_0 + \Delta \Gamma \quad (38)$$

where  $\Delta V$  and  $\Delta \Gamma$  are the incremental changes in local velocity and circulation, respectively, due to propeller slipstream. Now the corresponding spanwise load distribution for the basic wing immersed in the propeller slipstream can be written as

$$l = \rho V_s' \Gamma_s' \quad (39)$$

Substituting equations (37) and (38) into equation (39) yields a general expression for the spanwise load distribution of a wing immersed in the propeller slipstream, as follows:

$$\begin{aligned}
 d &= \rho (v_0 + \Delta v) (\Gamma_0 + \Delta\Gamma) \\
 &= \rho (v_0 + \Delta v) \Gamma_0 + \rho (v_0 + \Delta v) \Delta\Gamma \\
 &= \rho v_s' \Gamma_0 + \rho v_s' \Delta\Gamma \quad (40) \\
 &= \rho v_s' \Gamma_0 + \rho v_s' \Gamma_2 \\
 &= d_1 + d_2
 \end{aligned}$$

where  $\Gamma_2 \equiv \Delta\Gamma$  is the change in wing circulation due to propeller slipstream alone.

It can be noted from equation (40) that the first component  $d_1$  of the total lift distribution is that which would be obtained if the local velocity increased while the circulation  $\Gamma_0$  remained unchanged. If the circulation is unchanged, then there is no change in the trailing vorticity and therefore no change in the wing downwash field. The second term  $d_2$  represents the change in spanwise lift distribution due to the circulation  $\Gamma_2$  and is therefore associated with wing downwash changes caused by the propeller slipstream.

The problem of a wing immersed in the propeller slipstream is now reduced to proper determination of local values for the resultant velocity  $v_s'$  and the circulation  $\Gamma_2$  for the entire wing. This analysis is developed below.

For typical propeller/wing configurations, the resultant local velocity  $v_s'$  can be equated (within the small angle assumption) to the combined freestream and slipstream component along the wing section zero-lift line, thus

$$v_s \approx v_s' \quad (41)$$

Using the nomenclature of Figure 4, this velocity component can be expressed as

$$V_s = V_{s_0} \cos (\alpha_s + \alpha_e) - V_{s_t} \sin (\alpha_s + \alpha_e) \quad (42)$$

Also, the corresponding component of the total flow normal to the wing section zero-lift line is given by

$$V_n = V_{s_0} \sin (\alpha_s + \alpha_e) + V_{s_t} \cos (\alpha_s + \alpha_e) \quad (43)$$

The quantities  $V_{s_0}$  and  $V_{s_t}$  in the above equations represent the axial and swirl velocity components of the combined freestream and slipstream flow and are given by equations (33) and (34) respectively. Also, the angles  $\alpha_s$  and  $\alpha_e$  are known quantities which represent inclinations of the slipstream and the zero-lift line relative to the remote freestream velocity, respectively.

The extra wing circulation  $\Gamma_2$ , caused by the action of the propeller slipstream, is determined by equating the resulting change in wing upwash to the downwash change associated with  $\Gamma_2$ . This upwash change, in non-dimensional form, is defined as

$$v = \frac{V_n}{V_0} - \sin \alpha_e \quad (44)$$

Substituting equation (43) into equation (44) yields the extra upwash due to the slipstream as

$$v = \frac{V_{s_0}}{V_0} \sin (\alpha_s + \alpha_e) + \frac{V_{s_t}}{V_0} \cos (\alpha_s + \alpha_e) - \sin \alpha_e \quad (45)$$

In order to satisfy the wing boundary condition of no flow through the surface, this extra upwash or crossflow must be balanced by the combined influence of the extra bound vorticity,  $\Gamma_2$ , and the associated streamwise (i.e. chordwise and trailing) vorticity,  $-\frac{d\Gamma_2}{dy} dy$ .

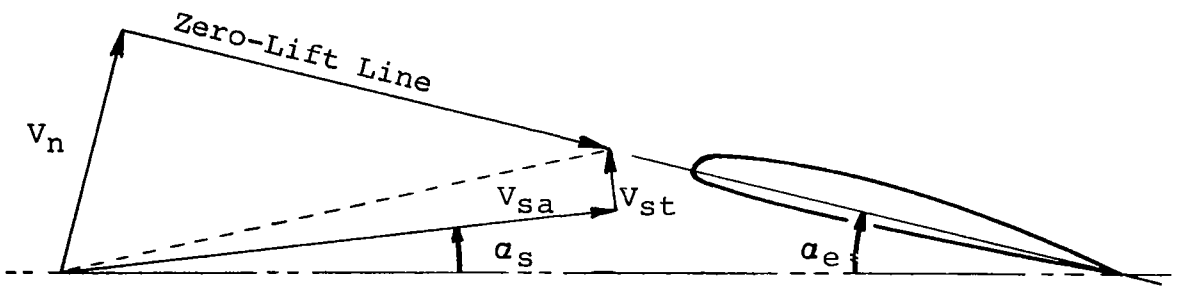
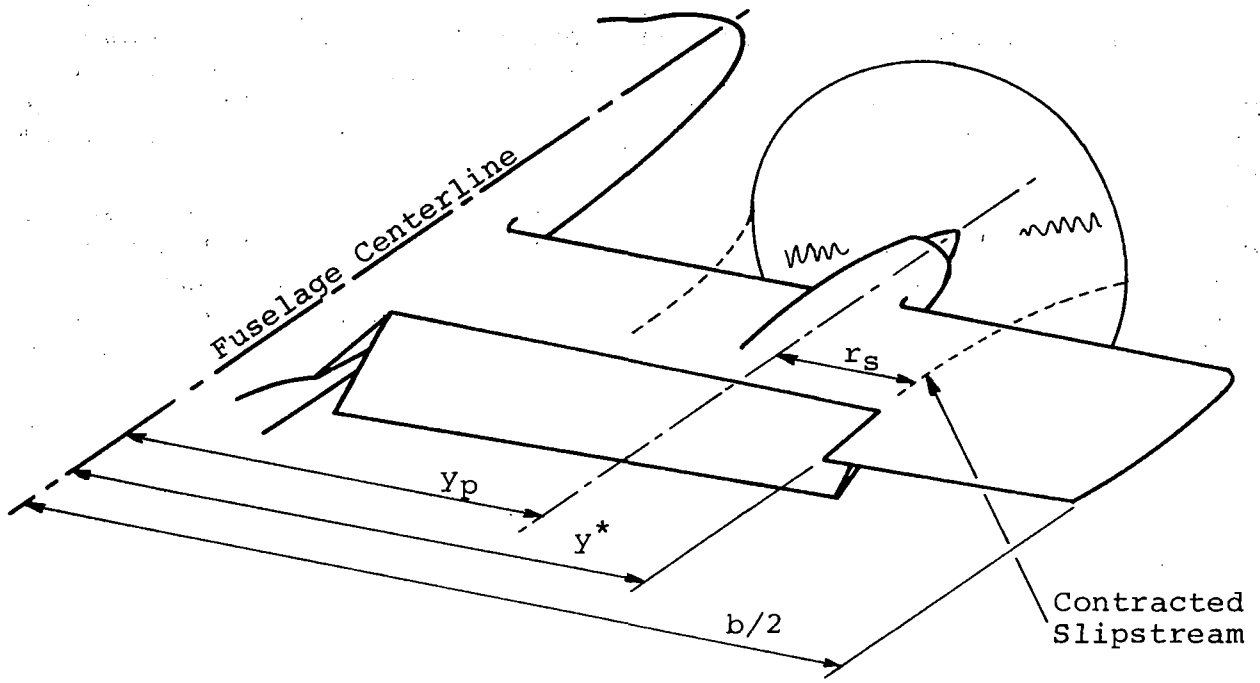


Figure 4. Notation for Wing-in-Slipstream Model



Observation of the lift on wings with slipstreams shows that the major portion of the extra loading caused by the slipstream is concentrated on and near that portion actually immersed in the slipstream and, for most configurations, the "aspect ratio" of this immersed portion is small, usually about 1.0. It is herein postulated that the distribution of extra vorticity caused by the slipstream exhibits the characteristics of that found on low aspect-ratio wings. Kuchemann, in Reference 22, shows that for low aspect-ratio wings only the chordwise and trailing vortices are required to fulfill the boundary conditions. In fact, as the aspect ratio tends to zero, the trailing vortices cancel half the upwash, and the chordwise vortices cancel the remainder.

In the present case, the net extra upwash is  $V_0 v$  and the downwash change due to the trailing vortices associated with the extra circulation,  $\Gamma_2$ , is given by

$$W_{i_2} = \frac{1}{4\pi} \int_{-b/2}^{b/2} \frac{-\frac{d\Gamma_2}{dy_1} dy_1}{y_1 - y} \quad (46)$$

Therefore, from the above considerations it follows that

$$W_{i_2} = 1/2 V_0 v \quad (47)$$

and hence

$$v = \frac{1}{2\pi V_0} \int_{-b/2}^{b/2} \frac{-\frac{d\Gamma_2}{dy_1} dy_1}{y_1 - y} \quad (48)$$

Equation (48) is supported by the analysis of Reference 23, which deals with the determination of the lift on a wing passing close to a line vortex. This reference states that lifting line theory always overestimates the lift induced by rapidly changing upwash fields (such as from propellers and line vortices) by a factor of 2, due to a corresponding underestimation of the wing downwash.

Now, expressing the circulation distribution,  $\Gamma_2$ , as a Fourier sine series in terms of the wing spanwise angular coordinate,  $\theta = \cos^{-1} \left( \frac{2y}{b} \right)$ , yields

$$\Gamma_2 = 1/2 b V_0 \sum_{n=1}^{\infty} B_n \sin n\theta \quad (49)$$

Combining equations (48) with (49) and performing the required mathematical operations, the Fourier coefficients  $B_n$  can be expressed as

$$B_n = \frac{4}{n\pi} \int_0^{\pi} v \sin \theta \sin n\theta d\theta \quad (50)$$

By limiting the series for  $\Gamma_2$  to  $r-1$  terms, equation (49) becomes

$$\Gamma_{2m} = 1/2 b V_0 \sum_{n=1}^{r-1} B_n \sin n \frac{m\pi}{r} \quad (51)$$

where  $m = 1, 2, \dots, \overline{r-1}$

and equation (50) is reduced to the summation

$$B_n = \frac{4}{nr} \sum_{m=1}^{r-1} v_m \sin \frac{m\pi}{r} \sin n \frac{m\pi}{r} \quad (52)$$

From equation (40) the lift  $\mathcal{L}_2$  associated with the slipstream may be expressed as

$$\mathcal{L}_2 = \rho V_s \Gamma_2 = 1/2 \rho V_0^2 C_{\mathcal{L}_2} c \quad (53)$$

where the lift coefficient is based on  $V_0$ . Therefore

$$\Gamma_{2m} = 1/2 b V_0 \left( \frac{C_{\mathcal{L}_2} c}{b} \frac{V_0}{V_s} \right)_m \quad (54)$$

Comparing equations (51 and (54) there results

$$\left(\frac{C_{d_2c}}{b}\right)_k = \left(\frac{V_s}{V_0}\right)_k \sum_{n=1}^{r-1} B_n \cdot \sin n \frac{k\pi}{r} \quad (55)$$

If the relationship for the coefficients,  $B_n$  is substituted into equation (55), the lift distribution associated with the slipstream is obtained in the form

$$\left(\frac{C_{d_2c}}{b}\right)_k = \left(\frac{V_s}{V_0}\right)_k \cdot \frac{4}{r} \sum_{n=1}^{r-1} \frac{\sin n \frac{k\pi}{r}}{n} \sum_{m=1}^{r-1} V_m \cdot \sin \frac{m\pi}{r} \cdot \sin n \frac{m\pi}{r} \quad (56)$$

Having determined the lift associated with the slipstream upwash the overall wing lift is calculated as follows.

Let  $\alpha_{i_1}$  and  $\alpha_{i_2}$  be the induced angles of attached associated with the lift distributions  $d_1$  and  $d_2$  respectively, as given by equation (40). Then the total induced angle of attack at any point  $k$  is given by

$$\alpha_{i_k} = \alpha_{i_{1k}} + \alpha_{i_{2k}} \quad (57)$$

Also, re-expressing equation (40) in terms of the lift coefficients based on  $V_0$  yields

$$\left(\frac{C_{d_c}}{b}\right)_k = \left(\frac{C_{d_1c}}{b}\right)_k + \left(\frac{C_{d_2c}}{b}\right)_k \quad (58)$$

Using the multipliers  $\beta_{mk}$  from Reference 1 in equation (58) there follows

$$\sum_{m=1}^{r-1} \left(\frac{C_{d_c}}{b}\right)_m \beta_{mk} = \sum_{m=1}^{r-1} \left(\frac{C_{d_1c}}{b}\right)_m \beta_{mk} + \sum_{m=1}^{r-1} \left(\frac{C_{d_2c}}{b}\right)_m \beta_{mk} \quad (59)$$

Now, by definition

$$\alpha_{i_{1k}} = \sum_{m=1}^{r-1} \left(\frac{C_{d_1c}}{b}\right)_m \beta_{mk} \quad (60)$$

Adding  $\alpha_{i2k}$  to both sides of equation (59) and using equations (57) and (60) leads to

$$\alpha_{ik} = \sum_{m=1}^{r-1} \left( \frac{C_{l2c}}{b} \right)_m \beta_{mk} + \alpha_{i2k} - \sum_{m=1}^{r-1} \left( \frac{C_{l2c}}{b} \right)_m \beta_{mk} \quad (61)$$

Equation (61) gives the total induced angle of attack in terms of the unknown wing lift distribution,  $C_{l2c}/b$ , the known induced angle of attack,  $\alpha_{i2} = V_0 v/V_s$ , and the known slip-stream lift distribution,  $C_{l2c}/b$ , given by equation (56). The solution is obtained by iteration as follows.

An approximation to the overall lift distribution is calculated and equation (61) is used to obtain a first approximation to the induced angle of attack. The effective angle of attack at the wing section is obtained from

$$\alpha_{ek} = \left[ \alpha_{gk} + \frac{V_0 v_k}{V_{sk}} - \alpha_{ik} - (1-E) \alpha_{lok} \right] \frac{1}{E} \quad (62)$$

Where  $\alpha_{gk}$  is the section geometric angle of attack,  $\alpha_{lok}$ , is the section zero-lift angle and  $E$  is the edge-velocity factor of Reference (1). This value of effective angle of attack is then used with the two-dimensional section lift curves at the effective section Reynolds number  $R_{ek}$  to obtain the lift coefficient  $C_l$ . The value of  $C_l/b$  thus calculated is compared to the initial approximation and, if sufficient agreement is not obtained, a new value is computed using the method given in Reference 1. This iteration process is then repeated until guessed and calculated values agree to within prescribed tolerance.

It should be noted that the above analysis is also applicable to a wing with full-span deflected flaps, provided that appropriate airfoil characteristics are employed for wing sections with flaps.

### 3.2.2 Analysis for a Wing with Part-Span Deflected Flaps

The deflection of a part-span flap causes a discontinuity  $\delta$  in the distribution of absolute angle of attack at the end of the flap, and produces a corresponding discontinuity in the slipstream-induced crossflow. The effect of these discontinuities on the span load distribution is treated below.

The analysis is developed for a wing having a deflected part-span flap  $\delta_f$  extending from  $y = -b/2$  to  $y = y^*$ . The most general case is that of a flap whose end lies within the slipstream, as illustrated in Figure 5.

Following the preceding treatment of a wing with no flaps or with full-span deflected flaps, the total wing lift distribution given by equation (40) can be divided into two portions and can be expressed in non-dimensional form as

$$\left(\frac{C_{Lc}}{b}\right) = \left(\frac{C_{L_1c}}{b}\right) + \left(\frac{C_{L_2c}}{b}\right) \quad (63)$$

where  $C_{L_2c}/b$  is the lift distribution associated with slipstream-induced upwash and  $C_{L_1c}/b$  is the remainder of the distribution.

In the present case, however, the slipstream-induced upwash  $V_0v$ , given by equation (48), is discontinuous at the end of the flap as shown in Figure 5. The net discontinuity in crossflow at the edge of the flap,  $y = y^*$ , can be obtained from equation (45) by considering the upwash on both sides of the flap end. Thus, using equation (45) for the flapped side of the wing, at  $y = y^*-0$ , this extra upwash can be expressed as follows

$$V_0v(y^*-0) = V_{s0}^* \sin(\alpha_s^* + \alpha_e^* + \delta) + V_{s1}^* \cos(\alpha_s^* + \alpha_e^* + \delta) - V_0 \sin(\alpha_e^* + \delta) \quad (64)$$

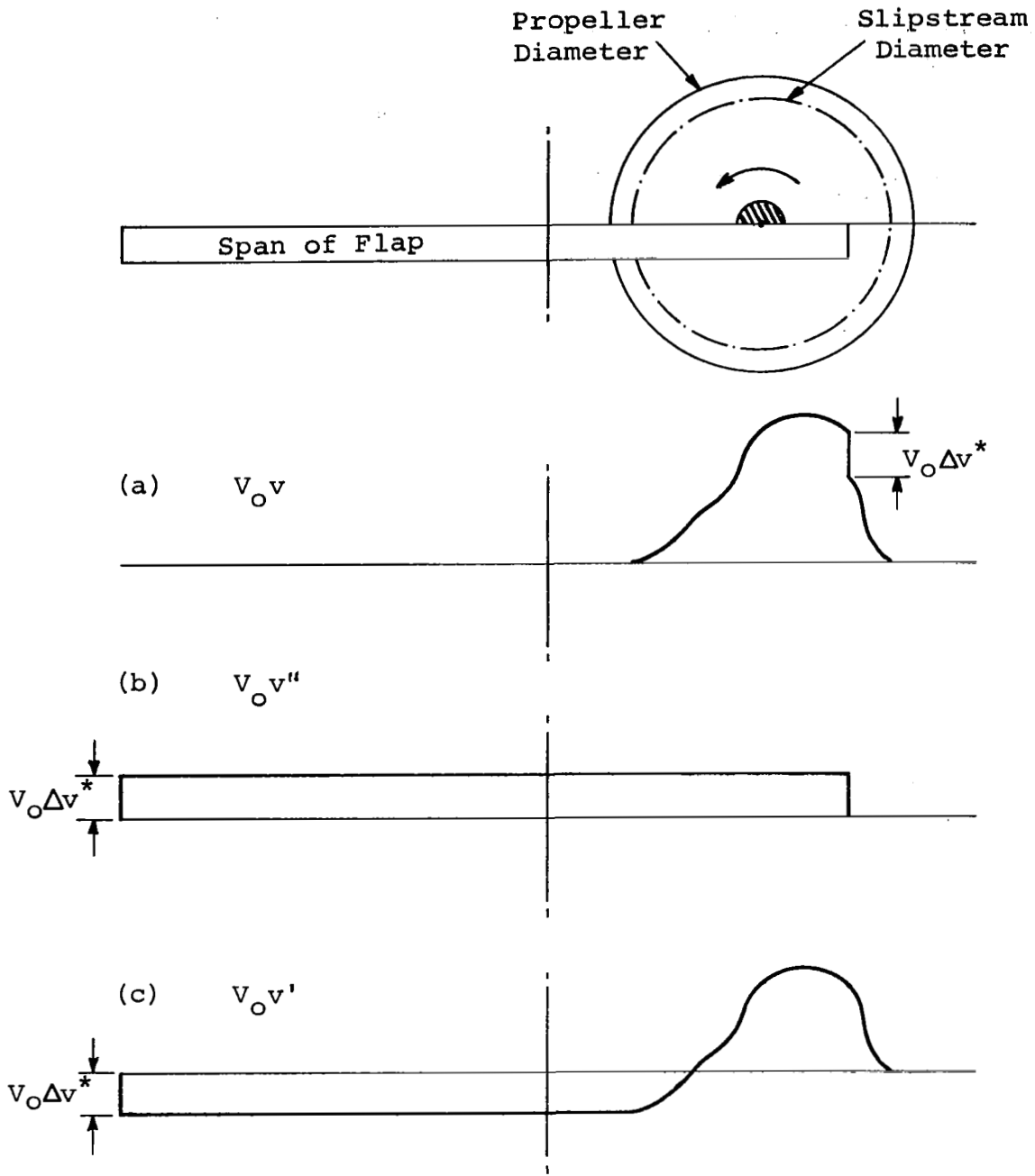


Figure 5. Mathematical Representation of Flap Discontinuity

Similarly, for the unflapped side at  $y = y^* + 0$ , the crossflow is given by

$$V_0 v(y^* + 0) = V_{sa}^* \sin(\alpha_s^* + \alpha_e^*) + V_{st}^* \cos(\alpha_s^* + \alpha_e^*) - V_0 \sin(\alpha_e^*) \quad (65)$$

The net discontinuity in crossflow is obtained as the difference between equations (64) and (65), thus

$$V_0 v(y^* - 0) - V_0 v(y^* + 0) = V_0 \Delta v^* \quad (66)$$

Because of the discontinuity in crossflow,  $V_0 \Delta v^*$ , given by equation (66), the solution for the lift distribution  $C_{l2}$  can not be obtained from a simple Fourier series for  $\Gamma_2$ , as was possible in equation (48). Therefore, the distribution  $V_0 v$  is split into two portions, one a continuous distribution  $V_0 v'$  and the other a step function distribution  $V_0 v''$ , where.

$$V_0 v = V_0 v' + V_0 v''$$

$$\text{and } V_0 v'' = V_0 \Delta v^* \quad \text{for } -b/2 \leq y < y^* \quad (67)$$

$$= 0 \quad \text{for } y^* \leq y \leq b/2$$

Now, it is necessary to relate the velocity distributions given by equation (67) to their corresponding circulation distributions. Since  $\Gamma_2$  is the total circulation corresponding to  $V_0 v$ , as given by equation (48), it can also be split into two distributions, i.e.,  $\Gamma_2'$ , corresponding to  $V_0 v'$  and  $\Gamma_2''$  corresponding to  $V_0 v''$ , where

$$\Gamma_2 = \Gamma_2' + \Gamma_2'' \quad (68)$$

Thus, using equations (48) and (68), the velocity distributions given by equation (67) can now be re-expressed in terms of the corresponding circulation distributions  $\Gamma_2'$  and  $\Gamma_2''$  as follows:

$$\begin{aligned} V_0 v &= V_0 v' + V_0 v'' \\ &= \frac{1}{2\pi} \int_{-b/2}^{b/2} \frac{-d\Gamma_2'}{dy_1} \cdot \frac{dy_1}{y_1 - y} + \frac{1}{2\pi} \int_{-b/2}^{b/2} \frac{-d\Gamma_2''}{dy_1} \cdot \frac{dy_1}{y_1 - y} \end{aligned} \quad (69)$$

where

$$V_0 v' = \frac{1}{2\pi} \int_{-b/2}^{b/2} \frac{-d\Gamma_2'}{dy_1} \cdot \frac{dy_1}{y_1 - y} \quad (70)$$

and

$$V_0 v'' = \frac{1}{2\pi} \int_{-b/2}^{b/2} \frac{-d\Gamma_2''}{dy_1} \cdot \frac{dy_1}{y_1 - y} \quad (71)$$

Now the problem reduces to determining  $\Gamma_2'$  and  $\Gamma_2''$  and the corresponding lift distribution  $C_{d_2} \cdot c/b$ . This is accomplished as outlined below.



Since  $V_0.v^I$  is continuous then, following the analysis of subsection 3.2.1,  $\Gamma_2^I$  can be expressed as the simple Fourier series

$$\Gamma_2^I = \frac{1}{2} b V_0 \sum_{n=1}^{r-1} B_n \sin n\theta \quad (72)$$

where the coefficients  $B_n$  are given by:

$$B_n = \frac{4}{n.r} \sum_{m=1}^{r-1} (v-v^{II})_m \sin \frac{m\pi}{r} \sin n \frac{m\pi}{r} \quad (73)$$

The relationship for  $\Gamma_2^{II}$  is obtained from the analysis of Reference 24 in the form

$$\frac{2 \Gamma_2^{II}}{b V_0} = \frac{\Delta v^*}{\pi} \left[ 2 (\pi - \theta^*) \sin \theta - (\cos \theta - \cos \theta^*) \log \left\{ \frac{1 - \cos (\theta + \theta^*)}{1 - \cos (\theta - \theta^*)} \right\} \right] \quad (74)$$

The distribution  $\Gamma_2^{II}$  given by equation (74) satisfies the required discontinuity in the crossflow,  $V_0.v^{II} = V_0.\Delta v^*$  in equation (71).

The circulation distributions  $\Gamma_2^I$  and  $\Gamma_2^{II}$ , determined in equations (72) and (74) respectively, can now be used to obtain the corresponding lift distribution  $C_{l2} c/b$  associated with the slipstream-induced upwash. This is accomplished by rearranging equation (54) and using equation (68), thus

$$\begin{aligned} \frac{C_{l2} c}{b} &= \left( \frac{V_s}{V_0} \right) \left( \frac{2 \Gamma_2}{b V_0} \right) \\ &= \left( \frac{V_s}{V_0} \right) \left( \frac{2 \Gamma_2^I}{b V_0} + \frac{2 \Gamma_2^{II}}{b V_0} \right) \end{aligned} \quad (75)$$

Finally, substituting equations (72), (73) and (74) into equation (75) yields the lift distribution  $C_{d_2} c/b$  at any point  $k$  on the wing, in the form

$$\left(\frac{C_{d_2} c}{b}\right)_k = \left(\frac{V_s}{V_0}\right)_k \left[ \frac{4}{r} \sum_{n=1}^{r-1} \frac{\sin n \frac{k\pi}{r}}{n} \sum_{m=1}^{r-1} (v_m - v_m'') \sin \frac{m\pi}{r} \sin n \frac{m\pi}{r} \right. \\ \left. + \frac{\Delta v^*}{\pi} \left\{ 2(\pi - \theta^*) \sin \frac{k\pi}{r} - \left( \cos \frac{k\pi}{r} - \cos \theta^* \right) \log \frac{1 - \cos \left( \frac{k\pi}{r} + \theta^* \right)}{1 - \cos \left( \frac{k\pi}{r} - \theta^* \right)} \right\} \right] \quad (76)$$

The above analysis gives the solution for the case where the flap extends from the left wing tip to a point  $y=y^*$  on the right wing. The solution for a flap extending between  $-y^* \leq y \leq y^*$ , or any other combination of flap positions, is obtained by superposition of solutions as shown in Figure 6.

It should be noted that equation (76) represents only one part of the solution for the total lift distribution  $C_{d_1} c/b$  as given in equation (63). It is now necessary to obtain an appropriate solution for the distribution  $C_{d_1} c/b$ . This is accomplished as outlined below.

The discontinuity  $\delta$  in absolute angle of attack caused by the flap deflection also affects the distribution  $C_{d_1} c/b$ . This distribution, although continuous, possesses an infinite derivative at  $y=y^*$ . Therefore, the multipliers  $\beta_{mk}$  developed in Reference 1 can not be used directly to obtain the induced angle of attack due to this distribution. This restriction is removed by the following analytical approach.

The distribution  $C_{d_1} c/b$  can also be divided into two portions, thus

$$\left(\frac{C_{d_1} c}{b}\right) = \left(\frac{C_{d_1}^I c}{b}\right) + \delta \left(\frac{C_{d_1}^{II} c}{b \delta}\right) \quad (77)$$

where  $C_{d_1}^{II} c/b \delta$  is the lift distribution due to a unit

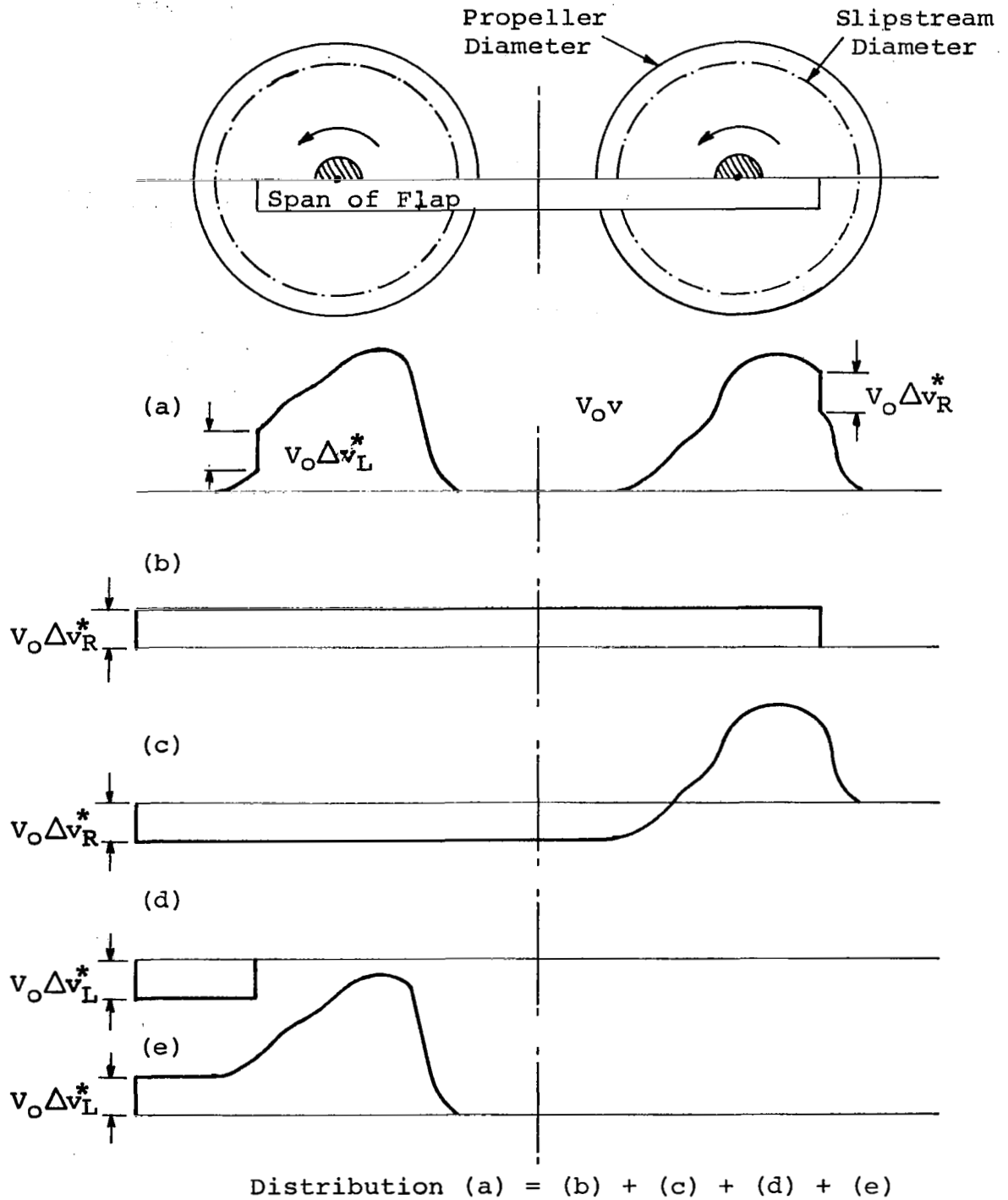


Figure 6. Method for Superposition of Solutions

discontinuity  $\delta$ , and  $C_{d1} c/b$ , is the remainder.

Applying the multipliers  $\beta_{mk}$  to equation (77) yields the following

$$\sum_{m=1}^{r-1} \left( \frac{C_{d1} c}{b} \right)_m \beta_{mk} = \sum_{m=1}^{r-1} \left( \frac{C_{d1} c}{b} \right)_m \beta_{mk} + \sum_{m=1}^{r-1} \left( \frac{C_{d1}'' c}{b \delta} \right)_m \delta \beta_{mk} \quad (78)$$

Also, applying the multipliers  $\beta_{mk}$  to equation (63) yields the total lift distribution  $C_d c/b$  as

$$\sum_{m=1}^{r-1} \left( \frac{C_d c}{b} \right)_m \beta_{mk} = \sum_{m=1}^{r-1} \left( \frac{C_{d1} c}{b} \right)_m \beta_{mk} + \sum_{m=1}^{r-1} \left( \frac{C_{d2} c}{b} \right)_m \beta_{mk} \quad (79)$$

Substituting equation (78) into equation (79), yields

$$\sum_{m=1}^{r-1} \left( \frac{C_d c}{b} \right)_m \beta_{mk} = \sum_{m=1}^{r-1} \left( \frac{C_{d1} c}{b} \right)_m \beta_{mk} + \sum_{m=1}^{r-1} \left( \frac{C_{d1}'' c}{b \delta} \right)_m \delta \beta_{mk} + \sum_{m=1}^{r-1} \left( \frac{C_{d2} c}{b} \right)_m \beta_{mk} \quad (80)$$

In order to obtain the iterative solution to equation (80), it is now necessary to relate the lift distributions given in equations (63) and (77) to their corresponding induced angle of attack distributions. If  $\alpha_i$  is the induced angle of attack distribution corresponding to the total lift distribution

$C_d c/b$ , and  $\alpha_{i1}$  and  $\alpha_{i2}$  are the induced angle of attack distributions corresponding to the lift components  $C_{d1} c/b$  and  $C_{d2} c/b$ , then from equation (63) there follows

$$\alpha_i = \alpha_{i1} + \alpha_{i2} \quad (81)$$

Also, applying similar considerations to equation (77) there

results

$$\alpha_{i_1} = \alpha_{i_1}' + \alpha_{i_1}'' \quad (82)$$

Substituting equation (82) into equation (81) yields the relationship for the induced total angle of attack as follows:

$$\alpha_i = \alpha_{i_1}' + \alpha_{i_1}'' + \alpha_{i_2} \quad (83)$$

where  $\alpha_{i_1}'' = \delta$  over the flap span  
 0 outside the flap span

It can be noted in equation (83) that the induced angle of attack distribution  $\alpha_{i_1}'$  must be continuous, since its corresponding lift distribution  $C_{d_1}' c/b$  as given in equation (77) is continuous. Therefore, this induced angle of attack distribution is obtained directly using the multipliers, thus

$$\alpha_{i_1 k}' = \sum_{m=1}^{r-1} \left( \frac{C_{d_1} c}{b} \right)_m \beta_{mk} \quad (84)$$

The above relationship can be re-expressed in terms of the total induced angle of attack distribution  $\alpha_i$  by using equation (83), thus

$$\sum_{m=1}^{r-1} \left( \frac{C_{d_1} c}{b} \right)_m \beta_{mk} = \alpha_{i k} - \alpha_{i_1 k}'' - \alpha_{i_2 k} \quad (85)$$

Now, equation (85) can be substituted into equation (80) to eliminate the  $C_{d_1}' c/b$  distribution and to yield the total lift distribution  $C_{d_1} c/b$  in the desired multiplier form as follows

$$\sum_{m=1}^{r-1} \left( \frac{C_{l_1} c}{b} \right)_m \beta_{mk} = \alpha_{i_k} - \alpha_{i_{1k}}'' - \alpha_{i_{2k}} + \sum_{m=1}^{r-1} \left( \frac{C_{l_1}'' c}{b \delta} \right)_m \beta_{mk} + \sum_{m=1}^{r-1} \left( \frac{C_{l_2} c}{b} \right)_m \beta_{mk} \quad (86)$$

Finally, rearranging the equation (86), the total induced angle of attack at any point  $k$  on the wing can be related to the corresponding total lift distribution and the known distributions of induced angle of attack  $\alpha_{i_1}''$  and  $\alpha_{i_2}$  and their corresponding lift distributions  $C_{l_1}'' c/b$  and  $C_{l_2} c/b$ , respectively. The resulting relationship is

$$\alpha_{i_k} = \sum_{m=1}^{r-1} \left( \frac{C_{l_1} c}{b} \right)_m \beta_{mk} + \delta \left[ \frac{\alpha_{i_k}}{\delta} - \sum_{m=1}^{r-1} \left( \frac{C_{l_1}'' c}{b \delta} \right)_m \beta_{mk} \right] + \alpha_{i_{2k}} - \sum_{m=1}^{r-1} \left( \frac{C_{l_2} c}{b} \right)_m \beta_{mk} \quad (87)$$

where from the analysis of Reference 1

$$\left( \frac{C_{l_1}'' c}{b \delta} \right)_k = \frac{2}{\pi} \left[ (\cos \theta^* - \cos \theta_k) \log \left\{ \frac{1 - \cos (\theta_k + \theta^*)}{1 - \cos (\theta_k - \theta^*)} \right\} + 2 (\pi - \theta^*) \sin \theta_k \right] \quad (88)$$

and  $C_{l_2} c/b$  has been already determined in equation (76).

Equation (87) is analogous to equation (61) developed in subsection 3.2.1 for no flap deflection. This equation is also solved by an iteration procedure, similar to that used for solving equation (61). Thus, upon obtaining the required convergence of the iterative solution, equation (87) yields the total lift distribution  $C_{l_1} c/b$  for a wing with a deflected flap within the propeller slipstream.

### 3.2.3 Extension of the Wing Analysis to Small Aspect Ratios

To provide added flexibility to the methodology developed herein, the wing analysis treated in Sections 3.2.1 and 3.2.2 is extended to include wings of small aspect ratio. This analysis is particularly useful for the current application, since much of the available test data on spanwise loadings for wings in slipstream falls within the low aspect ratio range. The correlations of this extended analysis with the corresponding test data where appropriate is shown in Section 5.0.

The modification of the present analysis to small aspect ratio wings is based on the wing theory of Kuchemann (Reference 22), as outlined below.

In equations (61) and (87) a set of multipliers was used to obtain the induced angle of attack distributions for a wing with no flaps and with part-span deflected flaps, respectively. These multipliers were obtained from the fundamental equation of the high-aspect-ratio, lifting-line theory which expresses the induced angle of attack in terms of the span loading,

$$\alpha_i = \frac{b}{8\pi} \int_{-b/2}^{b/2} \frac{\frac{d(C_{l,c/b})}{dy_1} dy_1}{y_1 - y} \quad (89)$$

Kuchemann, Reference 22, has shown that this equation may be generalized to wings of any aspect ratio by writing

$$\alpha_i = \frac{\omega' b}{8\pi} \int_{-b/2}^{b/2} \frac{\frac{d(C_{l,c/b})}{dy_1} dy_1}{y_1 - y} \quad (90)$$

where  $\omega'$  is a factor which varies between 1 for high aspect ratio ( $AR \rightarrow \infty$ ), and 2 for low aspect ratio ( $AR \rightarrow 0$ ).

Kuchemann obtained the following equation for  $\omega'$

$$\omega' = 2 - \left[ 1 + \frac{4}{AR^2} \right]^{-1/4} \quad (91)$$

If the multipliers  $\beta_{mk}$  are rederived using equation (91), a new set of multipliers,  $\beta'_{mk}$ , is obtained related to the old set by

$$\beta'_{mk} = \omega' \beta_{mk} \quad (92)$$

This new set of multipliers  $\beta'_{mk}$  may then be used to calculate induced angle of attack throughout the entire aspect ratio range.

The second equation that must be modified is that which defines the edge-velocity factor E. In Reference 1, this quantity is given by

$$\begin{aligned} E &= \frac{a_e - a_o}{a_o - a_{d0}} \\ &= \sqrt{1 + \frac{4}{AR^2}} \\ &= \frac{a_o}{a} \end{aligned} \quad (93)$$

where  $a_o$  is the two-dimensional lift curve slope ( $AR \rightarrow \infty$ ) and  $a$  is the corresponding value for finite aspect ratio.

Reference 22 presents an expression for the ratio of the lift curve slopes as

$$\frac{a_o}{a} = \frac{2 - \pi \omega' \cot\left(\frac{\pi \omega'}{2}\right)}{2 \omega'} \quad (94)$$

where  $\omega'$  is given by equation (91).



Thus, substituting equation (94) into equation (93) yields the edge-velocity factor E. applicable to all values of aspect ratio as

$$E = \frac{2 - \pi \omega' \cot\left(\frac{\pi \omega'}{2}\right)}{2 \omega'} \quad (95)$$

In the extended analysis equation (95) is used in place of equation (93).

Finally, the expression for the lift distribution associated with a discontinuity in induced angle of attack, as given by equation (88), must be modified in the following form

$$\left(\frac{C_{d1}'' c}{b \delta}\right) = \frac{2}{\pi \omega'} \left[ (\cos \theta^* - \cos \theta) \log \left\{ \frac{1 - \cos(\theta + \theta^*)}{1 - \cos(\theta - \theta^*)} \right\} + 2 (\pi - \theta^*) \sin \theta \right] \quad (96)$$

Equation (96) is now applicable to any value of aspect ratio. This equation is implemented in the computer program and extends the program capabilities to wings with low and high aspect ratios ranging from about 2.0 to infinity.

## SECTION 4

### DIGITAL COMPUTER PROGRAM

The theoretical analysis presented in Section 3 was programmed for use on the CDC 6600 series digital computer. This was accomplished by extensively modifying the computer program of Reference 1 to include the propeller slipstream and the wing in-slipstream analysis.

This section presents a description of the combined computer program logic, the selection and assembly of the pertinent airfoil section characteristics, and a sample computer output. Wherever appropriate, the discussion is directed towards those features of the modified program that are directly relevant to the treatment of the propeller slipstream and its effect on the wing spanwise loading. Additional information pertaining to computations of the wing loading for a basic wing/fuselage combination can be obtained from Reference 1.

#### 4.1 PROPELLER SLIPSTREAM COMPUTATIONS

This subsection presents the methodology and the associated airfoil section data used in computations of the propeller slipstream velocity distributions, which are later implemented in the overall solution for the wing spanwise loading of a general wing/propeller combination. The basic computational steps for implementing the slipstream velocity distributions into the wing analysis are summarized in subsection 4.2

The essential steps in the propeller slipstream solution are given below.

##### 4.1.1 Computational Procedures for Propeller Slipstream Velocity Distributions

(a) Calculate the propeller angle of attack and tip speed ratio from

$$\alpha_p = \alpha_B + i_{TL} \quad (97)$$

$$\mu_T = \frac{J \cos \alpha_p}{\pi} \quad (98)$$

(b) At each selected station on the propeller blade obtain local values of the solidity, blade speed ratio and inflow angle  $\phi_0$  from

$$\sigma = \frac{B \bar{c}_p}{2 \pi \bar{r}} \quad (99)$$

$$\mu = \frac{J \cos \alpha_p}{\pi \bar{r}} \quad (100)$$

$$\phi_0 = \tan^{-1} \mu \quad (101)$$

(c) obtain an approximate solution for the tip loss factor using

$$F_p = \frac{2}{\pi} \cos^{-1} \left[ \exp \left\{ -\frac{B}{2} (1-\bar{r}) \sqrt{1 + \left(\frac{1}{\mu_T}\right)^2} \right\} \right] \quad (102)$$

(d) Calculate an initial value for the quantity  $(u^*/\Omega r)$  from

$$\frac{u^*}{\Omega r} = \frac{1}{2} \left[ \sqrt{(\mu+k)^2 + 4k (\beta - \phi_0 - \alpha_{l_0})} - (\mu+k) \right] \quad (103)$$

where, by definition

$$k = \frac{\sigma \alpha_0}{4 F_p} \sqrt{1 + \mu^2} \quad (104)$$

and  $\alpha_0, \alpha_{l0}$  are the lift-curve slope and angle of attack at zero lift, respectively, for a linearized approximation to the tabulated airfoil section characteristics.

(e) Compute an initial inflow angle at each blade element station from

$$\phi' = \phi_0 + \frac{u^*}{\Omega r} \quad (105)$$

(f) Obtain an initial value for the quantity defined as

$$k_x = \frac{\left(\frac{u^*}{\Omega r}\right) \tan \phi'}{1 - \left(\frac{u^*}{\Omega r}\right) \tan \phi'} \quad (106)$$

(g) As the first step in the basic iteration routine, calculate a better approximation for the tip loss factor from

$$F = \left(\frac{F}{F_p}\right) \frac{2}{\pi} \cos^{-1} \left[ \exp \left\{ -\frac{B}{2} (1-\bar{r}) \sqrt{1 + \left(\frac{1}{\bar{r} \tan \phi'}\right)^2} \right\} \right] \quad (107)$$

where  $F/F_p$  is obtained by interpolating the results from the tip loss correction tables for specified values of  $B, \bar{r}$  and  $\sin \phi'$ . A listing of the tip loss correction tables stored and utilized by the computer program is presented in Appendix A.

(h) Calculate the blade section angle of attack and the blade section Mach number from

$$\begin{aligned} \alpha_b &= \beta - \phi' \\ M_v &= \frac{M_0 \pi \bar{r}}{J (1+k_x) \cos \alpha_p} \end{aligned} \quad (108)$$

Then obtain the section characteristics  $C_{dl}$  and  $C_d$  by interpolation and/or extrapolation of the data presented in the propeller airfoil tables, for the specified airfoil section geometry and values of  $\alpha_b$  and  $M_v$ .

(i) Compute the following quantities defined as

$$k_x = \frac{\sigma}{4F} \left[ \frac{C_{dl}}{\cos \phi'} + \frac{C_d}{\sin \phi'} \right] \quad (109)$$

$$k_y = \frac{\sigma}{4F} \left[ \frac{C_{dl}}{\sin \phi'} - \frac{C_d}{\cos \phi'} \right] \quad (110)$$

$$k_z = \mu (1 + k_x) + k_y \quad (111)$$

and then calculate a new value of  $\phi$  from

$$\phi'' = \tan^{-1} k_z \quad (112)$$

(j) If the absolute magnitude of  $(\phi'' - \phi') > 0.1$  degrees, then the solution for  $\phi$  requires reiteration. In this case the value of  $\phi$  to be substituted for  $\phi'$  in steps (g) through (i) is obtained from

$$\phi = \phi' + (\phi'' - \phi') \frac{1}{k_c} \quad (113)$$

where  $k_c$  is given by

$$k_c = 1 + \cos^2 \phi'' \left[ \mu k_x \left\{ \frac{a_0}{C_d} - \tan \phi' \right\} + k_y \left\{ \frac{a_0}{C_d} + \cot \phi' \right\} \right] \quad (114)$$

(k) If the absolute magnitude of  $(\phi'' - \phi') \leq 0.1$  degrees then the final slipstream velocity components for the streamtube element passing through the specified blade element station are determined as follows. First, calculate the true induced axial velocity ratio in the propeller disk plane using

$$\frac{u}{\Omega r} = \frac{1}{2} \left[ \sqrt{\mu^2 + \frac{4 F k_y k_z}{(1 + k_x)^2}} - \mu \right] \quad (115)$$

and then obtain the axial velocity ratio in the fully contracted slipstream from

$$\frac{V_{s_a}}{V} = 1 + \frac{2}{\mu} \left( \frac{u}{\Omega r} \right) \quad (116)$$

(l) Obtain the local radius in the fully contracted slipstream which corresponds to the specified blade element station from

$$\bar{r}_s = \left[ \bar{r}_{sp}^2 + (\bar{r}^2 - \bar{r}_p^2) \left( \frac{1}{2} + \frac{V_a}{V_{s_a} + V_{s_{ap}}} \right) \right] \quad (117)$$

where  $\bar{r}_{sp}$ ,  $\bar{r}_p$  and  $V_{s_{ap}}/V_a$  are the values corresponding to the immediately preceding inboard blade element station. The velocity ratio at the outer slipstream boundary is taken as unity, as is that at the hub/nacelle boundary unless a blade element station is specified at the hub.

(m) Compute the tangential velocity ratio in the fully contracted slipstream as

$$\frac{V_{st}}{V_a} = \frac{2}{\mu} \left( \frac{u}{\Omega r} \right) \frac{k_x \bar{r}}{k_y \bar{r}_s} \quad (118)$$

(n) Having obtained solutions for the flow corresponding to all propeller blade element stations  $m=1$  (at the hub) through  $m=M$  (at the blade tip), calculate the value of the integrated propeller thrust coefficient from

$$C_T = \sum_{m=2}^M \frac{1}{2} \left[ \left( \frac{d C_T}{d \bar{r}} \right)_m + \left( \frac{d C_T}{d \bar{r}} \right)_{m-1} \right] \left[ r_m - r_{m-1} \right] \quad (119)$$

where

$$\frac{d C_T}{d \bar{r}} = \left( \pi \bar{r} \right)^3 \frac{F k_y k_z}{(1 + k_x)^2} \quad (120)$$

(o) Obtain the momentum value of propeller thrust coefficient from

$$C_{TS} = \left[ \frac{1}{1 + \frac{\pi^3 \mu r^2}{8 C_T}} \right] \quad (121)$$

(p) Compute the integrated propeller torque coefficient using

$$C_Q = \sum_{m=2}^M \frac{1}{2} \left[ \left( \frac{d C_Q}{d \bar{r}} \right)_m + \left( \frac{d C_Q}{d \bar{r}} \right)_{m-1} \right] \left[ r_m - r_{m-1} \right] \quad (122)$$

where 
$$\frac{dC_Q}{d\bar{r}} = (\pi \bar{r})^3 \frac{r F k_x k_z}{2 (1+k_x)^2} \quad (123)$$

(q) Calculate the value of the momentum-weighted average axial velocity ratio in the fully contracted slipstream from

$$\frac{\bar{V}_{s0}}{V_0} = \sqrt{1 + \frac{8 C_T}{\pi^3 \mu_T^2}} \quad (124)$$

#### 4.1.2 Propeller Blade Section Characteristics

The analytical methods developed herein require that suitable aerodynamic characteristics be employed for the blade sections of propellers used on general aviation-type aircraft. The information on typical blade sections was obtained from the available technical literature and is summarized in Table I.

As can be noted from this table, early blade sections used in typical propellers are of the USNPS and Clark Y airfoil series. These sections have very similar profiles and members of each series are uniquely identified by the value of thickness/chord ratio alone.

Later blade sections are of the NACA 16-series family, which have a wider application in modern propeller design because of their superior low-drag characteristics (see Reference 25). These considerations also apply to the use of NACA 64 and 65 airfoil series. All of the latter airfoils are specified in terms of both a design lift coefficient and a thickness/chord ratio.

Based on a review of published experimental measurements of propeller airfoil section characteristics, it is evident that the most reliable data for the current application can be obtained from tests conducted in three wind tunnel



Table I. Typical Propeller Blade Sections.

Airfoil Series	Design Lift Coefficients	Thickness/Chord Ratios	References
USNPS	-	0.05 to 0.35	29
Clark Y	-	0.07 to 0.50	17,30,31
NACA 16XXX	0.2 to 0.7	0.04 to 0.40	17,30,32,33,34
NACA 64-XXX	0 to 0.2	0.07 to 0.26	35
NACA 65-XXX	0 to 0.2	0.04 to 0.40	35,36

facilities only. These are the Langley Low Turbulence Pressure Tunnel (Reference 26), for section data at low speed conditions ( $M \approx 0.15$ ), and both the Langley and Ames High Speed Wind Tunnels (References 27 and 28, respectively) for section data at high speeds ( $0.3 \leq M \leq 0.85$ ). Experimental data available from tests in these facilities were therefore used as the basis for preparation of the required section characteristics for all selected airfoils with the exception of the USNPS and Clark Y series. The section data for the latter two airfoils was generated from the measurements obtained in the Langley Variable-Density Tunnel.

Application of the present analytical methods requires information on the two-dimensional behavior of both lift and drag for the specified blade airfoils. However, an important simplification in preparing these airfoil characteristics is realized through the use of a constant value for drag coefficient on the basis of the following approximation.

From the propeller analysis it can be noted that the contributions of the blade section drag coefficient  $C_d$  to the axial and swirl velocity components in the slipstream are given, approximately, by  $(C_d/C_l) \tan \phi$  and  $(C_d/C_l) \cot \phi$  respectively, where  $\phi$  is the inflow angle. For low speed flight conditions appropriate to general aviation type aircraft, the contributions of blade section drag to the local axial velocity component in the slipstream are found to be negligible, whereas the contributions to the local swirl velocity are typically not more than a few percent. Thus it is considered a justifiable simplification in the computer program to substitute a representative constant value for  $C_d$  in place of the actual variations as a function of angle of attack and Mach number.

It is thus evident that realistic application of the propeller-slipstream analysis demands that selected data on blade section lift characteristics be accurately defined as a function of local angle-of-attack and Mach number for those typical airfoil sections identified above.

Table II summarizes the airfoil sections for which aerodynamic characteristics have been obtained and identifies the source references. In general it is apparent that insufficient data exist to enable a thorough coverage of all the possible variations in section geometry, angle-of-attack and

Table II. Summary of Propeller Airfoil Sections  
 Tabulated for Use in the Computer Program.

Airfoil Series	Thickness/Chord Ratios in Percent										Mach No. Range	Source References
USNPS	4	6	8	10	12	14	16	18	20		0.07	37
Clark Y	6	8	10	11.7	14	18	22				0.07	38
NACA 161XX	6	9	-	15	-	30					0.3 to 0.8	39
163XX	6	9	12	15	21	-						
165XX	6	9	12	15	21	30						
167XX	-	9	12	15	-	-						
NACA 64-0XX	6	9	12	15	18	21					0.15	40,41
64-2XX	6	9	12	15	18	21						
64-4XX	-	9	12	15	18	21						
NACA 65-0XX	6	9	12	15	18	21					0.15	40
65-2XX	6	9	12	15	18	21						
65-4XX	-	10	12	15	18	21						

Mach number range. Accordingly a number of simple empirical techniques have been developed to permit a reasonable extrapolation of the available data, as will be discussed later in the text.

Furthermore, in preparation of the final section characteristics, faired curves of the experimental  $C_d$  versus  $\alpha$  were utilized. The data was carefully selected so as to best define the non-linearities in the faired curves. In general the data represents the full range of the experimental measurements extending from the zero lift condition to a point close to stall and in most cases through the stall.

A complete computer listing of the tabulated section characteristics for the propeller airfoils listed in Table II, is presented in Appendix B. The airfoil tables are arranged so as to provide the maximum flexibility in their use in the computer program. These tables can be easily extended or deleted to include other airfoil families or specially modified aerodynamic characteristics of the selected sections.

These tables form the basis for look-up procedures which through interpolation and extrapolation of the stored data provide the required values of  $C_d$  for specified blade sections. These table look-up procedures are described in detail in the next subsection.

#### 4.1.3 Table Look-Up Procedures for Propeller Airfoil Characteristics

The propeller airfoil data tables are read in and stored by the computer immediately prior to execution of the propeller-slipstream calculations. The computer program provides data tables for up to 9 airfoil families, identified by an airfoil series code between 1 and 9 inclusive, but is capable of accepting a maximum of 150 tables. This storage capacity is considered more than adequate under most circumstances but could be extended, if required, by an internal program change. As a rule the only tables read in will be those sets corresponding to the blade sections of the propeller-wing configuration being evaluated.

Each table, as it is read in by the computer, is indexed consecutively in order to permit efficient operation of the look-up procedure. For proper utilization of these

data tables, it is essential that they be assembled in a special order. The assembly of all tables for each given airfoil family must be in ascending order of Mach number, thickness/chord ratio and design lift coefficient. However, the sets of tables for any airfoil family may be assembled in any order.

As an initial step in the table look-up procedure, the computer program first searches through the tables to locate and index those particular tables required for interpolation as each propeller blade element station is specified. The actual look-up procedure utilizes linear interpolation throughout and is performed first for the required value of  $\alpha$ , secondly for the value of Mach number, thirdly for the section thickness/chord ratio and finally for the design lift coefficient of the airfoil family specified.

To permit satisfactory operation of the computer program for conditions outside the range of the data tables a series of simple extrapolation procedures have been developed empirically from the available experimental data. These procedures are outlined below.

For angles of attack outside the tabulated range in each table it is assumed that the value of  $C_d$  remains constant, and for a Mach number outside the given range the extrapolation procedure determines a correction to the required value of  $\alpha$ , defined as  $\alpha_c$ , thus

$$\alpha_c = \alpha_{0T} + (\alpha - \alpha_{0T}) \sqrt{\frac{1 - M_T^2}{1 - M^2}} \quad (125)$$

where the subscript T denotes values for the table to be extrapolated.

This method is based on an application of the standard Prandtl-Glauert rule for the change in lift-curve slope with Mach number and assumes that the extrapolated family of lift curves can be represented by a simple adjustment of the angle of attack scale about  $\alpha_0$  point.

For section thickness/chord ratios outside the given range of tables at each value of design lift coefficient it is assumed that the airfoil characteristics will be invariant. While this assumption does not satisfactorily represent the

general reduction in lift-curve slope for thick sections ( $t/c \geq 0.2$ ) the existing data does not provide a base for a better approximation.

For a section design lift coefficient  $C_{d_i}$  outside the tabulated range, an extrapolation procedure is used to obtain a corrected value of  $C_d$  defined as  $C_{d_c}$ , thus

$$C_{d_c} = C_{d_T} + (C_{d_i} - C_{d_{iT}}) \sqrt{\frac{k_{C_{d_i}}}{1-M^2}} \quad (126)$$

where the subscript T denotes values for the table to be extrapolated and  $k_{C_{d_i}}$  is an empirical constant which generally varies for each airfoil family and thickness/chord ratio. This constant has been determined for each airfoil family used herein, and constitutes an inherent part of the computer program table look-up subroutine.

## 4.2 WING IN-SLIPSTREAM COMPUTATIONS

This subsection presents the method of implementation of the propeller slipstream distributions obtained above into the spanwise load calculations of a propeller/wing combination. The essential computational steps are described below.

### 4.2.1 Computational Procedures for Spanwise Loading on a Wing with no Flaps, or with Full-Span Deflected Flaps

(a) Obtain the wing basic geometric parameters namely, section chord ratio  $c/c_R$ , twist distribution  $\epsilon$ , thickness-chord ratio  $t/c$ , and camber distribution. Then calculate the wing section Reynolds number  $Re$  based on the local chord  $c$  and the local resultant velocity  $V$ , thus

$$Re = \frac{V c}{\nu} \quad (127)$$

where  $V$  is the combined freestream and slipstream velocity given in equation (3) and  $\nu$  is the kinematic viscosity. Also, obtain the section zero-lift angle  $\alpha_{d_0}$ .

(b) Compute the wing-induced upwash function,  $f$ ,

from the following equation which is based on a simple horse-shoe model of the wake (Reference 19)

$$f = \frac{\left(\frac{\pi}{4} - \bar{y}_p\right) \frac{1}{\bar{x}_p}}{\sqrt{\left(\frac{\pi}{4} - \bar{y}_p\right)^2 + \bar{x}_p^2}} + \frac{\left(\frac{\pi}{4} + \bar{y}_p\right) \frac{1}{\bar{x}_p}}{\sqrt{\left(\frac{\pi}{4} + \bar{y}_p\right)^2 + \bar{x}_p^2}} - \frac{\sqrt{\left(\frac{\pi}{4} + \bar{y}_p\right)^2 + \bar{x}_p^2} - \bar{x}_p}{\left(\frac{\pi}{4} + \bar{y}_p\right) \sqrt{\left(\frac{\pi}{4} + \bar{y}_p\right)^2 + \bar{x}_p^2}} - \frac{\sqrt{\left(\frac{\pi}{4} - \bar{y}_p\right)^2 + \bar{x}_p^2} - \bar{x}_p}{\left(\frac{\pi}{4} - \bar{y}_p\right) \sqrt{\left(\frac{\pi}{4} - \bar{y}_p\right)^2 + \bar{x}_p^2}} \quad (128)$$

where  $\bar{y}_p = 2y_p/b$  and  $\bar{x}_p = 2x_p/b$

are the non-dimensional spanwise and chordwise locations of the right-hand propeller hub.

(c) Calculate the geometric angle of attack at each wing station from

$$\alpha_g = \alpha_B + \alpha_R + \epsilon + \Delta\epsilon_N + \alpha_B T \left[ \frac{R}{d_u} \frac{d\bar{u}}{d\bar{u}} - 1 \right] \quad (129)$$

where  $\alpha_B$  is the fuselage angle of attack  
 $\alpha_R$  is the wing/fuselage root setting  
 $\epsilon$  is the local geometric twist

$T \left[ \frac{R}{d_u} \frac{d\bar{u}}{d\bar{u}} - 1 \right]$  is the correction factor for fuselage upwash given in Reference (1) and  $\Delta\epsilon_N$  is the setting of the equivalent chord line of the nacelle above the wing chord line at the nacelle station. The quantity  $\Delta\epsilon_N$  is only to be included when a computation station coincides with the nacelle location.

(d) Calculate the following initial approximation to the overall wing lift coefficient

$$C_{L\_APPROX} = \frac{1}{\left(1 + \frac{1.82}{AR}\right)} \left( \alpha_B + \alpha_R - 0.4 \alpha_{d_o\_TIP} - 0.6 \alpha_{d_o\_ROOT} \right) \quad (130)$$

(e) Compute the wing-induced upwash at the propeller disc using equation (128) as follows:

$$V_w = \frac{C_L \text{ APPROX. } f}{\pi^2 AR} \quad (131)$$

(f) Calculate the propeller thrust-line angle of attack and average inclination of the propeller slipstream to the freestream from

$$\alpha_p = \alpha_B + i_{TL} \quad (132)$$

$$\alpha_s = \tan^{-1} \left\{ \frac{V_0 \sin \alpha_p + V_w}{V_{sa}} \right\} \quad (133)$$

where  $i_{TL}$  is the propeller thrust-line angle relative to the fuselage centerline.

(g) At each wing station calculate the effective angles of attack, the resultant local slipstream velocity,  $V$ , and the non-dimensional slipstream upwash,  $v$ , from the following equations:

$$\alpha_e = \alpha_g - \alpha_{\ell_0} \quad (134)$$

$$V = V_{sa} / \cos (\alpha_p + \alpha_s) \quad (135)$$

$$v = \left( \frac{V_{sa}}{V_0} \right) \sin (\alpha_s + \alpha_e) + \left( \frac{V_{st}}{V_0} \right) \cos (\alpha_s + \alpha_e) - \sin \alpha_e \quad (136)$$

(h) Calculate the distribution of lift due to slipstream upwash  $Cd_2 c/b$  using equation (56).

(i) Using the effective angles of attack,  $\alpha_e$ , computed from equation (134) find the values of section lift coefficient,  $C_{\ell}$ , from the two-dimensional section data at the proper values of Reynolds number, thickness-chord ratio and camber level.



(j) Calculate an initial approximation to the spanwise loading distribution using

$$\frac{C_{d\ c}}{b} = C_{d\ c} \left( \frac{AR}{AR+1.8} \right) \left( \frac{c}{c_R} \right) \left( \frac{c_R}{b} \right) \left[ \frac{1}{2} + (1+\lambda) \sqrt{1 - \left( \frac{2y}{b} \right)^2} \right] \quad (137)$$

where  $\lambda$  is the wing taper ratio.

(k) Compute the values of induced angle of attack for this load distribution using equation (61) and determine the resultant section angles of attack from equation (62).

(l) From the section data obtain the values of lift coefficient corresponding to the resultant angles of attack from step (k) and calculate the new values of the span loading,  $C_{d\ c}/b$ .

(m) Compare the approximate values of span loading with the calculated values. If these are not in sufficiently close agreement, compute a new set of approximate values of  $C_{d\ c}/b$  using the procedures presented in subsection 3.2.2 of Reference 1. Repeat the iteration process until the required convergence is achieved.

(n) Integrate the new span load distribution to obtain the overall wing lift coefficient  $C_L$  and calculate a new value of wing-induced upwash at the propeller disc using equations (128) and (131).

(o) Repeat steps (f), (g), (h), (i), (k), (l), (m), (n) until the approximate and calculated values of span loading are in satisfactory agreement.

(p) Having determined the lift distribution obtain the section profile drag and pitching moment values from the section data and calculate the overall wing lift, drag, and pitching moment coefficients.

#### 4.2.2 Computational Procedures for Spanwise Loading on a Wing with Part-Span Deflected Flaps

(a) Calculate an initial approximation to the flapped wing lift distribution from the following equations

$$\begin{aligned} \frac{C_{dc}}{b} &= \frac{1}{2} C_{dR} \left(\frac{c}{c_R}\right) \left(\frac{c_R}{b}\right) \left\{ 1 + \sqrt{1 - \left(\frac{y}{y^*}\right)^2} \right\} \quad 0 \leq y \leq y^* \quad (138) \\ &= \frac{1}{2} C_{dR} \left(\frac{c}{c_R}\right) \left(\frac{c_R}{b}\right) \left\{ 1 - \sqrt{1 - \left(\frac{1-y}{1-y^*}\right)^2} \right\} \quad y^* \leq y \leq \frac{b}{2} \end{aligned}$$

where  $C_{dR}$  is the value of the lift coefficient at the root obtained from the flapped section data at the angle of attack

$$a = a_B + a_R \quad (139)$$

(b) Determine the uncorrected values of lift coefficient  $C_{du}^*$  at each flap end as follows

$$C_{du}^* = \frac{C_{dc}}{b} \left(\frac{b}{c}\right) \frac{1}{FF} \quad (140)$$

where FF is the correction factor which accounts for the change in the two-dimensional section data at the flap end. The calculation procedure for obtaining these correction factors is described in detail in subsection 4.1.3 of Reference 1, and will not be duplicated here.

(c) For the values of  $C_{du}^*$  obtained in step (b) above obtain the corresponding angles of attack  $a_0$  from the data for flapped sections. Calculate the corresponding corrected angles of attack  $a_{c\delta}$  at each end of the flap from

$$a_{c\delta} = E \cdot FF (a_0 - a_{d0}) + a_{d0} \quad (141)$$

(d) Using the same procedure as in step (c) above, calculate the values of angle of attack  $a_{c\delta=0}$  on the unflapped sides of the wing. Then obtain the first approximation for the values of the discontinuities in angle of attack  $\delta$ , thus

$$\delta = a_{c\delta=0} - a_{c\delta} \quad (142)$$

(e) Integrate the lift distribution given by equation (138) to obtain an approximate value of the overall flapped lift coefficient,  $C_L$ , and using equation (3), determine the wing-induced upwash at the propeller disc. Then calculate the value of slipstream inclination,  $\alpha_s$ , using equation (5).

(f) Using the values of  $\delta$  and  $\alpha_s$  from steps (d) and (e), respectively, calculate the distribution of slipstream crossflow from the following equation:

$$v = \left(\frac{V_{sa}}{V_0}\right) \sin(\alpha_s + \alpha_e) + \left(\frac{V_{st}}{V_0}\right) \cos(\alpha_s + \alpha_e) - \sin \alpha_e \quad (143)$$

and use equations (64) and (65) to determine the discontinuities in crossflow  $\Delta v^* = v''$ .

NOTE: In the most general case of a wing having two propellers, (one mounted on each wing panel), rotating in the same direction, the slipstream-induced crossflow distribution will be different at the same spanwise station  $y$  on each side of the fuselage centerline. This difference is caused by upward slipstream swirl velocities on one wing panel and downward on the other, occurring at the same spanwise stations on each side of the fuselage, i.e.  $v(y) \neq v(-y)$ . In the case of two propellers rotating in opposite directions, each slipstream-induced crossflow is symmetrical about the fuselage centerline and equation (143) need only be applied once, since  $v(y) = v(-y)$ .

(g) Using the appropriate values of the discontinuities  $\delta$  and  $\Delta v^* = v''$  from steps (d) and (f), respectively, compute the lift distribution  $C_{d2} \cdot c/b$  using equation (76).

NOTE: For the most general case, as discussed in step (f) above, this lift distribution must be calculated separately for each wing panel.

(h) Determine the lift distribution  $C_{d1}'' \cdot c/b$ , corresponding to the left and right spanwise discontinuities from equation (88).

(i) Calculate the overall induced angle-of-attack distribution  $\alpha_i$  from equation (87), using the approximate span load distribution computed in step (a) above.

(j) Compute the effective resultant section angle of distribution from the following equation

$$\alpha_e = \frac{\alpha_g - \alpha_i + \alpha_{i_e} - \alpha_{d_0} \left( 1 - E \frac{C_{d_{max}}}{(C_{d_{max}})_o} \right)}{E \frac{C_{d_{max}}}{(C_{d_{max}})_o}} \quad (144)$$

where  $\alpha_g$  is the geometric angle of attack,  $C_{d_{max}}$  is the value of  $C_{d_{max}}$  obtained from the corrected section data and  $(C_{d_{max}})_o$  is the uncorrected value of  $C_{d_{max}}$ .

(k) Using the values of  $\alpha_e$  from step (j) above, obtain the corresponding values of lift coefficient  $C_{d_0}$  from the uncorrected two-dimensional section lift data. Then determine the correct values of lift coefficient  $C_d$  by scaling, as follows:

$$C_d = C_{d_0} \frac{C_{d_{max}}}{(C_{d_{max}})_o} \quad (145)$$

(l) Calculate the distribution  $C_d c/b$  from (145) and compare this calculated distribution with the approximate distribution. If agreement between the distributions is not sufficiently close, calculate a new and better approximation using the procedures presented in subsection 3.2.2 of Reference 1.

(m) Repeat steps (b) through (l) above, until agreement is reached between the approximate and calculated values of the span load distribution.

(n) Having determined the lift distribution in step (m), calculate the corresponding value of the overall integrated wing lift coefficient  $C_L$ .

### 4.2.3 Wing Section Characteristics

The wing airfoil section characteristics for typical general aviation aircraft are presented in Section 4.2 of Reference 1, and will not be duplicated in this report. These characteristics are used directly in the current computer program and constitute a part of the overall tool for prediction of stalling characteristics of general wing/propeller combinations.

### 4.2.4 Table Look-Up Procedures for Wing Section Characteristics

The table look-up subroutine for wing section characteristics used in the current program is identical to that described in Section 4.2 of Reference 1.

## 4.3 DESCRIPTION OF THE COMPUTER PROGRAM LOGIC

The computational procedures described in Section 3.0 have been programmed for use on a CDC 6600 series digital computer. The program user instructions are given in Appendix C. The flow diagram for the program is shown in Figure 7 and a listing of the program is presented in Appendix D. The program was accomplished by an extensive restructuring and enlargement of the basic power-off wing stall analysis program contained in Reference 1.

The program is initiated by reading in the basic wing-fuselage configuration parameters. In this input format, provision has been made to include an increment representing the drag coefficient of the nacelles. If the calculations are to be performed for the power-on case this is indicated to the program by setting the parameter NSLIP equal to 1. If NSLIP=0, the slipstream calculation loops are bypassed and the program only computes the power-off characteristics.

The computer program arrays are dimensioned to enable calculations of the span loading to be made using 10 control points per semispan.

For twin propeller aircraft computations where the propellers are situated near the center of each wing panel or

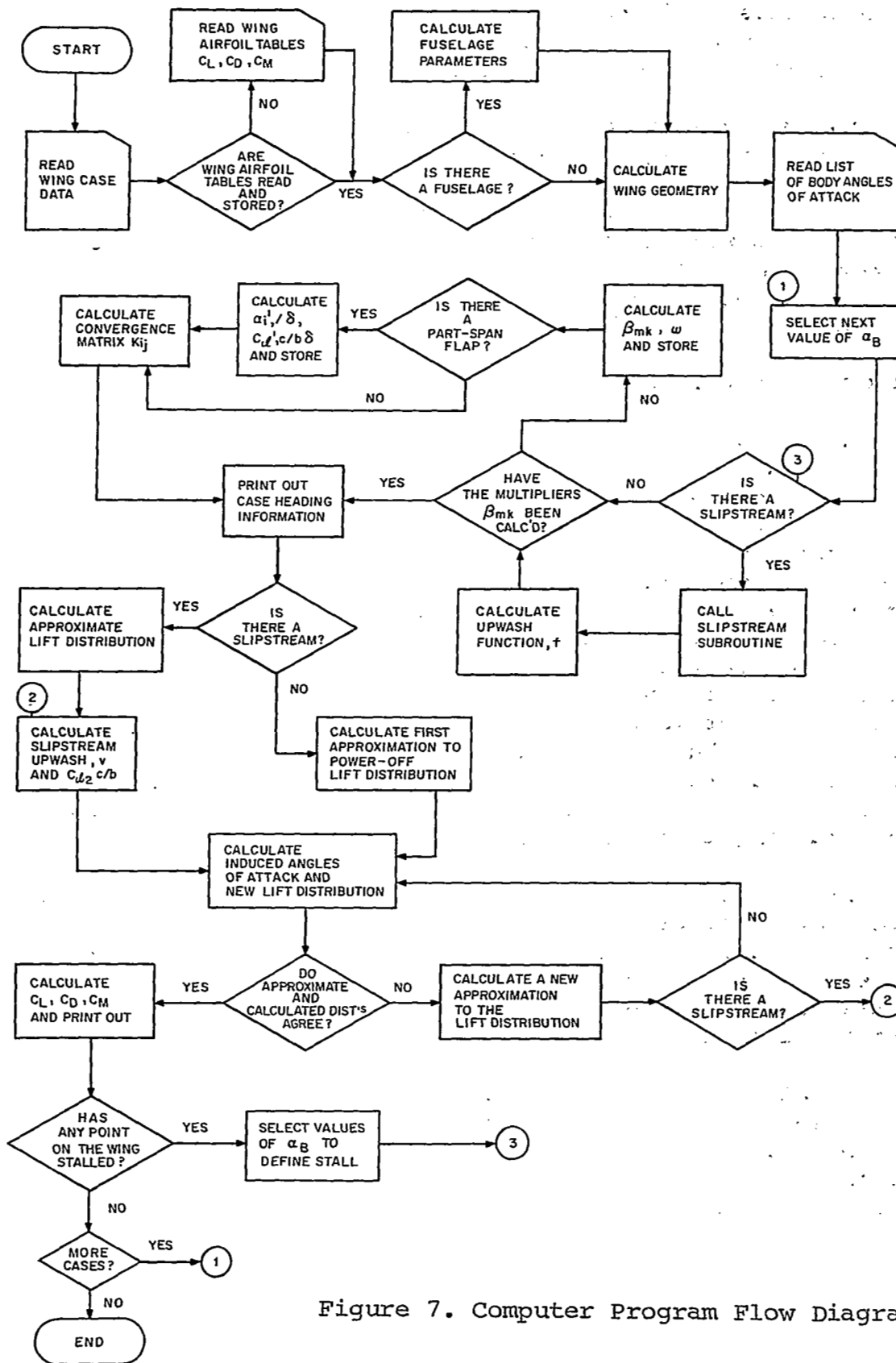


Figure 7. Computer Program Flow Diagram

at the wing tips, this number of wing control stations is adequate. However, for single propeller configurations, a better definition of the span loading in the slipstream region is obtained if the number of control stations is doubled to 20 per semispan. This is readily achieved by redimensioning the required arrays.

Having input the basic data, the required wing section data tables are read in and stored on tape. If the case is for a wing with fuselage the required transformation parameters are computed. The list of fuselage angles of attack is now read in and the first value in the list is selected. If the computation is to be performed for a power-on case the propeller slipstream subroutine is then called.

Execution of the slipstream subroutine shown in Figure 8 is initiated with input and storage at the propeller tip loss correction factor tables. This is followed by reading and storing the required blade section data tables, together with the data specifying the basic propeller geometry and operating condition. The program then proceeds with the main computations as the parameters for each successive blade element are read in. For each blade station, the solution for blade section angle of attack and lift is iterated to convergence. The velocity components for the corresponding streamtube element in the contracted slipstream are then computed. Finally, having obtained the complete velocity distribution for the slipstream, the slipstream velocities at the wing control stations are determined by interpolation before returning to the main program logic.

Having calculated the slipstream velocity distributions the wing upwash function and the induced angle-of-attack multipliers are now computed. If a part span deflected flap is present the parameters associated with the spanwise discontinuities are calculated together with the factors used to correct the two-dimensional section data.

The matrix of coefficients  $K_{ij}$  used in the iteration procedure is now computed and stored. If the calculations are to include slipstream effects, the slipstream inclination to the freestream, the slipstream upwash function,  $v$ , and the loading associated with this upwash function,  $Cd_2 c/b$ , are computed.

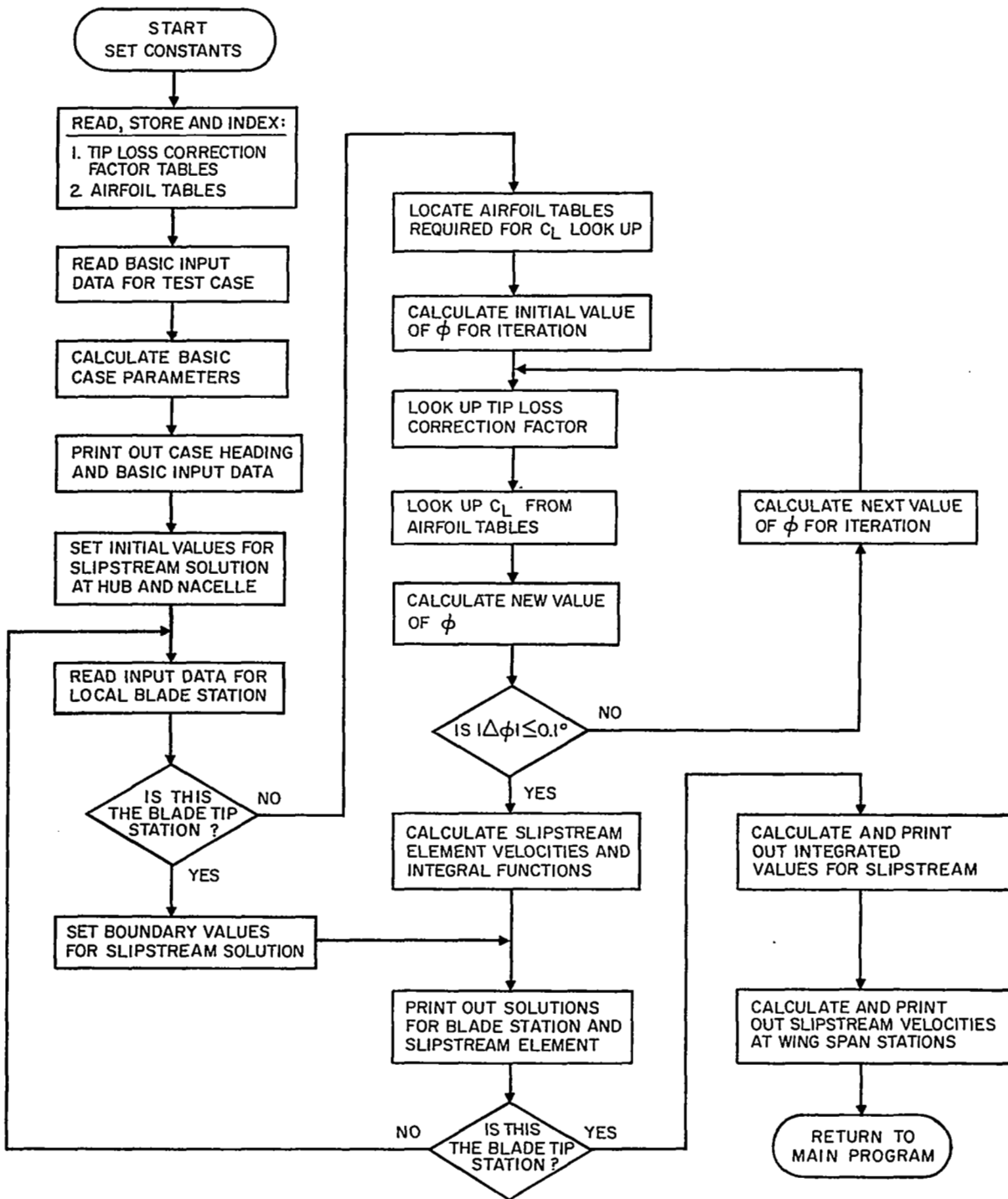


Figure 8. Logic Diagram for Propeller Slipstream Subroutine



The central program iteration loop is now entered. A new lift distribution is computed and compared to an approximate input value. If convergence is not achieved a new and better approximate value is computed. If slipstream effects are being considered, this new lift distribution is used to recalculate the upwash at the propeller discs and a modified slipstream inclination is obtained. A new upwash distribution is calculated and the basic iteration loop reentered.

Once convergence is obtained, the program computes and prints out the overall wing integrated values of  $C_L$ ,  $C_D$ , etc. together with the distributions. If stall is detected at any wing station, the program enters a routine to select values of fuselage angle of attack that will define the exact stall angle more closely.

#### 4.4 SAMPLE OUTPUT

A typical output obtained from the computer program, as described above, is presented in Tables III and IV. Table III shows sample computations for the spanwise lift distribution on a wing-in-slipstream, whereas Table IV presents a sample output for the slipstream velocity distribution used in the wing computations.

Table III - Sample Output for Lift Distribution on a Wing - In - Slipstream

LR 284 AR=3.04 WITH SS CT'=0.64

.....

BODY ANGLE OF ATTACK, DEG. . . . .	=	4.25	VALUE OF DISCRIMINANT. . . . .	=	0.001
BODY HEIGHT / SPAN . . . . .	=	0.00	BODY WIDTH / SPAN. . . . .	=	0.00
ASPECT RATIO . . . . .	=	3.04	WING HEIGHT / SPAN. . . . .	=	0.00
WING BODY INCIDENCE, DEG. . . . .	=	0.00	TIP THICKNESS CHORD. . . . .	=	0.15
ROOT THICKNESS CHORD . . . . .	=	0.15	GEOMETRIC TWIST, DEG. . . . .	=	0.00
NUMBER OF SPANWISE STATIONS. . . . .	=	20.00	AERODYNAMIC TWIST, DEG. . . . .	=	0.00
FLAP SPAN / WING SPAN. . . . .	=	0.00	TAPER RATIO. . . . .	=	1.00
FLAP SETTING, DEG. . . . .	=	0.00	REYNOLDS NUMBER. . . . .	=	0.63

COORDINATES OF MOMENT REFERENCE POINT X= 0.00 Z= 0.00

.....

3 ITERATIONS REQUIRED TO CONVERGE FOR ANGLE OF ATTACK EQUAL TO 4.25

SPANWISE STATIONS-2Y/B			
(.1)	0.987688E 00 ( 2)	0.951056E 00 ( 3)	0.891006E 00 ( 4)
(.6)	0.567786E 00 ( 7)	0.453991E 00 ( 8)	0.309018E 00 ( 9)
(.11)	-0.156432E 00 (12)	-0.309014E 00 (13)	-0.453988E 00 (14)
(.16)	-0.809015E 00 (17)	-0.891005E 00 (18)	-0.951055E 00 (19)

SECTION PITCHING MOMENT COEFFICIENT			
(.1)	0.000000E 00 ( 2)	0.000000E 00 ( 3)	0.000000E 00 ( 4)
(.6)	0.000000E 00 ( 7)	0.000000E 00 ( 8)	0.000000E 00 ( 9)
(.11)	0.000000E 00 (12)	0.000000E 00 (13)	0.000000E 00 (14)
(.16)	0.000000E 00 (17)	0.000000E 00 (18)	0.000000E 00 (19)

EFFECTIVE SECTION ANGLE OF ATTACK			
(.1)	0.216154E 01 ( 2)	0.427324E 01 ( 3)	0.589261E 01 ( 4)
(.6)	0.114550E 01 ( 7)	-0.328316E 01 ( 8)	-0.463838E 01 ( 9)
(.11)	0.149371E 01 (12)	-0.463839E 01 (13)	-0.328315E 01 (14)
(.16)	0.615531E 01 (17)	0.589264E 01 (18)	0.427328E 01 (19)

SECTION PROFILE DRAG COEFFICIENT			
(.1)	0.627499E-02 ( 2)	0.689538E-02 ( 3)	0.757830E-02 ( 4)
(.6)	0.604193E-02 ( 7)	0.666712E-02 ( 8)	0.703933E-02 ( 9)
(.11)	0.619995E-02 (12)	0.703933E-02 (13)	0.666712E-02 (14)
(.16)	0.801827E-02 (17)	0.757832E-02 (18)	0.689540E-02 (19)

SECTION INDUCED DRAG COEFFICIENT			
(.1)	0.716377E-02 ( 2)	-0.470249E-02 ( 3)	-0.264332E-01 ( 4)
(.6)	0.622957E-02 ( 7)	-0.482516E-01 ( 8)	-0.813102E-01 ( 9)
(.11)	0.733644E-02 (12)	-0.813105E-01 (13)	-0.482515E-01 (14)
(.16)	-0.309920E-01 (17)	-0.264338E-01 (18)	-0.470285E-02 (19)

DISTRIBUTION OF SECTION LIFT COEFFICIENT-CL			
(.1)	0.228259E 00 ( 2)	0.451254E 00 ( 3)	0.622260E 00 ( 4)
(.6)	0.120965E 00 ( 7)	-0.346702E 00 ( 8)	-0.489813E 00 ( 9)
(.11)	0.199976E 00 (12)	-0.469814E 00 (13)	-0.346701E 00 (14)
(.16)	0.650000E 00 (17)	0.622263E 00 (18)	0.451258E 00 (19)

DISTRIBUTION OF SECTION LIFT COEFFICIENT-CLS			
(.1)	0.836396E-01 ( 2)	0.165745E 00 ( 3)	0.228556E 00 ( 4)
(.6)	0.444305E-01 ( 7)	-0.127343E 00 ( 8)	-0.179908E 00 ( 9)
(.11)	0.734512E-01 (12)	-0.179909E 00 (13)	-0.127343E 00 (14)
(.16)	0.238745E 00 (17)	0.228557E 00 (18)	0.165747E 00 (19)

.....

FUSELAGE ANGLE OF ATTACK, DEGREES. . . . .	=	4.25000	INDUCED DRAG COEFFICIENT, CDI . . . . .	=	-0.01950
LIFT COEFFICIENT, CL . . . . .	=	0.13549	PROFILE DRAG COEFFICIENT, CD . . . . .	=	0.00678
LIFT COEFFICIENT, CLS . . . . .	=	0.04976	WACELLE DRAG COEFFICIENT, CDN . . . . .	=	0.00000
PITCHING MOMENT COEFFICIENT, CM. . . . .	=	0.00000	TOTAL DRAG COEFFICIENT, CD . . . . .	=	-0.01272
PITCHING MOMENT COEFFICIENT, CMS . . . . .	=	0.00000	TOTAL DRAG COEFFICIENT, CDS . . . . .	=	-0.00467

Table IV - Sample Output for Propeller Velocity Distribution

PROPELLER SLIPSTREAM ANALYSIS - NRC LR-284 FIG 26 CT'NOM=0.64, BETA75=25, J=0.605

PROPELLER - WING GEOMETRY

NUMBER OF PROPS = 2  
 PROP FWD COORD 2.YP/B = 0.5667  
 PROP SPAN COORD 2.YP/B = 0.6179  
 PROP DIA / WING SPAN = 0.4753

PROPELLER - NACELLE GEOMETRY

NO OF BLADES PER PROP = 4  
 HUB DIA / PROP DIA = 0.1673  
 NACELLE DIA / PROP DIA = 0.1673  
 PROP AXIS REL BODY AXIS = 0.000 DEG

PROPELLER OPERATING CONDITION

LEFT / RIGHT PROP ROTN = RH, LH  
 PROP ADVANCE RATIO = 0.6050  
 FLIGHT MACH NUMBER = 0.0581  
 PROP ANGLE OF ATTACK = 4.250 DEG

BLADE ELEMENT GEOMETRY

BLADE ELEMENT SOLUTION

SLIPSTREAM ELEMENT SOLUTION

RS/RP	CB/RP	PITCH	A/F SER	CLI	T/C	F	MACH	ALPHA	CL	CD	RS/RP	USA/UA	UST/UA	PHIS
0.2000	0.2500	55.350	NACA 16	0.500	0.153	1.040	0.082	3.461	0.582	0.010	0.1983	1.2525	0.3364	15.033
0.3000	0.2500	49.200	NACA 16	0.500	0.106	0.994	0.105	6.981	0.848	0.010	0.2878	1.4486	0.4344	16.694
0.4000	0.2500	43.350	NACA 16	0.500	0.090	0.972	0.131	7.968	0.970	0.010	0.3750	1.6170	0.4776	16.455
0.5000	0.2500	37.700	NACA 16	0.500	0.085	0.956	0.159	7.645	0.957	0.010	0.4610	1.7270	0.4672	15.139
0.6000	0.2500	32.350	NACA 16	0.500	0.080	0.933	0.188	6.403	0.878	0.010	0.5467	1.7843	0.4309	13.579
0.7000	0.2500	27.300	NACA 16	0.500	0.075	0.893	0.217	4.722	0.764	0.010	0.6326	1.7986	0.3810	11.962
0.8000	0.2500	22.850	NACA 16	0.500	0.070	0.811	0.246	2.739	0.655	0.010	0.7190	1.7895	0.3369	10.663
0.9000	0.2500	18.900	NACA 16	0.500	0.065	0.638	0.275	0.699	0.487	0.010	0.8067	1.6853	0.2688	9.063
0.9500	0.2500	17.100	NACA 16	0.500	0.062	0.473	0.289	-0.458	0.367	0.010	0.8518	1.5679	0.2195	7.970
1.0000	0.2500	15.350	NACA 16	0.500	0.060	0.000	0.307	0.000	0.000	0.000	0.9012	1.0000	0.0000	0.000

PROPELLER THRUST COEFFICIENT, CT' = 0.6327  
 PROPELLER THRUST COEFFICIENT, CT = 0.2462  
 PROPELLER TORQUE COEFFICIENT, CQ = 0.0374  
 MOMENTUM WGTD SLIPSTREAM VEL RATIO = 1.6455

SLIPSTREAM VALUES AT WING CONTROL STATIONS

K	ZY/B	RS/RP	USA/UA	UST/UD	UST/USA
1	0.9876	0.7780	1.7148	0.2903	0.1693
2	0.9510	0.7009	1.7865	0.3452	0.1932
3	0.8910	0.5745	1.7840	0.4136	0.2318
4	0.8090	0.4020	1.6470	0.4730	0.2872
5	0.7071	0.1876	1.2490	0.3175	0.2541
6	0.5877	0.0633	1.2490	-0.1071	-0.0858
7	0.4539	0.3448	1.5544	-0.4613	-0.2968
8	0.3090	0.6498	1.7918	-0.3712	-0.2071
12	-0.3090	0.6498	1.7918	-0.3712	-0.2071
13	-0.4539	0.3448	1.5544	-0.4613	-0.2968
14	-0.5877	0.0633	1.2490	-0.1071	-0.0858
15	-0.7071	0.1876	1.2490	0.3175	0.2541
16	-0.8090	0.4020	1.6470	0.4730	0.2872
17	-0.8910	0.5745	1.7840	0.4136	0.2318
18	-0.9510	0.7009	1.7865	0.3452	0.1932
19	-0.9876	0.7780	1.7148	0.2903	0.1693

## SECTION 5

### VERIFICATION OF THE DEVELOPED THEORY

This section presents a series of correlations between the predicted results, obtained from the computer program described in Section 4 and the available experimental data. A discussion of these correlations has been separated into two natural categories. The first part deals with a verification of the solution for an isolated propeller-nacelle configuration, while the second part considers the combined wing-in-slipstream case.

#### 5.1 CORRELATIONS FOR AN ISOLATED PROPELLER

A majority of the available experimental data on isolated propellers is limited to measurements of total thrust and torque. Even in the few reported studies where the propeller slipstream velocities were measured, the data presented is generally incomplete and insufficient to permit a comprehensive evaluation of the propeller analysis. It was therefore necessary to establish the overall adequacy of the analytical predictions by presenting a series of partial correlations with the applicable data from each experimental source.

Correlations of the elemental loading on a propeller blade are limited to the experimental data reported in Reference 30. This data is presented for two 2.8-foot diameter model propellers of similar design, but different twist distributions. The experimental loadings were obtained directly from measurements of the slipstream velocity and swirl angle in a plane immediately behind the propeller disc. This test information forms the basis for the correlations shown in Figures 9, 10, and 11.

Figure 9 presents comparisons between the predicted and measured elemental thrust and torque loadings, expressed as ratios of predicted over measured values, versus predicted local lift coefficient at a blade radius of 75.2 percent. As can be noted from this figure, the thrust loading predictions, employing the tabulated airfoil characteristics, are in satisfactory to good agreement with the test data throughout the range of the lift curve. Also, the

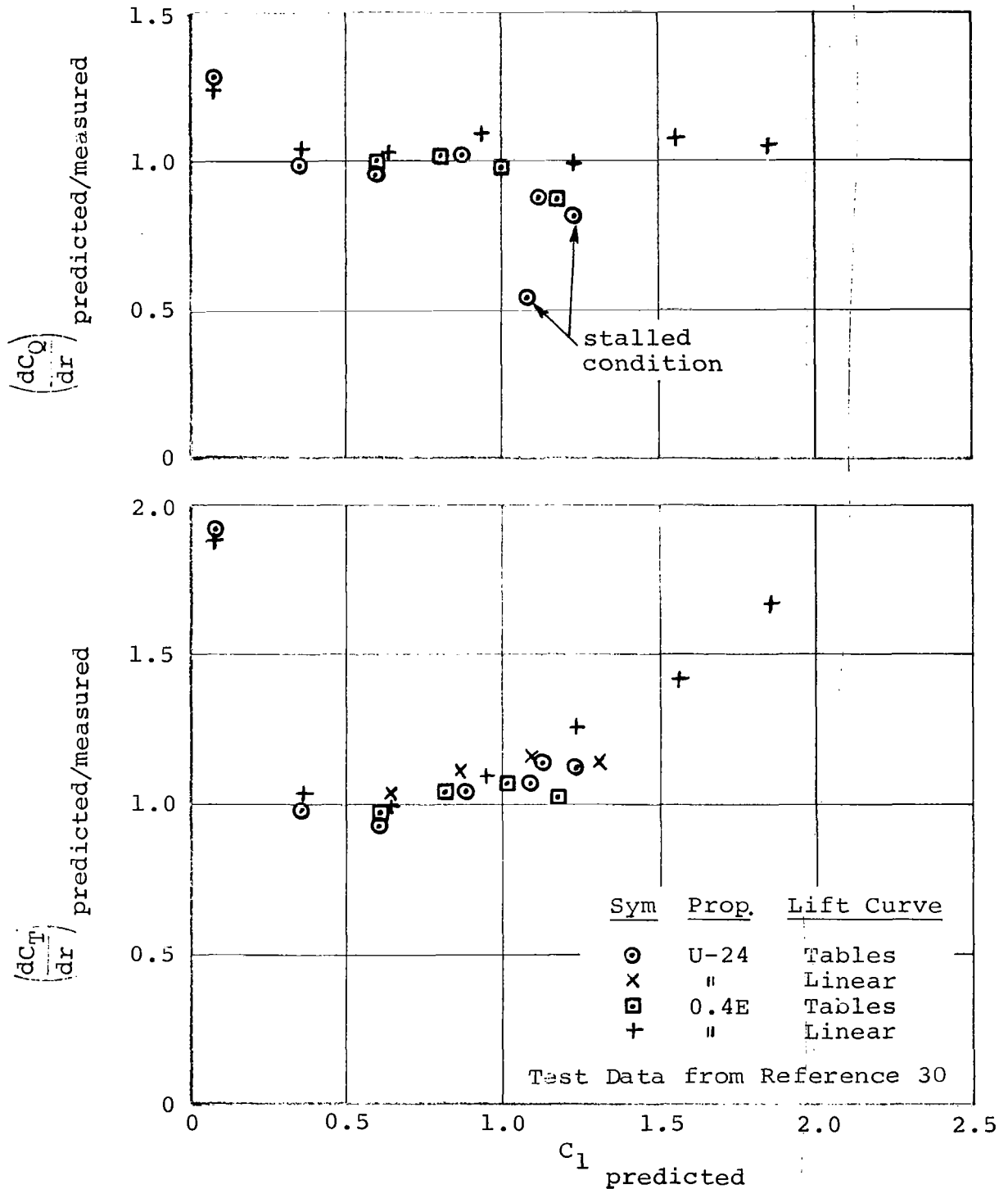


Figure 9. Correlation between Predicted and Measured Elemental Thrust and Torque Loadings at 75 Percent Radius.

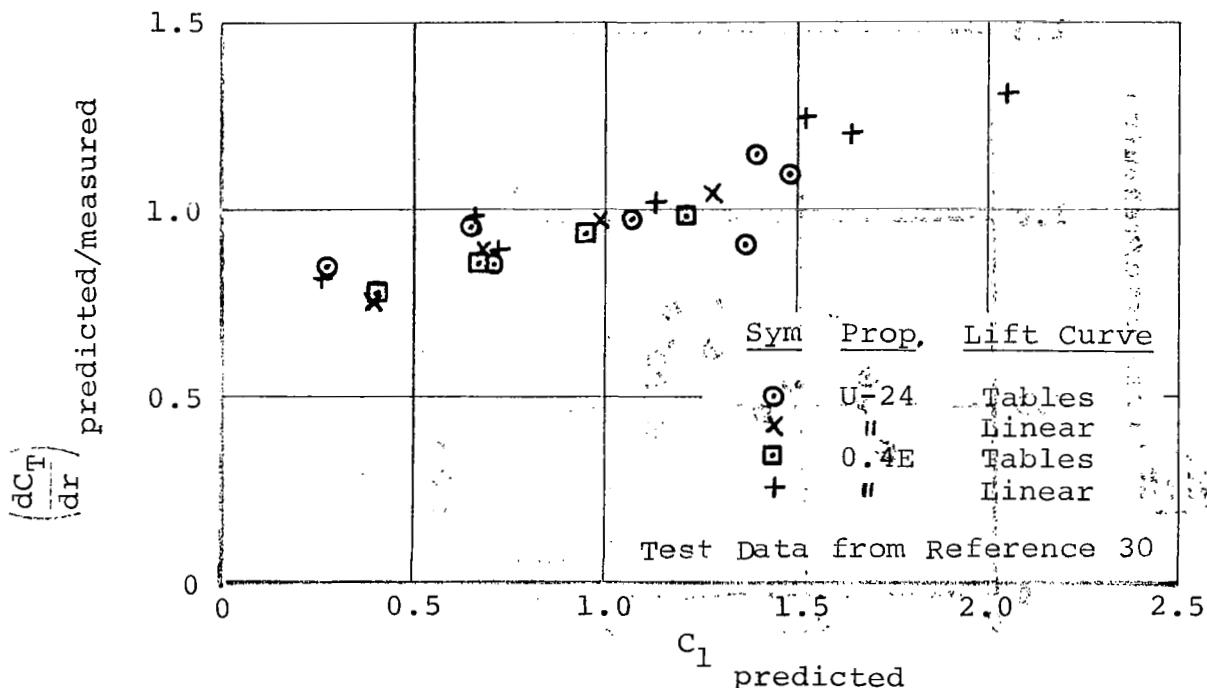
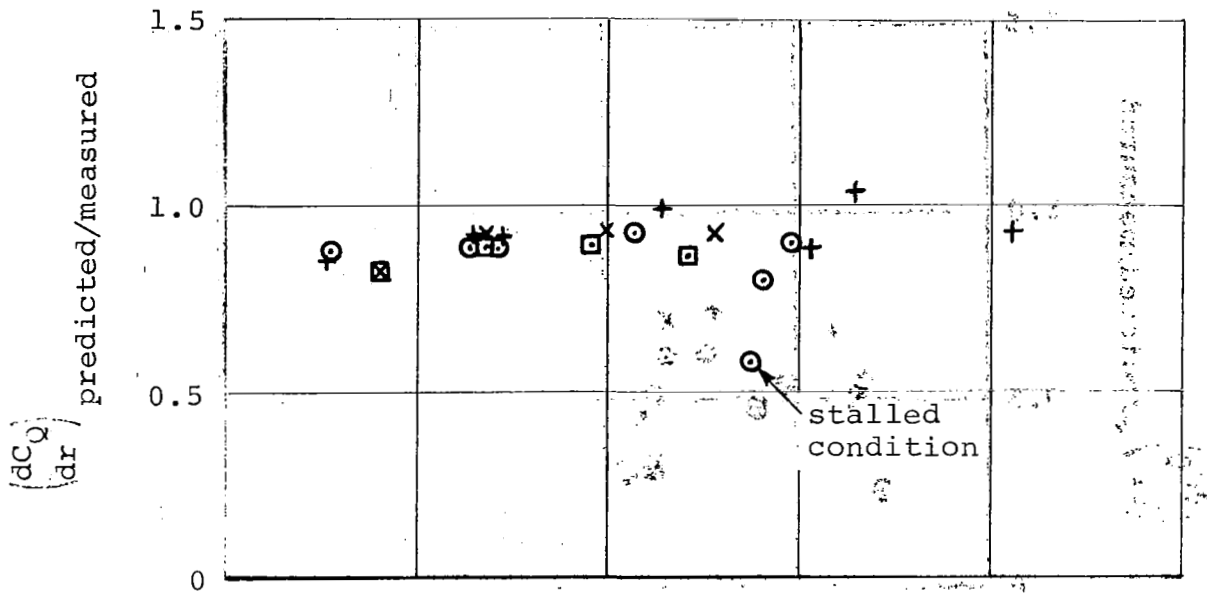


Figure 10. Correlation between Predicted and Measured Elemental Thrust and Torque Loadings, at 52 Percent Radius.

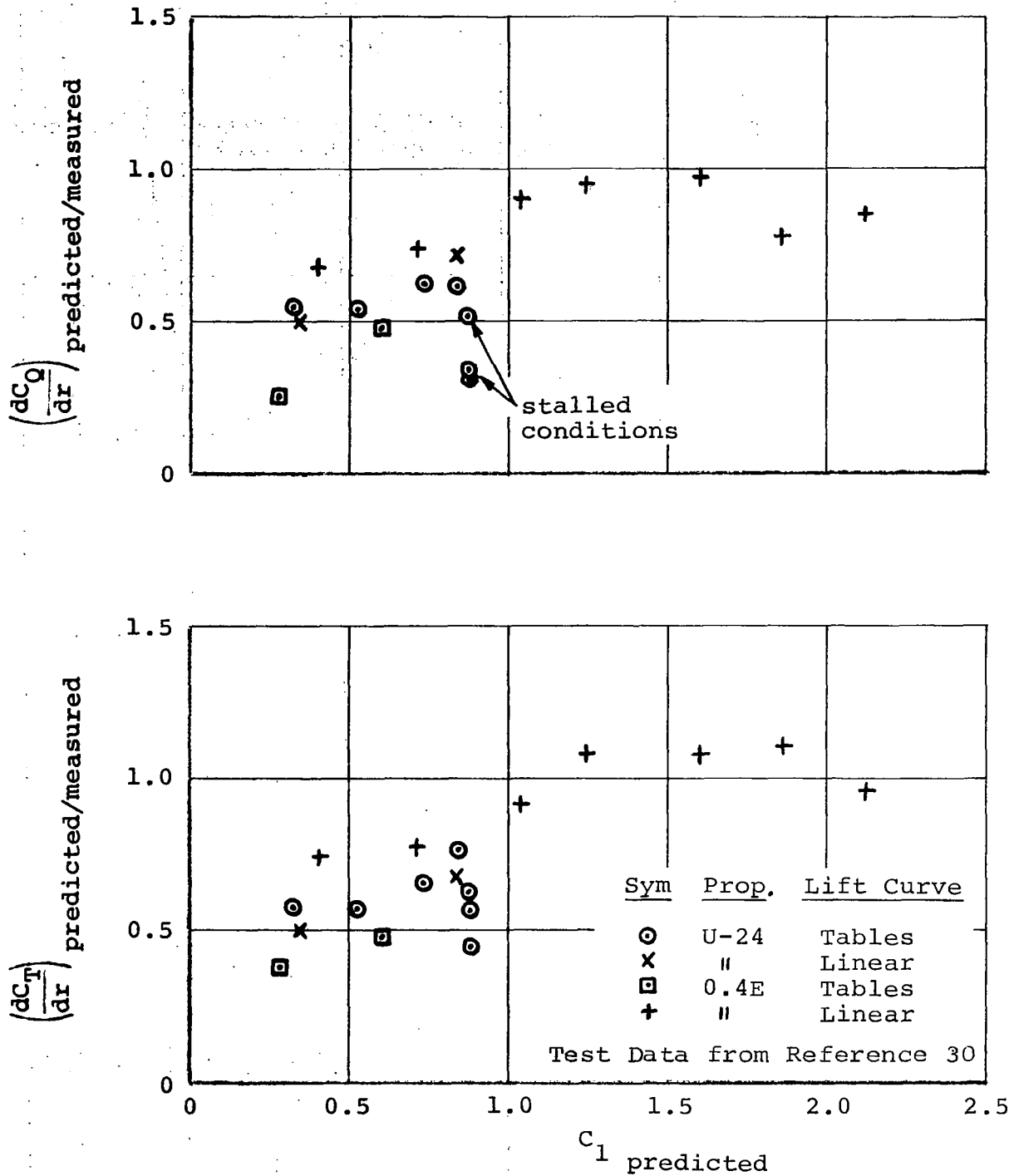


Figure 11. Correlation between Predicted and Measured Elemental Thrust and Torque Loadings at 25 Percent Radius.

corresponding torque loadings are in reasonable agreement, except at conditions near the stall, where the discrepancies may be attributed to an underestimation of the drag coefficient, assumed constant at a nominal value of 0.01. However, it should be noted that the experimental torque loading is particularly sensitive to the measurement of slipstream swirl angle, and therefore may be subject to appreciable experimental error. Figure 9 also includes a comparison of the predicted results obtained by using an unstallable linear lift curve to approximate the airfoil characteristics. The limitation of the linearized representation is reflected by an inferior prediction of thrust loadings near and above the stall point.

Figure 10 shows similar correlations, to those presented in Figure 9 but for a blade station further inboard at 52 percent radius. In this case, satisfactory to good correlations are also indicated.

Figure 11 shows similar comparisons to those shown in Figures 9 and 10, but at a blade radius near the hub, at 25.3 percent. While an increased scatter in the correlations may be partly attributed to the smaller magnitude of the measured quantities, it is evident that the assumption of an unstallable linear lift curve offers a better correlation for both the thrust and torque loadings. A suggestion that the stall point for this airfoil should be extended to a higher angle-of-attack, is consistent with the probable existence of a favorable boundary layer development caused by centrifugal pumping near the hub region.

In reviewing the correlations shown in Figures 9 through 11, it is apparent that there may be a restricted region of the blade close to the hub where stall delay effects are present. However, there is clearly an insufficient substantiation of this phenomenon to permit any rational empirical treatment.

Figures 12 and 13 present correlations between the predicted and measured values of the axial and swirl velocity distributions within the slipstream of propellers operating at relatively low advance ratios. The experimental data shown was obtained from Reference 17, which presents slipstream velocity measurements for two 39-inch diameter propeller-nacelle models, in a plane approximately 0.44 diameters



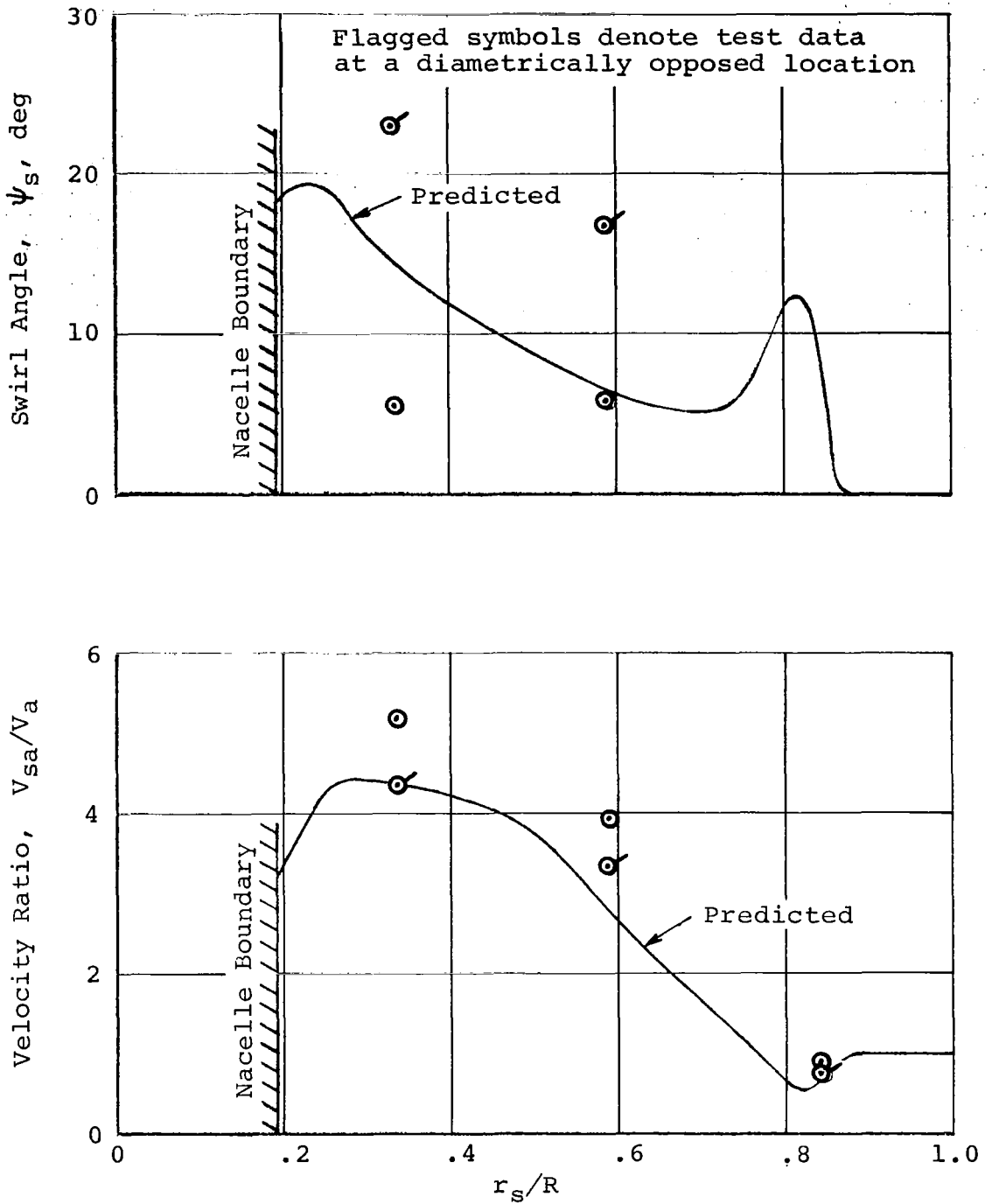


Figure 12. Comparison Between Predicted and Measured Distributions of Slipstream Axial Velocity and Swirl Angle for the P-2 Propeller of Reference 17 at  $J = 0.12$ .

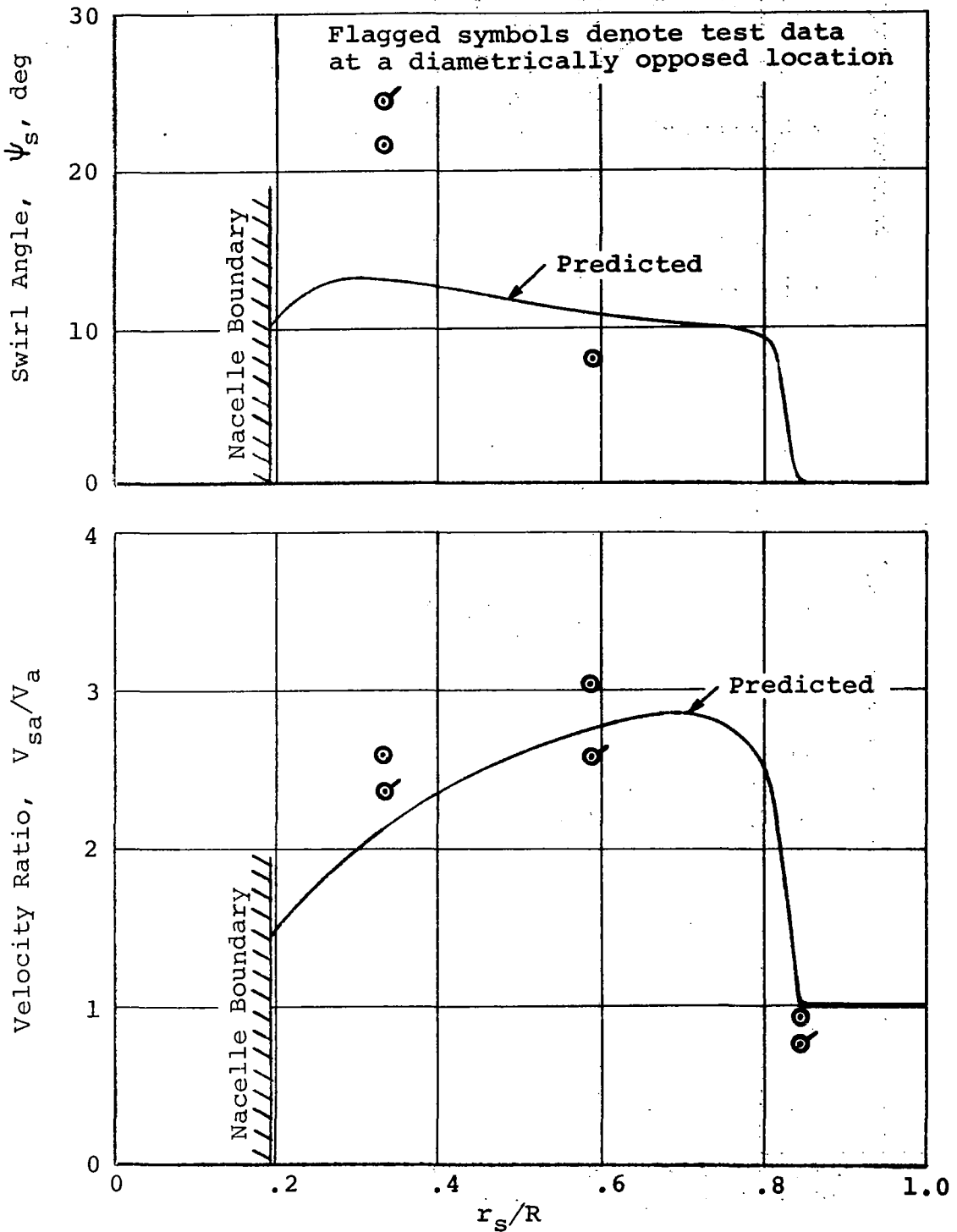


Figure 13. Comparison Between Predicted and Measured Distributions of Slipstream Axial Velocity and Swirl Angle for the P-1 Propeller of Reference 17 at  $J = 0.26$ .

downstream of the propeller disc. The slipstream velocity measurements were obtained using an eight-probe rake mounted symmetrically about the propeller axis.

Figure 12 shows a comparison between the predicted and measured slipstream velocities for a propeller designed with high taper and twist so as to produce an axial velocity peak well inboard. As can be seen from this figure, the predicted axial velocity distribution within the slipstream is in good agreement with the corresponding test data. However, the swirl angle prediction can not be properly assessed because of the excessive scatter of the experimental data points. It should be noted that flagged and unflagged test points shown in Figure 12 represent image positions on each side of the propeller.

Figure 13 shows a similar degree of correlation between the predicted and measured slipstream velocities for a propeller having a more conventional plan form and twist distribution. In this case, the predicted results are presented for a propeller speed reduced to 80 percent of the reported value. This correction was introduced to overcome an apparent discrepancy in the test measurements, as suggested by the authors of Reference 17.

Figure 14 presents two additional correlations for slipstream swirl angle distributions based on the test data of Reference 42. The experimental measurements were obtained at a distance of 2 diameters downstream of an isolated propeller. It can be seen from Figure 14 that the analysis generally predicts profiles of the experimental distributions, although an incremental shift in the swirl angle of up to 4 degrees is evident. However, the absence of the corresponding test data on the axial velocity distributions precludes a proper explanation of this shift in the slipstream swirl angle.

One aspect of the analysis not considered in the above correlations is an assumption that the slipstream may be considered as fully developed or fully contracted, for the purpose of predicting the wing span loading. While the effect of slipstream contraction on wing loading can only be properly assessed by comprehensive measurements, some observations on the rate of slipstream contraction can be made from the available test data.

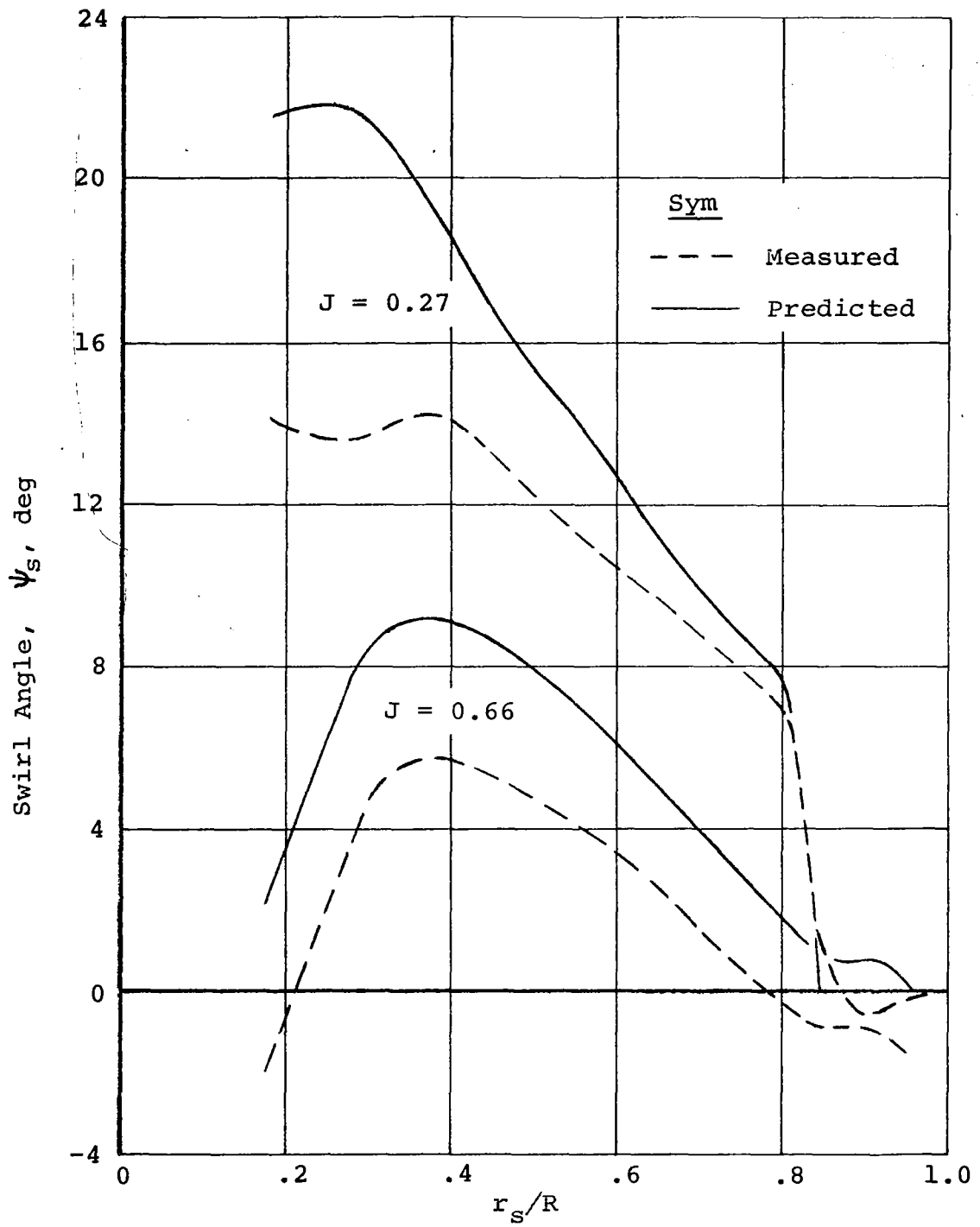


Figure 14. Comparison Between Predicted and Measured Distributions of Slipstream Swirl Angle for Typical Test Conditions Reported in Reference 42.

In practical aircraft configurations the propeller disc plane is generally located between one-half and one diameter forward of the wing quarter-chord line. From the correlations shown in Figures 12 and 13, it may be inferred that slipstream contraction could be fully developed at distances within 0.44 (D) behind the propeller. If this is the case, then the rate of slipstream contraction is significantly higher than that predicted by potential theory.

From the foregoing discussion and the correlations presented above, it can be concluded that the computerized analytical method developed herein yields more than adequate solution for the non-uniform propeller slipstream velocity distributions, which can be confidently used for prediction of wing spanwise loadings.

## 5.2 CORRELATIONS FOR WING-IN-SLIPSTREAM

This subsection presents the correlations of the theory with experimental data on wing spanwise loadings with slipstream effects. In selecting experimental data to thoroughly test the theoretical model the following criteria were used:

- Complete information on the geometric parameters of wings, nacelles and propellers.
- Adequate definition of the wing and propeller airfoil sections used in the tests.
- A thorough description of the propeller operating conditions in terms of blade angle, advance ratio, and rotational speed.
- An accurate determination of the spanwise lift distribution obtained by chordwise pressure surveys.

It was found that the amount of available test data that meets all of the above criteria is extremely limited. However, sufficient data was obtained from the technical literature to provide a fairly adequate basis for verification of the theoretical model. Some test data was obtained on wings immersed in jets, wings having centrally mounted

propellers, and wings with propellers placed at different spanwise stations up to and including the wing tips.

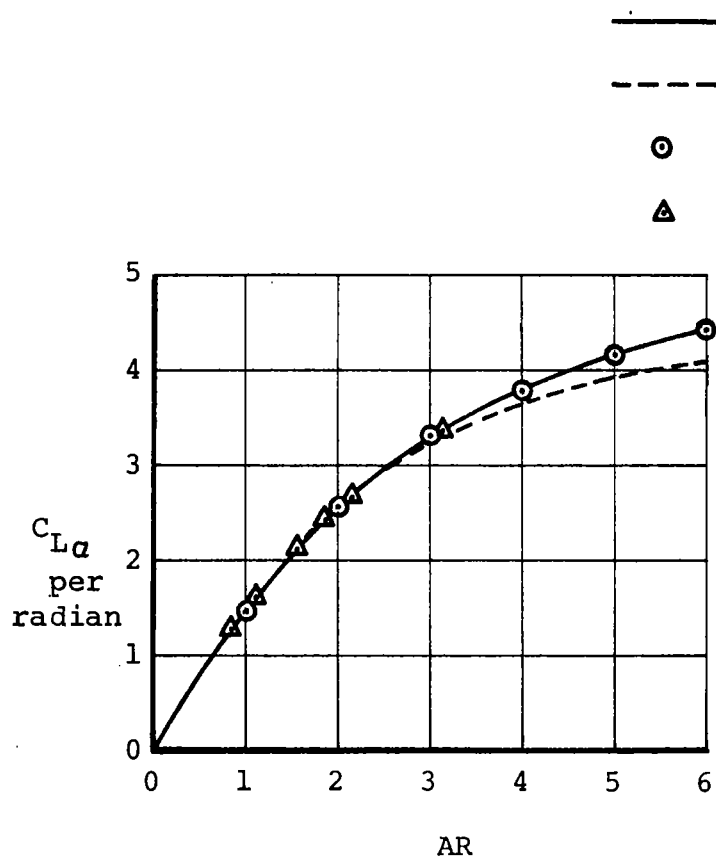
With few exceptions, the majority of the available test data was obtained at wing angles of attack below stall. Therefore, the adequacy of the developed methods to predict the span load distribution at the onset of stall could not be thoroughly verified. However, based on the correlations presented herein, at angles of attack close to stall, it can be inferred that the span loading at stall can be reasonably well predicted using the present analysis. Unfortunately, no test data is available on spanwise lift distributions for wings with part-span deflected flaps. Therefore, correlations for this case can not be presented at the present time.

The correlations that are presented below show the applicability of the analysis to low aspect-ratio wings, the capability to predict wing-in-jet effects, the prediction of span loading for single propeller configurations and, finally, the ability to predict the lift distributions on twin engine aircraft including those having tip-mounted propellers.

#### 5.2.1 Correlations for Low Aspect Ratio Wings

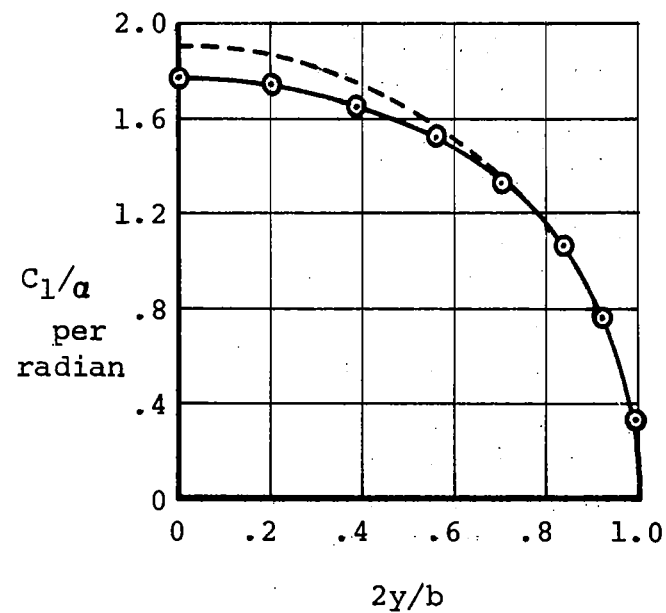
The applicability of the present method to low aspect ratio wings, (see subsection 3.2.3), was verified by performing correlations of the span loading on a rectangular wing of aspect ratio equal to 1.0. These correlations which are shown in Figure 15, are based on the analytical results of Reference 22 and the available test data obtained from a number of sources.

Figure 15 (a) shows a comparison of the predicted span loading (expressed as  $C_l/a$ ), with the analytical data of the two selected References. As can be noted from this figure, the predicted results are in satisfactory agreement with the results of References 22 and 43. Also Figure 15 (b) shows a comparison between the predicted and measured variations of lift-curve slope for a rectangular wing versus aspect ratio. Again, the computed results match those of References 22 and 43, and agree with the corresponding experimental values.



(b) Variation of Lift Curve Slope with Aspect Ratio

— Reference 22  
 - - - Reference 43  
 ○ Computer Program  
 △ Test Data



(a) Spanwise Lift Distribution for Rectangular Wing,  $AR = 1$

Figure 15. Verification of Low Aspect Ratio Analysis

### 5.2.2 Correlation for Centrally-Mounted Propellers and Jets

In Reference 6 Stuper measured the lift distribution on a rectangular wing having a uniform circular jet of air blowing over the center span. The jet was produced by a specially designed fan generating a uniform jet flow without rotation. This test data was chosen for comparison because it provides a check of the wing-in-slipstream theory, without reference to the propeller analysis.

Figure 16 shows a comparison between the predicted and measured spanwise lift distributions from Stuper's test; and again satisfactory agreement between the theory and the experimental data is obtained.

Measurements of lift distributions on wings with centrally mounted propellers are presented in Reference 29. In this series of tests, data was obtained for a full-scale wing/propeller combination in the large 30' X 60' wind tunnel at NASA, Langley. The propeller had a diameter of 4 feet and the wing was rectangular with a 5 foot chord. Aspect ratio was varied by changing the wing span.

Figure 17 presents a comparison between the theoretical predictions and the experimental data obtained for aspect ratio of 6.0 for wing alone, wing and nacelle, and wing, nacelle and propeller. Similar comparisons for a wing aspect ratio of 3.0 are shown in Figure 18. It can be noted from these figures that the combined wing/propeller theory predicts the span loading very well, except near the tips where the experimental data shows the characteristic square-tip loading which cannot be predicted using lifting line theory.

It should be noted that for both the Stuper jet case (Figure 16) and the central propeller cases (Figures 17 and 18), twenty stations per semispan were used in the computations in order to obtain adequate definition of the load distribution within the propeller slipstream region. If the propeller slipstream is not present, sufficient definition is generally achieved with the standard 10 points per semispan.



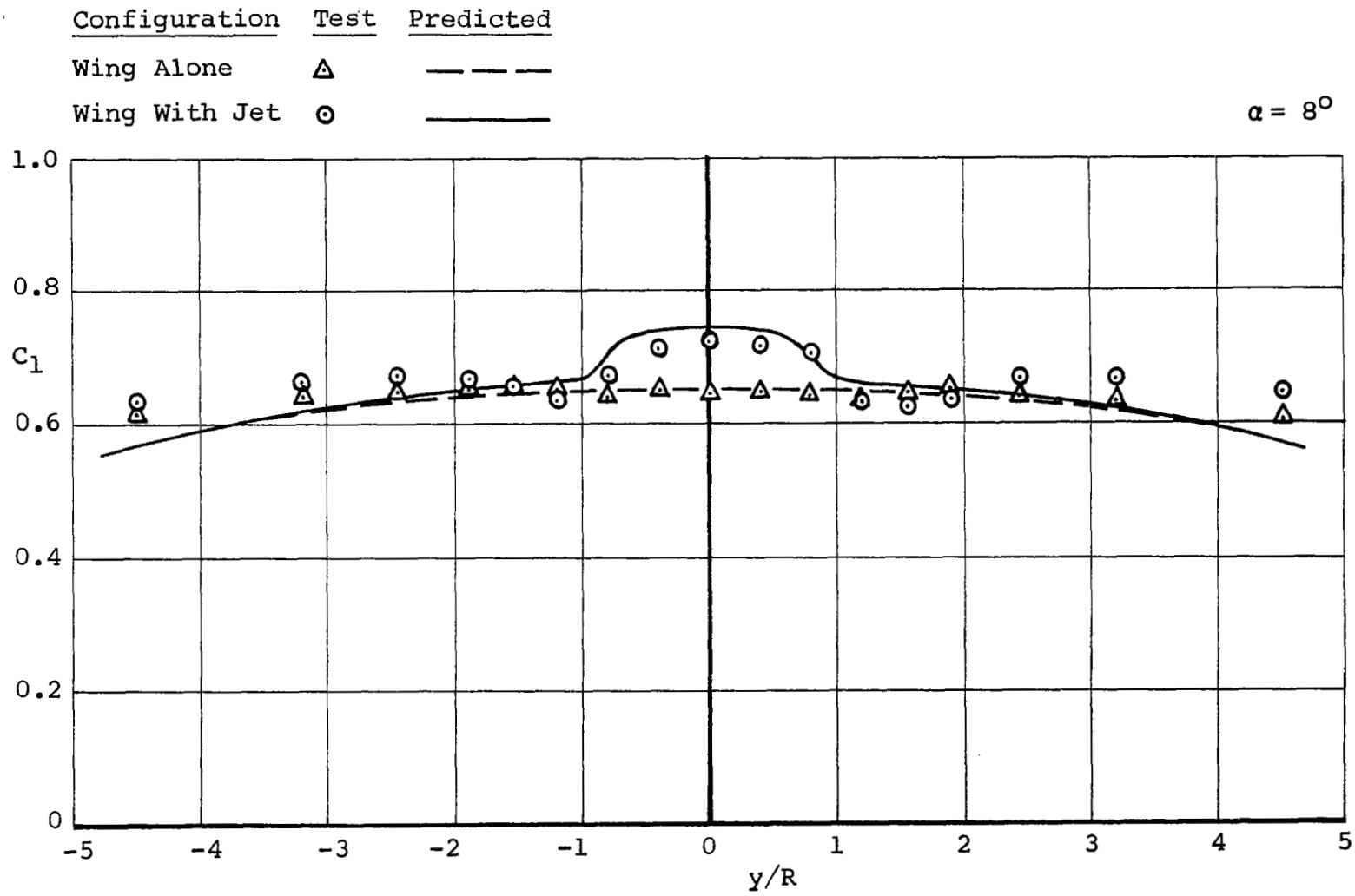


Figure 16. Comparison Between Predicted Spanwise Loading and Measurements of Reference 6 for a Rectangular Wing With End Plates Subjected to a Uniform Jet;  $V_s/V_o = 1.36$ .

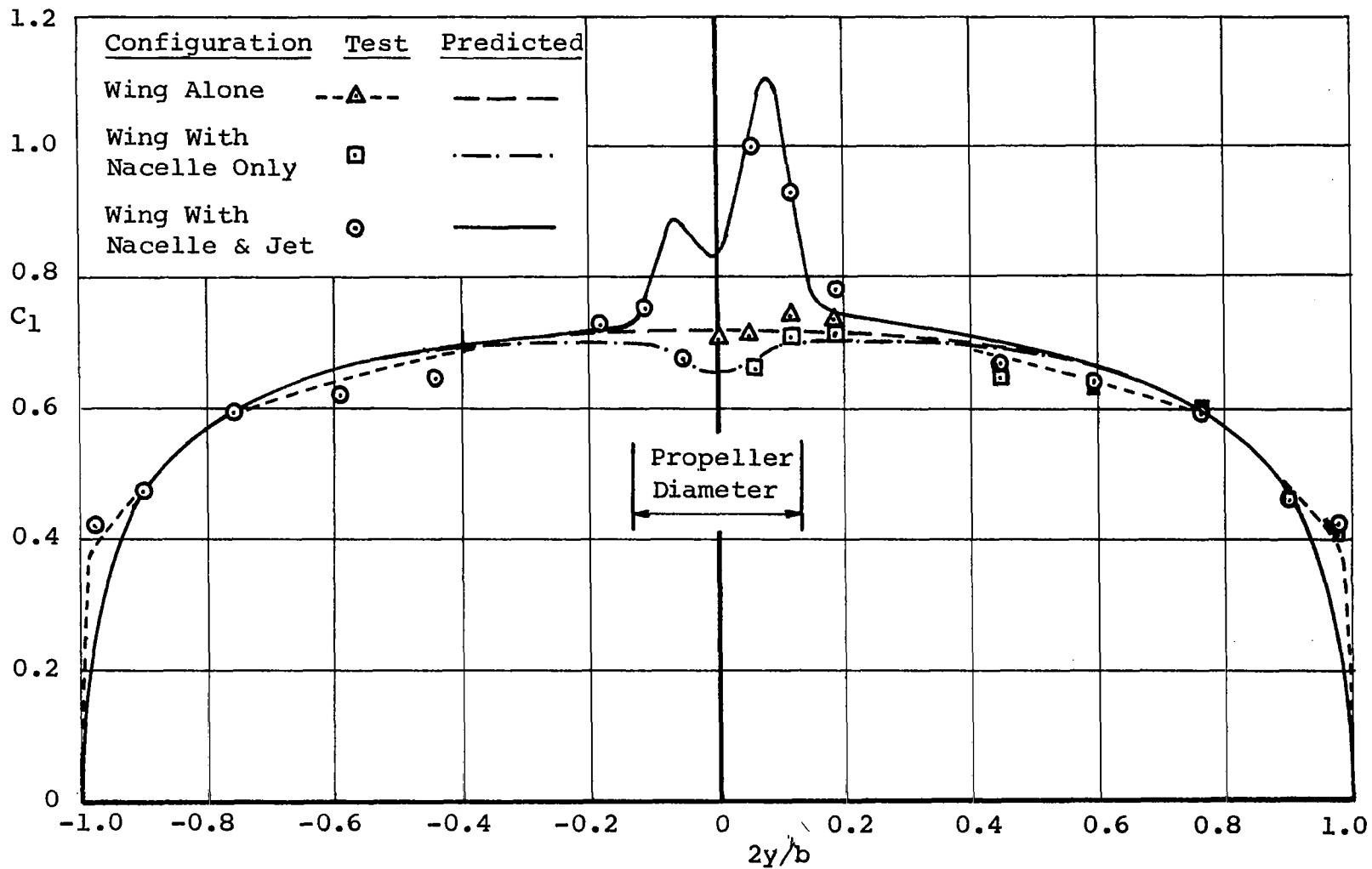


Figure 17. Predicted Versus Measured Spanwise Loadings for the Rectangular Wing of Reference 29 With a Centrally-Mounted Propeller; AR = 6.

$J = 0.42$  (Climb Condition)

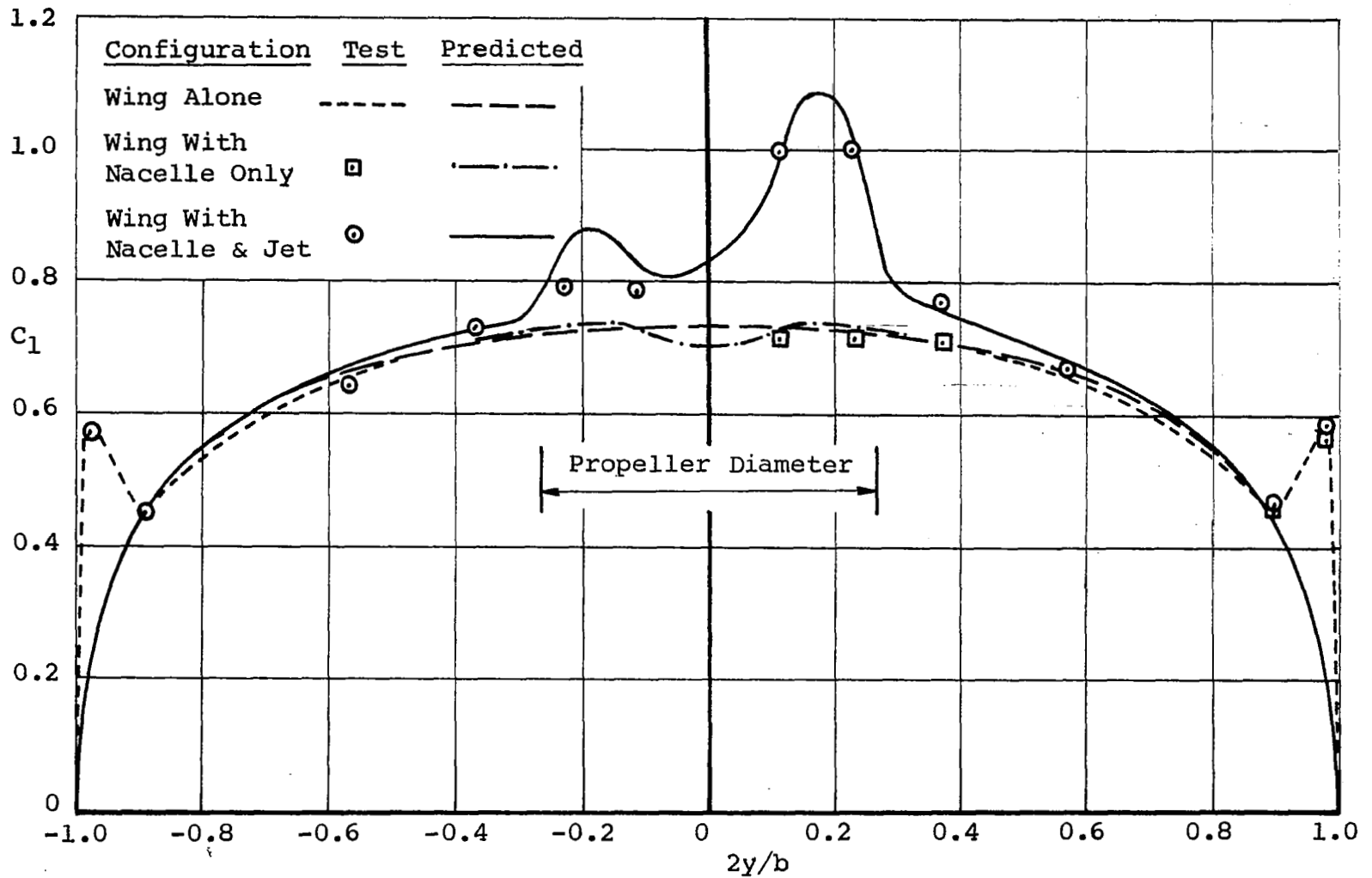


Figure 18. Predicted Versus Measured Spanwise Loadings for the Rectangular Wing of Reference 29 With a Centrally-Mounted Propeller;  $AR = 3$ .

### 5.2.3 Correlation for Twin Propeller Configurations

Reference 42 presents the results of wind tunnel tests on a reflection-plane model of a twin-engined tilt-wing VTOL configuration. The model tested consisted of a low aspect ratio rectangular (18" X 26") unswept wing with a nacelle and propeller situated at 62 percent of the semispan. The wing airfoil section was a NACA 0015, the propeller blade sections were of the NACA 16 series and the propeller diameter was 26". The test report presents measured spanwise load distributions at various wing angles of attack for a limited range of propeller thrust coefficients.

Figures 19, 20, and 21 show comparisons of the predicted and measured span loadings for power-off and power-on conditions, for propeller thrust coefficients of  $C_{T_S}=0$ , 0.36 and 0.64, respectively. It was found that in order to match the measured lift distributions power-off, the theoretical calculations had to be performed at angles of attack slightly below those values quoted in Reference 42. For example, in order to match the  $C_l$  distribution for  $5^\circ$  angle of attack, the calculations had to be made at  $4.25^\circ$ . The reason for this discrepancy is not clear since, as is shown elsewhere, predictions for other wings, power-off, agree with the experimental data. The discrepancy could be attributable to tunnel flow inclination effects. In the comparisons shown for power-on conditions, the angle of attack values used are those that match the power-off loading.

Despite the differences noted above, the theoretical predictions of the spanwise lift distribution agree well with the experimental data of Reference 42 except near the wing root. This discrepancy is attributed to the presence of tunnel wall boundary layer effects, as mentioned in Reference 42.

In Reference 44, a series of tests are reported that were made on rectangular wings or aspect ratio 2.28, 3.26, and 4.7 with an underslung nacelle and propeller placed at 83 percent, 58 percent and 40 percent of the semispan, respectively. The propeller was the same propeller used in the tests of Reference 42. The wing airfoil section was a NACA 4415 series. The tests were conducted for wing angles of attack of  $0^\circ$  through  $120^\circ$  at various values of propeller thrust coefficient.

Sym	Test	Predicted
△	$\alpha = 10^\circ$	$\alpha = 8.75^\circ$
□	$\alpha = 5^\circ$	$\alpha = 4.25^\circ$
○	$\alpha = 0^\circ$	$\alpha = 0^\circ$
◇	$\alpha = -5^\circ$	$\alpha = -4.25^\circ$
▽	$\alpha = -10^\circ$	$\alpha = -8.75^\circ$

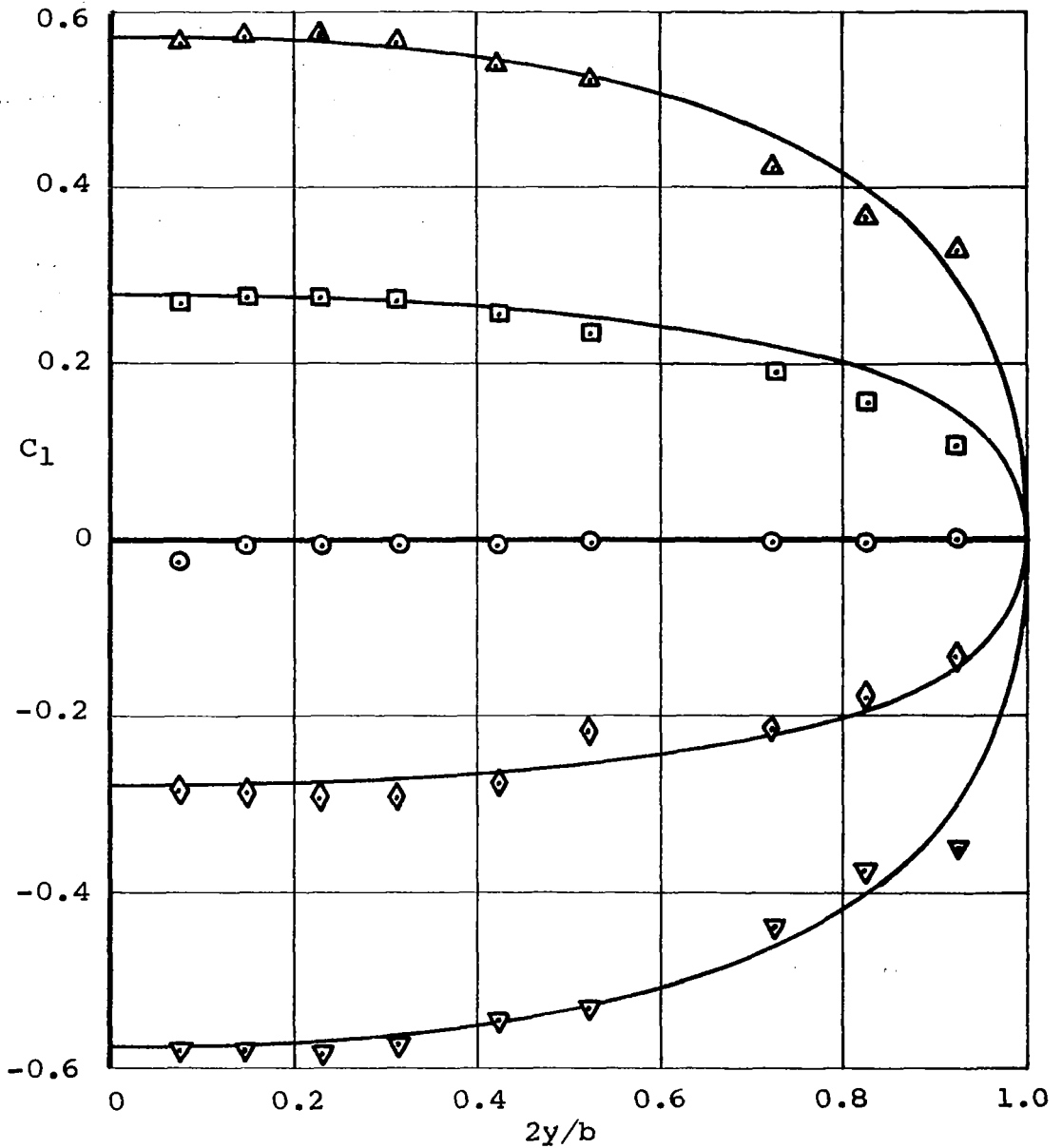


Figure 19. Predicted Versus Measured Spanwise Loadings for the Twin-Propeller Configuration of Reference 42; AR = 3.0,  $C_{TS} = 0$ .

Sym	Test	Predicted
△	$\alpha = 10^\circ$	$\alpha = 8.75^\circ$
□	$\alpha = 5^\circ$	$\alpha = 4.25^\circ$
○	$\alpha = 0^\circ$	$\alpha = 0^\circ$
◇	$\alpha = -5^\circ$	$\alpha = -4.25^\circ$
▽	$\alpha = -10^\circ$	$\alpha = -8.75^\circ$

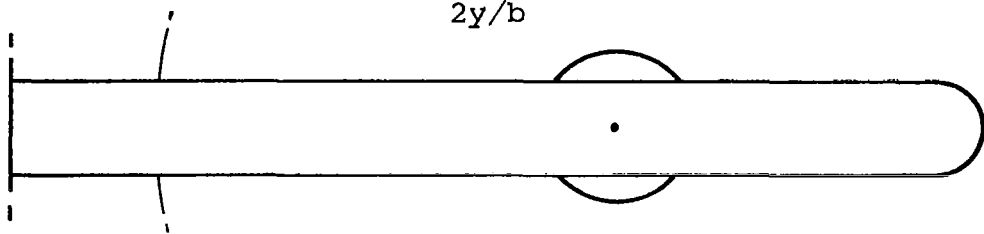
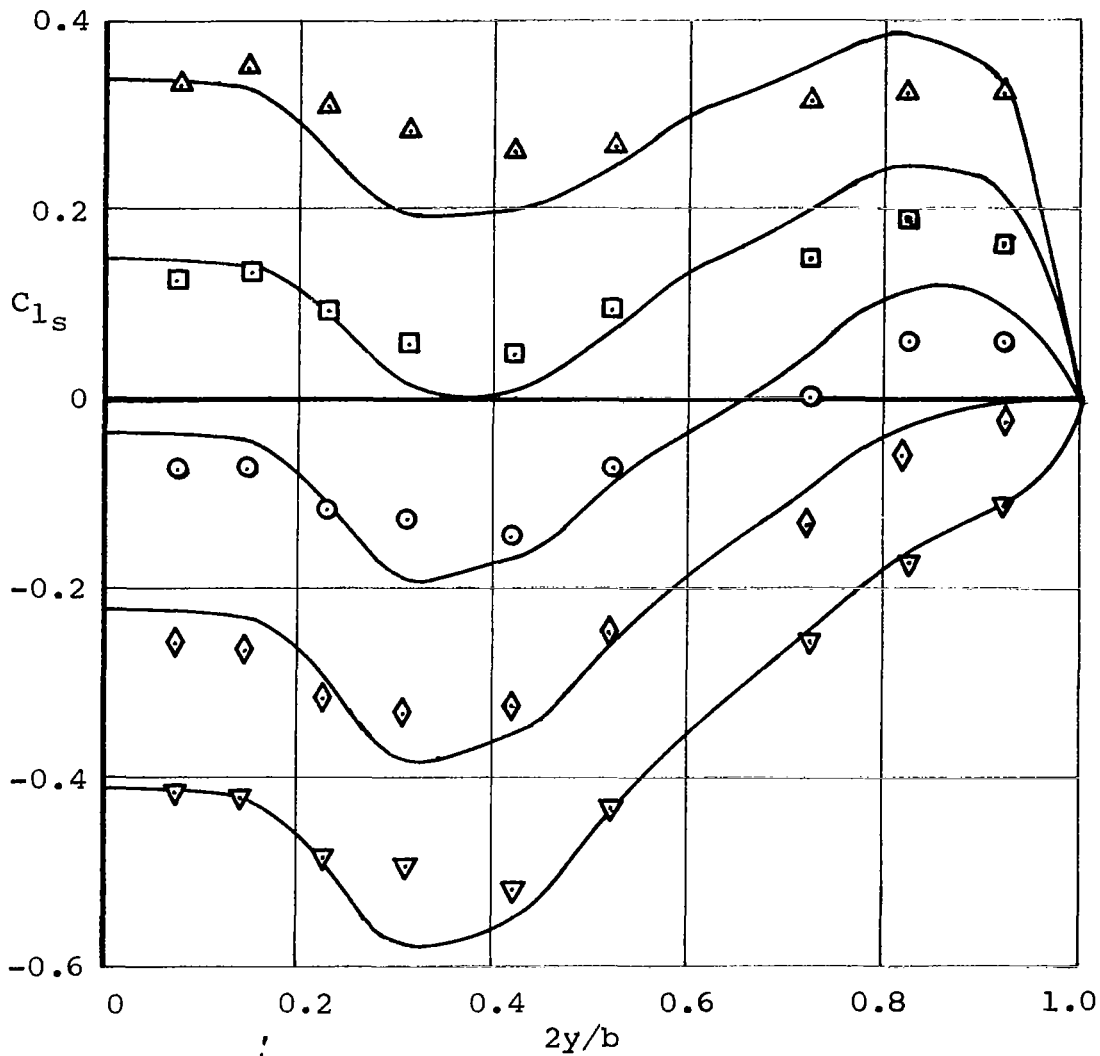


Figure 20. Predicted Versus Measured Spanwise Loadings for the Twin-Propeller Configuration of Reference 42;  $AR = 3.0$ ,  $C_{TS} = 0.36$ ,  $\beta_{75} = 25^\circ$ .

Sym	Test	Predicted
△	$\alpha = 10^\circ$	$\alpha = 8.75^\circ$
□	$\alpha = 5^\circ$	$\alpha = 4.25^\circ$
○	$\alpha = 0^\circ$	$\alpha = 0^\circ$
◇	$\alpha = -5^\circ$	$\alpha = -4.25^\circ$
▽	$\alpha = -10^\circ$	$\alpha = -8.75^\circ$

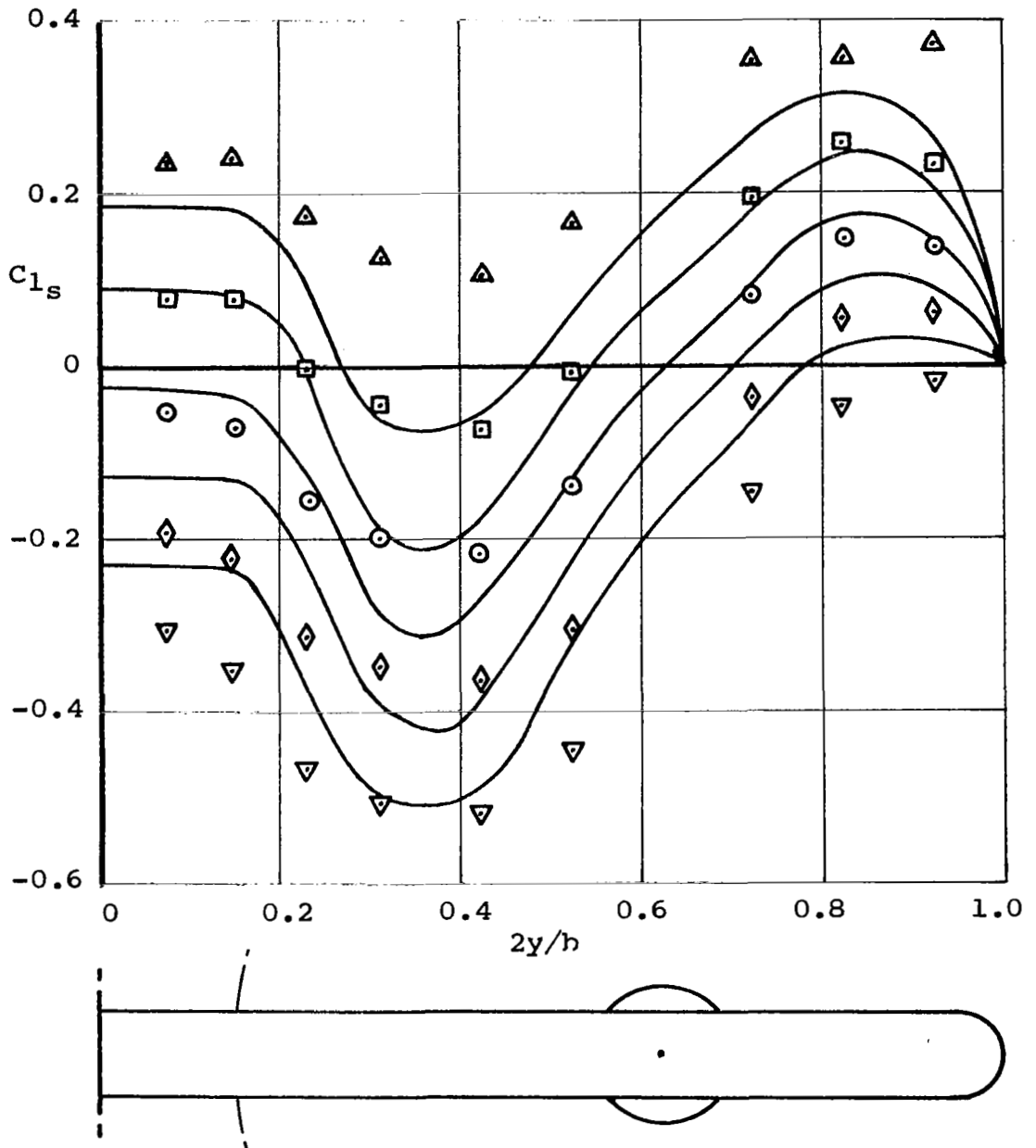


Figure 21. Predicted Versus Measured Spanwise Loadings for the Twin-Propeller Configuration of Reference 42;  $AR = 3.0$ ,  $C_{TS} = 0.64$ ,  $\beta_{75} = 25^\circ$ .

Figures 22, 23, and 24 show power-off correlations of the spanwise lift distribution obtained using the present theoretical analysis for the three wing aspect ratios at wing angles of attack below stall. The agreement between the theory and test is good throughout all values of wing aspect ratio except near the wing root where substantial wall effects are evident. Figures 25 through 27 show the theoretical span loading versus the measured loading for a propeller thrust coefficient  $C_{TS} = 0.4$ . In all cases, excellent agreement is obtained between the predictions and the test distributions.

Although test data was obtained at angles of attack up to  $120^\circ$ , the angles of attack were either below stall or well above stall. Thus no data was obtained at the point of initial stall onset. No check of the theory close to the stall point is, therefore, available from this test series.

#### 5.2.4 Effect of Propeller Rotation

The direction of rotation of propellers of multi-propeller configurations may introduce appreciable changes in the wing span loading. For example, rotation of propellers in the same direction of a twin-propeller configuration causes asymmetry in the span loading, which in turn gives rise to the aircraft rolling moment.

Although no test data exists to verify this aspect of the present theory, computations were performed for the configuration of Reference 42 to demonstrate the ability of the computer program to handle different propeller rotations. The predicted results showing the effect of propeller rotations on the wing span loading are presented in Figure 28. The results are applicable to wing aspect ratio of 3.0, wing angle of attack of  $10^\circ$  and propeller thrust coefficient of  $C_{TS} = 0.64$ .

As can be noted from Figure 28 counterclockwise rotation of both propellers (as viewed from the rear) results in the asymmetric span loading, which could be integrated to yield the aircraft rolling moment due to power effects.



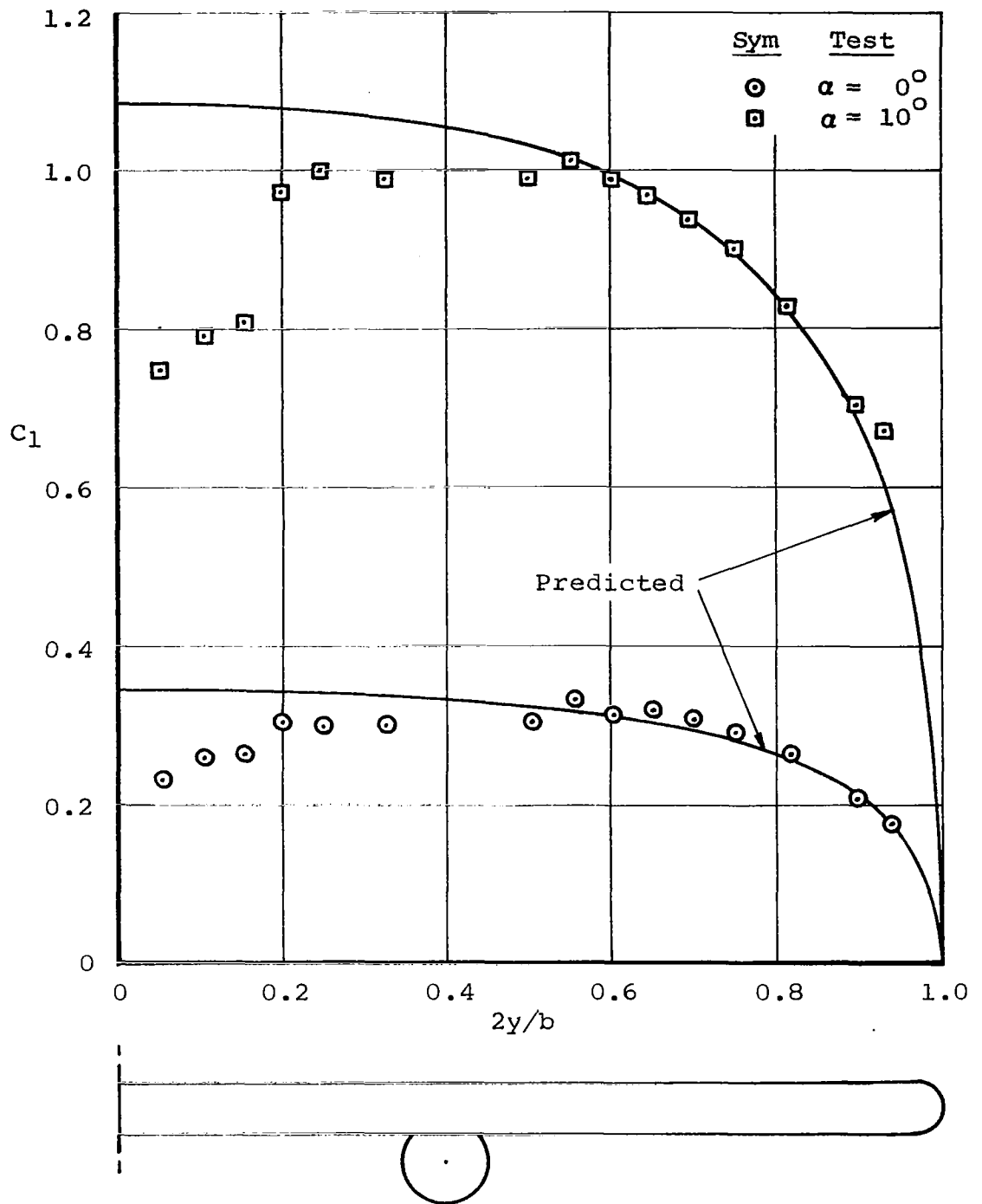


Figure 22. Predicted Versus Measured Spanwise Loadings for the Twin-Propeller Configuration of Reference 44;  $AR = 4.7$ ,  $C_{TS} = 0$ .

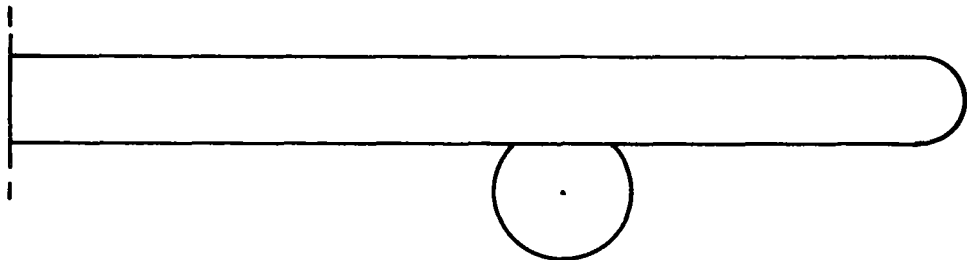
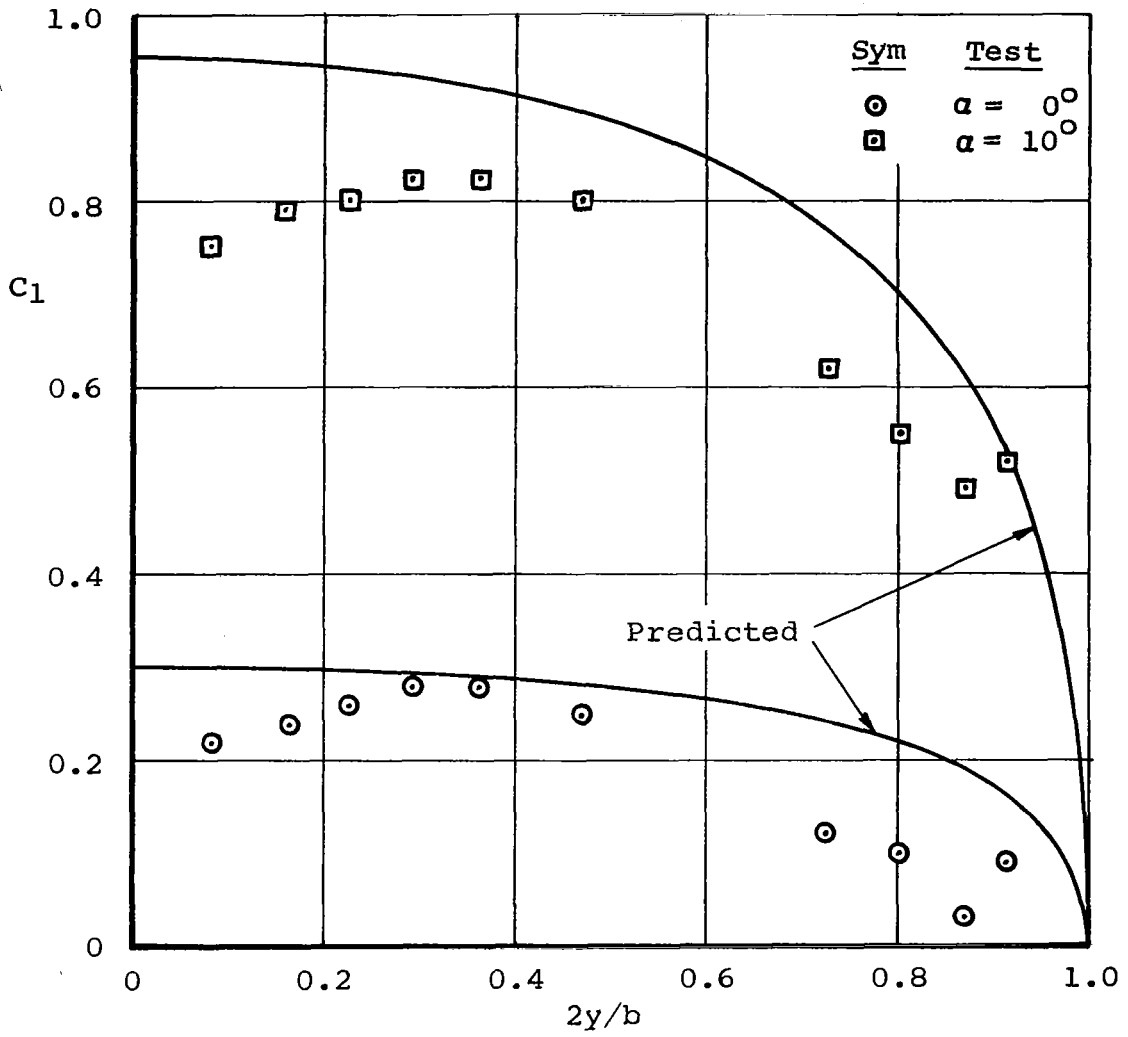


Figure 23. Predicted Versus Measured Spanwise Loadings for the Twin-Propeller Configuration of Reference 44;  $AR = 3.26$ ,  $C_{TS} = 0$ .

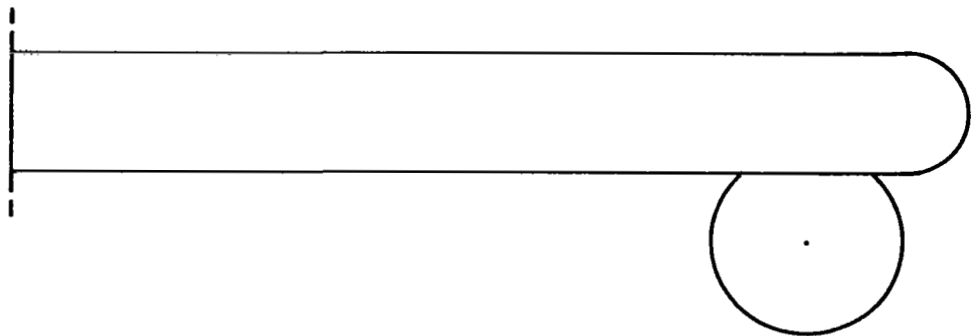
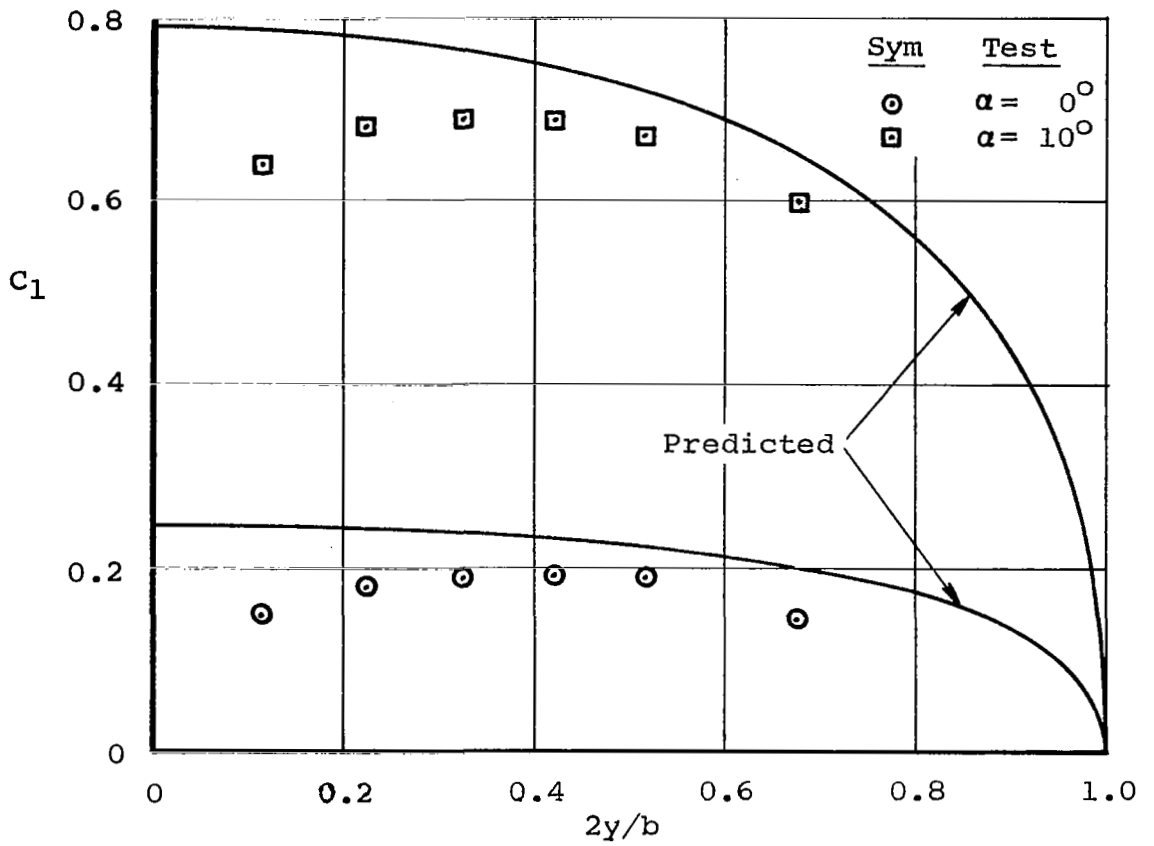


Figure 24. Predicted Versus Measured Spanwise Loadings for the Twin-Propeller Configuration of Reference 44;  $AR = 2.28$ ,  $C_{TS} = 0$ .

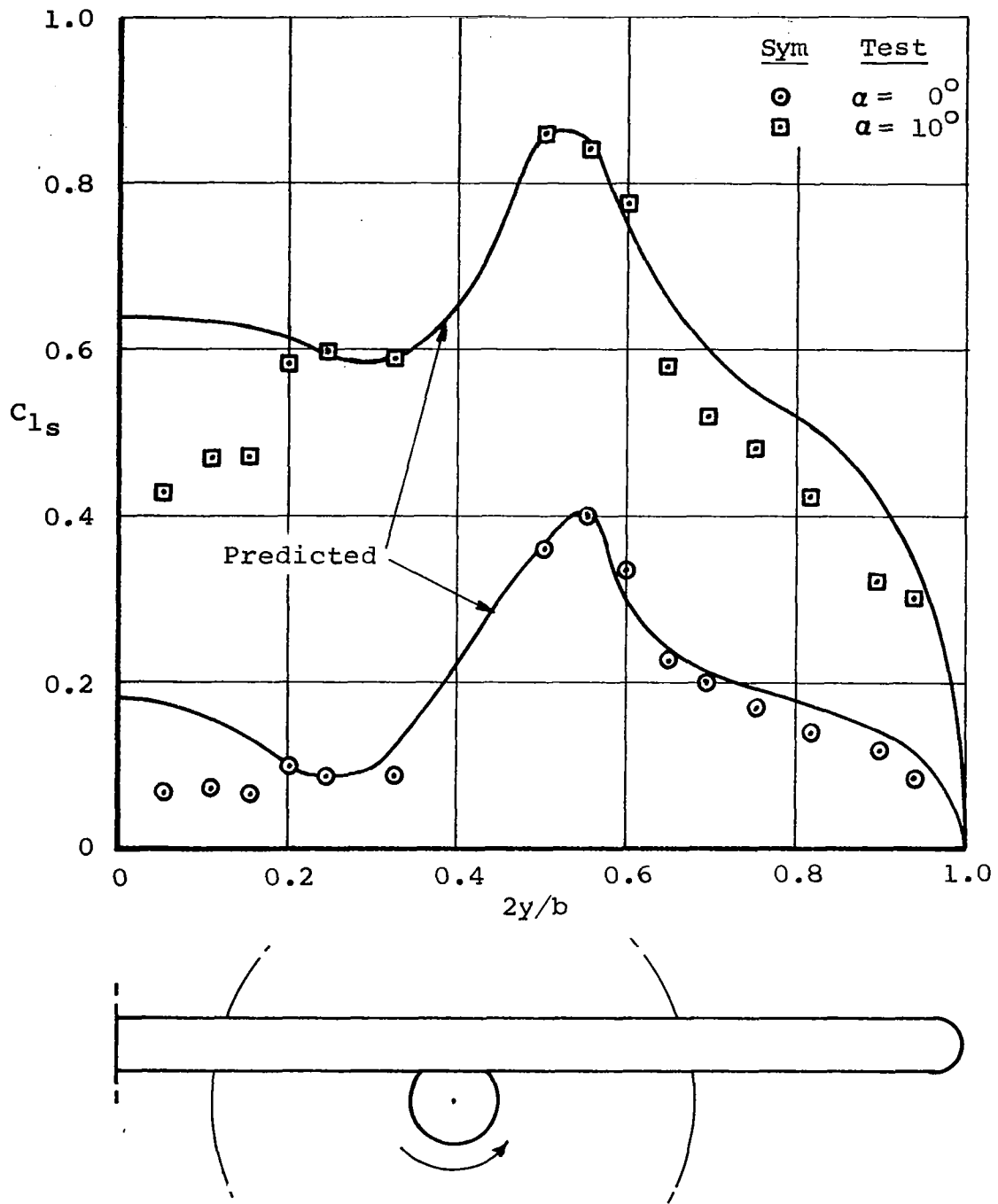


Figure 25. Predicted Versus Measured Spanwise Loadings for the Twin-Propeller Configuration of Reference 44;  $AR = 4.7$ ,  $C_{TS} = 0.4$ .

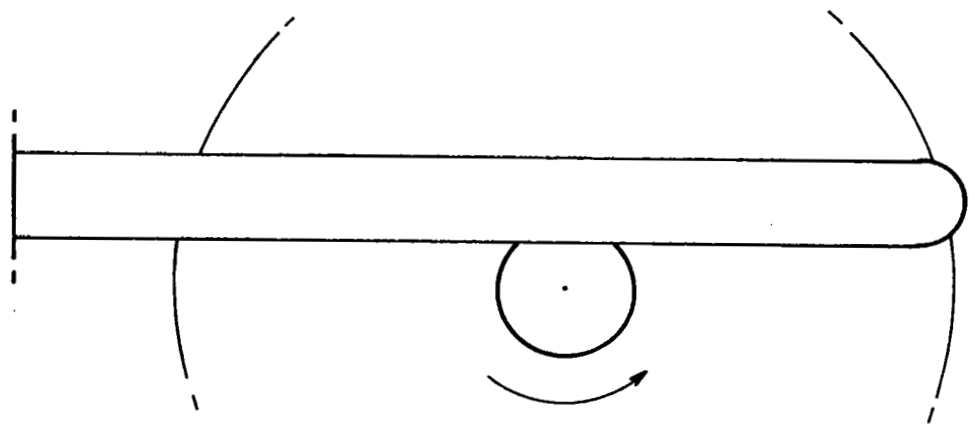
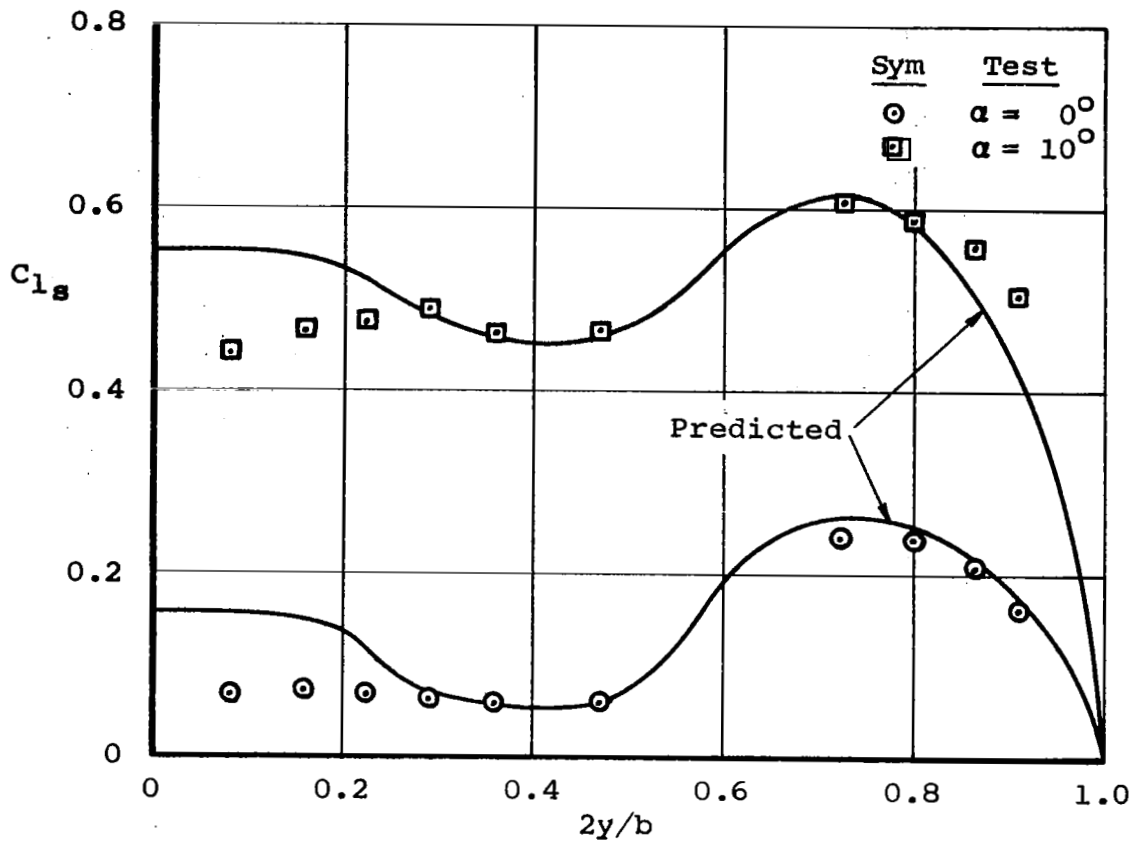


Figure 26. Predicted Versus Measured Spanwise Loadings for the Twin-Propeller Configuration of Reference 44;  $AR = 3.26$ ,  $C_{TS} = 0.4$ .

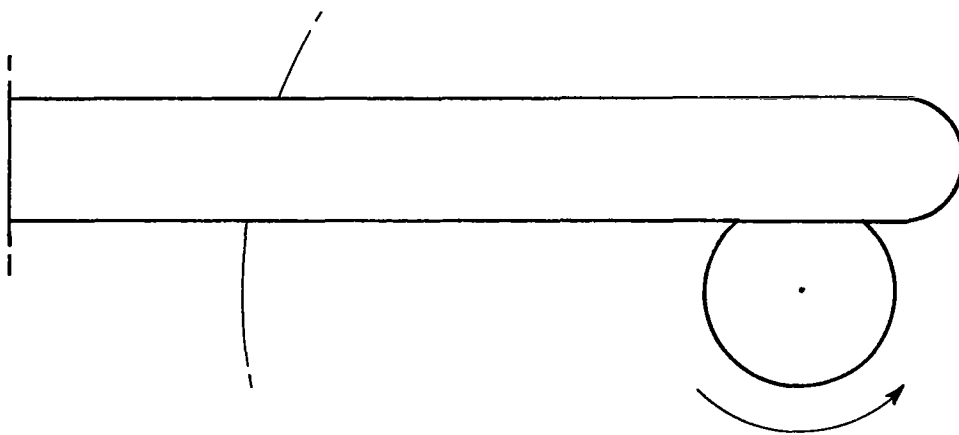
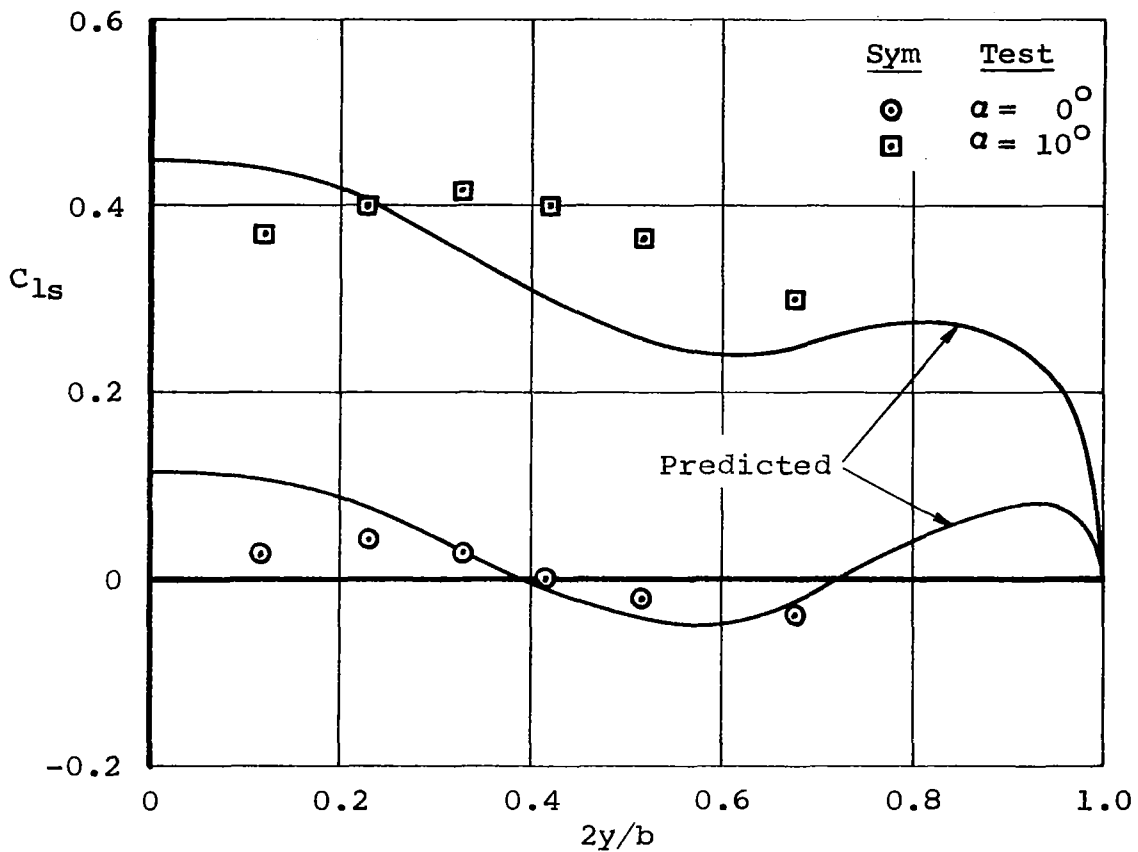


Figure 27. Predicted Versus Measured Spanwise Loadings for the Twin-Propeller Configuration of Reference 44;  $AR = 2.28$ ,  $C_{TS} = 0.4$ .

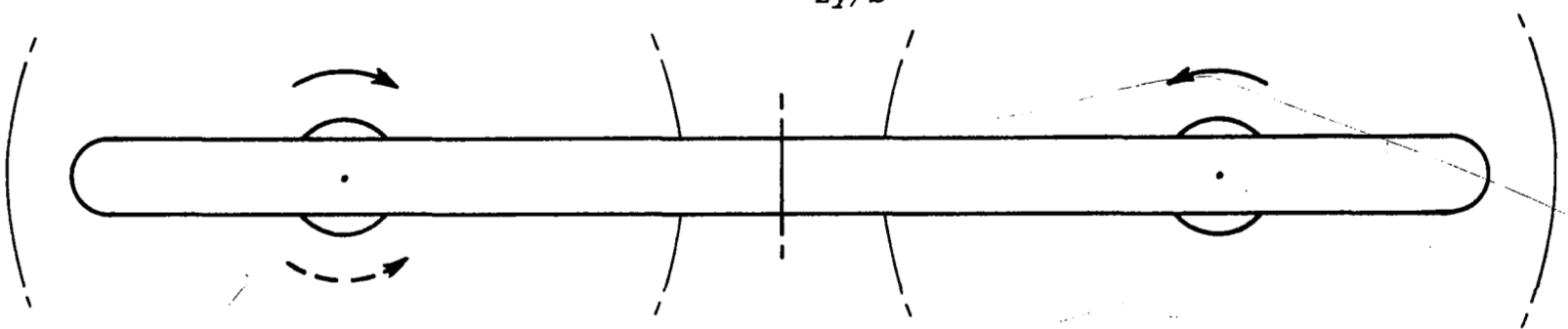
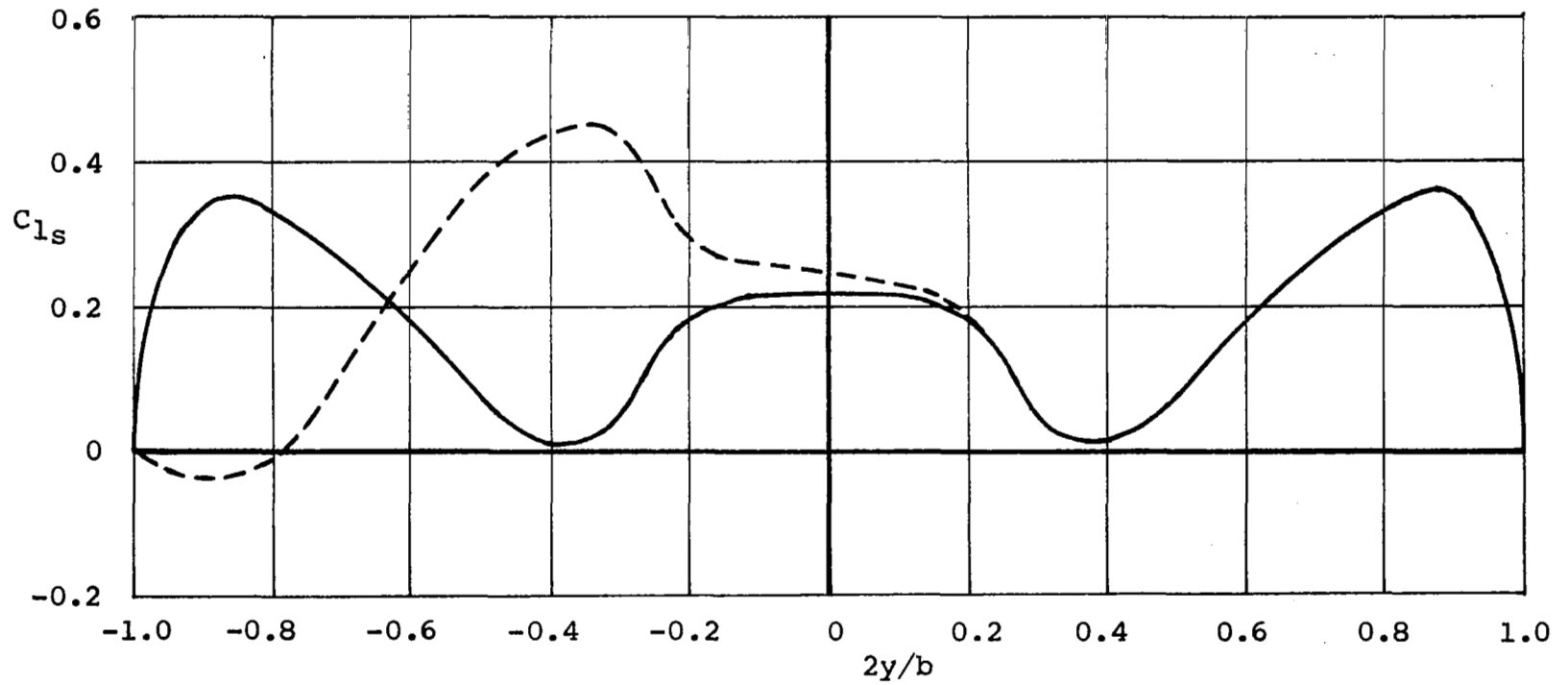


Figure 28. Effect of Propeller Rotation on Span Loading for the Configuration of Reference 42;  $AR = 3.0$ ,  $C_{TS} = 0.64$ ,  $\alpha = 10$  Degrees.

### 5.2.5 Effect of Flap Deflection

One of the prime concerns in the design of modern general aviation type aircraft is the effect of flap deflection (part-span and full-span) or bring stalling characteristics during take-off and landing, i.e. power-on and power-off conditions respectively. This effect can be readily predicted by the computer program developed herein, however the adequacy of the analysis can not be verified because of the lack of suitable experimental data.

Figure 29 demonstrates the capability of the current computer program to predict power-on span load distributions associated with the deflection of part-span flaps. This figure presents the computed results for the twin-propeller configuration of Reference 44, with an arbitrary flap of 60 percent span. The predicted power-off span loadings, with and without flap deflection, are also shown for comparison.

Based on the correlations presented in this section it is concluded that the wing-in-slipstream theory developed herein provides an effective analytical tool for predicting the effects of propeller slipstream on wing spanwise loadings. Unfortunately, due to the lack of suitable experimental data, these correlations had to be limited to unflapped wings operating at conditions below stall. It is expected, however, that if the pressure data was available for wings at the onset of stall and with part-span deflected flaps, the present theory would also prove satisfactory for these conditions. It is therefore recommended that this part of the theory be verified by wind tunnel tests which should include pressure measurements for both the wing and the slipstream for typical wing/propeller combinations operating close to stall.



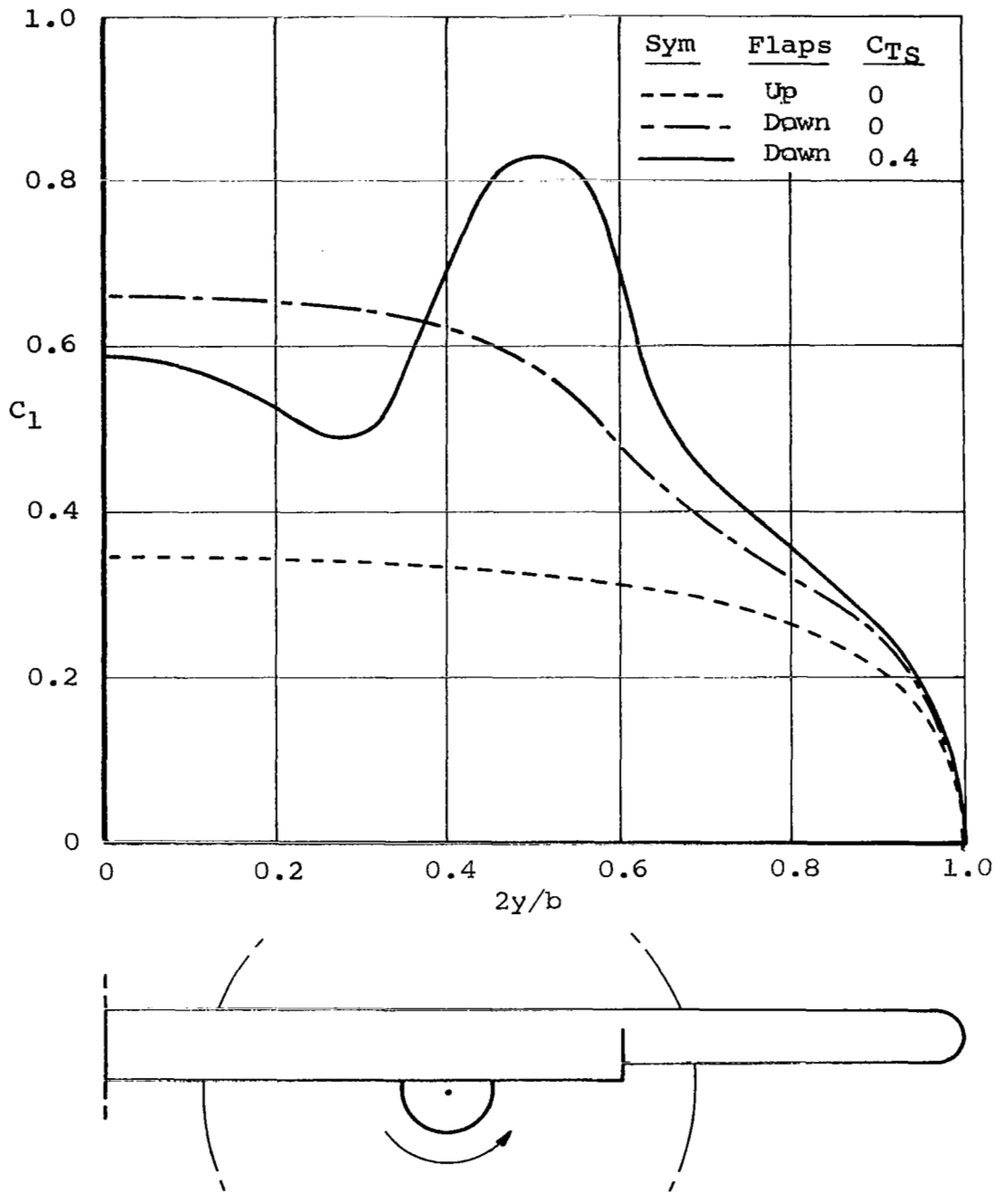


Figure 29. Predicted Spanwise Loadings for the Twin-Propeller Configuration of Reference 44 to Show the Effect of Flap Deflection;  $AR = 4.7$ ,  $\alpha = 10$  Degrees.

## SECTION 6

### CONCLUSIONS AND RECOMMENDATIONS

1. This report presents analytical methods for predicting spanwise load distributions of straight-wing/propeller combinations operating up to stall, for a range of aspect ratio from about 2.0 and higher.
2. The analytical methods developed herein employ non-linear lift curves, in the form of computerized table look-up subroutines, for a variety of wing airfoils and an extensive selection of typical propeller blade sections. These methods are therefore applicable to a wide range of wing/propeller configurations and operating conditions.
3. The predicted results for both propeller slipstream velocity distributions and for wing spanwise loadings are generally in good agreement with the limited test data. However, due to the lack of suitable experimental data involving pressure measurements on wings close to stall and with part-span deflected flaps, the full capability of the analysis could not be verified.
4. Based on the correlations shown in Section 5, it is concluded that the computerized methods developed herein represent an effective analytical tool for predicting the power-on and power-off stalling characteristics of general aviation aircraft.
5. In view of the promising results obtained in this study, it is strongly recommended that a comprehensive wind tunnel program be undertaken to provide the necessary experimental data base to complete verification of the analysis.
6. It is further recommended that the wind tunnel test program must include detailed pressure measurements for both the wing and the slipstream for typical wing/propeller combinations operating throughout the entire range of angle of attack up to and including stall.

## SECTION 7

### REFERENCES

1. McVeigh, M. A.: and Kisielowski, E.: Design Summary of Stall Characteristics of Straight Wing Aircraft. NASA CR 1646, June 1971.
2. Sivells, James C.: and Westrick, Gertrude, C.: Method for Calculating Lift Distributions for Unswept Wings with Flaps or Ailerons by use of Nonlinear Section Lift Data. NACA Rep. 1090, 1952.
3. Koning, C.: Influence of the Propeller on Other Parts of the Airplane Structure. Aerodynamic Theory (Durand, F. W., Editor) Vol. 4. Division M. Julius Springer, Berlin, 1935.
4. Glauert, H.: The Lift and Drag of a Wing Spanning a Free Jet. R & M 1603.
5. Franke, A.: and Weinig, F.: The Effect of the Slipstream on an Airplane Wing. NACA TM 920.
6. Stuper, J.: Effect of Propeller Slipstream on Wing and Tail. NACA TM874, 1938.
7. Graham, E. W.: Lagerstrom, P. A.: Licher, R. M.: and Beane, B. J.: A Preliminary Theoretical Investigation of the Effects of Propeller Slipstream on Wing Lift. Douglas Aircraft Co. Report SM-14991, 1953.
8. Weissinger, J.: The Lift Distribution of Swept-Back Wings. NACA TM 1120, 1947.
9. Ribner, H. S.: and Ellis, N. D.: Theory and Computer Study of a Wing in a Slipstream. AIAA Paper No. 66-466, 1966.
10. Brenckmann, J.: Experimental Investigation of the Aerodynamics of a Wing in a Slipstream, J. Aeron. Sci., Vol.25, No. 5 May 1958, pp. 324-328
11. Gobetz, F. W.: A Review of the Wing-Slipstream Problem with Experiments on a Wing Spanning a Circular Jet. Princeton University. Department of Aeronautical Engineering, Report 489, 1960.

12. Snedeker, Richard S.: Experimental Determination of Spanwise Lift Effects on a Wing of Infinite Aspect Ratio Spanning a Circular Jet. Princeton University, Department of Aeronautical Engineering, Report 525, 1961.
13. Rethorst, S.: Royce, W.: and Wu, T. Yao-tsu: Lift Characteristics of Wings Extending Through Propeller Slipstreams. Vehicle Research Corporation Report No. 1, 1958.
14. Goland, L.: Miller, N.: Butler, L.: Effects of Propeller Slipstream on V/STOL Aircraft Performance and Stability. USAAVLABS Technical Report 64-47, 1964.
15. Huang, K. P.: Goland, L.: and Balin, J.: Charts for Estimating Aerodynamic Forces on STOL Aircraft Wings Immersed in Propeller Slipstream. Dynasciences Report No. DCR-161, Bureau of Naval Weapons, Department of the Navy, Washington, D.C., November 1965.
16. Butler, L.: Huang, K. P.: and Goland, L.: An Investigation of Propeller Slipstream Effects on V/STOL Aircraft Performance and Stability. USAAVLABS Technical Report 65-81, February 1966.
17. George, M.: and Kisielowski, E.: Investigation of Propeller Slipstream Effects on Wing Performance. USAAVLABS Technical Report 67-67, 1967.
18. Fejer, A.: Lifting Line Theory for a Wing in Linearly Varying Flow. Ph.D. Thesis, California Institute of Technology, Pasadena, California, 1945.
19. Glauert, H.: The Elements of Airfoil and Airscrew Theory. Cambridge University Press, 1959.
20. Durand, W. F. (Editor in Chief): Aerodynamic Theory, Volume IV. Dover Publications, Inc., New York, 1963.
21. Lock, C. N. H.: and Yeatman, D.: Tables for Use in an Improved Method of Airscrew Strip Theory Calculation. Aeronautical Research Council, Reports and Memoranda 1674, October 1934.

22. Kuchemann, D.: A Simple Method for Calculating the Span and Chordwise Loading on Straight and Swept Wings of any Aspect Ratio. R & M 2935, August 1952.
23. Filotas, L. T.: Finite Chord Effects on Vortex Induced Wing Loads. AIAA Journal Volume II, No. 6, June 1973.
24. DeYoung, J.: Spanwise Loading for Wings and Control Surfaces of Low Aspect Ratio, NACA TN 2011, August, 1940.
25. Abbott, I. H. and Von Doenhoff, A. E.: Theory of Wing Sections. Dover, New York 1958.
26. Abbott, Jr., F. T. and Von Doenhoff, A. E.: The Langley Two-Dimensional Low-Turbulence Pressure Tunnel. NACA TN-1283
27. Stack, J.: Lindsey, W. F. and Littell, R. E.: The Compressibility Burble and the Effect of Compressibility on Pressures and Forces Acting on an Airfoil. NACA Rept. No. 646, 1938.
28. Summers, J. L. and Treon, S. L.: The Effects of Amount and Type of Camber on The Variation with Mach Number of the Aerodynamic Characteristics of a 10-Percent-Thick NACA 64A-Series Airfoil Section. NACA TN-2096.
29. Robinson, R. G. and Herrnstein, W. H.: Wing-Nacelle-Propeller Interference for Wings of Various Spans; Force and Pressure Distribution Tests. NACA Report No. 569, 1936.
30. Reid, E. G.: Wake Studies of Eight Model Propellers. NACA TN-1040, July, 1946.
31. Draper, J. W. and Kuhn, R. E.: Investigation of the Aerodynamic Characteristics of a Model Wing-Propeller Combination and of the Wing and Propeller Separately at Angles of Attack up to  $90^{\circ}$ , NACA TN-3304.
32. Hammach, J. and Bogeley, A. W.: Propeller Flight Investigation to Determine the Effects of Blade Loading, NACA TN-2022.

33. McLemore, H. C. and Cannon, M. D.: Aerodynamic Investigation of a Four-Blade Propeller Operating through an Angle-of- Attack Range from  $0^{\circ}$  to  $180^{\circ}$ , NACA TN-3228
34. Currie, M. M. and Dunsby, J. A.: Pressure Distributions and Force Measurements on a VTOL Tilting Wing-Propeller Model. Part II: Analysis of Results. National Research Council of Canada, NRC Aero. Rept. LR-284, June 1960.
35. Borst, H. V. and Ladden, R. M.: Propeller Testing at Zero Velocity, CAL/AVLABS Symposium Proceedings: Vol 1, June 1966.
36. Wickens, R. H.: Aerodynamic Force and Moment Characteristics of a Four-Bladed Propeller Yawed Through 120 Degrees. National Research Council of Canada. NRC Aero. Rept. LR-454, May 1966.
37. Weick, F. E.: Aircraft Propeller Design. McGraw Hill, 1960.
38. Pinkerton, R. M. and Greenberg, H.: Aerodynamic Characteristics of a Large Number of Airfoils Tested in the Variable-Density Wind Tunnel, NACA Report No. 628, 1938.
39. Lindsey, W. F.: Stevenson, D. B. and Daley, B. N.: Aerodynamic Characteristics of 24 NACA 16-Series Airfoils at Mach Numbers Between 0.3 and 0.8. NACA TN-1546, September 1948.
40. Abbott, I. H.: Von Doenhoff, A. E. and Stivers, L. S.: Summary of Airfoil Data. NACA TR-824, 1945.
41. Loftin, L. K., Jr. and Smith, H. A.: Aerodynamic Characteristics of 15 NACA Airfoil Sections at Seven Reynolds Numbers from  $0.7 \times 10^6$  to  $9.0 \times 10^6$ . NACA TN-1945, 1949.
42. Currie, M. M., and Dunsby, J. A.: Pressure Distribution and Force Measurements on a VTOL Tilting Wing-Propeller Model Part II; Analysis of Results. NRC LR-284, June 1960.

43. Falkner, V. M.: The Solution of Lifting Plane Problems by Vortex Lattice Theory. R & M 2591, September 1947.
44. Nishimura, Y.: An Experimental Investigation by Force and Surface Pressure Measurements of a Wing Immersed in a Propeller Slipstream Part II; Surface Pressure Measurements. NRC LR-525, June 1969.

## APPENDIX A

### PROPELLER TIP LOSS CORRECTION TABLES

This appendix presents a computer-generated listing of the propeller tip loss correction factors utilized by the computer program described herein. These correction factors are applied as described in Section 4.1 to obtain an improvement to the approximate tip loss factor given by equation (16).

These correction factors are based directly on the tabulated values generated by Lock, as given in Reference 21. However, the original tables given by Lock have been modified and enlarged to provide for more uniform increments in the two parametric variables,  $\bar{r}$  and  $\sin \phi$ . These changes permit a more efficient table look-up interpolation procedure and provide for an improved definition of the correction factors. The additional and intermediate values of these factors were obtained through crossplotting of the original tabulated data and by using suitably faired curves.

The following tables are presented for propellers having either 2, 3, or 4 blades. For propellers with more than 4 blades, the computer program assumes a correction factor of unity for all values of  $\bar{r}$  and  $\sin \phi$ .



TIP LOSS CORRECTIONS - TABULATION OF F/FP FOR 2 BLADED PROPELLERS

R/RP	0.3	0.4	0.5	0.6	0.7	0.8	0.9	1.0
SIN(PFI)								
0.00	1.000	1.000	1.000	1.000	1.000	1.000	1.000	1.000
0.05	1.000	1.000	1.000	1.000	1.000	0.998	0.994	0.990
0.10	1.000	1.000	0.999	0.998	0.996	0.990	0.983	0.976
0.15	0.999	0.998	0.997	0.994	0.987	0.978	0.966	0.955
0.20	0.995	0.994	0.990	0.984	0.972	0.959	0.940	0.923
0.25	0.987	0.984	0.979	0.965	0.949	0.929	0.906	0.877
0.30	0.978	0.974	0.965	0.945	0.923	0.894	0.865	0.827
0.35	0.969	0.963	0.949	0.924	0.894	0.858	0.820	0.785
0.40	0.961	0.952	0.931	0.902	0.863	0.822	0.781	0.746
0.45	0.956	0.941	0.913	0.879	0.831	0.786	0.746	0.711
0.50	0.954	0.929	0.894	0.852	0.801	0.757	0.717	0.681
0.55	0.953	0.918	0.876	0.827	0.777	0.734	0.694	0.656
0.60	0.955	0.907	0.856	0.806	0.759	0.715	0.674	0.635
0.65	0.963	0.900	0.843	0.791	0.746	0.699	0.656	0.616
0.70	0.975	0.897	0.835	0.780	0.735	0.685	0.639	0.598
0.75	0.992	0.899	0.833	0.777	0.726	0.671	0.622	0.581
0.80	1.015	0.911	0.840	0.777	0.718	0.658	0.607	0.564
0.85	1.056	0.942	0.855	0.780	0.710	0.646	0.592	0.547
0.90	1.128	0.990	0.877	0.784	0.704	0.634	0.577	0.531
0.95	1.240	1.060	0.906	0.791	0.698	0.623	0.563	0.515
1.00	1.512	1.170	0.940	0.798	0.692	0.612	0.550	0.500

TIP LOSS CORRECTIONS - TABULATION OF F/FP FOR 3 BLADED PROPELLERS

R/RP	0.3	0.4	0.5	0.6	0.7	0.8	0.9	1.0
SIN(PHI)								
0.00	1.000	1.000	1.000	1.000	1.000	1.000	1.000	1.000
0.05	1.000	1.000	1.000	1.000	1.000	0.999	0.997	0.995
0.10	1.000	1.000	0.999	0.999	0.999	0.995	0.992	0.987
0.15	0.999	0.999	0.997	0.997	0.995	0.990	0.985	0.976
0.20	0.997	0.996	0.994	0.993	0.990	0.982	0.972	0.960
0.25	0.995	0.993	0.991	0.987	0.981	0.971	0.953	0.938
0.30	0.992	0.990	0.986	0.980	0.968	0.955	0.931	0.910
0.35	0.989	0.985	0.979	0.971	0.954	0.935	0.905	0.879
0.40	0.985	0.979	0.970	0.959	0.938	0.910	0.876	0.844
0.45	0.980	0.973	0.961	0.945	0.919	0.886	0.845	0.809
0.50	0.976	0.967	0.953	0.931	0.900	0.861	0.815	0.777
0.55	0.975	0.964	0.947	0.918	0.882	0.837	0.789	0.749
0.60	0.978	0.965	0.941	0.906	0.865	0.816	0.765	0.724
0.65	0.986	0.968	0.939	0.897	0.849	0.796	0.744	0.701
0.70	0.999	0.976	0.938	0.890	0.835	0.779	0.725	0.680
0.75	1.020	0.986	0.939	0.885	0.823	0.763	0.706	0.661
0.80	1.051	1.001	0.944	0.882	0.815	0.750	0.689	0.644
0.85	1.099	1.028	0.957	0.886	0.812	0.739	0.675	0.627
0.90	1.163	1.073	0.984	0.897	0.814	0.730	0.663	0.611
0.95	1.255	1.145	1.025	0.914	0.815	0.722	0.652	0.597
1.00	1.535	1.275	1.080	0.935	0.817	0.715	0.642	0.583

## TIP LOSS CORRECTIONS - TABULATION OF F/FP FOR 4 BLADED PROPELLERS

R/RP	0.3	0.4	0.5	0.6	0.7	0.8	0.9	1.0
SIN(PHI)								
0.00	1.000	1.000	1.000	1.000	1.000	1.000	1.000	1.000
0.05	1.000	1.000	1.000	1.000	1.000	1.000	0.998	0.997
0.10	1.000	1.000	1.000	1.000	1.000	0.997	0.995	0.992
0.15	1.000	1.000	0.999	0.998	0.998	0.995	0.990	0.985
0.20	0.999	0.999	0.998	0.996	0.995	0.991	0.983	0.975
0.25	0.998	0.998	0.996	0.994	0.991	0.983	0.972	0.959
0.30	0.996	0.995	0.993	0.991	0.984	0.973	0.956	0.937
0.35	0.994	0.992	0.989	0.985	0.974	0.959	0.936	0.909
0.40	0.991	0.988	0.984	0.977	0.962	0.940	0.912	0.878
0.45	0.987	0.984	0.979	0.967	0.948	0.920	0.887	0.850
0.50	0.985	0.981	0.974	0.958	0.933	0.901	0.863	0.824
0.55	0.985	0.980	0.970	0.949	0.919	0.882	0.841	0.800
0.60	0.987	0.981	0.966	0.940	0.905	0.864	0.820	0.777
0.65	0.993	0.985	0.965	0.932	0.892	0.848	0.801	0.756
0.70	1.004	0.991	0.965	0.926	0.880	0.833	0.783	0.737
0.75	1.022	1.004	0.969	0.922	0.870	0.818	0.765	0.719
0.80	1.049	1.021	0.976	0.921	0.862	0.806	0.748	0.701
0.85	1.090	1.048	0.989	0.923	0.857	0.795	0.733	0.684
0.90	1.155	1.090	1.009	0.929	0.855	0.786	0.720	0.667
0.95	1.250	1.156	1.043	0.943	0.857	0.779	0.709	0.652
1.00	1.493	1.267	1.095	0.965	0.862	0.773	0.699	0.637

## APPENDIX B

### PROPELLER AIRFOIL TABLES

3

This appendix presents a computer-generated listing of the propeller blade section data tables that are available for use by the computer program.

Each table contains the values of lift coefficient versus angle of attack for a range of Mach number conditions for one specified airfoil section. At the head of each table is descriptive information on the airfoil name and data source. This is followed by the airfoil series code identification and the main geometric and test parameters.

The following tables contain the selected propeller station characteristics for airfoils of the U.S.N.P.S., Clark Y, NACA 16, NACA 64 and NACA 65 families. The sets of tables for each airfoil series are arranged in the specific order of increasing Mach number, thickness/chord ratio and design lift coefficient, as necessary for proper utilization by the computer program.

PROPELLER BLADE SECTION AIRFOIL TABLES

AIRFOIL SECTION	USNPS -M04		USNPS -M06		USNPS -M08		USNPS -M10		USNPS -M12		USNPS -M14	
TABLE DATA SOURCE	F E WEICK		F E WEICK		F E WEICK		F E WEICK		F E WEICK		F E WEICK	
AIRFOIL SER CODE	1		1		1		1		1		1	
DESIGN LIFT COEFF	0.000		0.000		0.000		0.000		0.000		0.000	
THICKNESS / CHORD	0.040		0.060		0.080		0.100		0.120		0.140	
MACH NUMBER	0.070		0.070		0.070		0.070		0.070		0.070	
ZERO LIFT ALPHA	-1.900		-2.600		-3.350		-4.300		-5.250		-6.300	
EXTRAP COEFF KCLI	0.000		0.000		0.000		0.000		0.000		0.000	
ALPHA, CL VALUES	-1.900	0.000	-2.600	0.000	-3.350	0.000	-4.300	0.000	-5.250	0.000	-6.300	0.000
	0.000	0.200	2.000	0.465	4.000	0.735	4.000	0.800	2.000	0.700	-4.000	0.200
	2.000	0.420	4.000	0.660	6.000	0.925	6.000	0.985	4.000	0.880	-2.000	0.390
	4.000	0.615	6.000	0.850	8.000	1.105	8.000	1.145	6.000	1.055	2.000	0.765
	6.000	0.760	8.000	1.020	10.000	1.200	10.000	1.310	8.000	1.220	4.000	0.935
	8.000	0.860	10.000	1.075	11.000	1.215	11.000	1.395	10.000	1.370	6.000	1.090
	10.000	0.915	12.000	1.040	12.000	1.160	12.000	1.435	12.000	1.470	8.000	1.230
	12.000	0.930	14.000	1.010	14.000	1.105	14.000	1.235	13.200	1.490	10.000	1.355
	14.000	0.925	16.000	0.990	16.000	1.060	16.000	1.095	14.000	1.480	12.000	1.440
	16.000	0.885	0.000	0.000	0.000	0.000	0.000	0.000	16.000	1.240	13.000	1.430
	0.000	0.000	0.000	0.000	0.000	0.000	0.000	0.000	0.000	0.000	14.000	1.385
	0.000	0.000	0.000	0.000	0.000	0.000	0.000	0.000	0.000	0.000	16.000	1.230
AIRFOIL SECTION	USNPS -M16		USNPS -M18		USNPS -M20							
TABLE DATA SOURCE	F E WEICK		F E WEICK		F E WEICK							
AIRFOIL SER CODE	1		1		1		0		0		0	
DESIGN LIFT COEFF	0.000		0.000		0.000		0.000		0.000		0.000	
THICKNESS / CHORD	0.160		0.180		0.200		0.000		0.000		0.000	
MACH NUMBER	0.070		0.070		0.070		0.000		0.000		0.000	
ZERO LIFT ALPHA	-7.400		-8.700		-10.200		0.000		0.000		0.000	
EXTRAP COEFF KCLI	0.000		0.000		0.000		0.000		0.000		0.000	
ALPHA, CL VALUES	-7.400	0.000	-8.700	0.000	-10.200	0.000	0.000	0.000	0.000	0.000	0.000	0.000
	-6.000	0.110	-4.000	0.320	-6.000	0.215	0.000	0.000	0.000	0.000	0.000	0.000
	-4.000	0.270	-2.000	0.490	-4.000	0.345	0.000	0.000	0.000	0.000	0.000	0.000
	-2.000	0.450	0.000	0.650	-2.000	0.490	0.000	0.000	0.000	0.000	0.000	0.000
	2.000	0.795	2.000	0.795	0.000	0.630	0.000	0.000	0.000	0.000	0.000	0.000
	4.000	0.950	4.000	0.950	2.000	0.760	0.000	0.000	0.000	0.000	0.000	0.000
	6.000	1.095	6.000	1.070	4.000	0.890	0.000	0.000	0.000	0.000	0.000	0.000
	8.000	1.210	8.000	1.165	6.000	1.010	0.000	0.000	0.000	0.000	0.000	0.000
	10.000	1.305	10.000	1.240	8.000	1.110	0.000	0.000	0.000	0.000	0.000	0.000
	12.000	1.375	12.000	1.285	10.000	1.165	0.000	0.000	0.000	0.000	0.000	0.000
	13.000	1.365	14.000	1.220	11.000	1.180	0.000	0.000	0.000	0.000	0.000	0.000
	14.000	1.305	16.000	1.135	12.000	1.170	0.000	0.000	0.000	0.000	0.000	0.000
	16.000	1.195	0.000	0.000	14.000	1.135	0.000	0.000	0.000	0.000	0.000	0.000
	0.000	0.000	0.000	0.000	16.000	1.060	0.000	0.000	0.000	0.000	0.000	0.000

## PROPELLER BLADE SECTION AIRFOIL TABLES

AIRFOIL SECTION	CLARK.Y-M06		CLARK.Y-M08		CLARK.Y-M10		CLARK.Y		CLARK.Y-M14		CLARK.Y-M18	
TABLE DATA SOURCE	NACA TR-628		NACA TR-628		NACA TR-628		NACA TR-628		NACA TR-628		NACA TR-628	
AIRFOIL SER CODE	2		2		2		2		2		2	
DESIGN LIFT COEFF	0.000		0.000		0.000		0.000		0.000		0.000	
THICKNESS / CHORD	0.060		0.080		0.100		0.117		0.140		0.180	
MACH NUMBER	0.060		0.060		0.060		0.060		0.060		0.060	
ZERO LIFT ALPHA	-2.950		-3.560		-4.560		-5.000		-6.200		-7.600	
EXTRAP COEFF KCLI	0.000		0.000		0.000		0.000		0.000		0.000	
ALPHA, CL VALUES	-6.000	-0.300	-6.000	-0.235	-6.000	-0.130	-6.000	-0.095	-6.200	0.000	-7.600	0.000
	-2.950	0.000	-3.560	0.000	-4.560	0.000	-5.000	0.000	2.000	0.800	-6.000	0.160
	4.000	0.680	6.000	0.925	2.000	0.640	-2.000	0.285	4.000	0.985	-4.000	0.350
	6.000	0.865	8.000	1.110	4.000	0.830	6.000	1.030	6.000	1.160	2.000	0.890
	8.000	0.985	10.000	1.280	6.000	1.015	8.000	1.200	8.000	1.315	4.000	1.040
	10.000	1.060	11.500	1.370	8.000	1.195	10.000	1.360	10.000	1.465	6.000	1.185
	12.000	1.070	12.000	1.290	10.000	1.365	12.000	1.485	12.000	1.590	8.000	1.315
	14.000	1.050	14.000	1.170	12.000	1.500	14.000	1.610	14.000	1.720	10.000	1.420
	16.000	1.020	16.000	1.100	14.000	1.635	15.300	1.680	16.000	1.550	12.000	1.470
	0.000	0.000	0.000	0.000	14.800	1.680	16.000	1.500	20.000	1.430	13.000	1.480
	0.000	0.000	0.000	0.000	16.000	1.420	20.000	1.300	0.000	0.000	14.000	1.470
	0.000	0.000	0.000	0.000	20.000	1.220	0.000	0.000	0.000	0.000	16.000	1.430
	0.000	0.000	0.000	0.000	0.000	0.000	0.000	0.000	0.000	0.000	20.000	1.360
AIRFOIL SECTION	CLARK.Y-M22		NACA 16106		NACA 16106		NACA 16106		NACA 16106		NACA 16106	
TABLE DATA SOURCE	NACA TR-628		NACA TN-1546		NACA TN-1546		NACA TN-1546		NACA TN-1546			
AIRFOIL SER CODE	2		3		3		3		3		3	
DESIGN LIFT COEFF	0.000		0.100		0.100		0.100		0.100		0.100	
THICKNESS / CHORD	0.220		0.060		0.060		0.060		0.060		0.060	
MACH NUMBER	0.060		0.300		0.450		0.600		0.700		0.750	
ZERO LIFT ALPHA	-9.290		-1.050		-1.100		-1.100		-1.000		-1.000	
EXTRAP COEFF KCLI	0.000		0.760		0.760		0.760		0.760		0.760	
ALPHA, CL VALUES	-9.290	0.000	-2.000	-0.085	-2.000	-0.090	-2.000	-0.105	-2.000	-0.130	-2.000	-0.145
	-6.000	0.300	-1.050	0.000	0.000	0.105	0.000	0.110	0.000	0.120	2.000	0.405
	-4.000	0.480	0.000	0.100	2.000	0.305	2.000	0.340	2.000	0.375	0.000	0.000
	0.000	0.800	2.000	0.305	4.000	0.540	4.000	0.600	3.000	0.540	0.000	0.000
	2.000	0.950	4.000	0.510	6.000	0.705	5.000	0.705	3.770	0.725	0.000	0.000
	4.000	1.085	6.000	0.670	8.000	0.820	6.000	0.780	0.000	0.000	0.000	0.000
	6.000	1.185	8.000	0.815	9.000	0.835	0.000	0.000	0.000	0.000	0.000	0.000
	8.000	1.265	9.000	0.850	10.000	0.810	0.000	0.000	0.000	0.000	0.000	0.000
	10.000	1.320	10.000	0.855	0.000	0.000	0.000	0.000	0.000	0.000	0.000	0.000
	12.000	1.350	0.000	0.000	0.000	0.000	0.000	0.000	0.000	0.000	0.000	0.000
	13.000	1.360	0.000	0.000	0.000	0.000	0.000	0.000	0.000	0.000	0.000	0.000
	14.000	1.340	0.000	0.000	0.000	0.000	0.000	0.000	0.000	0.000	0.000	0.000
	16.000	1.300	0.000	0.000	0.000	0.000	0.000	0.000	0.000	0.000	0.000	0.000
	20.000	1.240	0.000	0.000	0.000	0.000	0.000	0.000	0.000	0.000	0.000	0.000

PROPELLER BLADE SECTION AIRFOIL TABLES

AIRFOIL SECTION	NACA 16106		NACA 16109		NACA 16109		NACA 16109		NACA 16109		NACA 16109	
TABLE DATA SOURCE	NACA TN-1546		NACA TN-1546		NACA TN-1546		NACA TN-1546		NACA TN-1546		NACA TN-1546	
AIRFOIL SER CODE	3		3		3		3		3		3	
DESIGN LIFT COEFF	0.100		0.100		0.100		0.100		0.100		0.100	
THICKNESS / CHORD	0.060		0.090		0.090		0.090		0.090		0.090	
MACH NUMBER	0.800		0.300		0.450		0.600		0.700		0.750	
ZERO LIFT ALPHA	-0.950		-1.000		-1.100		-1.000		-1.000		-0.850	
EXTRAP COEFF KCLF	0.760		0.730		0.730		0.730		0.730		0.730	
ALPHA, CL VALUES	-2.000	-0.175	-2.000	-0.085	-2.000	-0.080	-2.000	-0.090	-2.000	-0.100	-2.000	-0.110
	-0.950	0.000	-1.000	0.000	0.000	0.095	0.000	0.100	0.000	0.115	-1.000	-0.025
	1.770	0.450	0.000	0.090	2.000	0.295	2.000	0.320	2.000	0.365	0.000	0.125
	0.000	0.000	2.000	0.295	4.000	0.470	4.000	0.500	4.000	0.520	2.000	0.420
	0.000	0.000	4.000	0.465	6.000	0.665	6.000	0.700	0.000	0.000	3.770	0.630
	0.000	0.000	6.000	0.660	8.000	0.785	7.000	0.750	0.000	0.000	0.000	0.000
	0.000	0.000	8.000	0.790	9.000	0.805	8.000	0.780	0.000	0.000	0.000	0.000
	0.000	0.000	10.000	0.835	10.000	0.795	10.000	0.790	0.000	0.000	0.000	0.000
	0.000	0.000	11.000	0.850	11.000	0.775	12.000	0.785	0.000	0.000	0.000	0.000
	0.000	0.000	0.000	0.000	12.000	0.755	0.000	0.000	0.000	0.000	0.000	0.000
AIRFOIL SECTION	NACA 16109		NACA 16115		NACA 16115		NACA 16115		NACA 16115		NACA 16130	
TABLE DATA SOURCE	NACA TN-1546		NACA TN-1546		NACA TN-1546		NACA TN-1546		NACA TN-1546		NACA TN-1546	
AIRFOIL SER CODE	3		3		3		3		3		3	
DESIGN LIFT COEFF	0.100		0.100		0.100		0.100		0.100		0.100	
THICKNESS / CHORD	0.090		0.150		0.150		0.150		0.150		0.300	
MACH NUMBER	0.800		0.300		0.450		0.600		0.700		0.300	
ZERO LIFT ALPHA	-1.000		-0.800		-0.800		-0.800		-0.800		0.500	
EXTRAP COEFF KCLF	0.730		0.600		0.600		0.600		0.600		-0.190	
ALPHA, CL VALUES	-2.000	-0.130	-2.000	-0.110	-2.000	-0.110	-2.000	-0.115	-2.000	-0.130	-2.000	-0.110
	-1.000	0.000	-0.800	0.000	0.000	0.080	0.000	0.085	-0.800	0.000	0.000	-0.025
	1.770	0.360	0.000	0.080	2.000	0.260	2.000	0.280	0.000	0.085	0.500	0.000
	0.000	0.000	2.000	0.260	4.000	0.330	4.000	0.355	2.000	0.295	2.000	0.100
	0.000	0.000	4.000	0.350	5.000	0.380	5.000	0.405	3.770	0.400	4.000	0.195
	0.000	0.000	5.000	0.390	6.000	0.445	6.000	0.470	0.000	0.000	6.000	0.245
	0.000	0.000	6.000	0.445	8.000	0.620	8.000	0.620	0.000	0.000	8.000	0.260
	0.000	0.000	7.000	0.515	10.000	0.790	10.000	0.860	0.000	0.000	10.000	0.295
	0.000	0.000	8.000	0.620	11.000	0.800	11.000	0.830	0.000	0.000	11.770	0.345
	0.000	0.000	10.000	0.785	11.770	0.780	11.770	0.690	0.000	0.000	0.000	0.000
	0.000	0.000	11.770	0.855	0.000	0.000	0.000	0.000	0.000	0.000	0.000	0.000







## PROPELLER BLADE SECTION AIRFOIL TABLES

AIRFOIL SECTION	NACA 16506		NACA 16506		NACA 16506		NACA 16506		NACA 16509		NACA 16509	
TABLE DATA SOURCE	NACA TN-1546		NACA TN-1546		NACA TN-1546		NACA TN-1546		NACA TN-1546		NACA TN-1546	
AIRFOIL SER CODE	3		3		3		3		3		3	
DESIGN LIFT COEFF	0.500		0.500		0.500		0.500		0.500		0.500	
THICKNESS / CHORD	0.060		0.060		0.060		0.060		0.090		0.090	
MACH NUMBER	0.450		0.600		0.700		0.750		0.300		0.450	
ZERO LIFT ALPHA	-3.900		-3.700		-3.500		-3.400		-4.200		-4.250	
EXTRAP COEFF KCLI	0.760		0.760		0.760		0.760		0.730		0.730	
ALPHA, CL VALUES	-4.000	-0.010	-4.000	-0.040	-4.000	-0.080	-3.400	0.000	-4.200	0.000	-4.000	0.025
	2.000	0.660	1.000	0.605	-2.000	0.230	-2.000	0.240	2.000	0.615	2.000	0.645
	3.000	0.720	2.000	0.730	1.770	0.830	0.000	0.595	4.000	0.710	4.000	0.730
	4.000	0.795	3.770	0.765	0.000	0.000	1.770	0.850	7.770	0.990	5.000	0.805
	6.000	0.970	0.000	0.000	0.000	0.000	0.000	0.000	0.000	0.000	6.000	0.905
	7.770	1.085	0.000	0.000	0.000	0.000	0.000	0.000	0.000	0.000	7.770	1.040
AIRFOIL SECTION	NACA 16509		NACA 16509		NACA 16509		NACA 16512		NACA 16512		NACA 16512	
TABLE DATA SOURCE	NACA TN-1546		NACA TN-1546		NACA TN-1546		NACA TN-1546		NACA TN-1546		NACA TN-1546	
AIRFOIL SER CODE	3		3		3		3		3		3	
DESIGN LIFT COEFF	0.500		0.500		0.500		0.500		0.500		0.500	
THICKNESS / CHORD	0.090		0.090		0.090		0.120		0.120		0.120	
MACH NUMBER	0.600		0.700		0.750		0.300		0.450		0.600	
ZERO LIFT ALPHA	-4.200		-4.200		-4.100		-4.200		-4.250		-4.200	
EXTRAP COEFF KCLI	0.730		0.730		0.730		0.690		0.690		0.690	
ALPHA, CL VALUES	-4.000	0.020	-5.000	-0.085	-4.100	0.000	-4.200	0.000	-4.000	0.025	-4.000	0.025
	1.000	0.605	-4.000	0.020	0.000	0.560	2.000	0.545	2.000	0.570	0.000	0.420
	2.000	0.720	1.770	0.780	1.770	0.750	4.000	0.700	3.000	0.645	2.000	0.620
	4.000	0.810	0.000	0.000	0.000	0.000	6.000	0.770	4.000	0.700	3.000	0.705
	5.770	0.930	0.000	0.000	0.000	0.000	8.000	0.905	6.000	0.790	4.000	0.775
	0.000	0.000	0.000	0.000	0.000	0.000	10.000	1.010	7.770	0.910	5.770	0.840
	0.000	0.000	0.000	0.000	0.000	0.000	11.770	1.070	0.000	0.000	0.000	0.000

PROPELLER BLADE SECTION AIRFOIL TABLES

AIRFOIL SECTION	NACA 16512		NACA 16512		NACA 16515		NACA 16515		NACA 16515		NACA 16515	
TABLE DATA SOURCE	NACA TN-1546		NACA TN-1546		NACA TN-1546		NACA TN-1546		NACA TN-1546		NACA TN-1546	
AIRFOIL SER CODE	3		3		3		3		3		3	
DESIGN LIFT COEFF	0.500		0.500		0.500		0.500		0.500		0.500	
THICKNESS / CHORD	0.120		0.120		0.150		0.150		0.150		0.150	
MACH NUMBER	0.700		0.750		0.300		0.450		0.600		0.700	
ZERO LIFT ALPHA	-4.100		-3.600		-4.400		-4.500		-4.600		-4.700	
EXTRAP COEFF KCLI	0.690		0.690		0.600		0.600		0.600		0.600	
ALPHA, CL VALUES	-4.000	0.005	-3.600	0.000	-4.400	0.000	-4.000	0.040	-4.000	0.045	-4.000	0.065
	-2.000	0.225	-2.000	0.200	-4.000	0.025	-2.000	0.195	-2.000	0.220	-2.000	0.235
	0.000	0.440	0.000	0.380	-2.000	0.155	0.000	0.325	0.000	0.325	-1.000	0.265
	2.000	0.675	2.000	0.530	0.000	0.305	2.000	0.520	2.000	0.525	0.000	0.315
	3.000	0.780	3.770	0.680	2.000	0.495	3.000	0.600	4.000	0.720	2.000	0.530
	3.770	0.825	0.000	0.000	4.000	0.660	4.000	0.655	6.000	0.780	3.770	0.710
	0.000	0.000	0.000	0.000	6.000	0.710	6.000	0.715	7.000	0.840	0.000	0.000
	0.000	0.000	0.000	0.000	8.000	0.815	8.000	0.825	7.770	0.915	0.000	0.000
	0.000	0.000	0.000	0.000	10.000	0.920	10.000	0.940	0.000	0.000	0.000	0.000
	0.000	0.000	0.000	0.000	12.000	1.010	12.000	1.025	0.000	0.000	0.000	0.000
	0.000	0.000	0.000	0.000	13.770	1.030	13.770	1.010	0.000	0.000	0.000	0.000
AIRFOIL SECTION	NACA 16515		NACA 16521		NACA 16521		NACA 16521		NACA 16521		NACA 16530	
TABLE DATA SOURCE	NACA TN-1546		NACA TN-1546		NACA TN-1546		NACA TN-1546		NACA TN-1546		NACA TN-1546	
AIRFOIL SER CODE	3		3		3		3		3		3	
DESIGN LIFT COEFF	0.500		0.500		0.500		0.500		0.500		0.500	
THICKNESS / CHORD	0.150		0.210		0.210		0.210		0.210		0.300	
MACH NUMBER	0.750		0.300		0.450		0.600		0.700		0.300	
ZERO LIFT ALPHA	-1.600		-2.300		-2.000		-1.800		-0.400		1.500	
EXTRAP COEFF KCLI	0.600		0.370		0.370		0.370		0.370		-0.190	
ALPHA, CL VALUES	-2.000	-0.045	-2.000	0.030	-2.000	0.070	-2.000	0.120	-2.000	-0.210	0.000	-0.100
	-1.600	0.000	3.000	0.455	-1.000	0.000	-1.000	0.120	-1.000	-0.080	6.000	0.300
	0.000	0.145	4.000	0.540	0.000	0.180	0.000	0.170	-0.400	0.000	8.000	0.405
	1.000	0.210	5.000	0.605	2.000	0.360	3.000	0.440	0.000	0.035	9.770	0.470
	2.000	0.295	6.000	0.650	4.000	0.520	4.000	0.530	2.000	0.020	0.000	0.000
	3.770	0.480	8.000	0.685	6.000	0.620	5.000	0.590	3.000	0.190	0.000	0.000
	0.000	0.000	10.000	0.750	8.000	0.670	6.000	0.610	3.770	0.270	0.000	0.000
	0.000	0.000	11.770	0.860	11.770	0.840	7.000	0.660	0.000	0.000	0.000	0.000
	0.000	0.000	0.000	0.000	0.000	0.000	8.000	0.750	0.000	0.000	0.000	0.000
	0.000	0.000	0.000	0.000	0.000	0.000	9.770	0.910	0.000	0.000	0.000	0.000

PROPELLER BLADE SECTION AIRFOIL TABLES

AIRFOIL SECTION	NACA 16530	NACA 16530	NACA 16709	NACA 16709	NACA 16709	NACA 16709
TABLE DATA SOURCE	NACA TN-1546	NACA TN-1546	NACA TN-1546	NACA TN-1546	NACA TN-1546	NACA TN-1546
AIRFOIL SER CODE	3	3	3	3	3	3
DESIGN LIFT COEFF	0.500	0.500	0.700	0.700	0.700	0.700
THICKNESS / CHORD	0.300	0.300	0.090	0.090	0.090	0.090
MACH NUMBER	0.450	0.600	0.300	0.450	0.600	0.700
ZERO LIFT ALPHA	2.200	3.200	-5.400	-5.500	-5.500	-5.600
EXTRAP COEFF KCLI	-0.190	-0.190	0.730	0.730	0.730	0.730
ALPHA, CL VALUES	0.000 -0.120	0.000 -0.280	-6.000 -0.065	-6.000 -0.060	-6.000 -0.050	-6.000 -0.020
	2.000 -0.015	3.200 0.000	-5.400 0.000	-4.000 0.145	-4.000 0.150	-5.000 0.040
	4.000 0.115	4.000 0.070	-4.000 0.140	0.000 0.580	-2.000 0.395	-4.000 0.150
	6.000 0.245	6.000 0.120	-2.000 0.345	1.000 0.690	0.000 0.645	-2.000 0.445
	8.000 0.355	8.000 0.280	0.000 0.550	2.000 0.780	2.000 0.855	0.000 0.750
	9.770 0.415	9.770 0.430	2.000 0.755	4.000 0.880	4.000 1.010	2.000 0.915
	0.000 0.000	0.000 0.000	3.000 0.815	6.000 1.005	5.770 1.110	0.000 0.000
	0.000 0.000	0.000 0.000	4.000 0.850	8.000 1.140	0.000 0.000	0.000 0.000
	0.000 0.000	0.000 0.000	5.000 0.895	9.000 1.200	0.000 0.000	0.000 0.000
	0.000 0.000	0.000 0.000	6.000 0.965	9.770 1.210	0.000 0.000	0.000 0.000
	0.000 0.000	0.000 0.000	7.770 1.080	0.000 0.000	0.000 0.000	0.000 0.000
AIRFOIL SECTION	NACA 16709	NACA 16709	NACA 16712	NACA 16712	NACA 16712	NACA 16712
TABLE DATA SOURCE	NACA TN-1546	NACA TN-1546	NACA TN-1546	NACA TN-1546	NACA TN-1546	NACA TN-1546
AIRFOIL SER CODE	3	3	3	3	3	3
DESIGN LIFT COEFF	0.700	0.700	0.700	0.700	0.700	0.700
THICKNESS / CHORD	0.090	0.090	0.120	0.120	0.120	0.120
MACH NUMBER	0.750	0.775	0.300	0.450	0.600	0.700
ZERO LIFT ALPHA	-5.400	-3.500	-5.500	-5.600	-6.000	-6.000
EXTRAP COEFF KCLI	0.730	0.730	0.690	0.690	0.690	0.690
ALPHA, CL VALUES	-4.000 0.150	-4.000 -0.100	-6.000 -0.040	-6.000 -0.035	-6.000 0.000	-4.000 0.150
	-2.000 0.375	-3.500 0.000	-4.000 0.120	-4.000 0.130	-5.000 0.060	-2.000 0.365
	0.000 0.585	-2.000 0.205	0.000 0.495	-2.000 0.340	-4.000 0.150	0.000 0.575
	1.000 0.620	0.000 0.460	2.000 0.685	2.000 0.740	2.000 0.825	1.770 0.760
	2.000 0.670	1.770 0.535	4.000 0.885	4.000 0.910	3.770 1.040	0.000 0.000
	3.770 0.820	0.000 0.000	6.000 0.930	6.000 0.960	0.000 0.000	0.000 0.000
	0.000 0.000	0.000 0.000	8.000 1.025	8.000 1.085	0.000 0.000	0.000 0.000
	0.000 0.000	0.000 0.000	10.000 1.140	9.770 1.175	0.000 0.000	0.000 0.000
	0.000 0.000	0.000 0.000	11.770 1.210	0.000 0.000	0.000 0.000	0.000 0.000

PROPELLER BLADE SECTION AIRFOIL TABLES

AIRFOIL SECTION	NACA 16715		NACA 16715		NACA 16715		0		0		0	
TABLE DATA SOURCE	NACA TN-1546		NACA TN-1546		NACA TN-1546							
AIRFOIL SER CODE	3		3		3		0		0		0	
DESIGN LIFT COEFF	0.700		0.700		0.700		0.000		0.000		0.000	
THICKNESS / CHORD	0.150		0.150		0.150		0.000		0.000		0.000	
MACH NUMBER	0.300		0.450		0.600		0.000		0.000		0.000	
ZERO LIFT ALPHA	-5.400		-5.500		-5.400		0.000		0.000		0.000	
EXTRAP COEFF KCLI	0.600		0.600		0.600		0.000		0.000		0.000	
ALPHA, CL VALUES	-6.000	-0.045	-6.000	-0.050	-6.000	-0.040	0.000	0.000	0.000	0.000	0.000	0.000
	-5.400	0.000	-4.000	0.130	-5.400	0.000	0.000	0.000	0.000	0.000	0.000	0.000
	-4.000	0.110	-2.000	0.300	-4.000	0.120	0.000	0.000	0.000	0.000	0.000	0.000
	-2.000	0.295	0.000	0.460	-2.000	0.325	0.000	0.000	0.000	0.000	0.000	0.000
	0.000	0.445	2.000	0.660	-1.000	0.390	0.000	0.000	0.000	0.000	0.000	0.000
	2.000	0.625	4.000	0.850	0.000	0.470	0.000	0.000	0.000	0.000	0.000	0.000
	4.000	0.800	5.000	0.895	2.000	0.720	0.000	0.000	0.000	0.000	0.000	0.000
	5.000	0.865	6.000	0.915	3.000	0.840	0.000	0.000	0.000	0.000	0.000	0.000
	6.000	0.905	8.000	0.975	4.000	0.930	0.000	0.000	0.000	0.000	0.000	0.000
	8.000	0.950	9.770	1.090	6.000	1.050	0.000	0.000	0.000	0.000	0.000	0.000
	10.000	1.050	0.000	0.000	7.770	1.150	0.000	0.000	0.000	0.000	0.000	0.000
	11.770	1.110	0.000	0.000	9.770	1.280	0.000	0.000	0.000	0.000	0.000	0.000

## PROPELLER BLADE SECTION AIRFOIL TABLES

AIRFOIL SECTION	NACA 64-006		NACA 64-009		NACA 64-012		NACA 64-015		NACA 64-018		NACA 64-021	
TABLE DATA SOURCE	NACA TR-824		NACA TR-824		NACA TR-824		NACA TR-824		NACA TR-824		NACA TR-824	
AIRFOIL SER CODE	4		4		4		4		4		4	
DESIGN LIFT COEFF	0.000		0.000		0.000		0.000		0.000		0.000	
THICKNESS / CHORD	0.060		0.090		0.120		0.150		0.180		0.210	
MACH NUMBER	0.150		0.150		0.150		0.150		0.150		0.150	
ZERO LIFT ALPHA	0.000		0.000		0.000		0.000		0.000		0.000	
EXTRAP COEFF KCLI	0.740		0.740		0.740		0.740		0.740		0.740	
ALPHA, CL VALUES	-4.000	-0.430	-6.000	-0.700	-6.000	-0.650	-6.000	-0.670	-6.000	-0.650	-6.000	-0.630
	4.000	0.430	0.000	0.000	6.000	0.650	6.000	0.670	6.000	0.650	6.000	0.630
	6.000	0.620	6.000	0.620	8.000	0.830	8.000	0.870	8.000	0.840	8.000	0.800
	8.000	0.790	8.000	0.770	10.000	0.930	10.000	1.000	10.000	0.980	10.000	0.900
	10.000	0.810	10.000	0.870	12.000	0.910	12.000	1.100	12.000	1.040	12.000	0.980
	12.000	0.770	12.000	0.890	14.000	0.850	14.000	0.900	14.000	1.070	14.000	1.010
	0.000	0.000	14.000	0.870	16.000	0.800	0.000	0.000	16.000	1.040	16.000	1.030
	0.000	0.000	16.000	0.800	0.000	0.000	0.000	0.000	17.200	0.640	17.000	1.030
	0.000	0.000	0.000	0.000	0.000	0.000	0.000	0.000	0.000	0.000	18.000	0.900
	0.000	0.000	0.000	0.000	0.000	0.000	0.000	0.000	0.000	0.000	19.000	0.700
	0.000	0.000	0.000	0.000	0.000	0.000	0.000	0.000	0.000	0.000	20.000	0.680
AIRFOIL SECTION	NACA 64-206		NACA 64-209		NACA 64-212		NACA 64-215		NACA 64-218		NACA 64-221	
TABLE DATA SOURCE	NACA TR-824		NACA TR-824		NACA TR-824		NACA TR-824		NACA TR-824		NACA TR-824	
AIRFOIL SER CODE	4		4		4		4		4		4	
DESIGN LIFT COEFF	0.200		0.200		0.200		0.200		0.200		0.200	
THICKNESS / CHORD	0.060		0.090		0.120		0.150		0.180		0.210	
MACH NUMBER	0.150		0.150		0.150		0.150		0.150		0.150	
ZERO LIFT ALPHA	-1.330		-1.400		-1.240		-1.440		-1.220		-1.260	
EXTRAP COEFF KCLI	0.740		0.740		0.740		0.740		0.740		0.740	
ALPHA, CL VALUES	-6.000	-0.490	-6.000	-0.490	-6.000	-0.520	-6.000	-0.490	-6.000	-0.530	-6.000	-0.540
	-1.330	0.000	-1.400	0.000	-1.240	0.000	-1.440	0.000	-1.220	0.000	-1.260	0.000
	4.000	0.560	6.000	0.790	6.000	0.790	6.000	0.800	6.000	0.800	4.000	0.600
	6.000	0.770	8.000	0.970	8.000	0.980	8.000	0.990	8.000	0.930	6.000	0.800
	8.000	0.900	10.000	1.050	10.000	1.125	10.000	1.120	10.000	1.060	8.000	0.940
	10.000	1.000	12.000	1.040	11.000	1.160	12.000	1.200	12.000	1.135	10.000	1.030
	12.000	1.010	14.000	1.010	12.000	1.130	13.000	1.200	14.000	1.180	12.000	1.090
	14.000	0.970	16.000	0.960	14.000	1.010	14.000	1.150	16.000	1.200	14.000	1.130
	16.000	0.910	18.000	0.860	0.000	0.000	16.000	1.020	17.000	1.200	16.000	1.140
	0.000	0.000	0.000	0.000	0.000	0.000	0.000	0.000	18.000	0.790	18.000	1.000
	0.000	0.000	0.000	0.000	0.000	0.000	0.000	0.000	20.000	0.760	20.000	0.920

PROPELLER BLADE SECTION AIRFOIL TABLES

AIRFOIL SECTION	NACA 64-409		NACA 64-412		NACA 64-415		NACA 64-418		NACA 64-421	
TABLE DATA SOURCE	NACA TN-1945		NACA TR-824		NACA TR-824		NACA TR-824		NACA TR-824	
AIRFOIL SER CODE	4		4		4		4		0	
DESIGN LIFT COEFF	0.400		0.400		0.400		0.400		0.400	
THICKNESS / CHORD	0.090		0.120		0.150		0.180		0.210	
MACH NUMBER	0.150		0.150		0.150		0.150		0.150	
ZERO LIFT ALPHA	-2.540		-2.860		-2.820		-2.800		-2.570	
EXTRAP COEFF KCLI	0.740		0.740		0.740		0.740		0.740	
ALPHA, CL VALUES	-6.000	-0.360	-6.000	-0.340	-6.000	-0.360	-6.000	-0.360	-6.000	-0.400
	-2.540	0.000	-2.860	0.000	0.000	0.320	-2.800	0.000	-2.570	0.000
	6.000	0.890	6.000	0.960	6.000	0.950	2.000	0.540	0.000	0.300
	8.000	1.040	8.000	1.150	8.000	1.110	4.000	0.740	2.000	0.530
	10.000	1.110	10.000	1.290	10.000	1.220	6.000	0.930	4.000	0.720
	11.000	1.120	11.000	1.340	12.000	1.290	8.000	1.080	6.000	0.890
	12.000	1.090	12.000	1.340	13.000	1.300	10.000	1.170	8.000	1.000
	14.000	1.020	14.000	1.220	14.000	1.290	12.000	1.230	10.000	1.070
	15.000	0.960	16.000	1.100	16.000	1.240	14.000	1.240	12.000	1.120
	0.000	0.000	0.000	0.000	18.000	1.050	16.000	1.230	14.000	1.160
	0.000	0.000	0.000	0.000	0.000	0.000	18.000	1.170	16.000	1.180
	0.000	0.000	0.000	0.000	0.000	0.000	0.000	0.000	18.000	1.180
	0.000	0.000	0.000	0.000	0.000	0.000	0.000	0.000	20.000	1.000
	0.000	0.000	0.000	0.000	0.000	0.000	0.000	0.000	0.000	0.000

AIRFOIL SECTION	NACA 65-006		NACA 65-009		NACA 65-012		NACA 65-015		NACA 65-018		NACA 65-021	
TABLE DATA SOURCE	NACA TR-824		NACA TR-824		NACA TR-824		NACA TR-824		NACA TR-824		NACA TR-824	
AIRFOIL SER CODE	5		5		5		5		5		5	
DESIGN LIFT COEFF	0.000		0.000		0.000		0.000		0.000		0.000	
THICKNESS / CHORD	0.060		0.090		0.120		0.150		0.180		0.210	
MACH NUMBER	0.150		0.150		0.150		0.150		0.150		0.150	
ZERO LIFT ALPHA	0.000		0.000		0.000		0.000		0.000		0.000	
EXTRAP COEFF KCLI	0.740		0.740		0.740		0.740		0.740		0.740	
ALPHA, CL VALUES	-6.000	-0.640	-6.000	-0.630	-6.000	-0.650	-6.000	-0.630	-6.000	-0.600	-6.000	-0.580
	0.000	0.000	6.000	0.630	0.000	0.000	-4.000	-0.440	-4.000	-0.420	-4.000	-0.390
	4.000	0.420	8.000	0.820	6.000	0.670	6.000	0.660	0.000	0.000	0.000	0.000
	6.000	0.620	10.000	0.900	8.000	0.870	8.000	0.840	6.000	0.620	4.000	0.400
	8.000	0.770	11.000	0.920	10.000	0.970	10.000	1.000	8.000	0.800	6.000	0.590
	10.000	0.870	12.000	0.910	12.000	0.950	11.000	1.030	10.000	0.930	8.000	0.740
	12.000	0.920	14.000	0.850	14.000	0.900	12.000	1.020	12.000	1.020	10.000	0.850
	14.000	0.880	0.000	0.000	16.000	0.840	14.000	0.880	14.000	1.070	12.000	0.930
	16.000	0.790	0.000	0.000	0.000	0.000	16.000	0.790	16.000	0.900	14.000	1.020
	0.000	0.000	0.000	0.000	0.000	0.000	18.000	0.680	0.000	0.000	16.000	1.070
	0.000	0.000	0.000	0.000	0.000	0.000	0.000	0.000	0.000	0.000	18.000	1.080
	0.000	0.000	0.000	0.000	0.000	0.000	0.000	0.000	0.000	0.000	20.000	0.860





## APPENDIX C - PROGRAM USER INSTRUCTIONS

### 1.0 INTRODUCTION

This appendix contains a guide to the setting up and running of the computer program. The essential computational steps are described in Section 4, and the underlying theory in Section 3 of this report, and Section 3 of Reference 1. It should be noted that whereas this program is an extension and modification of the computer program developed in Reference 1, considerable differences exist between the two programs. Users of the old program are, therefore, cautioned against attempting modification of the former program without a careful study of the present program layout and data format requirements.

### 2.0 PROGRAM LANGUAGE

The program is written entirely in Fortran IV, Version 2.3 for a Scope 3.1 operating system and library tape.

### 3.0 MACHINE REQUIREMENTS

The program is designed to run on a CDC-6600 computer. The program makes use of the overlay capability and requires 15 disc files and a tape unit for peripheral storage.

### 4.0 INPUT DATA

The input data required by the program to compute a series of solutions at specified angles of attack up to stall for each wing-fuselage-propeller configuration constitutes one input case. This input data must include tabulations of applicable wing-section and propeller blade-section aerodynamic characteristics, propeller tip loss correction factors, and a range of geometric and flight condition parameters together with specification of several computational control and sequence options.

The input data for each case is in the form of punched cards arranged in sequential groups as shown in Figure 30. The principal card groups are identified as follows:

<u>CARD GROUP</u>	<u>DESCRIPTION</u>
A	Wing-fuselage geometry and control and sequencing options
B	Wing-section aerodynamic data
C	Wing geometry if not straight-tapered
D	Fuselage angles of attack
E	Propeller tip loss factors
F	Propeller blade-section aerodynamic data
G	Propeller geometry and operating conditions

In general, the first case requires a full specification of the input data contained in each group. However, for the second and subsequent cases, card groups specifying tabulated data (Groups B, C, E, and F) may be omitted where there is no change in the input data requirements. See Figure 30.

#### 4.1 Wing Fuselage Geometry (Card Group A)

Wing-fuselage geometry is entered on the first three cards as follows:

<u>CARD</u>	<u>COL.LOC</u>	<u>VARIABLE TYPE</u>	<u>PROGRAM NAME</u>	<u>VARIABLE</u>	<u>DESCRIPTION</u>
1	1-10	Real	ASPEC	AR	Wing aspect ratio
	11-20	Real	TAUT	$(t/c)_T$	Wing tip thickness/ chord ratio
	21-30	Real	TAUR	$(t/c)_R$	Wing root thickness/ chord ratio

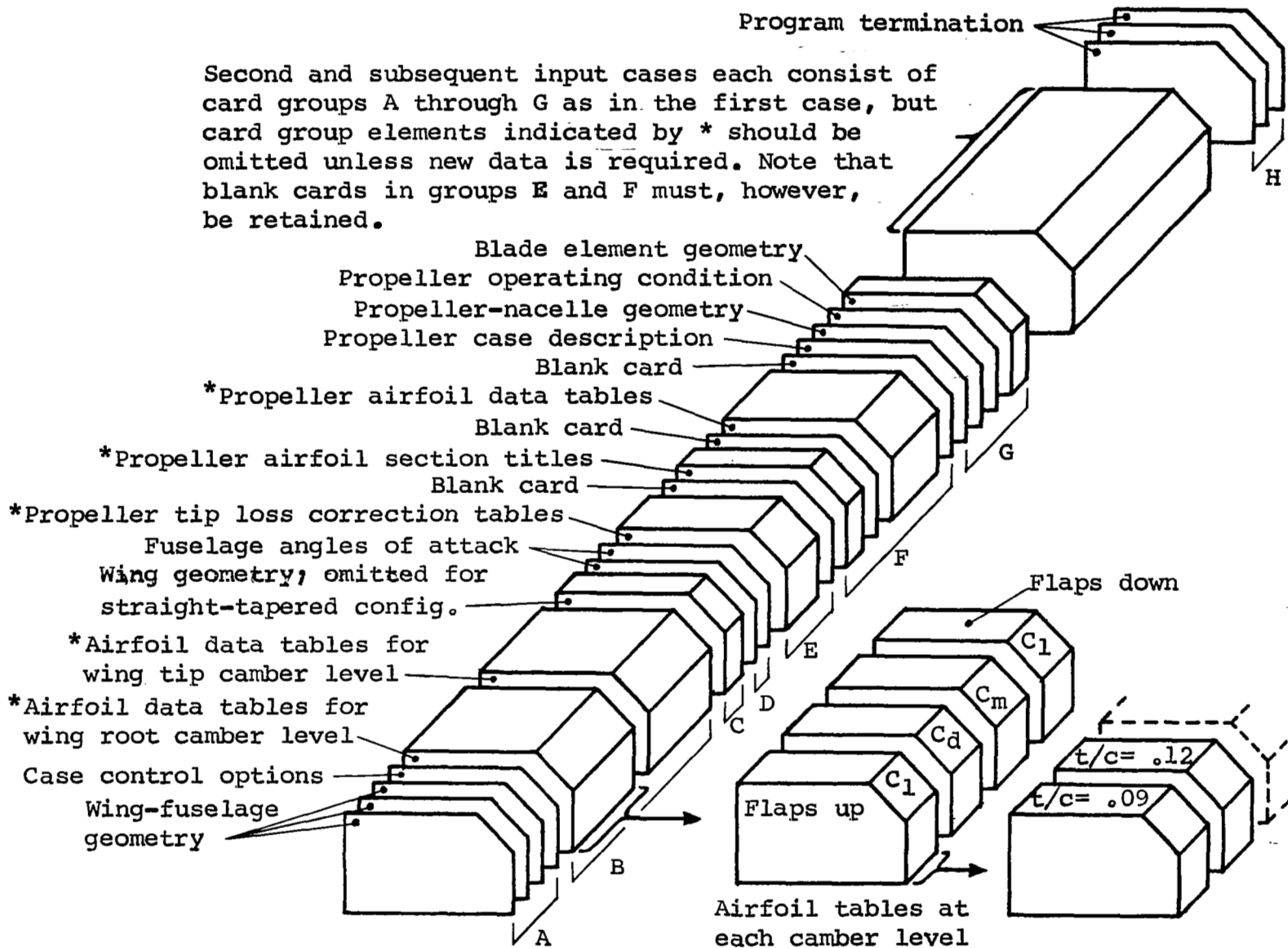


Figure 30. Assembly of Computer Program Input Data Card Deck

<u>CARD</u>	<u>COL,LOC</u>	<u>VARIABLE TYPE</u>	<u>PROGRAM NAME</u>	<u>VARIABLE</u>	<u>DESCRIPTION</u>
1	31-40	Real	TAPER	$\lambda$	Wing taper ratio
	41-50	Real	TWIST	$\epsilon_g$	Wing geometric twist (If geometric twist is specified, TWISA on card 2 must be set to 100.0)
	51-60	Real	R	r	Number of spanwise stations
	61-70	Real	BF	$b_f/b$	Flap span/wing span
	71-80	Real	REYND	$Re^l$	Reynolds number in millions based on wing mean aerodynamic chord
2	1-10	Real	DISCR	$\Delta$	Criterion for converg- ence of iteration loop
	11-20	Real	A	A	Fuselage semi-height/ wing semi-span
	21-30	Real	B	B	Fuselage semi-width/ wing semi-span
	31-40	Real	H	H	Height of wing above fuselage centerline/ wing semi-span
	41-50	Real	ALPHR	$\alpha_R$	Wing/body incidence - degrees
	60	Integer	NFLAP	--	Flap indicator: if NFLAP = 1, Flap is deflected; if NFLAP = 0, Flap is undeflected

<u>CARD</u>	<u>COL.LOC</u>	<u>VARIABLE TYPE</u>	<u>PROGRAM NAME</u>	<u>VARIABLE</u>	<u>DESCRIPTION</u>
2	61-65	Real	FLAP	$\delta_f$	Flap setting - degrees: If $\delta_f$ is zero, ie, flaps not deflected, then BF on card 1 should be set to 1.0
	66-70	Real	X	X	X-coordinate of moment reference point
	71-75	Real	Z	Z	Z-coordinate of moment reference point
	76-80	Real	TWISA	$\epsilon_0$	Aerodynamic twist - degrees (If aerodyn- amic twist is speci- fied, TWIST on card 1 must be set to 100.0)
3	1-10	Real	CAMBT	$K_T$	Tip airfoil series camber level
	11-20	Real	CAMBR	$K_R$	Root airfoil series camber level
	21-30	Integer	NSLIP	--	NSLIP = 0, power off case, no propeller data required; NSLIP = 1, power on case, propeller data required
	31-40	Real	CDNAC	$C_{DN}$	Total drag coefficient of all nacelles based on wing area, set to zero if no nacelles

## 4.2 Control and Sequencing Options (Card Group A)

Card 4 of Group A controls data read-in and optional printout features, in addition to standard output. The card layout is shown below.

<u>CARD</u>	<u>COL.LOC</u>	<u>VARIABLE</u> <u>TYPE</u>	<u>PROGRAM</u> <u>NAME</u>	<u>VARIABLE</u>	<u>DESCRIPTION</u>
4	1	Integer	NLVL	--	Number of values of thickness chord ratio (limit 5)
	2	Integer	ISWIT(1)	--	Option for reading in wing geometric parameters
	3	Integer	ISWIT(2)	--	Option to print out intermediate calculations as they are performed
	4	Integer	ISWIT(3)	--	Option to print out matrices
	5	Integer	IG	--	Switch used to set up data tables
	6-55	Alphanumeric	--	--	Run number, date, etc.

The options are as follows:

### ISWIT(1)

This control option is used for wings having nonlinear taper. The local values of Reynolds number, geometric twist, and ratios of thickness/chord and local chord/root chord must be key-punched for each spanwise station together with the values of edge velocity factor and the ratios of mean aerodynamic chord/root chord and root chord/span. By setting ISWIT(1) = 1, these values (Card Group C) are read in the following order using Format (16F5.0):

<u>PROGRAM</u> <u>VARIABLE</u> <u>NAME</u>	<u>DESCRIPTION</u>	<u>TYPE</u>	<u>NUMBERS</u> <u>OF</u> <u>VALUES</u>
TAU	Thickness/chord ratios	array	R-1
REY	Reynolds numbers	array	R-1
C	Chord/root chord ratios	array	R-1
EPS	Geometric twist	array	R-1
EDGE	Edge velocity factor	single value	1
CRB	Root chord/span ratio	single value	1
ACC	Mean aerodynamic chord	single value	1

If ISWIT(1) = 0, the program assumes a straight-tapered wing and calculates the values. Normally this is the case.

#### ISWIT(2)

This option allows for different types of printout required in the computation.

Setting ISWIT(2) = 1, causes the program to print out intermediate calculations as they are performed. This printout is very lengthy and should be used only when absolutely necessary to aid in debugging.

If ISWIT(2) = 0, intermediate calculations are not printed.

#### ISWIT(3)

If this control option is set to 1, the two major matrices of the program will be listed. First,  $\beta_{mk}$  (BETA), the matrix of multipliers used to obtain induced angles of attack is printed out. Then this is followed by the matrix  $K_{ij}$  (TRIX) which is used in the iteration cycle.

If ISWIT(3) is set to zero, no printout of the matrices will be obtained.

## IG

This control option is used to set up the wing airfoil data tables. For the case of a wing having the root airfoil series the same as the tip airfoil series, or for a wing with a deflected part-span flap, set:

IG = 3, if airfoil data is being read for the first time from cards

or IG = 1, if the airfoil data has already been read in and stored on tape

If the root airfoil series is different from the tip series then set:

IG = 4, if airfoil data is being read for the first time from cards

or IG = 2, if the airfoil data has already been read and stored on tape

Note that for a wing with a deflected part-span flap, the airfoil series from root to tip must be the same. The value of IG causes the computer to perform the following operations.

<u>VALUE OF IG</u>	<u>OPERATION</u>
1	Read airfoil data from peripheral storage device (PSD) to cube 1 on disc then copy cube 1 to cube 2 (See Figure 7).
2	Read root series airfoil data from PSD to cube 1 on disc, then read tip series data from PSD to cube 2 on disc.
3	Read airfoil data from cards, load to PSD, then read from PSD to cube 1 on disc. Copy cube 1 to cube 2.
4	Read root series airfoil data from cards, load to PSD, then to cube 1 on disc. Read tip series airfoil data from cards, then load to PSD, then to cube 2 on disc.



### 4.3 Wing Section Aerodynamic Data (Card Group B)

The aerodynamic section characteristics of the airfoil are read into the computer in the form of tables of lift coefficient ( $C_l$ ) versus angle of attack ( $\alpha$ ), drag coefficient ( $C_d$ ) versus  $C_l$ , pitching moment coefficient ( $C_m$ ) versus  $C_l$  and lift coefficient with flap deflected versus  $\alpha$ . The tables must be selected to cover the range of values of thickness/chord ratio, Reynolds number, and camber associated with the wing under consideration.

For each value of thickness/chord ratio, the data tables are arranged as indicated in Table V. The first card (punched in columns 1 through 7) indicates the number of rows in the table (columns 1 and 2), the number of columns in the table (columns 3 and 4) and the airfoil thickness/chord ratio (columns 5, 6, and 7). The second card (in alphanumeric format) indicates the airfoil type and the type of data e.g. NACA 230XX,  $C_l$ .

All cards in the table have format (F7.3,9F8.3). The first card contains the values of Reynolds number (in millions) and begins with a blank in columns 1 through 7. If the table is to contain  $C_l$  values, the next card reads -90.0 in columns 1 through 7, and -9.0 in columns 8 through 80. If the table is for values of  $C_d$ , the card reads -10.0 in columns 1 through 7, and 2.0 in columns 8 through 80. If the table is to contain  $C_m$  values, the card reads -10.0 in columns 1 through 7, and zeros in columns 8 through 80.

The remaining cards contain either: (1) a value of angle of attack (columns 1 through 7) followed by the values of  $C_l$  corresponding to each Reynolds number, or (2) a value of  $C_l$  (columns 1 through 7) followed by the values of  $C_d$ , or (3) a value of  $C_l$  (columns 1 through 7) followed by the values of  $C_m$ , depending on whether the table contains  $C_l$ ,  $C_d$ , or  $C_m$  data. The last three cards in each table are:

Table V. Card Format for Wing Section Airfoil Tables

Col. Loc.	1	8	16
Header Cards	1311-12		
	NACA 23012 Lift Coefficient $C_L$		
Reynolds Numbers		0.5	1.0
	-90.0	-9.0	-9.0
	-14.0	-0.5	-0.45
	$\alpha$ Values		$C_d$ Values
	:		:
	+90.0	4.0	9.0
$C_d$ Max Values		1.51	1.54
$\alpha$ Max Values		17.2	17.0
	1511.12		
	NACA 23012 Drag Coefficient $C_D$		
		0.5	1.0
	-10	2.0	2.0
	-0.3	0.004	0.0042
	$C_d$ Values		$C_d$ Values
	:		:
	10.0	2.0	2.0
		Blank card	
		Blank card	
	1611.12		
	NACA 23012 Pitching Moment Coefficient		
	CML/4 Chord		
	-10.0	0.0	0.0
	-0.36	-0.40	-0.41
	$C_d$ Values		$C_m$ Values
	:		:
	10.0	0.0	0.0
		Blank card	
		Blank card	

C<sub>1</sub> Table

<u>Card No.</u>	<u>Columns 1 through 7</u>	<u>Remaining Fields</u>
1	90.0	9.0 9.0 etc.
2*	blank	Values of C <sub>1</sub> max
3*	blank	Values of $\alpha$ at C <sub>1</sub> max i.e. $\alpha_{max}$

\* In the C<sub>1</sub> tables the values of C<sub>1max</sub> and  $\alpha_{max}$  appearing on cards 2 and 3 respectively, must also appear in the main body of the table.

C<sub>d</sub> Table

1	10.0	2.0 2.0 etc.
2	blank card	
3	blank card	

C<sub>m</sub> Table

1	10.0	0.0 0.0 etc.
2	blank card	
3	blank card	

Up to 5 "levels" of thickness/chord ratio may be used. Within each level the table size is limited to 8 columns (7 values of Reynolds number) and 25 rows (22 different values of  $\alpha$  or C<sub>1</sub>).

The airfoil data cards are assembled as shown in Figure 30.

#### 4.4 Fuselage Angles of Attack (Card Group D)

The fuselage angles-of-attack at which calculations are to be made are read in on 2 cards, Format (10F8.0). These are used sequentially as punched until either 99.0 is encountered or stall is reached. If the former condition is encountered, the program will automatically proceed to the next case; if stall is reached, the program will search for an angle-of-attack close to the value of angle-of-attack at which stall just occurs. The accuracy of this search depends on how closely the angles-of-attack are chosen near stall.

Note that all the lift tables are artificially extended beyond the  $C_{l \max}$  point with a positive slope. For example, in all tables  $C_l$  at  $\alpha = \pm 90$  is set to  $\pm 9.0$ . This is done to ensure convergence. The effect of this is that the overall wing  $C_L$  versus  $\alpha$  curve predicted by the program will be correct up to the angle-of-attack at which stall first occurs on the wing. Thereafter, the predicted  $C_L$  is incorrect. This is consistent with the purpose of the program which is to predict the point of stall onset only.

#### 4.5 Propeller Tip Loss Correction Factors (Card Group E)

The propeller tip loss correction tables are defined by a three-dimensional array of size (3, 21, 8). The data values are read in on a total of 63 data cards, each card containing 8 values and having the following format:

<u>COL.LOC</u>	<u>VARIABLE TYPE</u>	<u>PROGRAM SYMBOL</u>	<u>ALGEBRAIC SYMBOL</u>	<u>DESCRIPTION</u>
1	Integer	IB	(B-1)	Array index identifying number of blades per propeller, less one
2-3	Integer	IP	$(1+20 \sin \phi)$	Array index identifying value of $\sin \phi$
4-32	--	--	--	Blank
33-38	Real	TLOSS(1)	F/FP	Data value at $r/R = 0.3$
39-44	Real	TLOSS(2)	F/FP	Data value at $r/R = 0.4$

<u>COL. LOC.</u>	<u>VARIABLE TYPE</u>	<u>PROGRAM SYMBOL</u>	<u>ALGEBRAIC SYMBOL</u>	<u>DESCRIPTION</u>
75-80	Real	TLOSS(8)	F/FP	Data value at r/R = 1.0

These 63 data cards may be assembled in any order.

#### 4.6 Propeller Blade Section Aerodynamic Data (Card Group F)

Up to 150 propeller blade-section data tables\* can be accepted and stored by the computer program. Each table contains an array of up to 20 pairs of  $\alpha$  and  $C_1$  values for one airfoil section at one Mach number condition. Up to 25 airfoil sections may be specified for each airfoil family. A maximum of 9 families can be stored, each being assigned an arbitrary single-digit airfoil series code between 1 and 9 inclusive.

The standard blade-section data tables available with the program use preassigned airfoil series codes (as given below) for which the computer program stores the following titles and values of two constants,  $k_1$  and  $k_2$ .

<u>Code</u>	<u>Airfoil Series Name</u>	<u><math>k_1</math></u>	<u><math>k_2</math></u>
1	USNPS	0.	-40.0
2	Clark, Y	0.	-40.0
3	NACA 16XXX	-7.3	0.
4	NACA 64-XXX	-6.9	0.
5	NACA 65-XXX	-6.9	0.
6-9	Blank	0.	0.

\*See section 4.1.3 of main report for order of assembly.

The constants  $k_1$ ,  $k_2$  are empirical values that permit an initial value for  $\alpha_0$ , angle-of-attack at zero lift used in equation 104, to be obtained from a linearized approximation to the airfoil characteristics given by the expression

$$\alpha_0 = k_1 \times (\text{design lift coefficient}) + k_2 \times (\text{thickness/chord ratio}) \quad (146)$$

The airfoil series title card is used to reassign airfoil series names and  $k_1$ ,  $k_2$  values as required. One card is used for each reassignment and has the following format:

<u>COL.LOC.</u>	<u>VARIABLE TYPE</u>	<u>PROGRAM NAME</u>	<u>ALGEBRAIC SYMBOL</u>	<u>DESCRIPTION</u>
1	Integer	I	--	Airfoil series code
11-18	Alphanumeric	AFSER(I)	--	Airfoil series name
21-30	Real	AK(I,1)	$k_1$	} Empirical constants defined in preceding text
31-40	Real	AK(I,2)	$k_2$	

Each airfoil table is defined on a sequence of from 2 to 5 cards. The first card in the sequence contains header information specifying the airfoil section and other pertinent parameters as follows:

<u>COL.LOC.</u>	<u>VARIABLE TYPE</u>	<u>PROGRAM NAME</u>	<u>ALGEBRAIC SYMBOL</u>	<u>DESCRIPTION</u>
1-2	Integer	IHEDD(1)	--	Number of pairs of $\alpha$ , $C_l$ values in table
5	Integer	IHEDD(2)	--	Airfoil series code
9-16	Real	THEDD(1)	$C_{li}$	Design lift coefficient
17-24	Real	THEDD(2)	t/c	Thickness/chord ratio

<u>COL.LOC.</u>	<u>VARIABLE TYPE</u>	<u>PROGRAM NAME</u>	<u>ALGEBRAIC SYMBOL</u>	<u>DESCRIPTION</u>
25-32	Real	THEDD(3)	Mo	Mach number
33-40	Real	THEDD(4)	$\alpha_0$	Angle-of-attack for zero lift
41-48	Real	THEDD(5)	$k_{Cl_i}$	Extrapolation coefficient given by equation (126)
57-68*	Alphanumeric	--	--	Table data source
69-80*	Alphanumeric	--	--	Airfoil section name

\* For reference only; these columns not read by program.

The second and subsequent cards in each airfoil table sequence contain the pairs of  $\alpha$  and  $C_1$  values. These values must be arranged in order of  $\alpha$  increasing. The format is as follows:

<u>COL.LOC.</u>	<u>VARIABLE TYPE</u>	<u>PROGRAM NAME</u>	<u>ALGEBRAIC SYMBOL</u>	<u>DESCRIPTION</u>
1-8	Real	TALFA(1)	$\alpha$	} 1st pair of values
9-16	Real	TLIFT(1)	$C_1$	
17-24	Real	TALFA(2)	$\alpha$	} 2nd pair of values
25-32	Real	TLIFT(2)	$C_1$	
65-72	Real	TALFA(5)	$\alpha$	} 5th pair of values
73-80	Real	TLIFT(5)	$C_1$	

#### 4.7 Propeller Geometry and Operating Conditions (Card Group G)

Information to specify the propeller geometric and operating parameters is provided on a series of cards of four types. These cards must be arranged in the order described below. Each card type is assigned a numerical code value in column 80. The value is read by the program to ensure that the cards are in proper sequence.

The first card provides for the inclusion of arbitrary title information as follows:

<u>COL.LOC.</u>	<u>VARIABLE TYPE</u>	<u>PROGRAM NAME</u>	<u>DESCRIPTION</u>
1-76	Alphanumeric	TITLE	Propeller identification title
80	Integer	IDENT	Card identification code = 1

The second card provides information specifying the propeller and nacelle geometry as follows:

<u>COL.LOC.</u>	<u>VARIABLE TYPE</u>	<u>PROGRAM NAME</u>	<u>ALGEBRAIC SYMBOL</u>	<u>DESCRIPTION</u>
1-2	Integer	NP	--	Number of propellers
11-12	Integer	NB	B	Number of blades per propeller
21-30	Real	DPB	D/b	Propeller diameter/wing span
31-40	Real	RHBR	$r_{\text{hub}}/R$	Hub radius/tip radius
41-50	Real	RNBR	$r_{\text{nacelle}}/R$	Nacelle radius/tip radius
80	Integer	IDENT	--	Card identification code = 2



The third card provides information specifying the operating conditions for the propeller(s) as follows:

<u>COL.LOC.</u>	<u>VARIABLE TYPE</u>	<u>PROGRAM NAME</u>	<u>ALGEBRAIC SYMBOL</u>	<u>DESCRIPTION</u>
1-2	Integer	NROT(1)	--	L.H. propeller rotation index
11-12	Integer	NROT(2)	--	R.H. propeller rotation index
21-30	Real	AJ	J	Propeller advance ratio
31-40	Real	AMCHU	$M_0$	Flight Mach number
80	Integer	IDENT	--	Card identification code = 3

The positive value (01) for the propeller rotation index is used to specify a right-hand rotation for either propeller. The negative value (-1) is used to specify a left-hand rotation. Where a single-propeller configuration is considered, the rotation index for the L.H. propeller must be set to zero (00) while the R.H. propeller index has the appropriate value for the single propeller rotation sense.

The fourth-through-last cards of the series provide information specifying the blade section geometry. One card is required for each selected blade station between hub and tip, up to a maximum of 12 cards. These cards must be assembled in order of increasing blade station radius. The first selected station need not be at the hub, but the last card must specify the station at the tip with a value of 1.0 in columns 1-10.

<u>COL.LOC.</u>	<u>VARIABLE TYPE</u>	<u>PROGRAM NAME</u>	<u>ALGEBRAIC SYMBOL</u>	<u>DESCRIPTION</u>
1-10	Real	RPBR	r/R	Blade station radius/ tip radius
11-20	Real	CPBR	C/R	Blade-section chord/ tip radius

<u>COL. LOC.</u>	<u>VARIABLE TYPE</u>	<u>PROGRAM NAME</u>	<u>ALGEBRAIC SYMBOL</u>	<u>DESCRIPTION</u>
21-30	Real	BETA	$\beta$	Blade section pitch angle, degrees
31	Integer	NA	--	Blade section airfoil series code
41-50	Real	CLI	$C_{li}$	Blade section design lift coefficient
51-60	Real	TOC	t/c	Blade section thickness/chord ratio
80	Integer	IDENT	--	Card identification code = 4

#### 4.8 Program Termination (Card Group H)

The program operation is terminated by three input data cards located at the end of the input data deck. The first card uses the format of card number 1 of Group A with the value of ASPEC set to 99.0. The second and third cards must be blank.

#### 4.9 Data Restrictions

The following is a list of input quantities together with the restrictions and normal range of values.

<u>QUANTITY</u>	<u>SIGN-RESTRICTIONS-NORMAL RANGE</u>
ASPEC	+, $\geq$ 2.0
TAUT, TAUR, TAPER	+, $\leq$ 1.0
TWIST, TWISA	between $+15^\circ$ and $-15^\circ$
R	+20 only*
BF	+, $\leq$ 1.0

<u>QUANTITY</u>	<u>SIGN-RESTRICTIONS-NORMAL RANGE</u>
REYND	+
DI SCR	+, suggested value .001
A, B, H	+, $\leq 1.0$
ALPHR	between $+10^\circ$ and $-10^\circ$
NFLAP	0 or 1
FLAP	+, between $0^\circ$ and $90^\circ$
X, Z	+ or -
NSLIP	0 or 1
CDNAC	+, $0 \leq 1.0$

\* R, which must be an even integer, may be changed to allow calculation at a greater number of spanwise stations. This requires changing the DIMENSION statements.

## 5.0 OUTPUT

### 5.1 Printout Options

All output is from a standard 120-characters-per-line printer. The amount and type of data output depends on the options exercised and on whether the computation is for a wing with or without a deflected flap/ with or without slipstream. For the standard run (without the debug print-out), the output data is self-explanatory. When the option for printing intermediate calculations is exercised, the output contains the following additional parameters whose meaning is given below.

<u>QUANTITY</u>	<u>TYPE</u>	<u>DESCRIPTION</u> (see also Reference 1)
A1	single value	Angle of attack corresponding to $C_1$ at flap end, from flapped section data
A2	single value	Angle of attack corresponding to $C_1$ at flap end, from unflapped section data
A3	single value	Zero-lift angle at flap end - flapped section data
A4	single value	Zero-lift angle at flap end - unflapped section data
ALPC	array	Angle of attack corrections for flap effect
ALPH	array	Angles of attack corrected for downwash, flap effects and body upwash
ALPHE	array	Effective angles of attack
ALPG	array	Wing section geometric angles of attack
ALPHU	array	Section downwash angles corrected for fuselage effects
ALPHZ	array	Section zero-lift angles
ALFPR	single value	Propeller shaft angle of attack in radians
ASBAR	single value	Average slipstream angle
CBC	array	Calculated values of $C_{1c}/b$
CBG	array	Approximate values of $C_{1c}/b$
CDOC	array	Values of $C_{dc}/b$
CL	single value	Integrated lift coefficient used to normalize CLADD

<u>QUANTITY</u>	<u>TYPE</u>	<u>DESCRIPTION</u> (see also Reference 1)
CLADD	array	Additional lift coefficient distribution
CLAD1	array	Modified distribution of additional lift coefficients from tip to flap end
CLAD2	array	Modified distribution of additional lift coefficients from flap end to wing/fuselage junction
CL2CB	array	Distribution of lift associated with equation (56)
CLDEL	array	Distribution of lift coefficient due to flap deflection only
CLMAX	array	Values of section maximum lift coefficients
CLSTA	single value	Section lift coefficient at flap end
CLSTU	single value	Uncorrected section lift coefficient at flap end
CVAL	array	Lift coefficients corresponding to ALPG
DELTA	array	Differences between guessed and calculated lift distributions
DDCLMA	single value	Increment in section maximum lift coefficient at flap end due to flap deflection
EDGE	single value	Edge velocity factor
F	array	Factors used in altering two-dimensional section data to three-dimensional data

<u>QUANTITY</u>	<u>TYPE</u>	<u>DESCRIPTION</u> (see also Reference 1)
FF	single value	Factors used at flapside of flap end to alter 2-dimensional data
F1	single value	Factor used to scale additional lift distribution CLADD
F2	single value	Factor used to scale CLDEL
FUNC	single value	Wing-on-propeller upwash function, equation (128)
GENE	array	Values of equation (88) for $\theta^* = \pi - \theta^*$
HOPP	array	Values of $\alpha_{cK} / \delta$ - see Reference 1 equation (38)
RDUBAR/DU	single value	Real part of the derivative of the conformal transformation function, equation (9) of Ref. 1
SGENE	array	Function associated with equation (76)
STONY	array	Function associated with equation (76)
SIGMA	array	Function associated with HOPP
SV	array	Slipstream crossflow distribution
TONY	array	Values of equation (88)
VW	single value	Wing-induced upwash in propeller disc plane

## 5.2 Error Messages

In developing the program it was found that the most common source of error was the airfoil data tables. In particular, the tables of  $C_l$  versus  $\alpha$  are most critical. The variation of  $C_l$  with increasing  $\alpha$  should be smooth

without sudden breaks, especially for values higher than  $\alpha_{max}$ . A sharp break in the slope of  $C_l$  versus  $\alpha$  after  $\alpha_{max}$  may cause the iteration procedure to diverge. If this occurs a message is printed as follows:

UNABLE TO CONVERGE AFTER 30 ITERATIONS ABORTED

The last values of DELTA and the values of lift coefficient are then listed together with a dump of the airfoil tables in core at that time.

A second error message associated with table interpolation is as follows:

ERROR CODE (N)

IF 1 CVAL GTR THAN MAX VALUE LISTED

IF 2 CVAL GTR THAN TABLE VALUE

IF 3 ALPHA VALUE GTR THAN TABLE VALUE

IF 6 THICKNESS CHORD RATIO VALUE CANNOT BE FOUND

If these errors occur, the tables should be examined for mistakes in key punching, etc.

Several error messages are associated with the propeller slipstream analysis subroutine and operate as follows:

- (a) If an invalid number of tip loss correction cards are read, i.e. other than 0 or 63, this is indicated by the message:

XX TIP LOSS CORRECTION TABLE DATA CARDS READ IS  
INVALID - SLIPSTREAM COMPUTATIONS ABORTED

- (b) If the propeller geometry and operating condition data cards are read out of sequence, this is indicated by the message:

CARD IDENT XX HAS BEEN READ OUT OF SEQUENCE,  
SLIPSTREAM COMPUTATIONS ABORTED

- (c) If propeller airfoil tables are not stored for the airfoil series code specified on a blade station data card (IDENT 4), this is indicated by the following message:

AIRFOIL TABLES NOT STORED FOR AIRFOIL SERIES XX  
SPECIFIED AT RB/RP = XX•XXXX - THIS ELEMENT IS  
DELETED FROM THE ANALYSIS

- (d) If the propeller-slipstream analysis fails to converge within 9 iterations, then the following message appears after printing out the solution for the last iteration:

SOLUTION FOR PRECEEDING ELEMENT FAILED TO CONVERGE  
IN 9 ITERATIONS AND IS DELETED FROM THE SLIPSTREAM  
ANALYSIS

## 6.0 PROGRAM STRUCTURE

The program is written to operate in OVERLAY mode. The central controlling portion of the overall program is called STALL. The remainder of the program is split into 3 parts, ONE, TWO, THREE, which are overlaid. STALL calls ONE which then calls either TWO or THREE depending on whether the calculation is for a flapped wing or not. The major subroutines called by each overlay are as follows:

ONE	calls	MAIN, MAINA, MAIN1
TWO	calls	MAIN2, MAN2A, MAIN4
THREE	calls	MAIN2, MAIN3, MAIN5

These major subroutines call the remaining subroutines in the program as follows:

MAIN	calls	MAINA, SETSW, AERDA, DATSW, ZZZ
MAINA	calls	SLIP, AAA, DATSW, ZZZ, BRIDG, MAIN1
MAIN1	calls	DATSW, AAA, MINV, GRIDG, SSS
MAN2A	calls	DATSW, AAA, BRIDG, ZZZ, MAIN4
MAIN3	calls	DAGET, DATSW, AAA, ARC, ZZZ, MAIN5
MAIN4	calls	BRIDG, AAA, DATSW, MAN2A
MAIN5	calls	DAGET, ARC, DATSW, AAA, ZZZ
BRIDG	calls	DAGET, ARC
ARC	calls	LOOK



## 7.0 OPERATING PROCEDURE

Logical TAPE5 is named as the working (scratch) tape. The program deck and data deck are loaded in the following sequence: job card, system control cards, end-of-record card, program deck, end-of-record card, data deck, end-of-file card.

## 8.0 PROGRAM TIMING

Central processor unit time for an average run of six (6) angles-of-attack is approximately 60 seconds.

APPENDIX D

INTERNAL LISTING OF THE COMPUTER PROGRAM

Presented in this appendix is an internal listing of the computer program developed under the present contract.

```

OVERLAY(BLINDA,C,C)
PRCGRAM STALL(INPUT=2C1,OUTPUT=10C1,TAPE8=INPUT,TAPE6=OUTPUT,TAPE1
1=2C1,TAPE2=2C1,TAPE3=2C1,TAPE4=201,TAPE5=201,TAPE10=201,TAPE15=201
2,TAPE20=201,TAPE44=2C1,TAPE7=1CC1,TAPE9=2C1)
DIMENSION C(15),EPS(19),TRANS(19),REY(19),ETA(19),FCPP(19),CLMAX(1
19),ZHERE(2,6),WFERE(2,6),ARRAY(5,25,8),Y(19),TAU(19),BETA(19,19),
2MAZZ(6),MZCCL(6),MAXX(6),MXCCL(6),YHERE(2,6),MYCCL(6),MAYY(6),TRIX
3(19,19),CM(19),LIST(19),YCA(19),YDAX(19),YX(19),TONY(19),ALPG(19),
4XHERE(2,6),MWCCCL(6),MAWw(6)
DIMENSION CVAL(19),ALPHU(19),CBC(19),CBG(19),DELTA(19),ALPHZ(19),
1ALPH(19),ALPHE(19),CLACC(19),CLDEL(19),CLAD2(19),CLAD1(19),F(19),
CCMMCN KCR,KIR,KIL,KCL,VSA(19),SW(19),VSEAR,EYETL,CTS,XPB,YPB,JP,
1IPRAB,ALPFB,KSTAL,ISTAL,KCLNT,AB(3)
CCMMCN NSLIP,VR(19),DA(19),AS(19),TL(19),SV(19),FUNC,YO,CDNAC,
1ALPHV(16)
CCMMCN INNCW,ISWIT(3),ALPHA,REYN,CLL,REYCN,XMAX,ALMAX(19),CLMAX,C,
1EPS,TRANS,REY,ETA,FCPP,ZHERE,WFERE,ARRAY,Y,BETA,TFAC,TRIX,TAU,MAXX
2,MAZZ,MXCCL,MZCCL,ASPEC,TAPER,BF,REYND,DISCK,PIER,CRB,Q,TSTAX,EDGE
3,SIG,ALPHR,NFLAP,NLVL,NP,IY,IZ,IR,IP,IS,ISTAR,A,B,H,TAUT,TAUR,
4TWIST,R,BAX,YHERE,MYCCL,MAYY,FLAP,TONY,TWISA,X,Z,CM,ACC,XHERE,
5MWCCCL,MAWw,CAMB(19),CAMBR,CAMBT,DUPY1,DUPY2,NAME(25),AHERE(2,6),
6MAAAA(6),MACCL(6),BHERE(2,6),MABB(6),MCCOL(6),CHERE(2,6),MACC(6),
7MCCCL(6),DHERE(2,6),MADD(6),MCCOL(6),STONY(19),SGENE(19),CVAL,
8ALPHU,CBC,CBG,DELTA,ALPHZ,ALPH,ALPHE,CLACC,CLDEL,CLAD2,CLAD1,
9F,IRI,FF,LCCER
BLINDA=CLBLINDA
RECALL=6HRECALL
30 IR=8
50 CALL CVERLAY(BLINDA,1,0,RECALL)
IF(NFLAP.NE.C) GO TO 10
GC TC 2C
10 CALL CVERLAY(BLINDA,3,C,RECALL)
GC TC 4C
20 CALL CVERLAY(BLINDA,2,0,RECALL)
40 IF(IR.FC.C) GC TO 50
GC TC 3C
END
OVERLAY(BLINDA,1,C)
PRCGRAM CNE
DIMENSION C(19),EPS(19),TRANS(19),REY(19),ETA(19),FCPP(19),CLMAX(1
19),ZHERE(2,6),WFERE(2,6),ARRAY(5,25,8),Y(19),TAU(19),BETA(19,19),
2MAZZ(6),MZCCL(6),MAXX(6),MXCCL(6),YHERE(2,6),MYCCL(6),MAYY(6),TRIX
3(19,19),CM(19),LIST(19),YCA(19),YDAX(19),YX(19),TONY(19),ALPG(19),
4XHERE(2,6),MWCCCL(6),MAWw(6)
DIMENSION CVAL(19),ALPHU(19),CBC(19),CBG(19),DELTA(19),ALPHZ(19),
1ALPH(19),ALPHE(19),CLACC(19),CLDEL(19),CLAD2(19),CLAD1(19),F(19),
CCMMCN KCR,KIR,KIL,KCL,VSA(19),SW(19),VSEAR,EYETL,CTS,XPB,YPB,JP,
1IPRAB,ALPFB,KSTAL,ISTAL,KCLNT,AB(3)
CCMMCN NSLIP,VR(19),DA(19),AS(19),TL(19),SV(19),FUNC,YO,CDNAC,
1ALPHV(16)
CCMMCN INNCW,ISWIT(3),ALPHA,REYN,CLL,REYCN,XMAX,ALMAX(19),CLMAX,C,
1EPS,TRANS,REY,ETA,FCPP,ZHERE,WFERE,ARRAY,Y,BETA,TFAC,TRIX,TAU,MAXX
2,MAZZ,MXCCL,MZCCL,ASPEC,TAPER,BF,REYND,DISCK,PIER,CRB,Q,TSTAX,EDGE
3,SIG,ALPHR,NFLAP,NLVL,NP,IY,IZ,IR,IP,IS,ISTAR,A,B,H,TAUT,TAUR,
4TWIST,R,BAX,YHERE,MYCCL,MAYY,FLAP,TONY,TWISA,X,Z,CM,ACC,XHERE,
5MWCCCL,MAWw,CAMB(19),CAMBR,CAMBT,DUPY1,DUPY2,NAME(25),AHERE(2,6),
6MAAAA(6),MACCL(6),BHERE(2,6),MABB(6),MCCOL(6),CHERE(2,6),MACC(6),
7MCCCL(6),DHERE(2,6),MADD(6),MCCOL(6),STONY(19),SGENE(19),CVAL,
8ALPHU,CBC,CBG,DELTA,ALPHZ,ALPH,ALPHE,CLACC,CLDEL,CLAD2,CLAD1,
9F,IRI,FF,LCCER
IF(IR.EG.0) GC TC 2C
10 CALL MAIN
20 CALL MAINA
IF(ALPHE.EQ.99.) GC TC 1C
IF(IPRAB.NE.1) GO TO 3C
CALL MAINI
30 RETURN
END
OVERLAY(BLINDA,2,0)
PRCGRAM ThC
DIMENSION C(19),EPS(19),TRANS(19),REY(19),ETA(19),FCPP(19),CLMAX(1
19),ZHERE(2,6),WFERE(2,6),ARRAY(5,25,8),Y(19),TAU(19),BETA(19,19),
2MAZZ(6),MZCCL(6),MAXX(6),MXCCL(6),YHERE(2,6),MYCCL(6),MAYY(6),TRIX
3(19,19),CM(19),LIST(19),YCA(19),YDAX(19),YX(19),TONY(19),ALPG(19),
4XHERE(2,6),MWCCCL(6),MAWw(6)
DIMENSION CVAL(19),ALPHU(19),CBC(19),CBG(19),DELTA(19),ALPHZ(19),
1ALPH(19),ALPHE(19),CLACC(19),CLDEL(19),CLAD2(19),CLAD1(19),F(19),
CCMMCN KCR,KIR,KIL,KCL,VSA(19),SW(19),VSEAR,EYETL,CTS,XPB,YPB,JP,
1IPRAB,ALPFB,KSTAL,ISTAL,KCLNT,AB(3)
CCMMCN NSLIP,VR(19),DA(19),AS(19),TL(19),SV(19),FUNC,YO,CDNAC,

```

```

1ALPHV(16)
  CCMCN INNCN, ISWIT(3), ALPHA, REYN, CLL, REYCN, XMAX, ALMAX(19), CLMAX, C,
1EPS, TRANS, REY, ETA, FCPP, ZFERE, WFERE, ARKAY, Y, BETA, TFAC, TRIX, TAU, MAX)
2, MAZZ, MXCCL, MZCCL, ASPEC, TAPER, BF, REYND, DISCR, PIER, CRB, G, TSTAX, EDGE
3, SIG, ALPHR, NFLAP, NLVL, NP, IY, IZ, IX, IP, IS, ISTAR, A, B, F, TAU, TAUR,
4TWIST, R, BAX, YFERE, MYCCL, MAYY, FLAP, TLNY, TWISA, X, Z, CM, ACC, XHERE,
5MCCCL, MAWW, CAMB(19), CAMBR, CAMBT, DUMY1, DUMY2, NAME(25), AHERE(2,6),
6MAAA(6), MACCL(6), BFERE(2,6), MABB(6), MCOL(6), CHERE(2,6), MACC(6),
7MCCCL(6), DFERE(2,6), MACD(6), MCCCL(6), STONY(19), SGENE(19), CVAL,
8ALPHU, CBC, CBG, DELTA, ALPHZ, ALPH, ALPHE, CLADD, CLDEL, CLAD2, CLAD1,
9F, IRI, FF, LCCER
  CALL MAIN2
  CALL MANZA
  RETURN
  END
  CVERLAY(BLINDA,3,C)
  PRCCGRAM THREE
  DIMENSION C(19), EPS(19), TRANS(19), REY(19), ETA(19), FCPP(19), CLMAX(1
19), ZFERE(2,6), WFERE(2,6), ARRAY(5,25,8), Y(19), TAL(19), BETA(19,19),
2MAZZ(3), MZCCL(6), MAXX(6), MXCCL(6), YHERE(2,6), MYCCL(6), MAYY(6), TRI
3(19,19), CM(19), DIST(19), YCA(19), YCAX(19), YX(19), TONY(19), ALPG(19),
4XFERE(2,6), MCOL(6), MAWW(6)
  DIMENSION CVAL(19), ALPHU(19), CBC(19), CBG(19), DELTA(19), ALPHZ(19),
1ALPH(19), ALPHE(19), CLADD(19), CLDEL(19), CLAD2(19), CLAD1(19), F(19)
  CCMCN KGR, KIR, KIL, KCL, VSA(19), SV(19), VSBAR, EYETL, CTS, XPB, YPE, JP,
1IPRAB, ALPHB, KSTAL, ISTAR, KGLNT, AB(3)
  CCMCN NSLIP, VR(19), DA(19), AS(19), TL(19), SV(19), FUNC, YO, CDNAC,
1ALPHV(16)
  CCMCN INNCN, ISWIT(3), ALPHA, REYN, CLL, REYCN, XMAX, ALMAX(19), CLMAX, C,
1EPS, TRANS, REY, ETA, FCPP, ZFERE, WFERE, ARRAY, Y, BETA, TFAC, TRIX, TAU, MAX)
2, MAZZ, MXCCL, MZCCL, ASPEC, TAPER, BF, REYND, DISCR, PIER, CRB, G, TSTAX, EDGE
3, SIG, ALPHR, NFLAP, NLVL, NP, IY, IZ, IR, IP, IS, ISTAR, A, B, F, TAU, TAUR,
4TWIST, R, BAX, YFERE, MYCCL, MAYY, FLAP, TONY, TWISA, X, Z, CM, ACC, XHERE,
5MCCCL, MAWW, CAMB(19), CAMBR, CAMBT, DUMY1, DUMY2, NAME(25), AHERE(2,6),
6MAAA(6), MACCL(6), DFERE(2,6), MABB(6), MCOL(6), CHERE(2,6), MACC(6),
7MCCCL(6), DFERE(2,6), MACD(6), MCCCL(6), STONY(19), SGENE(19), CVAL,
8ALPHU, CBC, CBG, DELTA, ALPHZ, ALPH, ALPHE, CLADD, CLDEL, CLAD2, CLAD1,
9F, IRI, FF, LCCER
  CALL MAIN2
  CALL MAIN3
  RETURN
  END
  SUBROUTINE MINV(A,N,D,L,M)

```

I

C  
C  
C  
C  
C

MATRIX INVERSION SUBROUTINE

DIMENSION A(1),L(1),M(1)

SEARCH FOR LARGEST ELEMENT

```

D=1.0
NK=-N
DC 180 K=1,N
NK=NK+N
L(K)=K
M(K)=K
KK=NK+K
BICA=A(KK)
DC 2C J=K,N
IZ=N*(J-1)
CC 2C I=K,N
IJ=IZ+I
IF(ABS(BICA)-ABS(A(IJ))) 10,20,20
10 BICA=A(IJ)
L(K)=I
M(K)=J
20 CCNTINUE

```

C  
C  
C

INTERCHANGE ROWS

```

J=L(K)
IF(J-K) 50,50,30
30 KI=K-N
DC 4C I=J,N
KI=KI+N
HCLD=-A(KI)
JI=KI-K+J
A(KI)=A(JI)
40 A(JI)=HCLD

```

C

INTERCHANGE COLUMNS

```

50 I=M(K)
   IF(I-K) 80,80,60
60 JP=N*(I-1)
   DC 70 J=1,N
   JK=NK+J
   JI=JP+J
   HCLC=-A(JK)
   A(JK)=A(JI)
70 A(JI)=+CLC

```

DIVIDE COLUMN BY MINUS PIVOT (VALUE OF PIVOT ELEMENT IS CONTAINED IN BIGA)

```

80 IF(ABS(BIGA)-1.E-20) 90,90,100
90 D=C.C
   RETURN
100 DC 120 I=1,N
   IF(I-K) 110,120,110
110 IK=NK+I
   A(IK)=A(IK)/(-BIGA)
120 CCNTINUE

```

REDUCE MATRIX

```

DC 150 I=1,N
IK=NK+I
HCLC=A(IK)
IJ=I-N
DC 150 J=1,N
IJ=IJ+N
IF(I-K) 130,150,130
130 IF(J-K) 140,150,140
140 KJ=IJ-I+K
   A(IJ)=+CLC*A(KJ)+A(IJ)
150 CCNTINUE

```

DIVIDE ROW BY PIVOT

```

KJ=K-N
DC 170 J=1,N
KJ=KJ+N
IF(J-K) 160,170,160
160 A(KJ)=A(KJ)/BIGA
170 CCNTINUE

```

PRODUCT OF PIVOTS

D=C\*BIGA

REPLACE PIVOT BY RECIPROCAL

```

A(KK)=1.0/BIGA
180 CCNTINUE

```

FINAL ROW AND COLUMN INTERCHANGE

```

K=N
190 K=K-1
   IF(K) 260,260,200
200 I=L(K)
   IF(I-K) 230,230,210
210 JC=N*(K-1)
   JR=N*(I-1)
   DC 220 J=1,N
   JK=JC+J
   HCLC=A(JK)
   JI=JR+J
   A(JK)=-A(JI)
220 A(JI)=+CLC
230 J=M(K)
   IF(J-K) 190,190,240
240 KI=K-N
   DC 250 I=1,N
   KI=KI+N
   HCLC=A(KI)
   JI=KI-K+J
   A(KI)=-A(JI)

```

```

250 A(JI)=FCLD
GC TC 190
260 RETURN
END
SUBROUTINE CAGET(ARKAY,IFILE,II)

```

```

SUBROUTINE TO GET TABLE FROM DISK AND PUT
IT INTO CORE

```

```

DIMENSION ARRAY(5,25,8),CRRAY(5,25,8)
COMMON KCR,KIR,KIL,KOL,VSA(19),SW(19),VSBAR,EYETL,CTS,XPB,YPB,JP,
1 IPRAE,ALPH3,KSTAL,ISTAL,KCLNT,AB(3)
COMMON NSLIP,VR(19),CA(19),AS(19),TL(19),SV(19),FUNC,YO,CDNAC,
1 ALPHV(16)
COMMON INNCW,ISWIT(3),ALPHA,REYN,CLL,REYCN,XMAX,ALMAX(19),CLMAX(15
1),C(19),EPS(19),TRANS(19),RLY(19),ETA(19),HCPP(19),ZHERC(2,6),
2 ZHERE(2,6),CRRAY,Y(19),BETA(19,19),TFAC,TRIX(19,19),TAL(19),MAXX(6
3),MAZZ(6),MXCCL(6),MZCCL(6),ASPEC,IAPER,BF,REYND,DISCR,PIER,CRB,Q,
4 ISTAR,A,B,H,
5 STAGT,TALR,THIST,R,BFX,YFERE(2,6),MYCCL(6),MAYY(6),FLAP,TCNY(19),
6 T,ISA,X,Z,CM(19),ACC,XFERE(2,6),MWCCL(6),MAWW(6),CAMB(19),CAMER,
7 CAMBT,CLMY1,CLMY2,NAME(25),AFERE(2,6),MAAA(6),MACCL(6)

```

```

TABLE PRESENTLY IN CORE IS INNOW

```

```

IF TABLE IS ALREADY IN CORE THEN RETURN
IF NOT THEN GET TABLE FROM DISK

```

```

10 IF(IFILE-INNCW) 10,90,10
II=1
REWIND IFILE
READ(IFILE) ARRAY
REWIND IFILE

```

```

RESET TABLE PRESENTLY IN CORE INDICATOR

```

```

INNCW=IFILE
IF(IFILE=5) 50,30,90
30 DC 4C JFCX=1,NLVL
KRCW=MAAA(JFCX)-2
KCCL=MACCL(JFCX)
DC 4C KBCB=2,KCCL
ARRAY(JFCX,2,KBCB)=-9.0
40 ARRAY(JFCX,KRCW,KBCB)=9.0
GC TC 90
50 IF(IFILE=1) 90,60,90
60 DC 8C JFCX=1,NLVL
KRCW=MAXX(JFCX)-2
KCCL=MXCCL(JFCX)
DC 7C KBCB=2,KCCL
ARRAY(JFCX,2,KBCB)=-9.0
70 ARRAY(JFCX,KRCW,KBCB)=9.0
80 CONTINUE
90 RETURN
END
SUBROUTINE AAA(CLIST,NV)

```

```

SUBROUTINE TO OUTPUT A ONE DIMENSIONAL
ARRAY

```

```

DIMENSION CLIST(1)
IP=6
WRITE(IP,10) (J,CLIST(J),J=1,NV)
WRITE(IP,20)
RETURN

```

```

10 FORMAT(5(1X,I1(,I2,2H) ,E16.6))
20 FORMAT(2(1F ))
END
SUBROUTINE ZZZ(VALUE)

```

```

SUBROUTINE TO OUTPUT A SINGLE VALUE
OUTPUT VALUE IN BOTH F AND E FORMAT

```

```

IP=6
WRITE(IP,10) VALUE,VALUE
RETURN

```

```

10 FORMAT(1X,F15.8,E16.8/1X)

```

```

C
C
C
C
C
END
SUBROUTINE SSS(A,NP)
C
C
C
C
C
C
SUBROUTINE TC OUTPUT A SQUARE TWO
DIMENSIONAL ARRAY
DIMENSION A(19,19)
IP=6
WRITE(IP,1C) ((J,K,A(J,K),K=1,NP),J=1,NP)
WRITE(IP,2C)
RETURN
C
C
C
C
10 FCRMAT(5(1X,1F,12,1F,12,2F) ,E13.6))
20 FCRMAT(3(1FC/))
END
FUNCTION TERP(R1,R2,R3,C1,C3)
C
C
C
C
C
C
INTERPOLATION FUNCTION
IF(R1-R3) 2C,10,20
10 TERP=C1
RETURN
20 TERP=C1+((C3-C1)*((R2-R1)/(R3-R1)))
RETURN
END
SUBROUTINE SETSW
C
C
C
C
C
SUBROUTINE CHECKS SWITCH SETTINGS ON DATA
CARD AND LISTS OPTIONS SELECTED
COMMON KOR,KIR,KIL,KCL,VSA(19),SW(19),VSBAR,EYETL,CTS,XPB,YPB,JP,
1 IPRAB,ALPHB,KSTAL,ISTAL,KCLNT,AB(3)
COMMON NSLIP,VR(19),CA(19),AS(19),TL(19),SV(19),FUNC,YO,CDNAC,
1 ALPHV(1C)
COMMON INNCK,ISWIT(3)
K=C
IP=6
WRITE(IP,90)
IF(ISWIT(1)) 2C,20,10
10 K=K+1
WRITE(IP,10C)
20 IF(ISWIT(2)) 40,40,30
30 K=K+1
WRITE(IP,11C)
40 IF(ISWIT(3)) 6C,60,50
50 K=K+1
WRITE(IP,12C)
60 IF(K) 8C,70,80
70 WRITE(IP,13C)
80 RETURN
C
90 FCRMAT(11F1/1FC/1HC,5CX,29FSPECIAL FEATURES FOR THIS RUN/1HO)
100 FCRMAT(51X,14FREAD IN VALUES/1FC)
110 FCRMAT(51X,34FTRACE (OUTPUT OF KEY CALCULATIONS)/1HO)
120 FCRMAT(51X,2CFPRINT MATRICES BETA AND TRIX/1HO)
130 FCRMAT(51X,31FC SWITCH SETTINGS REGULAR RUN)
END
SUBROUTINE DATSW(N,ICOND)
SUBROUTINE MAKES DECISION BASED ON SETTING OF THE SWITCH,
SET=1,NOT SET=C. ICCOND=1 IF SWITCH IS SET,ICOND=2 IF
SWITCH IS NOT SET
COMMON INNCK,ISWIT(3)
IF(N=3) 1C,2C,3C
10 IF(ISWIT(1)) 4C,4C,50
10 IF(ISWIT(2)) 4C,4C,50
10 IF(ISWIT(3)) 4C,4C,50
40 ICCOND=2
RETURN
50 ICCOND=1
RETURN
END
SUBROUTINE AERCA(ARRAY,NLVL,WHERE,MAXCOL,MAXX,IFILE,KEEP)
C
C
C
C
C
SUBROUTINE TC READ AERODYNAMIC TABLES FROM
CARDS AND PUT TABLES ON DISK
DIMENSION NAME(4C),MAXX(6),MAXCOL(6),WHERE(2,6),ARRAY(5,25,8)
COMMON KOR,KIR,KIL,KCL,VSA(19),SW(19),VSBAR,EYETL,CTS,XPB,YPB,JP,
1 IPRAB,ALPHB,KSTAL,ISTAL,KCLNT,AB(3)
COMMON NSLIP,VR(19),CA(19),AS(19),TL(19),SV(19),FUNC,YO,CDNAC,

```





```

7MCCCL(6),DHERE(2,6),MADD(6),MCCOL(6)
                                INITIALIZATION
                                IF REYCN=999 THEN SPECIAL CASE

                                DCMY2=C.0
                                DCMY1=C.0
                                IF(REYCN=999.) 20,10,20
10  KEY=1
20  GC TC 30
    KEY=2

                                STORE C VALUE

30  CLT=CLL

                                NEW IS THE FILE NUMBER OF THE OTHER CUBE
                                PRIMARY CUBES ARE NUMBERED 1,2,3,4
                                SECONDARY CUBES ARE NUMBERED 5,10,15,20

    NEW=LCM*5

                                STORE XMAX

    XMX=XMAX

                                DETERMINE IF SINGLE VALUE IS TO BE USED OR
                                LIST OF VALUES IS TO BE USED IN LOOK UP

40  IF(IS=1P) 50,40,50
    KCC=1

                                SET UP FOR CONSTANT VALUE OF X

    ATMP(1)=XX(1)
    GC TC 7C

                                SET UP FOR VARIABLE VALUE OF X

50  KCC=2
    DC 6C J=NS,AP
60  ATMP(J)=XX(J)

                                PUT PROPER TABLE IN CORE

70  CALL DACET(ARRAY,NEW,IZXY)

                                SET UP ALPHA EITHER VARIABLE OR CONSTANT

    DC 19C K=NS,AP
    GC TC (80,90), KGC
80  ALPFA=ATMP(IS)
    GC TC 10C
90  ALPFA=ATMP(K)

                                GET TAU VALUE FROM ARRAY

100 TAUX=TAL(K)
    GC TC (120,110), KEY

                                GET PROPER REYNCLDS NUMBER EITHER REGULAR
                                OR MAX NUMBER

110 REYCN=REY(K)
    REYN=999.
    GC TC 130
120 REYN=REY(K)
130 CLL=CLT
    XMAX=XMX

                                PERFORM LOOK FOR LIFT, DRAG, PITCHING
                                MOMENT OR FLAP CASE

    GC TC (140,150,160,170), LCM
140 CALL ARC(ARRAY,TAUX,MAAA,MACCL,IE,AHERE,NLVL)
    GC TC 180
150 CALL ARC(ARRAY,TALX,MABB,MCCCL,IE,BHERE,NLVL)
    GC TC 180
160 CALL ARC(ARRAY,TAUX,MACC,MCCCL,IE,CHERE,NLVL)
    GC TC 180

```

```

17C CALL ARC(ARRAY,TAUX,MADD,MCCCL,IE,DHERE,NLVL)
                                STORE VALUES FOUND IN LOCK UP
18C CCZ2(K)=YY
  CCLR2(K)=DUMY1
  CALR2(K)=DUMY2
                                REPEAT FOR NUMBER OF VALUES TO BE FOUND
19C CCNTINUE
                                GET NEXT TABLE IN CORE
  CALL CAGET(ARRAY,LCM,IY)
                                SET UP ALPHA VALUE
  DC 310 K=NS,NP
  GC TC (20C,21C), KGO
20C ALPHA=ATMP(15)
  GC TC 220
21C ALPHA=ATMP(K)
                                SET UP REYNOLDS NUMBER
22C GC TC (24C,23C), KEY
23C REYN=REY(K)
  REYN=999.
  GC TC 250
24C REYN=REY(K)
                                SET UP CVAL, TAU, AND XMAX VALUE
25C CLL=CLT
  TAU=TAL(K)
  XMAX=XMX
                                LOCK UP FOR SECOND LIFT, DRAG, PITCHING
                                MCMENT, OR FLAP CASE
  GC TC (26C,27C,28C,29C), LCM
26C CALL ARC(ARRAY,TAUX,MAXX,MXCCL,IE,WHERE,NLVL)
  GC TC 30C
27C CALL ARC(ARRAY,TALX,MAZZ,MZCCL,IE,ZHERE,NLVL)
  GC TC 30C
28C CALL ARC(ARRAY,TAUX,MAYY,MYCCL,IE,YHERE,NLVL)
  GC TC 30C
29C CALL ARC(ARRAY,TAUX,MAHH,MHCCL,IE,XHERE,NLVL)
                                STORE VALUES FOUND IN LOCK UP
30C CCZ1(K)=YY
  CCLR1(K)=DUMY1
  CALR1(K)=DUMY2
31C CCNTINUE
                                SPECIAL CASE FOR LIFT LOCK UP
  GC TC (32C,40C,40C,40C), LCM
                                REPEAT FOR ALL VALUES OF TAU
32C DC 39C K=NS,NP
  ALPHA=ATMP(K)
  CCLR=TERP(CAMBR,CAMB(K),CAMBT,CCLR1(K),CCLR2(K))
  CALR=TERP(CAMBR,CAMB(K),CAMBT,CALR1(K),CALR2(K))
  IF((ALPHA-CALR1(K))*(ALPHA-CALR2(K))) 34C,33C,33C
33C CCZ1(K)=TERP(CAMBR,CAMB(K),CAMBT,CCZ1(K),CCZ2(K))
  GC TC 35C
34C IF(CALR2(K)-CALR1(K)) 35C,350,360
35C IF(ALPHA-CALR) 37C,37C,38C
36C IF(ALPHA-CALR) 38C,38C,37C
37C CLA=TERP(CALR1(K),CALR2(K),ALPHA,CCLR1(K),CCZ1(K))
  CLC=TERP(CAMBR,CAMB(K),CAMBT,CLA,CCLR2(K))
  CCZ1(K)=TERP(CALR2(K),ALPHA,CALR,CLC,CCLR)
  GC TC 390
38C CLB=TERP(CALR2(K),CALR1(K),ALPHA,CCLR2(K),CCZ2(K))
  CLC=TERP(CAMBR,CAMB(K),CAMBT,CCLR1(K),CLB)
  CCZ1(K)=TERP(CALR1(K),ALPHA,CALR,CLC,CCLR)

```

390 CONTINUE  
RETURN

REGULAR INTERPOLATION BETWEEN TABLES

400 DC 410 K=NS,NP

410 CCZ1(K)=TERP(CAMBR,CAMB(K),CAMBT,CCZ1(K),CCZ2(K))  
RETURN

EAC

SUBROUTINE ARC(ARRAY,TAU,ARCWS,NCCLS,IE,WHERE,NLVLS)

SUBROUTINE TO INTERPOLATE BETWEEN LEVELS OF  
A GIVEN TABLE

DIMENSION ARRAY(5,25,8),ARCWS(6),NCCLS(6),CLR(2),ALR(2),TCNY(19),  
1 WFERE(2,6),YHERE(2,6),MYCCL(6),MAYY(6),CM(19),XHERE(2,6),MAWW(6),  
2 MWCCL(6),C(19),EPS(19),TRANS(19),REY(19),ETA(19),HCPP(19),CLMAX(19,  
3),ZHERE(2,6),HERE(2,6),Y(19),UAU(19),BETA(19,19),TRIX(19,19),MAZZ(  
4),MZCCL(6),MAXX(6),MXCCL(6)

COMMON KGR,KIR,KIL,KGL,VSA(19),SW(19),VSEAR,EYETL,CTS,XPB,YPB,JP,  
1 IPRAB,ALPHA,KSTAL,ISTAL,KCLNT,AB(3)

COMMON NSLIP,VR(19),DA(19),AS(19),TL(19),SV(19),FUNC,YO,CDNAC,  
1 ALPHA(16)

COMMON INNOW,ISWIT(3),ALPHA,REYN,CVAL,REYON,XMAX,ALMAX(19),CLMAX,C  
1,EPS,TRANS,REY,FIA,FOPP,ZHERE,HERE,ARRAY,Y,BETA,IFAC,TRIX,UAU,MAXX  
2,MAZZ,MXCCL,MZCCL,ASPEC,TAPEK,BF,REYND,DISCR,PIEK,CRB,C,TSTAX,EDGE  
3,SIG,ALPHR,NFLAP,NLVL,NP,IY,IZ,IR,IP,IV,ISTAR,A,B,H,TAUT,TAUR,  
4 TWIST,R,BWX,YHERE,MYCCL,MAYY,FLAP,TCNY,TWISA,X,Z,CM,ACC,XHERE,  
5 MWCCL,MAWW,CAMB(19),CAMBR,CAMBT,DUMY1,DUMY2,NAME(25),AHERE(2,6),  
6 MAJAA(C),MACCL(6),BHERE(2,6),MABB(6),MBCOL(6),CHEKE(2,6),MACC(6),  
7 MCCCL(6),EHERE(2,6),MADD(6),MDCOL(6)

IE=C  
XTRAL=C.  
XTRAU=C.

IS TAU LESS THAN OR EQUAL TO LOWEST LEVEL  
TAL VALUE

10 IF(TAL-WHERE(2,1)) > 10,20,20  
J=2  
XTRAL=1.  
GC TC 8C

20 IF(TAL-WHERE(2,NLVLS)) 40,30,30  
YES, SET J EQUAL TO MAX LEVEL

30 J=NLVLS  
XTRAU=1.  
GC TC 80

NC, SEARCH LIST OF LEVELS (TAU VALUES)  
UNTIL ONE GIVEN IS GREATER THAN ONE TO BE  
FOUND

40 DC 50 J=2,NLVLS  
IF(TAL-WHERE(2,J)) 90,90,50  
50 CONTINUE

ERROR IF NONE CAN BE FOUND

IE=6  
IF(IE) 70,70,60  
60 WRITE(IP,54C) IE,INNOW,CVAL,ALPHA,REYN,REYON,XMAX  
70 RETURN

80 CONTINUE  
90 LVL=WHERE(1,J)  
MAXR=ARCWS(J)  
MAXC=NCCLS(J)

IF(ALPHA-999.) 100,130,100  
100 IF(REYN-999.) 110,120,110  
110 IF(CVAL-999.) 260,250,260  
120 IF(CVAL-999.) 240,260,240  
130 IF(CVAL-999.) 140,150,140  
140 IF(REYN-999.) 230,260,230  
150 IF(REYN-999.) 260,160,260  
160 IF(REYON-999.) 180,170,180  
170 IF(XMAX) 220,260,220  
180 IF(XMAX) 200,190,200  
190 IF(LP=1

```

GC TC 210
200 IFLP=2
210 IS=5
GC TC 270
220 IS=4
GC TC 270
230 IS=1
GC TC 270
240 IS=2
GC TC 270
250 IS=3
GC TC 270
260 IE=6
RETURN
270 CALL LOCK(ARRAY,LVL,MAXR,MAXC,IE)
CLR(2)=DUMY2
ALR(2)=DUMY1
GC TC (280,290,300,310,320), IS
280 FIND=ALPHA
ALPHA=999.
GC TC 350
290 FIND=REYN
REYN=999.
GC TC 350
300 FIND=CVAL
CVAL=999.
GC TC 350
310 FIND=REYON
REYON=999.
GC TC 350
320 FIND=XMAX
GC TC (330,340), IFLP
330 XMAX=C.
GC TC 350
340 XMAX=100.
350 LVL=WFERE(1,J-1)
MAXR=NROWS(J-1)
MAXC=NCOLS(J-1)

```

SPECIAL PROCEDURE FOR INTERPOLATION IN THE  
NEIGHBORHOOD OF CL MAX

```

CALL LOCK(ARRAY,LVL,MAXR,MAXC,IE)
CLR(1)=DUMY2
ALR(1)=DUMY1
IF(IE) 360,360,60
360 R1=WFERE(2,J-1)
R2=TAL
R3=WFERE(2,J)
C3=FIND
GC TC (490,500,370,520,530), IS
370 IF(INNCW-1) 380,390,380
380 IF(INNCW-5) 510,390,510
390 DUMY1=TERP(R1,R2,R3,CLR(1),CLR(2))
DUMY2=TERP(R1,R2,R3,ALR(1),ALR(2))
IF((ALPHA-ALR(1))*(ALPHA-ALR(2))) 400,510,510
400 IF(XTRAL-1.) 410,420,410
410 IF(XTRAL-1.) 440,430,440
420 CVAL=DUMY1-CLR(1)+TERP(ALPHA,DUMY2,ALR(1),CLR(1),CVAL)
RETURN
430 CVAL=DUMY1-CLR(2)+TERP(ALPHA,DUMY2,ALR(2),CLR(2),C3)
RETURN
440 IF(ALR(2)-ALR(1)) 450,450,460
450 IF(ALPHA-DUMY2) 470,470,480
460 IF(ALPHA-DUMY2) 480,480,470
470 CLA=TERP(ALR(1),ALR(2),ALPHA,CLR(1),CVAL)
CLC=TERP(R1,R2,R3,CLA,CLR(2))
CVAL=TERP(ALR(2),ALPHA,DUMY2,CLC,DUMY1)
RETURN
480 CLB=TERP(ALR(2),ALR(1),ALPHA,CLR(2),C3)
CLC=TERP(R1,R2,R3,CLR(1),CLB)
CVAL=TERP(ALR(1),ALPHA,DUMY2,CLC,DUMY1)
RETURN
490 C1=ALPHA
ALPHA=TERP(R1,R2,R3,C1,C3)
RETURN
500 C1=REYN
REYN=TERP(R1,R2,R3,C1,C3)
RETURN
510 C1=CVAL

```

```

CVAL=TERP(R1,R2,R3,C1,C3)
RETURN
520 C1=REYN
REYCN=TERP(R1,R2,R3,C1,C3)
RETURN
530 C1=XMAX
XMAX=TERP(R1,R2,R3,C1,C3)
RETURN

```

```

540 FORMAT(20X,12HEXERRR CCDE (,12,42H ) IF 1 CVAL GREATER THAN MAX VAL
1UE LISTEC/37X,34HIF 2 CVAL GREATER THAN TABLE VALUE/37X,41HIF 3 AL
2PFA VALUE GREATER THAN TABLE VALUE/37X,29HIF 6 TAU VALUE CANNOT BE
3FCUNC/37X,13HTABLE NUMBER ,12,IF IN CCRE/10X,8HC-VALUE=,F10.2,5X,
46HALPHA=,F10.2,5X,13HREYNCLDS NO.=,F10.2,5X,6HREYCN=,F10.2,5X,5HXM
5AX=,F10.2/12C(1H/))
END

```

```

SUBROUTINE LCCK(AR,LVL,MAXR,MAXC,IE)

```

```

SUBROUTINE FOR TWO DIMENSIONAL TABLE LOOKUP

```

```

DIMENSION A(5,25,8),TCNY(19),YHERE(2,6),MYCCL(6),MAYY(6),CM(19),
1XFERE(2,6),MAWW(6),MWCC(6),C(19),EPS(19),TRANS(19),REY(19),ETA(19
2),FCPP(19),CLMAX(19),ZHERE(2,6),HERE(2,6),Y(19),LAC(19),BETA(19,19
3),TRIX(19,19),MAZZ(6),MZCCL(6),MAXX(6),MXCOL(6)
CCMCMN KOR,KIR,KIL,KOL,VSA(19),SW(19),VSBAR,EYETL,CTS,XPB,YPB,JP,
1IPRAB,ALPHB,KSTAL,ISTAL,KCLNT,Ab(3)
CCMCMN ASLIP,VR(19),DA(19),AS(19),TL(19),SV(19),FUNC,YO,CDNAC,
1ALPHV(16)
CCMCMN INCH,ISWIT(3),ALPHA,REYN,CVAL,REYCN,XMAX,ALMAX(19),CLMAX,C
1,EPS,TRANS,REY,ETA,FCPP,ZHERE,HERE,A,Y,BETA,TFAC,TRIX,UAU,MAXX,
2MAZZ,MXCCL,MZCCL,ASPEC,TAPER,BF,REYND,DISCR,PIER,CRR,O,ISTAX,EDGE,
3SIG,ALPHR,NFLAP,NLVL,NP,IY,IZ,IR,IP,IS,ISTAR,AA,B,F,TAUT,TAUR,
4T,IST,R,BWX,YHERE,MYCCL,MAYY,FLAP,TCNY,TWISA,X,Z,CM,ACC,XHERE,
5MWCC,MAWW,CAMB(19),CAMBR,CAMBT,DUMY1,DUMY2

```

```

SECTION TO LOCATE REYNOLDS NUMBER IN TABLE

```

```

XTRAL=0.
XTRAU=C.

```

```

LRCW IS THE LAST ROW CONTAINING INFORMATION
IN ANY TABLE. THE LAST TWO ROWS OF ANY
TABLE CONTAIN MAX DATA.

```

```

LRCW=MAXR-2
IS=1

```

```

IS REYCN EQUAL TO 999.
IF YES THEN NORMAL AND WE WILL ALREADY HAVE
SET THE SWITCH IS TO 1 AND WE WILL USE THE
VALUE OF REYN
IF NO THEN SET REYN TO REYCN AND SET SWITCH
IS TO 2

```

```

10 IF(REYCN-999.) 10,20,10
REYN=REYCN
IS=2

```

```

IS THE REYNOLDS NUMBER WE ARE LOOKING FOR
GREATER THAN OR EQUAL TO THE REYNOLDS
NUMBER GIVEN ALONG THE FIRST ROW OF THE
TABLE

```

```

20 IF(REYN-A(LVL,1,MAXC)) 40,30,30
30 LCCR=MAXC
XTRAL=1.
GC TC 7C

```

```

NORMAL CASE. IF REYNOLDS NUMBER IS LESS
THAN MAX REYN NUMBER IN TABLE THEN WE
CHECK TC SEE IF IT IS GREATER THAN THE
MINIMUM REYNOLDS NUMBER LISTED IN THE TABLE

```

```

40 IF(REYN-A(LVL,1,2)) 50,60,60

```

```

IF LESS THAN MINIMUM WE WANT TO USE THE
MINIMUM VALUE IN THE TABLE

```

```

50 LCCR=3
XTRAL=1.

```

GC TC 70

IF LESS THAN MAXIMUM AND GREATER THAN  
MINIMUM WE WANT TO SEARCH TABLE UNTIL WE  
FIND A REYNOLDS NUMBER GREATER THAN THE  
GIVEN REYNOLDS NUMBER  
IF REYN LESS THAN KEEP LOOKING  
IF REYN GREATER THAN SET UP R1,R3 FOR  
INTERPLATION

60 DC 61C LCCR=3,MAXC  
IF(REYN-A(LVL,1,LCCR)) 70,70,610  
70 R1=A(LVL,1,LCCR-1)  
R3=A(LVL,1,LCCR)  
GC TC (80,150), IS

SECTION FOR NORMAL LOOK UP OF ALPHA AND  
CVAL. A VALUE OF 999 SPECIFIES THAT THIS  
VARIABLE IS THE ONE WHOSE VALUE IS TO BE  
FOLLO IN THE TABLE.

80 IF(ALPHA-999.) 90,110,90  
90 IF(REYN-999.) 100,600,100  
100 IF(CVAL-999.) 600,190,600  
110 IF(CVAL-999.) 120,130,120  
120 IF(REYN-999.) 160,600,160  
130 IF(REYN-999.) 600,140,600  
140 IF(REYN-999.) 150,600,150

SECTION FOR LOOKING UP MAX VALUES

150 IF(XMAX) 580,590,580

SECTION TO LOOK UP ALPHA FOR GIVEN CVAL BY  
INTERPLATING BETWEEN COLUMNS WHERE  
REYNOLDS NUMBERS BRACKET GIVEN REYN

160 DC 170 J=3,LRCW  
CCC=TERP(R1,REYN,R3,A(LVL,J,LCCR-1),A(LVL,J,LOCR))  
IF(CVAL-CCC) 180,180,170  
170 CCNTINLE  
JE=2  
GC TC 600  
180 CC2=TERP(R1,REYN,R3,A(LVL,J-1,LOCR-1),A(LVL,J-1,LOCR))  
ALPHA=TERP(CC2,CVAL,CCC,A(LVL,J-1,1),A(LVL,J,1))  
GC TC 600

LOOK UP CVAL FOR GIVEN ALPHA. CHECK TO SEE  
IF WE HAVE A LIFT OR DRAG TABLE IN AT THIS  
TIME. DRAG TABLES HAVE ZERO VALUES FOR ALL  
MAXIMUM VALUES (LAST TWO ROWS).

190 IF(A(LVL,MAXR,LCCR-1)) 210,200,210  
200 IF(A(LVL,MAXR,LCCR)) 210,550,210

FOR LIFT TABLE. DUMY1 AND DUMY2 ARE THE  
MAXIMUM INTERPLATED VALUES FOR GIVEN  
REYNOLDS NUMBERS OF ALPHA MAX AND CVAL MAX

210 CCNTINLE  
DUMY1=TERP(R1,REYN,R3,A(LVL,MAXR,LCCR-1),A(LVL,MAXR,LOCR))  
DUMY2=TERP(R1,REYN,R3,A(LVL,MAXR-1,LOCR-1),A(LVL,MAXR-1,LOCR))  
IF(XTRAL-1.) 220,240,220  
220 IF(XTRAL-1.) 230,240,230  
230 CCNTINLE  
IF((ALPHA-A(LVL,MAXR,LCCR-1))\*(ALPHA-A(LVL,MAXR,LCCR)))240,250,250  
240 IF(A(LVL,MAXR,LCCR)-A(LVL,MAXR,LCCR-1)) 270,260,260  
250 GC TC 550  
260 ALPHA1=A(LVL,MAXR,LCCR-1)  
ALPHA2=A(LVL,MAXR,LCCR)  
GC TC 280  
270 ALPHA1=A(LVL,MAXR,LCCR)  
ALPHA2=A(LVL,MAXR,LCCR-1)  
280 IF(XTRAL-1.) 290,300,290  
290 IF(XTRAL-1.) 480,390,480  
300 IF(ALPHA2-DUMY1) 350,550,310  
310 IF((ALPHA-DUMY1)\*(ALPHA-ALPHA2)) 320,550,550  
320 DC 330 J=3,LRCW  
IF(ALPHA2-A(LVL,J,1)) 340,340,330  
330 CCNTINLE

```

IE=3
GC TC 600
340 C1=A(LVL,J,LCCR-1)
CVAL=DUMY2+(A(LVL,MAXR-1,LCCR-1)-C1)/(ALPH1-ALPH2)*(ALPHA-DUMY1)
GC TC 600
350 IF((ALPHA-DUMY1)*(ALPHA-ALPH1)) 360,550,550
360 DC 370 J=3,LRCW
IF(ALPH1-A(LVL,J,1)) 380,380,370
370 CCNTINUE
IE=3
GC TC 600
380 C1=A(LVL,J,LCCR-1)
CVAL=DUMY2+(A(LVL,MAXR-1,LCCR-1)-C1)/(ALPH2-ALPH1)*(ALPHA-DUMY1)
GC TC 600
390 IF((ALPH2-DUMY1) 400,550,440
400 IF((ALPHA-DUMY1)*(ALPHA-ALPH1)) 410,550,550
410 DC 420 J=3,LRCW
IF(ALPH1-A(LVL,J,1)) 430,430,420
420 CCNTINUE
IE=3
GC TC 600
430 C1=A(LVL,J,LCCR)
CVAL=DUMY2+(A(LVL,MAXR-1,LCCR)-C1)/(ALPH2-ALPH1)*(ALPHA-DUMY1)
GC TC 600
440 IF((ALPHA-DUMY1)*(ALPHA-ALPH2)) 450,550,550
450 DC 460 J=3,LRCW
IF(ALPH2-A(LVL,J,1)) 470,470,460
460 CCNTINUE
IE=3
GC TC 600
470 C1=A(LVL,J,LCCR)
CVAL=DUMY2+(A(LVL,MAXR-1,LCCR)-C1)/(ALPH2-ALPH1)*(ALPHA-DUMY1)
GC TC 600
480 IF((ALPHA-DUMY1) 490,490,520
490 DC 500 J=3,LRCW
IF(ALPH1-A(LVL,J,1)) 510,510,500
500 CCNTINUE
IE=3
GC TC 600
510 C1=A(LVL,J,LCCR-1)
C3=A(LVL,J,LCCR)
C1=TERP(R1,REYN,R3,C1,C3)
CVAL=TERP(ALPH1,ALPHA,DUMY1,C1,DUMY2)
GC TC 600
520 DC 530 J=3,LRCW
IF(ALPH2-A(LVL,J,1)) 540,540,530
530 CCNTINUE
IE=3
GC TC 600
540 C1=A(LVL,J,LCCR-1)
C3=A(LVL,J,LCCR)
C3=TERP(R1,REYN,R3,C1,C3)
CVAL=TERP(DUMY1,ALPHA,ALPH2,DUMY2,C3)
GC TC 600
550 DC 560 J=3,LRCW

SEARCH FOR ALPHA

IF(ALPHA-A(LVL,J,1)) 570,570,560
560 CCNTINUE
IE=3
GC TC 600
570 CCC=TERP(R1,REYN,R3,A(LVL,J-1,LCCR-1),A(LVL,J-1,LCCR))
CC2=TERP(R1,REYN,R3,A(LVL,J,LCCR-1),A(LVL,J,LCCR))
CVAL=TERP(A(LVL,J-1,1),ALPHA,A(LVL,J,1),CCC,CC2)
GC TC 600
580 XMAX=TERP(R1,REYN,R3,A(LVL,MAXR,LCCR-1),A(LVL,MAXR,LCCR))
GC TC (600,620), IS
590 XMAX=TERP(R1,REYN,R3,A(LVL,MAXR-1,LCCR-1),A(LVL,MAXR-1,LCCR))
GC TC (600,620), IS
600 RETURN
510 CCNTINUE
IE=1
GC TC 600
620 REYN=999.
GC TC 600
ENC
SUBROUTINE FCISK(ITNC,TLCS)

```

SUBROUTINE TO STORE TABULATED PROPELLER  
TIP LOSS CORRECTION DATA ON DISK

```
REAL TLCS(8)  
READ(11*ITNC) TLOSS  
RETURN  
ENC  
SUBROUTINE GDISK(ITNC,TALFA,TLIFT)
```

SUBROUTINE TO STORE TABULATED PROPELLER  
AIRFOIL SECTION DATA ON DISK -  
ALPHA AND CL VALUES ONLY

```
REAL TALFA(20),TLIFT(20)  
READ(12*ITNC) TALFA  
READ(13*ITNC) TLIFT  
RETURN  
ENC  
SUBROUTINE SLIP
```

SUBROUTINE TO CALCULATE PROPELLER  
SLIPSTREAM VELOCITY DISTRIBUTION USING  
NACA - LINEAR BLADE AIRFOIL SECTION  
LIFT CHARACTERISTICS

```
DIMENSION NS(19),YBW(19),RSBW(19),RSBA(19),VST(19),  
1RSBR(12),LSAPR(12),USTBR(12),BDATA(12,5),NDATA(12),TITLE(19),  
2ITFAC(150,2),THEAC(150,5),TALFA(20),TLIFT(20),TLCS(8),  
3AFSER(5,2),AK(5,2),NG(5),ITA(5,2),ITN(5,2),ITC(4,2),ITM(2),FR(2),  
4TCLI(4),TICC(4),TXCL(4),CLG(4),CLM(2),CLC(2),NRCT(2),RUI(2),  
5IFECC(2),THECC(5)  
COMMON KCR,KIR,KIL,KGL,VSA(19),SW(19),VSBAR,EYETL,CTS,XPB,YPB,JP,  
1IPRAB,ALPHA
```

\*\*\*\*\* INITIALIZE DATA ARRAYS

```
DATA AK/10*C.C/  
DATA NG/9*0/  
DATA ITA/18*C/  
DATA AFSEK/18*4F /  
DATA AFSER(1,1),AFSER(1,2)/4F US,4FNPS /  
DATA AFSEK(2,1),AFSER(2,2)/4F CLA,4FRK.Y/  
DATA AFSEK(3,1),AFSER(3,2)/4F NAC,4FA 16/  
DATA AFSEK(4,1),AFSER(4,2)/4F NAC,4FA 64/  
DATA AFSEK(5,1),AFSER(5,2)/4F NAC,4FA 65/  
DATA ARCTL,ARCTC,ARCTR/3F LH,3H RH/
```

CHECK VALUE OF IPRAB

```
EQ 1 - NEW CASE, READ CARD INPUT  
NE 1 - NEW ALPHA ONLY, SKIP CARD INPUT
```

```
IF (IPRAB-1) 2350,2000,2350  
CONTINUE
```

SET FIXED CONSTANTS

```
KP=6  
KR=8  
PI=3.1415927  
RTC=57.29578
```

SET AIRFOIL CONSTANTS FOR INITIAL SOLUTION

```
AK(1,2)=-40.C  
AK(2,2)=-40.C  
AK(3,1)=-7.3  
AK(4,1)=-0.9  
AK(5,1)=-6.9  
.....
```

READ, STORE AND INDEX TIP LOSS CORR TABLES

```
**  
** DATA CARDS ACCEPTED IN ANY ORDER, **  
** BUT MUST NUMBER EITHER C OR 63 **  
**  
** NONE REQUIRED IF TIP LOSS TABLES **  
** ARE ALREADY STORED ON DISK FILE **  
**  
** FOLLOWING CARD MUST BE BLANK **
```





```

WRITE(12,IT) TALFA
WRITE(13,IT) TLIFT
2230 IF (I-HEAD(IT,2)-IA) 2230,2250,2230
      NG(IA)=IG
      IC=IG+1
      ITA(IA,IG)=IT
      ITA(IA,2)=IT-1
2240 IF (I-HEAD(IT,2)) 2210,2240,2210
      NT=IT-1
      GC TC 2295
2250 IF (I-HEAD(IT,1)-THEC1) 2270,2260,2270
2260 IF (I-HEAD(IT,2)-THEC2) 2280,2220,2280
C
C
2270 THEC1=THEAD(IT,1)
      IF (I-HEAD(IT,2)-THEC2) 2280,2290,2280
C
2280 THEC2=THEAD(IT,2)
C
      SET AIRFOIL SECTION INDEX
2290 IC=IG+1
      ITA(IA,IG)=IT
      GC TC 2220
2295 CCNTINUE
C
      PRINT SUMMARY OF AIRFOIL TABLES READ IN
2296 WRITE(KP,2983) NT
      WRITE(KP,2984) (I,I=1,9)
      WRITE(KP,2985) (AFSER(I,1),AFSER(I,2),I=1,9)
      WRITE(KP,2986) (NG(I),I=1,9)
      WRITE(KP,2987) (ITA(I,1),ITA(I,2),I=1,9)
C
C
C
C
      READ CASE INPUT DATA CARDS IDENT 1 - 4
      READ TITLE CARD
      READ(KR,2921) TITLE,IDENT
      IF (IDENT-1) 2897,2330,2897
C
      READ PROPELLER-NACELLE GEOMETRY CARD
2330 READ(KR,2923) NP,NB,DPB,RFB,RNR,IDENT
      IF (IDENT-2) 2897,2340,2897
C
      READ PROPELLER OPERATING CONDITION CARD
2340 READ(KR,2924) ARCT(1),ARCT(2),AJ,AMCHU,IDENT
      IF (IDENT-3) 2897,2341,2897
2341 DC 2345 I=1,2
      IF (ARCT(I)) 2342,2343,2344
2342 RCT(I)=ARCTL
      GC TC 2345
2343 RCT(I)=ARCTC
      GC TC 2345
2344 RCT(I)=ARCTR
2345 CCNTINUE
C
C
2350 ***** CALCULATE BASIC CASE PARAMETERS
      ALFP=ALPHB+EYETL
      ALFPR=ALFP/RTC
      CA=CCS(ALFPR)
      AMLT=AJ*CA/PI
      AMCFI=PI*AMCFI/AJ
      DNP=CPB*RNR
C
      PRINT MAIN HEADER TITLES AND INPUT VALUES
      WRITE(KP,2951) TITLE
      WRITE(KP,2952) NP,NB,RCT(1),RCT(2),XPC,RFB,AJ
      WRITE(KP,2954) YPB,RNR,AMCFI,CPB,EYETL,ALFP
      WRITE(KP,2956)
C
      INITIALIZE SLIPSTREAM VALUES
      AT FUB AND NACELLE
      IS=C
      RFBXR=RFB
      RNBXR=RNR
      USBRX=1.0
      OCTX=C.C
      OCCX=C.C
      CT=C.C
      CC=C.C
C
      READ BLADE STATION DATA CARD IDENT 4

```

```

C
C
C
C
C
C
C
C
**
**  LAST DATA CARD MUST HAVE RPBR=1.0
**
C
2360 IS=IS+1
IF (IPRAB-1) 2370,2365,2370
2365 REAC(KR,2925) (BCATA(IS,1),I=1,3),NDATA(IS),
1 (BCATA(IS,1),I=4,5),ICENT
IF (ICENT-4) 2897,2370,2897
2370 RPBR=BCATA(IS,1)
CPBR=BCATA(IS,2)
BFTA=BCATA(IS,3)
CLI=BCATA(IS,4)
TLC=BCATA(IS,5)
NA=NDATA(IS)
C
C
CHECK FOR LAST BLADE STATION DATA CARD
C
IF (RPBR-1.C) 2400,2380,2380
C
C
CALCULATE BOUNDARY VALUES FOR SLIPSTREAM
2380
.....
NIT=C
F=C.O
AMACT=AMCT*SQRT(1.O+AMUT**2)
ALPHA=C.O
CL=C.C
CC=C.C
RSBR(IS)=SQRT(RSBR**2+(1.C-RPBR**2)*(0.5+1.O/(1.O+USBR)))
RSTPR=RSBR(IS)
USAPR(IS)=1.O
USTPR(IS)=C.O
PHIS=C.C
CI=CI+C.O*CCCX*(1.C-RPBR)
CC=CC+C.O*CCCX*(1.C-RPBR)
GC TC 2750
2400
.....
LOCATE AND INDEX AIRFOIL TABLES
AND GEOMETRIC DATA AS REQUIRED
TO LOCK UP CL FOR SPECIFIED
AIRFOIL SECTION GEOMETRY
C
C
IT=ITN(NA,1)
IF (IT) 2410,2405,2410
2405 WRITE(KP,2994) NA,RPBR
IS=IS-1
GC TC 2360
2410 THEC1=THEAC(IT,1)
DC 2411 I=1,4
ITC(I,1)=C
2411 ITC(I,2)=C
IA=1
IB=2
IC=1
IC=C
IF=C
IG=C
2415 IG=IG+1
IT=ITN(NA,IG)
IF (THEAD(IT,1)-CLIX 2420,2440,2445
2420 IF (THEAD(IT,1)-TFED1) 2425,2430,2425
2425 IC=IG
THEC1=THEAC(IT,1)
2430 IF (IC-NG(NA)) 2415,2435,2415
2435 IG=IC
IT=ITN(NA,IG)
GC TC 2455
2440 THEC1=THEAD(IT,1)
GC TC 2435
2445 IF (IG-1) 2450,2455,2450
2450 IC=IG
IG=IC
2455 IF (THEAD(IT,2)-TCC) 2460,2475,2470
2460 IE=1
ITG(IA,1)=IT
TCL(IA)=THEAC(IT,1)
ITCC(IA)=THEAC(IT,2)
TXCL(IA)=THEAC(IT,5)
IG=IG+1
IT=ITN(NA,IG)
ITG(IA,2)=IT-1
IF (IG-NG(NA)) 2465,2465,2485

```

```

2465 IF (THEAD(IT,1)-TFED1) 2485,2455,2485
2470 IF (IE) 248C,2475,248C
2475 ITG(IA,1)=IT
      TCL1(IA)=THEAD(IT,1)
      TTCC(IA)=THEAD(IT,2)
      TXCL(IA)=THEAD(IT,5)
      IG=IG+1
      IT=ITN(NA,IG)
      ITG(IA,2)=IT-1
2480 GC TC 2485
      ITG(IB,1)=IT
      ITCC(IB)=THEAD(IT,2)
      TXCL(IB)=THEAD(IT,5)
      IC=IC+1
      IT=ITN(NA,IG)
      ITG(IB,2)=IT-1
2485 IF (IC) 249C,2495,249C
2490 IG=IC
      IT=ITN(NA,IG)
      THEC1=THEAD(IT,1)
      IA=3
      IB=4
      IC=C
      IE=C
      GC TC 2455
2495 CCONTINUE
C ..... CALCULATE INITIAL VALUES OF PHIR AND CX FOR
C BASIC ITERATION ROUTINE
C
SCL=NB*CPBR/(2.C*PI*RPBR)
AMU=AMLT/RPBR
PHICR=ATAN(AMU)
PHIC=PHICR*RTC
AMACH=AMCHT*RPBR/CCS(PHICR)
AC=C.1/SQRT(1.C-AMACH**2)
ALPFC=CL1*AK(NA,1)+TCC*AK(NA,2)
X=-C.5*NB*(1.C-KPBR)*SQRT(1.C+(1.0/AMU)**2)
Y=EXP(X)
FP=(2.C/PI)*ATAN((SQRT(1.C-Y**2))/Y)
X=SCL*AC*RTC*SQRT(1.C+AMU**2)/(4.C*FP)
Y=(PETA-PHIC-ALPFC)/RTC
UXCZR=C.5*(SQRT((AMU+X)**2+4.C*X*Y)-(AMU+X))
PHIR=PHICR+LXCZR
PHI=PHIR*RTC
X=UXCZR*SIN(PHIR)/COS(PHIR)
CX=X/(1.0-X)
NIT=1
2500 CCONTINUE
C ..... BASIC ITERATION ROUTINE
C
CP=CCS(PHIR)
SP=SIN(PHIR)
C ..... LOCK UP TIP LOSS CORRECTION FACTOR
C
X=-C.5*NB*(1.C-RPBR)*SQRT(1.C+(1.0/((RPBR*SP/CP)**2)))
Y=EXP(X)
FP=(2.C/PI)*ATAN((SQRT(1.C-Y**2))/Y)
C ..... CHECK IF NB GT 4 - SET FCFP = 1.0
C
IF (NB-4) 252C,252C,251C
2510 FCFP=1.C
      GC TC 256C
2520 IB=NB-1
C ..... CHECK IF RPBR LT 0.3 - ASSUME RPBR = 0.3
C
AR=10.C*RPBR
IR=AR
IF (IR-3) 253C,254C,254C
2530 IR=3
      AR=3.C
C ..... CONTINUE - COMPUTE INTERPOLATION FRACTIONS
C AND ARRAY INDICES FOR TIP LOSS CORRECTION
C VALUES TO BE INTERPOLATED
2540 DR=AR-IR
      IC=IR-2
      ID=IC+1
      AP=2C.C*SP
      IP=AP
      DP=AP-IP
C ..... INTERPLATE FOR RPBR AT EACH SIN(PHI)
      DC 255C I=1,2

```

```

IP=IP+1
IA=21*(IB-1)+IP
2550 CALL FCISK(IA,TLCS)
FR(1)=TLCS(IC)+(TLCS(IC)-TLCS(IC))*DR
C
C
C          INTERPLATE FOR SIN(PHI)
FCFP=FR(1)+(FR(2)-FR(1))*CP
2560 F=FP*FCFP
ALPHA=BETA-PHI
AMACH=APCFI*RPBR/((1.0+CX)*CP)
C
C
C          ..... LOCK UP CL FOR EACH AIRFOIL TABLE
C          AS REQUIRED, THEN INTERPLATE CL
C          FOR ALPHA AND AMACH
DC 2695 IA=1,4
IT=ITG(IA,1)
2605 IF (IT) 2605,2695,2605
ALPHC=ALPHA
ITM(2)=0
IE=C
2610 IF (THEAD(IT,3)-AMACH) 2615,2620,2625
2615 IE=1
ITM(1)=IT
TMCH1=THEAD(IT,3)
IT=I[+1
IF (IT-ITG(IA,2)) 2610,2610,2640
2620 IE=1
ITM(1)=IT
TMCH1=THEAD(IT,3)
GC TC 2645
2625 IF (IE) 2635,2630,2635
2630 IE=1
ITM(1)=IT
TMCH1=THEAD(IT,3)
GC TC 2640
2635 IE=2
ITM(2)=IT
TMCH2=THEAD(IT,3)
GC TC 2645
2640 IT=ITM(1)
ALPHC=THEAD(IT,4)+(ALPHA-THEAD(IT,4))*SQRT((1.0-THEAD(IT,3)**2)/
2645 1*(1.0-AMACH**2))
DC 2690 IC=1,2
IT=ITM(IC)
2650 IF (IT) 2650,2690,2650
IE=1
IE=C
CALL CRISK(IT,TALFA,TLIFT)
2655 IF (TALFA(IC)-ALPHC) 2660,2665,2670
2660 IE=1
TALF1=TALFA(IC)
TLFT1=TLIFT(IC)
IC=IC+1
IF (IC-THEAD(IT,1)) 2655,2655,2685
2665 IE=1
TALF1=TALFA(IC)
TLFT1=TLIFT(IC)
GC TC 2685
2670 IF (IC) 2680,2675,2680
2675 IE=1
TALF1=TALFA(IC)
TLFT1=TLIFT(IC)
GC TC 2685
2680 IE=2
TALF2=TALFA(IC)
TLFT2=TLIFT(IC)
2685 GC TC (2680,2687),IE
C
C          EXTRAPCLATE FOR ALPHA
2686 CLM(IC)=TLFT1
GC TC 2690
C
C          INTERPLATE FOR ALPHA
2687 CLM(IC)=TLFT1+(TLFT2-TLFT1)*(ALPHC-TALF1)/(TALF2-TALF1)
2690 CONTINUE
GC TC (2691,2692),IE
C
C          EXTRAPCLATE FOR AMACH
2691 CLG(IA)=CLM(1)

```

```

C
GC TC 2695
C
2692 LIG(IA)=CLM(1)+(CLM(2)-CLM(1))*(AMACH-TMCH1)/(TMCH2-TMCH1)
2695 CCNTINUE
C
INTERPCLATE CL FOR TOC AND CLI
DC 2720 IC=1,2
IA=2*IC-1
IB=2*IC
CLC(IC)=0
IF (ITG(IA,1)) 2705,2720,2705
IF (ITG(IB,1)) 2710,2715,2710
C
C
C
INTERPCLATE FOR TOC
2710 CLC(IC)=CLG(IA)+(CLG(IB)-CLG(IA))*
1(TTCC-TTCC(IA))/(TTCC(IB)-TTCC(IA))
TXCL(IC)=TXCL(IA)+(TXCL(IB)-TXCL(IA))*
1(TTCC-TTCC(IA))/(TTCC(IB)-TTCC(IA))
TCLI(IC)=TCLI(IA)
GC TC 2720
C
EXTRAPCLATE FOR TOC
2715 CLC(IC)=CLG(IA)
TCLI(IC)=TCLI(IA)
TXCL(IC)=TXCL(IA)
2720 CCNTINUE
IF (CLC(2)) 2725,2730,2725
C
C
C
INTERPCLATE FOR CLI
2725 CL=CLC(1)+(CLC(2)-CLC(1))*(CLI-TCLI(1))/(TCLI(2)-TCLI(1))
GC TC 2735
C
EXTRAPCLATE FOR CLI OUTSIDE TABLE LIMIT
2730 CL=CLC(1)+TXCL(1)*(CLI-TCLI(1))/SQRT(1.0-AMACH**2)
2735 CCNTINUE
C
SET BLADE SECTION DRAG CD = 0.010
CD=C.C1
X=SCL/(4.0*F)
CX=X*(CL/CP+CD/SP)
CY=X*(CL/SP-CD/CP)
CZ=AMU*(1.0+CX)+CY
PHIN=ATAN(CZ)*RTD
IF (ABS(PHIN-PHI)-0.1) 2745,2745,2740
X=AML*CX*(AC*RTD/CL-SP/CP)
Y=CX*(AC*RTD/CL+CP/SP)
CC=1.0+(X+Y)/(1.0+CZ**2)
PHI=PHI+(PHIN-PHI)/CC
PHIR=PHI/RTD
NIT=NIT+1
IF (NIT-9) 2500,2500,2745
C
C
C
CALCULATE VALUES FOR DISK PLANE ELEMENT
2745 UCZR=C.5*(SQRT(AMU**2+4.0*F*CY*CZ/(1.0+CX)**2)-AMU)
UCLA=UCZR/AML
WCZC=UCZR*CX/CY
C
CALCULATE VALUES FOR SLIPSTREAM ELEMENT
USABR(IS)=1.0+2.0*UCLA
RSPR(IS)=SQRT(RSBRX**2+(RPBR**2-RPBRX**2)*
1(0.5+1.0/(USABR(IS)+USERX)))
USTBR(IS)=2.0*WCZC*RPBR/(RSBR(IS)*AMU)
PHIS=RTD*ATAN(USTBR(IS)/USABR(IS))
DCT=(PI*RPBR)**3*F*CY*CZ/(1.0+CX)**2
DCG=DCT*(RPBR/2.0)*CX/CY
C
C
C
PRINT BLADE ELEMENT SOLUTION
2750 WRITE(KP,2957) RPBR,CPBR,BETA,AFSER(NA,1),AFSER(NA,2),CLI,TOC,
IF,AMACH,ALPFA,CL,CD,RSBR(IS),USABR(IS),USTBR(IS),PHIS
IF (RPBR-1.0) 2755,2810,2810
2755 IF (NIT-9) 2800,2800,2760
2760 WRITE(KP,2955)
IS=IS-1
GC TC 2360
2800 CCNTINUE
C
SUM INTEGRAL TERMS FOR SLIPSTREAM ELEMENT
CT=CT+C.5*(DCT+DCTX)*(RPBR-RPBRX)

```

```

      CC=CC+C.5*(CCC+CCCX)*(RPER-RPBRX)
C
      RESET LAST VALUES OF INTEGRAL TERMS
      RPBRX=RPBR
      RSRX=RSBR(IS)
      USBRX=USABR(IS)
      DCTX=CCT
      DCCX=CCC
      GC TC 2860
      CCNTINCE
2810 ..... CALCULATE FINAL SLIPSTREAM INTEGRALS
C
      VSBAR=CA*SQRT(1.0+E.0*CT/(PI*(PI*AMUT)**2))
      CTS=1.C/(1.C+(PI*(PI*AMUT)**2)/(E.0*CT))
C
      PRINT FINAL SLIPSTREAM INTEGRALS
      WRITE(KP,2958) CTS,CT,CQ,VSBAR
C
      CALCULATE SLIPSTREAM VALUES FOR
      INPUT TO WING ANALYSIS
C
      IF (NRCT(1)) 2812,2811,2812
2811 NR=-1
      GC TC 2813
2812 NR=-1+IABS(NRCT(2)-NRCT(1))
2813 KCR=C
      Nk=2*JP
      DC 286C K=1,JP
      YBw(K)=CCS(K*PI/Nw)
      RSBw(K)=(YBw(K)-YPB)/CPB
      RSBA(K)=ABS(RSBw(K))
      IF (RSBA(K)-RSTBR) 2815,2850,2850
2815 NS(K)=1
      IF (KCR) 2817,2816,2817
2816 KCR=K
2817 KIR=K
      ISIGN=-ARCT(2)*RSBw(K)/RSBA(K)
      IA=C
      IH=1
2820 IF (RSBR(IB)-RSBA(K)) 2825,2830,2835
2825 IA=IB
      IB=IE+1
      GC TC 282C
2830 VSA(K)=CA*USABR(IB)
      VST(K)=CA*USTBR(IB)*ISIGN
      Sw(K)=VST(K)/VSA(K)
      GC TC 2855
2835 IF (IA) 2845,2840,2845
2840 VSA(K)=CA*USABR(IB)
      VST(K)=CA*USTBR(IB)*ISIGN*RSBA(K)/RSBR(IB)
      Sw(K)=VST(K)/VSA(K)
      GC TC 2855
2845 X=(RSBA(K)-RSBR(IA))/(RSBR(IE)-RSBR(IA))
      VSA(K)=CA*(USABR(IA)+(USABR(IE)-USABR(IA))*X)
      VST(K)=CA*(USTBR(IA)+(USTBR(IE)-USTBR(IA))*X)*ISIGN
      Sw(K)=VST(K)/VSA(K)
      GC TC 2855
2850 NS(K)=C
      VSA(K)=1.0
      VST(K)=C.0
      Sw(K)=C.0
2855 L=Nw-K
      NS(L)=NS(K)
      YBw(L)=YBw(K)*(-1.0)
      RSBA(L)=RSBA(K)
      VSA(L)=VSA(K)
      VST(L)=VST(K)*NR
      Sw(L)=VST(L)/VSA(L)
2860 CCNTINCE
      IF (KIR-JP) 2862,2861,2862
2861 KIR=Nw-KCR
2862 KIL=Nw-KIR
      KCL=Nw-KCR
C
      PRINT SLIPSTREAM VALUES AT WING STATIONS
      WRITE(KP,2961)
      IC=Nw-1
      DC 287C K=1,IC
      IF (NS(K)) 2870,2870,2865
2865 *RITE(KP,2962) K,YBw(K),RSBA(K),VSA(K),VST(K),Sw(K)

```

287C CCNTINUE  
2897 WRITE(KP,2991) IDENT  
2899 CCNTINUE

..... READ FORMATS

2901 FCRMAT(11,12,29X,8F6.0)  
2911 FCRMAT(11,9X,2A4,2X,2F10.C)  
2912 FCRMAT(12,2X,11,3X,5F8.0)  
2913 FCRMAT(10F8.C)  
2921 FCRMAT(19A4,3X,11)  
2923 FCRMAT(12,8X,12,8X,3F10.C,29X,11)  
2924 FCRMAT(2(12,8X),2F10.C,35X,11)  
2925 FCRMAT(3F10.C,11,9X,2F10.C,19X,11)

..... PRINT FORMATS

2951 FCRMAT(1H1//EX,32HPRPELLER SLIPSTREAM ANALYSIS -,2X,19A4/1X)  
2952 FCRMAT(1HG,7X,25HPROPELLER - WING GEOMETRY,14X,  
A 25HPROPELLER - NACELLE GEOMETRY,12X,  
B 25HPROPELLER OPERATING CONDITION/1X)  
2953 FCRMAT(1H ,4X,25HNUMBER OF PROPS =,12,13X,  
A 25HNO OF BLADES PER PROP =,12,13X,  
B 25HLEFT / RIGHT PROCP ROTN =,A3,1F,,A3/  
C 5X,25HPRCP FWC CCCRD 2.XP/B =,F7.4,8X,  
D 25HPRCP DIA / PROCP DIA =,F7.4,8X,  
E 25HPRCP ADVANCE RATIO =,F7.4)  
2954 FCRMAT(1H ,4X,25HPRCP SPAN CCCRD 2.YP/B =,F7.4,8X,  
A 25HNACELLE DIA / PROCP DIA =,F7.4,8X,  
B 25HFLIGHT MACH NUMBER =,F7.4/  
C 5X,25HPRCP DIA / WING SPAN =,F7.4,8X,  
D 25HPRCP AXIS REL BODY AXIS =,F7.3,4H DEG,4X,  
E 25HPRCP ANGLE OF ATTACK =,F7.3,4H DEG)

2956 FCRMAT(1H-,12X,22HBLADE ELEMENT GEOMETRY,22X,  
A22HBLADE ELEMENT SOLUTION,14X,27HSLIPSTREAM ELEMENT SOLUTION//  
B2X,5HRS/RP,3X,5HCB/RP,3X,5HPITCH,2X,7HA/F SER,  
C3X,3HCL1,4X,3H1/C,9X,1HF,5X,4HMACT,2X,5HALPHA,4X,2HCL,  
D5X,2HCC,8X,5HRS/RP,2X,6HUSA/LA,2X,6HUST/LA,4X,4HPHIS/1X)

2957 FCRMAT(1H-,F6.4,F8.4,F8.3,1X,2A4,2F7.3,4X,5F7.3,4X,3F8.4,F8.3)  
2958 FCRMAT(1H-,4X,36HPROPELLER THRUST COEFFICIENT, CT'' =,F7.4/  
A 5X,36HPROPELLER THRUST COEFFICIENT, CT =,F7.4/  
B 5X,36HPROPELLER TORQUE COEFFICIENT, CQ =,F7.4/  
C 5X,36HMENTUM WGTD SLIPSTREAM VEL RATIO =,F7.4)

2961 FCRMAT(1H-,4X,42HSLIPSTREAM VALUES AT WING CONTROL STATIONS//6X,  
A1HK,7X,4H2Y/B,7X,5HRS/RP,7X,6HUSA/LC,6X,6HUST/LC,5X,7HUST/USA/1X)

2962 FCRMAT(1H ,4X,12,5(5X,F7.4))

2981 FCRMAT(1H1,9X,13,42H TIP LOSS CORRECTION TABLE DATA CARDS READ/1X)

2982 FCRMAT(1H ,13X,44HIS INVALID - SLIPSTREAM COMPUTATIONS ABORTED/1X)

2983 FCRMAT(1H-,9X,13,41H PROPELLER AIRFOIL TABLES READ AS FOLLOWS/1X)

2984 FCRMAT(1HC,14HAIRFOIL CODES,9(5X,13,3X))

2985 FCRMAT(1HC,14HAIRFOIL SERIES,9(2X,2A4))

2986 FCRMAT(1HC,14HNO OF SECTIONS,9(5X,13,3X))

2987 FCRMAT(1HC,14HTABLE NUMBERS,9(3X,13,2H -,13))

2988 FCRMAT(1H-,11X,32HC PROPELLER AIRFOIL TABLES READ,,13,47H PREVIOUS  
A TABLES READ AND STORED ARE AS FOLLOWS)

2991 FCRMAT(1H-,10X,10HCARD IDENT,12,  
A62H HAS BEEN READ OUT OF SEQUENCE, SLIPSTREAM COMPUTATION ABORTED)

2994 FCRMAT(1H-,44HAIRFOIL TABLES NOT STORED FOR AIRFOIL SERIES,12,  
A21H SPECIFIED AT RB/RP =,F7.4,  
B46H - THIS ELEMENT IS DELETED FROM THE ANALYSIS/1X)

2995 FCRMAT(1HC,10HSOLUTION FOR PRECEDING ELEMENT FAILED TO CONVERGE I  
AN S ITERATIONS AND IS DELETED FROM THE SLIPSTREAM ANALYSIS/1X)

RETURN  
END  
SUBROUTINE MAIN  
DIMENSION C(19),EPS(19),TRANS(19),REY(19),ETA(19),FCPP(19),CLMAX(1  
19),ZHERE(2,6),WHERE(2,6),ARRAY(5,25,8 ),Y(19),TAL(19),BLTA(19,19),  
2MAZZ(6),MZCCL(6),MAXX(6),MXCCL(6),YHERE(2,6),MYCCL(6),MAYY(6),TRIX  
3(19,19),CY(19),LIST(19),YCA(19),YDAX(19),YX(19),TCNY(19),ALPG(19),  
4XHERE(2,6),MWCC(6),MAHW(6)  
DIMENSION CVAL(19),ALPFL(19),CPC(19),CBG(19),DELTA(19),ALPHZ(19),  
1ALPF(19),ALPHE(19),CLADD(19),CLUB(19),CLAD2(19),CLAD1(19),F(19),  
CCMCM KCR,KIR,KIL,KCL,VSA(19),SW(19),VSHAR,EYETL,CFS,XPB,YPB,JP,  
1IPRAH,ALPFB,KSTAL,ISTAL,KCNT,AB(3)  
CCMCM NSLIP,VR(19),CA(19),AS(19),TL(19),SV(19),FUNC,YG,CDNAC,  
1ALPFW(16)  
CCMCM INACH,ISWIT(3),ALPHA,REYN,CLL,KEYCN,XMAX,ALMAX(19),CLMAX,C,  
1EPS,TRANS,REY,ETA,FCPP,ZHERE,WHERE,ARRAY,Y,BETA,TFAC,TRIX,TAL,MAXX  
2,MAZZ,MXCCL,MZCCL,ASPEC,TAPER,UF,KEYND,DISCR,PIEK,CRB,Q,ISTAX,EDGE  
3,SIG,ALPHK,NFLAP,NLVL,NP,IY,IZ,IR,IP,IS,ISTAR,A,B,F,TAUT,TAUR,



```

4 TWIST,R,BHX,YFERE,MYCCL,MAYY,FLAP,TCNY,TWISA,X,Z,CM,ACC,XHERE,
5 MCCL,MAWH,CAMB(19),CAMBR,CAMBT,DCMY1,DCMY2,NAME(25),AHERE(2,6),
6 MAAA(6),MACCL(6),BFERE(2,6),MABB(6),MBCUL(6),CHEKE(2,6),MACC(6),
7 MCCLL(6),CFERE(2,6),MACC(6),MCCOL(6),STORY(19),SGENE(19),CVAL,
8 ALPFU,CBC,CHG,DELTA,ALPFZ,ALPF,ALPFE,CLAED,CLDEL,CLAD2,CLAD1,
9 F,IRI,FF,LCCER
ACCS(X)=ATAN(SCRT(1.-X*X)/X)

```

READER (IR) AND PRINTER (IP) LOGICAL UNIT NUMBERS

```

IR=8
IP=6
REWIND 1
REWIND 2
REWIND 3
REWIND 4
REWIND 5
REWIND 10
REWIND 15
REWIND 20
REWIND 7
KEEP=1

```

INPUT DATA SECTION

```

IS=1
READ(IR,65C) ASPEC,TALT,TALR,TAPER,TWIST,K,BF,REYNC,DISCR,A,B,H,
1 ALPFR,NFLAP,FLAP,X,Z,TWISA,CAMBT,CAMBR,NSLIP,CONAC
IF(ASPEC-99.) 2C,1C,1C
10 CALL EXIT
20 CCATINUE

```

LAYOUT OF FOURTH DATA CARD

```

FIELD 1  I1  NUMBER OF TAL VALUES PER TABLE
FIELD 2  I1  1 FOR READ IN OF TAL, REY, ETC.
              0 FOR NO READ IN
FIELD 3  I1  1 FOR DUMP OF COMPUTED ARRAYS
              0 FOR NO DUMP
FIELD 4  I1  1 FOR DUMP OF BETA ARRAY
              0 FOR NO DUMP
FIELD 5  I1  1 READ CUBE 1 FROM TAPE, LOAD
              TO DISK, COPY CUBE 1 TO CUBE
              2 ON DISK.
              2 READ CUBE 1 FROM TAPE, LOAD
              TO DISK, READ CUBE 2 FROM
              TAPE, LOAD TO DISK.
              3 READ CUBE 1 FROM CARDS, LOAD
              TO TAPE, LOAD TO DISK, COPY
              CUBE 1 TO CUBE 2 ON DISK
              4 READ CUBE 1 FROM CARDS, LOAD
              TO TAPE, LOAD TO DISK, READ
              CUBE 2 FROM CARDS, LOAD TO
              TAPE, LOAD TO DISK
FIELD 6  25A2 FIFTY COLUMNS OF IDENTIFYING
              INFORMATION. THIS IS PRINTED
              AT THE TOP OF EACH PAGE OF
              OUTPUT

```

READ (IR,66C) NLVL,ISWIT,IG,NAME

SWITCH ZERO ON WILL READ IN VALUES FROM CARDS FOR TAL, REY, C, EPS, EDGE, CRG, AND ACC. FORMAT IS 16F5.C. ARRAYS ARE READ IN ROWWISE

```

CALL SETSW
DC 30 J=1,6
WHERE(1,J)=C.
WHERE(2,J)=C.
MAWH(J)=0
30 MACCL(J)=C
IY=C
IF(IG-3) 80,4C,40

```

```

40 DC 5C J=1,4
   CALL AERDA(ARRAY,NLVL,WHERE,MACCL,MAWH,7,KEEP)
   WRITE(7) ARRAY
50 WRITE(7) WHERE,MACCL,MAWH
   IF(IG-4) 80,6C,80
60 DC 7C J=1,4
   CALL AERDA(ARRAY,NLVL,WHERE,MACCL,MAWH,7,KEEP)
   WRITE(7) ARRAY
70 WRITE(7) WHERE,MACCL,MAWH
80 IK=1
   REWIND 7
   READ(7) ARRAY
   READ(7) WHERE,MAXCCL,MAXX
   WRITE(7) ARRAY
   IK=IK+1
   READ(7) ARRAY
   READ(7) ZHERE,MZCCL,MAZZ
   WRITE(7) ARRAY
   IK=IK+1
   READ(7) ARRAY
   READ(7) YHERE,MYCCL,MAYY
   WRITE(7) ARRAY
   IK=IK+1
   READ(7) ARRAY
   READ(7) XHERE,MXCCL,MAWH
   WRITE(7) ARRAY
   REWIND 1
   REWIND 2
   REWIND 3
   REWIND 4
90 IF(IG-1) 10C,10C,9C
   IF(IG-3) 13C,10C,13C
100 IK=1
   DC 11C J=1,4
   READ(7) ARRAY
   KK=IK*5
   IK=IK+1
110 WRITE(KK) ARRAY
   DC 12C J=1,6
   AHERE(1,J)=WHERE(1,J)
   AHERE(2,J)=WHERE(2,J)
   BHERE(1,J)=ZHERE(1,J)
   BHERE(2,J)=ZHERE(2,J)
   CHERE(1,J)=YHERE(1,J)
   CHERE(2,J)=YHERE(2,J)
   DHERE(1,J)=XHERE(1,J)
   DHERE(2,J)=XHERE(2,J)
   MACCL(J)=MXCCL(J)
   MBCCL(J)=MZCCL(J)
   MCCCL(J)=MYCCL(J)
   MDCCL(J)=MXCCL(J)
   MAAA(J)=MAXX(J)
   MABB(J)=MAZZ(J)
   MACC(J)=MAYY(J)
120 MACC(J)=MAWH(J)
   GC TC 140
130 IK=5
   READ(7) ARRAY
   READ(7) AHERE,MACCL,MAAA
   WRITE(7) ARRAY
   IK=IK+5
   READ(7) ARRAY
   READ(7) BHERE,MBCCL,MABB
   WRITE(7) ARRAY
   IK=IK+5
   READ(7) ARRAY
   READ(7) CHERE,MCCCL,MACC
   WRITE(7) ARRAY
   IK=IK+5
   READ(7) ARRAY
   READ(7) DHERE,MDCCL,MACD
   WRITE(7) ARRAY
140 ALPC(1)=C.C
   REWIND 5
   REWIND 10
   REWIND 15
   REWIND 20
   REWIND 1
   REWIND 2
   REWIND 3

```

```

REWIND 4
NP=R-1.
JP=R/2.
PIER=3.14159/R
CALL CATSW(C,I)
GC TC (15C,16C), I
150 READ(IR,67C) (TAU(I),I=1,NP)
    READ(IR,67C) (REY(I),I=1,NP)
    READ(IR,67C) (C(I),I=1,NP)
    READ(IR,67C) (EPS(I),I=1,NP)
    READ(IR,67C) EDGE
    READ(IR,67C) CRB
    READ(IR,67C) ACC
160 CONTINUE

                IF NO FUSE (FUSELAGE)

    IF(A) 410,410,170
170 YC=B*SQRT(1.-F**2/A**2)
    ECC=SQRT(A**2-B**2)
    CALL CATSW(C,I)
    GC TC (19C,18C), I
180 CRB=2.*(1.-YC)/(ASPEC*(1.+TAPER-2.*YO*TAPER))
190 TFAC=1.-(YC*TAUR*CRB/(3.14159*A*B))*4.
    JPP=JP+1

                Y'(I) (SEE CR1646 FOR EXPLANATIONS)

    DC 20C I=1,JPP
    XII=I-1
200 YCA(I)=YO+(1.-YC)*COS(XII*PIER)

                CHECK IF FUSE ELLIPTICAL OR CIRCULAR

    IF(A-B) 230,230,210

                ELLIPTICAL FUSE

210 CONTINUE
    DISTX=C.5*(SQRT(1.+(H-ECC)**2)+SQRT(1.+(H+ECC)**2))
    BWX=1./(A-B)*(A-B*DISTX/SQRT(DISTX**2-ECC**2))
    DC 22C I=1,JPP
    DIST(I)=0.5*(SQRT(YDA(I)**2+(H-ECC)**2)+SQRT(YDA(I)**2+(H+ECC)**2
1))

                Y BAR PRIME (I)

220 YCAX(I)=(YCA(I)/(A-B)*(A-B*DIST(I)/SQRT(DIST(I)**2-ECC**2)))/BWX
    GC TC 250

                Y BAR PRIME (I) FOR CIRCULAR FUSE

230 BWX=1.-A**2/(1.+H**2)
    DC 24C I=1,JPP
240 YCAX(I)=YCA(I)*(1.-A**2/(YCA(I)**2+H**2))/BWX

                COMMON TO ELLIPTIC AND CIRCULAR FUSE

250 DC 260 I=1,JPP

                Y BAR (I)

    AI=I-1
260 YX(I)=CCS(AI*PIER)

                Y (I)

    DC 270 I=2,JPP
270 Y(I)=TERP(YCAX(I-1),YX(I),YDAX(I),YCA(I-1),YDA(I))
    DC 280 I=1,JP
    Y(I)=Y(I+1)
280 YX(I)=YX(I+1)
    M=JP-1
    DC 29C I=1,M
    IRI=R
    IRI=IRI-I
    YX(IRI)=-YX(I)
290 Y(IRI)=-Y(I)
    IF(A-B) 36C,360,300

```

FLUSE IS ELLIPTICAL

```

C
C
300 DC 310 I=1,JP
DIST(I)=0.5*(SQRT(Y(I)**2+(H-ECC)**2)+SQRT(Y(I)**2+(H+ECC)**2))
C=CIST(I)/SQRT(CIST(I)**2-ECC**2)
S=1.+(ECC*Y(I)/(DIST(I)**2-ECC**2))**2
TRANS(I)=1./(A-B)*(A-B*C/S)
IRI=R
IRI=IRI-I
310 TRANS(IRI)=TRANS(I)

```

WING ON TOP OR BOTTOM OF FLUSELAGE

```

C
C
IF(A-F) 32C,320,330
320 TRANS(JP)=1.
330 IF(NFLAP) 52C,520,340
340 IF(BF-1.) 35C,520,520
350 DISF=C.5*(SQRT(BF**2+(H-ECC)**2)+SQRT(BF**2+(H+ECC)**2))
BFX=(BF/(A-B)*(A-B*DISF/SQRT(DISF**2-ECC**2)))/BWX
GC TC 460
360 DC 370 I=1,JP
TRANS(I)=1.+A**2*(Y(I)**2+H**2)/((Y(I)**2+H**2)**2)
IRI=R
IRI=IRI-I
370 TRANS(IRI)=TRANS(I)
IF(A-F) 38C,380,391
391 IF(NFLAP) 52C,520,390
380 TRANS(JP)=1.C
390 IF(BF-1.) 40C,520,520
400 BFX=(BF*(1.-A**2/(BF**2+H**2)))/BWX
GC TC 460
410 DC 420 I=1,AP
AI=I
Y(I)=CCS(AI*PIER)
IF(AI.EQ.JP) Y(I)=C.C
YY(I)=Y(I)
420 TRANS(I)=1.
YC=C.

```

SPECIAL CASE IF VALUES HAVE BEEN READ IN  
 DO NOT WANT TO COMPUTE CRB.  
 WILL NOT COMPUTE VALUES ALREADY READ IN

```

C
C
CALL DATSW(C,I)
GC TC (440,430), I
430 CRB=2.*(1.-YC)/(ASPEC*(1.+TAPER-2.*YO*TAPER))
440 TFAC=1.
HWX=1.
IF(BF-1.) 450,520,520
450 BFX=HF
460 TSTAX=ACOS(BFX/BWX)
DC 510 I=1,JP
AI=I
C3=AI*PIER
TSTX=TSTAX
IF(C3-TSTX) 510,470,480
470 TSTAX=C3
ISTAR=I
GC TC 520
480 AM=C3-TSTAX
C1=(AI-1.)*PIER
AK=TSTAX-C1
IF(AM-AK) 490,490,500
490 ISTAR=I
TSTAX=C3
GC TC 520
500 ISTAR=I-1
TSTAX=C1
GC TC 520
510 CCNTINLE
520 CALL DATSW(C,I)
GC TC (550,530), I
530 EDGE=SQRT(1.+4./(ASPEC**2))
EA=1.-C.5/SQRT(EDGE)
PI=3.14159
ECGE=C.5*(1./EA-PI*CCS(PI*EA)/SIN(PI*EA))
CALL DATSW(3,I)
GC TC (541,542), I
541 WRITE(IP,1011)
CALL ZZZ(ECGE)

```

```

542 DC 54C I=1, NP
C(I)=1.-(1.-TAPER)*(ABS(Y(I))-Y0)/(1.-Y0)
TAL(I)=TALR/C(I)*(1.-(1.-TAPER*TAUT/TAUK)*(ABS(Y(I))-Y0)/(1.-Y0))
CAMB(I)=CAMBR+(CAMBT-CAMER)*(ABS(Y(I))-YC)/(1.-YC)
ACC=C.666*(1.+TAPER*(1.+TAPER))/(1.+TAPER)
540 KEY(I)=KEYNC*C(I)/ACC
550 CALL MAINA
RETURN
1011 FCRMAT(10X,5FEDGE=)
650 FCRMAT(8F10.C/5F10.0,110,4F5.C/2F10.0,11C,1F10.C)
66C FCRMAT(511,25A2)
67C FCRMAT(16F5.C)
END
SUBROUTINE MAINA
***** MAINA-CONTINUATION OF SUBROUTINE MAIN *****
DIMENSION C(19),EPS(19),TRANS(19),KEY(19),ETA(19),FCPP(19),CLMAX(1
19),ZHERE(2,6),WHERF(2,6),ARRAY(5,25,8),Y(19),TAL(19),BETA(19,19),
2MAZZ(6),MZCCL(6),MAXX(6),MXCCL(6),YHERE(2,6),MYCCL(6),MAYY(6),TRIX
3(19,19),CM(19),TCNY(19),
4ALPHZ(19),XHERE(2,6),MXCCL(6),MAWH(6)
DIMENSION CVAL(19),ALPHC(19),CBC(19),CBG(19),DELTA(19),
1ALPH(19),ALPHE(19),CLADD(19),CLDEL(19),CLAD2(19),CLAD1(19),F(19),
CCMNCN,KGR,KIK,KIL,KGL,VSA(19),Sw(19),VSEAR,EY,TL,CTS,XPB,YPB,JP,
1IPRAB,ALPHB,KSTAL,ISTAL,KCLN1,AB(3)
CCMNCN,NSLIP,VR(19),CA(19),AS(19),TL(19),SV(19),FUNC,Y0,CDNAC,
1ALPHV(16)
CCMNCN,INACH,ISWIT(3),ALPHA,REYN,CLL,REYCN,XMAX,ALMAX(19),CLMAX,C,
1EPS,TRANS,KEY,ETA,FCPP,ZHERE,WHERE,ARRAY,Y,BETA,TFAC,TRIX,TAU,MAXX
2,MAZZ,MXCCL,MZCCL,ASPEC,TAPER,BF,REYND,DISCK,PIER,CRB,C,TSTAX,EDGE
3,SIG,ALPHR,NFLAP,NLVL,NP,IY,IZ,IR,IP,IS,ISTAK,A,B,F,TAUT,TAUR,
4TWIST,R,RKX,YHERE,MYCCL,MAYY,FLAP,TCNY,THISA,X,Z,CM,ACC,XHERE,
5MXCCL,MAWH,CAMB(19),CAMBR,CAMBT,DUMY1,DUMY2,NAML(25),AHERE(2,6),
6MAAA(6),MACCL(6),BHERE(2,6),MABB(6),MBCUL(6),CHERE(2,6),MACC(6),
7MCCL(6),CHERE(2,6),MADD(6),MCCCL(6),STONY(19),SGENE(19),CVAL,
8ALPHC,CBC,CBG,DELTA,ALPHZ,ALPH,ALPHE,CLADD,CLDEL,CLAD2,CLAD1,
9F,IRI,FF,LCCER
IF(IR-8) 20,10,10
10 IPRAB=1
KSTAL=C
ISTAL=C
KCUNT=C
RFAC(IP,320) ALPHV
GC TC 3C
20 IPRAB=IPRAB+1
30 ALPHE=ALPHV(IPRAB)
IF(ALPHE.EC.99.) GC TC 641
IF(IPRAB.NE.1) GC TO 61
DC 549 K=1, NP
VSA(K)=1.
VR(K)=1.0
Sw(K)=C.0
DA(K)=C.0
AS(K)=C.0
TL(K)=C.0
549 SV(K)=C.0
61 IF(NSLIP.EC.0) CO TO 552
CALL SLIP
IF(IPRAB.NE.1) GO TO 81
C READ(IR,320) (CA(K),TL(K),K=1,NP)
SUM=C.7854+YPB
DIFF=C.7854-YPB
SUM2=SUM**2
DIFF2=DIFF**2
RTSUM=SQRT(SUM2+XPB**2)
RTCIF=SQRT(DIFF2+XPB**2)
FLNC=DIFF/(XPB*RTCIF)+SLM/(XPB*RTSUM)-(RTSUM-XPB)/(SUM*RTSUM)
IF(ABS(YPB-C.7854)-.C1) 71,71,72
71 FUNC1=C.0
GC TC 73
72 FUNC1=(RTCIF-XPB)/(DIFF*RTCIF)
73 FLNC=FLNC-FUNC1
CALL DATSw(3,JUNK)
GC TC (80,81),JUNK
80 WRITE(IP,5491)
5491 FCRMAT(10X,4FFUNC)
CALL ZZZ(FLNC)
81 DC 553 J=1, NP
553 REY(J)=REY(J)*SQRT(VSA(J)**2+Sw(J)**2)
552 IF(IPRAB.NE.1) GO TO 641
LCCER=3

```

ALPHA=999.  
CLL=C.  
REYCN=999.  
XMAX=0.

LCKK UP ZERO LIFT ANGLE FOR TIP SECTION

CALL BRIDG(ALPHZ,1,1,1,IY,IE,REY,TAU,CAMB,ALPHA,1,1,ALPHA)  
IF(IE) 56C,56C,64C

LCKK UP ZERO LIFT ANGLE FOR ROOT SECTION

ALPHA=999.  
CALL BRIDG(ALPHZ,JP,JP,1,IY,IE,REY,TAU,CAMB,ALPHA,1,1,ALPHA)  
IF(IE) 57C,57C,64C

CALCULATE AERODYNAMIC AND GEOMETRIC TWIST

570 IF(TWISA-100.) 580,59C,59C  
580 TWIST=TWISA-(ALPHZ(JP)-ALPHZ(1))  
GC TC 600  
59C TWISA=TWIST+(ALPHZ(JP)-ALPHZ(1))  
60C CALL CATSW(C,I)  
GC TC (63C,61C), I  
61C DC 620 I=1,NP  
620 EPS(I)=TWIST\*TAPER\*(ABS(Y(I))-YO)/(C(I)\*(1.-YO))  
IF(NFLAP.NF.C) GO TO 641  
630 LCCER=J  
CLL=999.  
ALPHA=999.  
REYCN=999.  
REYCN=C.

FOR XMAX=100. ARC WILL LCKK UP ALPHA MAX  
FOR XMAX=C. ARC WILL LOOK UP CL MAX

XMAX=100.  
CALL BRIDG(ALMAX,1,NP,1,IY,IE,REY,TAU,CAMB,ALPHA,1,1,XMAX)  
640 WRITE(IP,68C) IE,LCCER  
CALL EXIT  
641 RETURN

320 FORMAT(8F10.0)  
680 FORMAT(1X,11#ERROR CODE ,12,13# -IN SECTION ,13,9# ABORTED)  
ENC  
SUBROUTINE MAIN1

MAIN1----CONTINUATION OF SUBROUTINE MAIN

DIMENSION C(19),EPS(19),TRANS(19),REY(19),ETA(19),FCPP(19),CLMAX(19),ZHERE(2,6),WHERE(2,6),ARRAY(5,25,8),Y(19),TAU(19),BETA(19,19),MAZZ(6),MZCCL(6),MAXX(6),MXCCL(6),YHERE(2,6),MYCCL(6),MAYY(6),TRIX(19,19),TCNY(19),GENE(19),SIGMA(19),LL(19),MM(19),CM(419),XHERE(2,6),MWCC(6),MAWW(6)  
DIMENSION CVAL(19),ALPHU(19),CBC(19),CBG(19),DELTA(19),ALPHZ(19),ALPH(19),ALPHE(19),CLADD(19),CLDEL(19),CLAD2(19),CLAD1(19),F(19)  
COMMON KCR,KIR,KIL,KCL,VSA(19),SW(19),VSBAR,EYEIL,CTS,XPB,YPB,JP,IPRAB,ALPHB,KSTAL,ISTAL,KCLNT,AB(3)  
COMMON NSLIP,VR(19),DA(19),AS(19),TL(19),SV(19),FUNC,YO,CDNAC,ALPHV(16)  
COMMON INNCW,ISWIT(3),ALPHA,REYN,CLL,REYCN,XMAX,ALMAX(19),CLMAX,C,EPS,TRANS,REY,ETA,FCPP,ZHERE,WHERE,ARRAY,Y,BETA,IFAC,TRIX,TAU,MAXX,MAZZ,MXCCL,MZCCL,ASPEC,TAPER,BI,KEYND,DISCK,PIER,CRB,G,TSTAX,EDGE,3,SIG,ALPHR,NFLAP,NLVL,NP,IY,IZ,IR,IP,IS,ISTAR,A,B,F,TAUT,TAUR,4TWIST,BWX,YHERE,MYCCL,MAYY,FLAP,TCNY,TWISA,X,Z,CM,ACC,XHERE,5MWCC,MAWW,CAMB(19),CAMBR,CAMBT,DUMY1,DUMY2,NAME(25),AHERE(2,6),6MAAA(6),MACCL(6),BHERE(2,6),MABB(6),MBCOL(6),CHERE(2,6),MACC(6),7MCCL(6),CHERE(2,6),MADD(6),MDCCL(6),STONY(19),SGENE(19),CVAL,8ALPHU,CBC,CBG,DELTA,ALPHZ,ALPH,ALPHE,CLADD,CLDEL,CLAD2,CLAD1,9F,IRI,FF,LCCER

COMPLTATION OF BETA

OMEGA=2.-1./((1.+4./(ASPEC\*\*2))\*C.25)  
DC 800 N=1,NP  
DC 800 K=1,NP  
AK=K  
AM=M  
IF(K-M) 2C,10,2C  
10 BETA(M,K)=180.\*R/(8.\*3.14159\*SIN(AK\*PIER))\*OMEGA

```

GC TC 50
20 KK=ABS(K-M)-2*((ABS(K-M))/2)
IF(KK-1) 4C,30,40
30 BETA(M,K)=18C./(4.*3.14159*R*SIN(AK*PIER))*(1./(1.-COS((AK+AM)*
13.14159/R))-1./(1.-COS((AK-AM)*3.14159/R)))*OMEGA
GC TC 5C
40 BETA(M,K)=C.
50 IF(M-K) 7C,60,70
60 TRIX(M,K)=1.+C.1*C(K)*CRB/BWX*BETA(M,K)*TRANS(K)/EDGE
GC TC 8C
70 TRIX(M,K)=C.1*C(K)*CRB/BWX*BETA(M,K)*TRANS(K)/EDGE
80 I=NP+1-M
J=NP+1-K
BETA(I,J)=BETA(M,K)
800 TRIX(I,J)=TRIX(M,K)
CALL CATSW(4,I)
GC TC (50,100), I
90 WRITE(IP,43C)
CALL SSS(BETA,NP)
100 DC 11C I=1,AP
AI=I
110 ETA(I)=C.523598/R*(3.-(-1.)**I)*SIN(AI*PIER)
CHECK IF FLAP CASE
IF(NFLAP) 31C,310,120
IS THERE A PART-SPAN FLAP
120 IF(BF-1.) 130,310,310
130 DC 170 I=1,AP
AI=I
THE=AI*PIER
IF(THE-TSTAX) 150,14C,150
140 TCNY(I)=1./45.*TSTAX*SIN(THE)
GC TC 16C
150 TCNY(I)=1./9C.*(CCS(THE)-CCS(TSTAX))*(ALCG(1.-COS(THE+TSTAX
1)))-ALCG(1.-COS(THE-TSTAX)))+2.*TSTAX*SIN(THE))
60 GENE(I)=1./9C.*(CCS(THE)+CCS(TSTAX))*(ALCG(1.+COS(THE-TSTAX
1)))-ALCG(1.+COS(THE+TSTAX)))+2.*(3.14159-TSTAX)*SIN(THE))
SGENE(I)=2.*SIN(THE)-90./3.14159*TCNY(I)
TCNY(I)=TCNY(I)/CMEGA
GENE(I)=GENE(I)/CMEGA
170 CCNTINUE
CHECK FOR DUMP
CALL CATSW(3,I)
GC TC (18C,19C), I
180 WRITE(IP,44C)
CALL AAA(GENE,NP)
WRITE(IP,45C)
CALL AAA(TCNY,NP)
190 DC 23C K=1,AP
SUM=C.
DC 200 M=1,AP
SUM=TCNY(M)*BETA(M,K)+SUM
IF(K-1STAR) 210,210,220
210 HCFF(K)=1.-SUM
GC TC 23C
220 HCFF(K)=-SUM
230 CCNTINUE
DC 270 K=1,AP
SUM=C.
DC 240 M=1,AP
SUM=GENE(M)*BETA(M,K)+SUM
IRI=R
IF(K-IRI+1STAR) 250,260,260
250 SIGMA(K)=1.-SUM
GC TC 27C
260 SIGMA(K)=-SUM
270 CCNTINUE
DC 280 K=1,AP
HCPP(K)=SIGMA(K)-FCPP(K)
280 TCNY(K)=GENE(K)-TONY(K)
CHECK FOR DUMP
CALL CATSW(3,I)

```

```

GC TC (29C,2CC), I
290 WRITE(IP,46C)
   CALL AAA(FCFP, NP)
   WRITE(IP,47C)
   CALL AAA(SIGMA, NP)
   WRITE(IP,44C)
   CALL AAA(GENE, NP)
   WRITE(IP,45C)
   CALL AAA(TCNY, NP)
   WRITE(IP,59C)
   CALL AAA(STCNY, NP)
   WRITE(IP,60C)
   CALL AAA(SGENE, NP)
300 CONTINUE
310 IBTA=1
CCCC
C
C
C STORE BETA TEMPORARILY ON DISK SO WE CAN
  CCMPUTE THE TRANSPCSF OF TRIX
C
C
C REWIND 44
  WRITE(44) BETA
  REWIND 44
CCCC
C
C STORE TRIX IN BETA
C
C DC 320 M=1, NP
  DC 320 K=1, NP
320 BETA(M, K)=TRIX(M, K)
CCCC
C
C NOW TRANSPOSE BETA (OLD TRIX)
C
C DC 330 M=1, NP
  DC 330 K=1, NP
330 TRIX(M, K)=BETA(K, M)
  IBTA=1
CCCC
C
C RESTORE BETA
C
C READ(44) BETA
CCCC
C
C INVERT TRIX
C
C CALL MINV(TRIX, NP, AK, LL, MM)
  IF(NFLAP-1) 36C,42C,42C
360 WRITE(IP,49C) NAME
   WRITE(IP,50C)
   CALL AAA(Y, NP)
   WRITE(IP,51C)
   CALL AAA(ALMAX, NP)
CCCC
C
C SET UP FOR CL MAX LOOK UP
C
C IY=1
  REYCN=C.
  ALPHA=599.
  CLL=599.
  REYN=559.
CCCC
C
C LOOK UP CL MAX VALUES
C
C XMAX=C.
  CALL BRIDGE(CLMAX, 1, NP, 1, IY, IE, REY, TAU, CAMB, ALPHA, 1, 1, XMAX)
  WRITE(IP,52C)
  CALL AAA(CLMAX, NP)
  WRITE(IP,53C)
  CALL AAA(TAU, NP)
  WRITE(IP,54C)
  CALL AAA(REY, NP)
  WRITE(IP,55C)
  CALL AAA(C, NP)
  WRITE(IP,56C)
  CALL AAA(EPS, NP)
  WRITE(IP,57C)
  CALL AAA(CAMB, NP)
420 RETURN
C
C 430 FORMAT(10X, 11#MATRIX BETA)
  440 FORMAT(10X, 4#GENE)
  450 FORMAT(10X, 4#TCNY)
  460 FORMAT(10X, 4#FCFP)

```



```

470 FCRMAT(10X,5F-SIGMA)
490 FCRMAT(1H1/1HC/35X,25A2/1X)
500 FCRMAT(1X/1CX,22F-SPANWISE STATIONS-2Y/8)
510 FCRMAT(10X,5F-ALPHA MAX)
520 FCRMAT(10X,7F-CL MAX)
530 FCRMAT(10X,30F-THICKNESS / CHORD DISTRIBUTION)
540 FCRMAT(10X,33F-SECTION REYNOLDS NUMBERS, MILLIONS)
550 FCRMAT(10X,18F-CHORD DISTRIBUTION)
560 FCRMAT(10X,18F-TWIST DISTRIBUTION)
570 FCRMAT(10X,19F-CAMBER DISTRIBUTION)
590 FCRMAT(10X,5F-STCNY)
600 FCRMAT(10X,5F-SENE)
    ENC
    SUBROUTINE MAIN2

```

CC

MAIN2-----GENERAL PRINT SUBROUTINE-----

```

DIMENSION ARRAY(5,25,8),C(19),EPS(19),TRANS(19),REY(19),ETA(19),
1HCPP(19),CLMAX(19),ZHERE(2,6),WHERE(2,6),Y(19),TAU(19),BETA(19,19)
2,TRIX(19,19),MAZZ(6),MZCCL(6),MAXX(6),MXCCL(6),CBG(19),CVAL(19),
3ALPG(19),CBC(19),ALPHU(19),ALPH(19),ALPHZ(19),ALPHE(19),DELTA(19),
4YHERE(2,6),MYCCL(6),MAYY(6),CM(19),XHERE(2,6),MAWW(6),MWCCL(6)
5DIMENSION CLADD(19),CLDEL(19),CLAD2(19),CLAD1(19),F(19)
6COMMON KCR,KIR,KIL,KCL,VSA(19),SW(19),VSBAR,EYETL,CTS,XPB,YPB,JP,
1IPRAB,ALPHB,KSTAL,ISTAL,KCLNT,AB(3)
7COMMON NSLIP,VR(19),DA(19),AS(19),TL(19),SV(19),FUNC,YO,CDNAC,
1ALPHV(16)
7COMMON INNCW,ISWIT(3),ALPHA,REYN,CLL,REYCN,XMAX,ALMAX(19),CLMAX,C,
1EPS,TRANS,REY,ETA,FCPP,ZHERE,WHERE,ARRAY,Y,BETA,TFAC,TRIX,TAU,MAXX
2,MAZZ,MXCCL,MZCCL,ASPEC,TAPER,BF,REYND,DISCR,PIER,CRB,C,TSTAX,EDGE
3,SIG,ALPHR,NFLAP,NLVL,NP,IY,IZ,IR,IP,IG,ISTAR,A,B,H,TAUT,TAUR,
4TWIST,R,BWX,YHERE,MYCCL,MAYY,FLAP,TCNY(19),TWISA,X,Z,CM,ACC,XHERE,
5MWCCL,MAWW,CAMB(19),CAMBR,CAMBT,DUMY1,DUMY2,NAME(25),AHERE(2,6),
6MAAAA(6),MACCL(6),BHERE(2,6),MABU(6),MBCCL(6),CHERE(2,6),MACC(6),
7MCCL(6),CHERE(2,6),MADD(6),MDCCL(6),STONY(19),SENE(19),CVAL,
8ALPHU,CBC,CBG,DELTA,ALPHZ,ALPH,ALPHE,CLADD,CLDEL,CLAD2,CLAD1,
9F,IRI,FF,LCCER
    ALPG(1)=ALPG(1)
    WRITE(IP,330) NAME
    WRITE(IP,340) ALPHB,CTS,A,B,ASPEC,H,ALPHR,TALT
    WRITE(IP,350) TAUR,TWIST,R,TWISA,BF,TAPER,FLAP,REYND,X,Z
    WRITE(IP,360)
    RETLRA
330 FCRMAT(1H1/1HC/35X,25A2/1X)
340 FCRMAT(1X,4C(3F./)/1HC/15X,3CHBODY ANGLE OF ATTACK, DEG. . =,F10.
12,1CX,3CHPRPELLER THRUST COEFFICIENT =,F11.3/15X,3CHBODY HEIGHT /
2 SPAN . =,F10.2,1CX,3CHBODY WIDTH / SPAN . =,F10.
32/15X,3CHASPECT RATIO . =,F10.2,1CX,3CHWING HEIGHT /
4 SPAN . =,F10.2/15X,3CHWING BODY INCIDENCE, DEG. . =,F10.
52,1CX,30FTIP THICKNESS CHORD . . . =,F10.2)
350 FCRMAT(15X,30FRCDT THICKNESS CHORD . . . =,F10.2,10X,30HGEOMETRI
1C TWIST, DEG . . . =,F10.2/15X,30FNUMBER OF SPANWISE STATIONS. =
2,F10.2,10X,30AERODYNAMIC TWIST, DEG . =,F10.2/15X,30HFLAP SPA
3N / WING SPAN . =,F10.2,1CX,30FTAPER RATIO . =
4,F10.2/15X,30HFLAP SETTING, DEG. =,F10.2,10X,30HREYNOLDS
5 ALMBER, MILLICNS . =,F10.2/15X,30FX-COORDINATE OF MOMENT REF . =
6,F10.2,10X,30HZ-COORDINATE OF MOMENT REF . =,F10.2)
360 FCRMAT(1HC/1X,4C(3F./)/1X)
    ENC
    SUBROUTINE MAN2A

```

CC

\*\*\*\*\*MAN2A--CONTINUATION OF MAIN2 \*\*\*\*\*

```

DIMENSION TCNY(19)
DIMENSION ARRAY(5,25,8),C(19),EPS(19),TRANS(19),REY(19),ETA(19),
1HCPP(19),CLMAX(19),ZHERE(2,6),WHERE(2,6),Y(19),TAU(19),BETA(19,19)
2,TRIX(19,19),MAZZ(6),MZCCL(6),MAXX(6),MXCCL(6),CBG(19),CVAL(19),
3ALPG(19),CBC(19),ALPHU(19),ALPH(19),ALPHZ(19),ALPHE(19),DELTA(19),
4YHERE(2,6),MYCCL(6),MAYY(6),CM(19),XHERE(2,6),MAWW(6),MWCCL(6)
5DIMENSION CLADD(19),CLDEL(19),CLAD2(19),CLAD1(19),F(19)
6COMMON KCR,KIR,KIL,KCL,VSA(19),SW(19),VSBAR,EYETL,CTS,XPB,YPB,JP,
1IPRAB,ALPHB,KSTAL,ISTAL,KCLNT,AB(3)
7COMMON NSLIP,VR(19),DA(19),AS(19),TL(19),SV(19),FUNC,YO,CDNAC,
1ALPHV(16)
7COMMON INNCW,ISWIT(3),ALPHA,REYN,CLL,REYCN,XMAX,ALMAX(19),CLMAX,C,
1EPS,TRANS,REY,ETA,FCPP,ZHERE,WHERE,ARRAY,Y,BETA,TFAC,TRIX,TAU,MAXX
2,MAZZ,MXCCL,MZCCL,ASPEC,TAPER,BF,REYND,DISCR,PIER,CRB,C,TSTAX,EDGE
3,SIG,ALPHR,NFLAP,NLVL,NP,IY,IZ,IR,IP,IS,ISTAR,A,B,H,TAUT,TAUR,
4TWIST,R,BWX,YHERE,MYCCL,MAYY,FLAP,TCNY,TWISA,X,Z,CM,ACC,XHERE,
5MWCCL,MAWW,CAMB(19),CAMBR,CAMBT,DUMY1,DUMY2,NAME(25),AHERE(2,6),

```

```

6AAA(6),MACCL(6),HERE(2,6),PABU(6),MUCOL(6),CHERE(2,6),MACC(6),
7MCCCL(6),CHERE(2,6),MACCL(6),MCCCL(6),STCKY(19),SGENE(19),CVAL,
8ALPHU,CBC,CBC,DELTA,ALPZ,ALPZ,ALPZ,CLACC,CLDEL,CLAD2,CLAD1,
9F,IRI,FF,LCCER

```

```

ITR=C
IY=1

```

```

DC 70 K=1, NP

```

```

ALPG(K)=ALPB+ALPR+EPS(K)+ALPB+TFAC+(TRANSLK)-1.)

```

```

SWITCH NUMBER 3 IS USED FOR AN INTERNAL
CLMP CF ARRAYS COMPUTED DURING ITERATION
PRCESS

```

70  
C  
C  
C  
C

```

CALL DATSW(3,JUNK)

```

```

GC TC (80,9C), JUNK

```

80 WRITE(IP,37C)

```

CALL AAA(ALPG,NP)

```

90

```

LCCER=3

```

```

ALPA=999.

```

```

CLI=C.C

```

```

REYCK=999.

```

```

XMAX=C.C

```

```

CALL BRIG(ALPZ,1,NP,1,IY,IE,REY,TAU,CAMB,ALPHA,1,1,ALPHA)

```

```

CALL DATSW(3,JUNK)

```

```

GC TC (66,67),JUNK

```

66

```

WRITE(IP,68)

```

```

CALL AAA(ALPZ,NP)

```

67

```

IF(IE) 101,101,310

```

101

```

IF(NSLIP-1) 135,102,102

```

135

```

DC 136 K=1, NP

```

136

```

TCNY(K)=0.0

```

```

GC TC 130

```

102

```

DC 103 K=1, NP

```

```

ALPG(K)=ALPG(K)+TL(K)

```

103

```

ALPZ(K)=ALPZ(K)+CA(K)

```

```

IF(ITR) 104,104,105

```

104

```

DLM=C.1*(ALPB+ALPR-C.4*ALPZ(1)-C.6*ALPZ(JP))/(1.+1.82/ASPEC)

```

105

```

GC TC 109

```

```

DLM=C.0

```

106

```

DC 106 K=1, NP

```

```

DLM=CBC(K)*ETA(K)+DLM

```

109

```

DLM=DLM*ASPEC*BWX**2

```

```

VW=DLM*FUNC/(9.87*ASPEC)

```

```

ALFPR=(ALPB+EYETL)/57.293

```

```

ASBAR=ATAN((SIN(ALFPR)+VW)/VSBAR)-ALFPR

```

```

CALL DATSW(3,JUNK)

```

50

```

GC TC (50,51),JUNK

```

1009

```

WRITE(IP,1009)

```

```

FCRMAT(10X,2F-VW)

```

```

CALL ZZZ(VW)

```

1010

```

WRITE(IP,1010)

```

```

FCRMAT(10X,5F-ALFPR)

```

```

CALL ZZZ(ALFPR)

```

1011

```

WRITE(IP,1011)

```

```

FCRMAT(10X,5F-ASBAR)

```

```

CALL ZZZ(ASBAR)

```

51

```

DC 1031 K=1, NP

```

1031

```

HCPP(K)=ALPG(K)-ALPZ(K)

```

```

DC 107 K=KCR,KIR

```

```

AS(K)=ASBAR

```

```

VR(K)=VSA(K)/CCS(ALFPR+ASBAR)

```

```

ANG=AS(K)+FCPP(K)/57.293

```

```

SYN=SIN(ANG)

```

```

CCZ=CCS(ANG)

```

107

```

SV(K)=VR(K)*SYN+VR(K)*Sw(K)*CCZ-SIN(HCPP(K)/57.293)

```

```

DC 108 K=KIL,KEL

```

```

AS(K)=ASBAR

```

```

VR(K)=VSA(K)/CCS(ALFPR+ASBAR)

```

```

ANG=AS(K)+FCPP(K)/57.293

```

```

SYN=SIN(ANG)

```

```

CCZ=CCS(ANG)

```

108

```

SV(K)=VR(K)*SYN+VR(K)*Sw(K)*CCZ-SIN(HCPP(K)/57.293)

```

```

CALL DATSW(3,JUNK)

```

52

```

GC TC (52,53),JUNK

```

1071

```

WRITE(IP,1071)

```

```

FCRMAT(10X,2F-SV)

```

```

CALL AAA(SV,NP)

```

1072

```

WRITE(IP,1072)

```

```

FCRMAT(10X,2F-VR)

```

```

CALL AAA(VR,NP)

```

178

```

53 DC 126 K=1, NP
    AK=K
    SUM1=C.C
    DC 121 M=1, NP
    AN=M
    SUM2=C.C
    DC 122 N=1, NP
    AM=M
122 SUM2=SUM2+SV(M)*SIN(AN*PIER)*SIN(AN*AM*PIER)
121 SUM1=SUM1+SUM2*SIN(AN*AK*PIER)/AN
120 TCNY(K)=VR(K)*SUM1*4./R
    CALL CATSW(3, JUNK)
    GC TC (54, 13C), JUNK
    54 WRITE(IP, 13C1)
1301 FCRMAF(10X, 5FCL2CB)
    CALL AAA(TCNY, NP)
130 IF(ITR) 131, 131, 14C
131 LCCER=2
    DC 1311 K=1, NP
1311 HCFP(K)=(ALPG(K)-ALPZ(K)*(1.-EDGE))/EDGE
    CLL=999.
    REYCN=999.
    XMAX=C.C
    CALL BRIDG(CVAL, 1, NP, 1, IY, IE, REY, TAU, CAMB, HOPP, 1, NP, CLL)
100 IF(IF) 10C, 10C, 31C
    DC 110 K=1, NP
    AK=K
110 CEG(K)=CVAL(K)*(ASPEC/(ASPEC+1.8))*C(K)*CRB*(0.5+
1(.1.+TAPER)*SIN(AK*PIER)/(3.14159*C(K)))
    CALL CATSW(3, JUNK)
    GC TC (12C, 14C), JUNK
120 WRITE(IP, 38C)
    CALL AAA(CVAL, NP)
140 DC 16C K=1, NP
    SIG=C.C
    DC 15C M=1, NP
150 SIG=(CEG(M)-TCNY(M))*BETA(M, K)+SIG
    ALPFL(K)=SIG*(1.+TFAC*(TRANS(K)-1.))
    ALPZ(K)=ALPG(K)-ALPFL(K)
160 ALPHE(K)=(ALPZ(K)-ALPZ(K)*(1.-EDGE))/EDGE
    C
    C
    C
    C
    LCCER=4
    CLL=999.
    REYCN=999.
    XMAX=C.C
    CALL BRIDG(CVAL, 1, NP, 1, IY, IE, REY, TAU, CAMB, ALPHE, 1, NP, CLL)
    IF(IE) 17C, 17C, 31C
170 DC 18C K=1, NP
    CEG(K)=CVAL(K)*C(K)*CRB/BWX
180 DELTA(K)=CEG(K)-CEG(K)
    C
    C
    C
    C
    CHECK FOR DUMR
    CALL CATSW(3, JUNK)
    GC TC (19C, 20C), JUNK
190 WRITE(IP, 39C)
    CALL AAA(CEG, NP)
    WRITE(IP, 40C)
    CALL AAA(ALPFL, NP)
    WRITE(IP, 41C)
    CALL AAA(ALPHE, NP)
    WRITE(IP, 38C)
    CALL AAA(CVAL, NP)
    WRITE(IP, 42C)
    CALL AAA(CEG, NP)
    WRITE(IP, 43C)
    CALL AAA(DELTA, NP)
    C
    C
    C
    CHECK TOLERANCE
200 DC 22C K=1, NP
    IF(ABS(DELTA(K))-DISCR) 21C, 210, 23C
210 IF(K-NP) 22C, 30C, 30C
220 CONTINUE
230 DC 25C I=1, NP
    SUM=C.C
    DC 24C J=1, NP

```

```

240 SUM=TRIX(I,J)*DELTA(J)+SUM
250 CBG(I)=CBG(I)+SUM
C
CALL DATSW(3,JUNK)
GC TC (260,270), JUNK
260 WRITE(IP,39C)
CALL AAA(CBG,AP)
C
REPEAT CYCLE
270 ITR=ITR+1
FF(ITR-30) 141,141,280
141 IF(NSLIP-1) 140,105,105
C
IF UNABLE TO CONVERGE AFTER 30 ITERATIONS
DUMP DELTA VALUES, C VALUES, AND TABLE
PRESENTLY IN CORE BEING USED FOR LOCK UP
280 WRITE(IP,440)
WRITE(IP,430)
CALL AAA(DELTA,AP)
WRITE(IP,380)
CALL AAA(CVAL,AP)
CALL EXIT
300 WRITE(IP,470) ITR,ALPH+B
CALL MAIN4
310 WRITE(IP,480) IE,LCCER
CALL EXIT
C
68 FCRMAT(10X,16+ZERC-LIFT ANGLES)
370 FCRMAT(10X,4+ALPG)
380 FCRMAT(10X,4+CVAL)
390 FCRMAT(10X,3+CBG)
400 FCRMAT(10X,5+ALPHU)
410 FCRMAT(10X,5+ALPHE)
420 FCRMAT(10X,3+CBC)
430 FCRMAT(10X,5+DELTA)
440 FCRMAT(1X,48+UNABLE TO CONVERGE AFTER 30 ITERATIONS ABORTED)
470 FCRMAT(10X,12,63+ ITERATIONS REQUIRED TO CONVERGE FOR ANGLE CF AT
1TACK EQUAL TO ,F8.2/1X)
480 FCRMAT(1X,1+ERRCK CODE,12,1X,1+HAT SECTION,13,1X,32+IN PROGRAM, E
1EXECUTION TERMINATED)
END
SUBROUTINE MAIN4
C
MAIN4-----CONTINUATION OF SUBROUTINE MAIN2
DIMENSION ARRAY(5,25,8 ),C(19),EPS(19),TRANS(19),REY(19),ETA(19),
1HCPP(19),CLMAX(19),ZHERE(2,6),WHERE(2,6),Y(19),TAU(19),BETA(19,19)
2,TRIX(19,19),MAZZ(6),MZCCL(6),MAXX(6),MXCCL(6),ALPG(19),ALPHE(19),
3CL(19),CDC(19),CACC(19),ALPH(19),CBC(19),CBG(19),DELTA(19),ALPHZ(
419),ALPH(19),CVAL(19),YHERE(2,6),MYCCL(6),MAYY(6),CM(19),
5XHERE(2,6),MAHW(6),MWCCL(6)
DIMENSION CLACC(19),CLDEL(19),CLAC2(19),CLAD1(19),F(19)
CCMPCN KCR,KIR,KIL,KCL,VSA(19),SK(19),VSEAR,EYETL,CTS,XPB,YPB,JP,
1FPRAB,ALPH+B,KSTAL,ISTAL,KCLNT,AB(3)
CCMPCN NSLIP,VR(19),DA(19),AS(19),TL(19),SV(19),FUNC,YO,CDNAC,
1ALPHV(16)
CCMPCN INACH,ISWIT(3),ALPHA,REYN,CLL,REYCN,XMAX,ALMAX(19),CLMAX,C,
1EPS,TRANS,REY,ETA,HCPP,ZHERE,WHERE,ARRAY,Y,BETA,TFAC,TRIX,TAU,MAXX
2,MAZZ,MXCCL,MZCCL,ASPEC,TAPER,BF,REYCN,DISCR,PIER,CRD,OTSTAX,EDGE
3,SIG,ALPHR,NFLAP,ALVL,NP,IY,IZ,IK,IP,IG,ISTAR,A,B,F,TAUT,TAUR,
4TWIST,R,BWX,YHERE,MYCCL,MAYY,FLAP,ICNY(19),THISA,X,Z,CM,ACC,XHERE,
5MWCCL,MAHW,CAMB(19),CAMBR,CAMBT,DUMY1,DUMY2,NAME(25),AHERE(2,6),
6MAAA(6),MACCL(6),CHERE(2,6),MABU(6),MBCOL(6),CHERE(2,6),MACC(6),
7MCCCL(6),CHERE(2,6),MACC(6),MBCOL(6),STONY(19),SCENE(19),CVAL,
8ALPHL,CBC,CBG,DELTA,ALPHZ,ALPH,ALPHE,CLACC,CLDEL,CLAD2,CLAD1,
9F,IRI,FF,LCCER
DC 10 K=1,AP
10 CL(K)=CVAL(K)
IZ=1
LCCER=5
C
CCMPLTE PROFILE DRAG COEFFICIENTS
C
CLL=999.
REYCN=999.

```

```

XMAX=C.
CALL BRIDG(CDC,1,NP,2,IZ,IE,REY,TAU,CAMB,CL,1,NP,CLL)
DC 2C K=1,NP
20 CL(K)=CVAL(K)

                                CCMPLTE QUARTER CHORD PITCHING MOMENT
                                CCEFFICIENTS

CLL=999.
KEYCN=999.
XMAX=C.
CALL BRIDG(CM,1,NP,3,Ih,IE,REY,TAU,CAMB,CL,1,NP,CLL)
DC 5C K=1,NP

                                CHECK IF SECTION STALLED

30 IF(ALPHE(K)-ALMAX(K)) 40,3C,3C
   WRITE(IP,26C) K,ALPHE(K),ALMAX(K)
   KSTAL=1

                                CCMPUTE SECTION PITCHING MCMENT

40 SUM1=CCS(3.14159/180.*(ALPB-ALPHU(K)))
   SUM2=SIN(3.14159/180.*(ALPB-ALPHU(K)))
   CM(K)=CM(K)-X/C(K)*(CL(K)*SUM1+CDC(K)*SUM2)-Z/C(K)*(CL(K)*SUM2-CDD
   I(K)*SUM1)
50 CCCC(K)=CDC(K)*C(K)*CRB/BWX
   WRITE(IP,39C)
   CALL AAA(Y,NP)
   WRITE(IP,27C)
   CALL AAA(CM,NP)

                                CHECK FOR DUMP

CALL DATSW(3,JUNK)
GC TC (60,7C), JUNK
60 WRITE(IP,28C)
   CALL AAA(CLMAX,NP)
   WRITE(IP,29C)
   CALL AAA(CCCC,NP)
70 WRITE(IP,30C)
   CALL AAA(ALPHE,NP)
   WRITE(IP,31C)
   CALL AAA(CDC,NP)
DC 8C K=1,NP
80 ALPG(K)=ALPHU(K)*CL(K)*3.14159/180.
   WRITE(IP,32C)
   CALL AAA(ALPG,NP)
   WRITE(IP,33C)
   CALL AAA(CL,NP)
   IF(NSLIP.EC.C) CTS=0.0
DC 8C1 K=1,NP
801 CDC(K)=CL(K)*(1.-CTS)
   WRITE(IP,32C)
   CALL AAA(CDC,NP)

                                CCMPLTE OVERALL LIFT, DRAG, AND PITCHING
                                MCMENT COEFFICIENTS

SUM1=C.
SUM2=C.
SUM3=C.
SUM4=C.
DC 5C I=1,NP
SUM1=CBC(I)*ETA(I)+SUM1
SUM2=CBC(I)*ALPHU(I)*ETA(I)+SUM2
SUM3=CDC(I)*ETA(I)+SUM3
90 SUM4=CM(I)*C(I)**2*ETA(I)+SUM4
Q=ASPEC*BWX**2
CLIFT=C*SUM1
CLPP=CLIFT*(1.-CTS)
CCI=C.C17453*C*SUM2
CDP=C*SUM3
CD=CCI+CDP+CDNAG
CCPP=CC*(1.-CTS)
ZM=ASPEC*BWX*CRB/ACC*SUM4
CMPP=ZM*(1.-CTS)
WRITE (IP,34C)
WRITE (IP,341) ALPB,CCI,CLIFT,CDP,CLPP,CDNAG,ZM,CD,CMPP,CDPP
WRITE (IP,34C)

```

```

C
C
C      IF((KSTAL.EQ.C).AND.(KCUNT.EQ.C)) GO TO 250
C      DEFINE EXACT STALL ANGLE CF ATTACK
C
C      IF((IPRAB.EQ.1).OR.(KCUNT.EQ.3)) GO TO 9900
C      KCUNT=KCUNT+1
C      GC TC (1000,2000,3000),KCUNT
1000  AB(1)=(ALPFB+ALPHV(IPRAB-1))/2.
C      ALPFB=AB(1)
C      GC TC 9900
2000  IF(KSTAL.EQ.C) GO TO 2100
C      ISTALL=1
C      AB(2)=(AB(1)+ALPHV(IPRAB-1))/2.
C      ALPFB=AB(2)
C      GC TC 9900
2100  ISTALL=C
C      AB(2)=(AB(1)+ALPHV(IPRAB))/2.
C      ALPFB=AB(2)
C      GC TC 9900
3000  IF(KSTAL+ISTALL-1) 3100,3200,3300
3100  AB(3)=(AB(2)+ALPHV(IPRAB))/2.
C      ALPFB=AB(3)
C      GC TC 9900
3200  AB(3)=(AB(2)+AB(1))/2.
C      ALPFB=AB(3)
C      GC TC 9900
3300  AB(3)=(AB(2)+ALPHV(IPRAB-1))/2.
C      ALPFB=AB(3)
9900  KSTAL=C
C      DC 17C K=1,AP
170  CDC(K)=CLMAX(K)-CL(K)
C      WRITE(IP,35C)
C      CALL AEA(CDC,AP)
C      IF((IPRAB.EQ.1).OR.(KCUNT.EQ.3)) GO TO 171
C      WRITE(IP,37C) NAME
C      WRITE(IP,36C) ALPFB
C      IR=100
C      CALL MAIN2A
250  IR=C
C      RETURN
171  IR=101
C      RETURN
C
C 260  FCRMAT(10X,19)STALLED AT STATION ,12,18H ANGLE OF ATTACK =,F7.3,
C      11CX,21)SECTION STALL ANGLE =,F7.3)
270  FCRMAT(10X,35)SECTION PITCHING MOMENT COEFFICIENT)
280  FCRMAT(10X,5)CLMAX)
290  FCRMAT(10X,4)CCLC)
300  FCRMAT(10X,33)EFFECTIVE SECTION ANGLE OF ATTACK)
310  FCRMAT(10X,32)SECTION PROFILE DRAG COEFFICIENT)
320  FCRMAT(10X,32)SECTION INCLCED DRAG COEFFICIENT)
330  FCRMAT(10X,43)DISTRIBUTION CF SECTION LIFT COEFFICIENT-CL)
340  FCRMAT(1X,4C(3F./.)/1FC/)
341  FCRMAT(1CX,36)FLSELAGE ANGLE OF ATTACK,DEGREES. =,F9.5,
C      11CX,32)INCLCED DRAG COEFFICIENT,CDI = ,F9.5/10X,
C      236)LIFT COEFFICIENT,CL . . . =,F9.5,
C      31CX,32)PROFILE DRAG COEFFICIENT,CD . . . =,F9.5/10X,
C      436)LIFT COEFFICIENT,CLS . . . =,F9.5,
C      510X,32)MACELLE DRAG COEFFICIENT,CDA = ,F9.5/10X,
C      636)PITCHING MOMENT COEFFICIENT,CM . . . =,F9.5,
C      71CX,32)TOTAL DRAG COEFFICIENT,CD . . . =,F9.5/10X,
C      836)PITCHING MOMENT COEFFICIENT,CMS . . . =,F9.5,
C      910X,32)TOTAL DRAG COEFFICIENT,CDS = ,F9.5/1H0/)
350  FCRMAT(10X,34)STALL MARGIN DISTRIBUTION,CLMAX-CL,/1X)
360  FCRMAT(1X,4C(3F./.)/1X/1CX,2)ADJUSTED ANGLE OF ATTACK TC,F8.3,32H
C      1,SEARCHING FOR EXACT STALL PCINT,/1X/1X,4C(3H./.)/1X)
370  FCRMAT(1H1/1H/35X,25A2/1X)
380  FCRMAT(10X,44)DISTRIBUTION CF SECTION LIFT COEFFICIENT-CLS)
390  FCRMAT(1CX,22)SPANWISE STATIONS-2Y/B)
C      ENC
C      SUBROUTINE MAIN3
C
C-----MAIN3--SUBROUTINE FOR THE CASE WITH PART-SPAN FLAPS-----
C
C      DIMENSION ARRAY(5,25,8 ),C(19),EPS(19),TRANS(19),REY(19),ETA(19),
C      1HCPP(19),CLMAX(19),ZHERE(2,6),WHERE(2,6),Y(19),TAL(19),BETA(19,19)
C      2,TRIX(19,19),PAZZ(6),MZCCL(6),MAXX(6),MXCCL(6),XHERE(2,6),MxCCL(6)
C      3,MAWH(6),CM(19),CBG(19),CVAL(19),ALPG(19),CBC(19),ALPHU(19),ALPH(1
C      49),ALPZ(19),ALPE(19),DELTA(19),CL(19),YHERE(2,6),PYCOL
C      5(6),MAYY(6),CLACD(19),CLCEL(19),CLAD2(19),CLAD1(19),F(19),ALPC(19)

```

```

6, ICNY(19)
CCMFCN KDR, KIR, KIL, KCL, VSA(19), SW(19), VSBAR, EYETL, CTS, XPB, YPB, JP,
1 IPRAF, ALPFE, KSTAL, ISTAR, KCLNT, AB(3)
CCMFCN NSLIP, VR(19), CA(19), AS(19), TL(19), SV(19), FUNC, YG, CDNAC,
1 ALPFV(14)
CCMFCN IRNCH, ISWIT(3), ALPHA, REYN, CLL, REYCN, XMAX, ALMAX(19), CLMAX, C,
1 EPS, TRANS, REY, ETA, FCPP, ZFERE, WFERE, ARRAY, Y, BETA, TFAC, TRIX, TAL, MAXX
2, MAZZ, MXCCL, MZCCL, ASPEC, TAPER, LF, REYND, DISCR, PIER, CRB, G, TSTAX, EDGE
3, SIG, ALPHR, AFLAP, NLVL, NP, IY, IZ, IR, IP, ISIS, ISTAR, A, B, H, TAUT, TAUR,
4 TWIST, R, SWX, YFERE, MYCCL, MAYY, FLAP, TCNY, TWISA, X, Z, CM, ACC, XHERE,
5 MCEL, MAH, CAMB(19), CAMER, CAMET, DUMY1, DUMY2, NAME(25), AHERE(2,6),
6 MAAA(6), MACCL(6), WFERE(2,6), MABB(6), MCOL(6), CHERE(2,6), MACC(6),
7 MCCCL(6), CHERE(2,6), MADD(6), MCCOL(6), STONY(19), SGENE(19), CVAL,
8 ALPFU, CBC, CBG, CELTA, ALPFZ, ALPH, ALPFE, CLADD, CLDEL, CLAD2, CLAD1,
9F, IRI, FF, LCCER
IF(IPRAE.NE.1)GC TO 690
ALPE=C.
CL(1)=C.
IRI=R
ITR=0
IY=1

```

CCC

PUT FLAPS-LP CL DATA INTO CORE

```

CALL LAGET(ARRAY,1,IY)
LCCER=2
DC 6C K=1,NP
ALPG(K)=3.

```

CCC

LCCK LP CL VALUES

```

CLL=999.
ALPFA=ALPG(K)
REYN=PEY(K)
TALX=TAL(K)
REYCN=999.
XMAX=C.
CALL ARC(ARRAY,TAUX,MAXX,MXCCL,IE,WHERE,NLVL)

```

CCC

CHECK FOR ERROR STOP

```

IF(IE) 50,5C,4C
4C WRITE(IP,720) IE,LCCER
CALL EXIT
5C CVAL(K)=CLL
AK=K
60 CBG(K)=CVAL(K)*(ASPEC/(ASPEC+1.8))*C(K)*CRB*(0.5+(1.+TAPER)*SIN(AK
1*PIER)/(3.14159*C(K)))
CALL DATSW(3,JUNK)
GC TO (70,8C), JUNK
70 WRITE(IP,730)
CALL AAA(CVAL,NP)
80 DC 12C K=1,NP
SIG=C.
DC 5C M=1,NP
90 SIG=CBG(M)*BETA(M,K)+SIG
ALPL(K)=SIG*(1.+TFAC*(TRANS(K)-1.))
ALPF(K)=ALPG(K)-ALPFU(K)

```

CCC

LCCK LP ALPHA FOR ZERO LIFT

```

LCCER=3
ALPFA=999.
CLL=C.0
REYN=REY(K)
TALX=TAL(K)
REYCN=999.
XMAX=C.
CALL ARC(ARRAY,TAUX,MAXX,MXCCL,IE,WHERE,NLVL)
IF(IE) 10G,10C,95
95 WRITE(IP,720) IE,LCCER
CALL EXIT
100 ALPFZ(K)=ALPFA
ALPFE(K)=(ALPF(K)-ALPFZ(K))*(1.-EDGE))/EDGE

```

CCC

LCCK LP CL VALUES

```

LCCER=4
CLL=999.
ALPFA=ALPFE(K)

```

```

      REYN=REY(K)
      TALX=TAL(K)
      REYCN=999.
      XMAX=C.
      CALL ARC(ARRAY,IAUX,MAXX,MAXCCL,IE,WHERE,NLVL)
      IF(IE) 11C,11C,95
110  CVAL(K)=CLL
      CBC(K)=CVAL(K)*C(K)*CR8/BWX
120  DELTA(K)=CBC(K)-CBG(K)
      CALL DATSW(3,JUNK)
      GC TC (13C,14C), JUNK
130  WRITE(IP,74C)
      CALL AAA(CBG,AP)
      WRITE(IP,75C)
      CALL AAA(ALPHL,AP)
      WRITE(IP,76C)
      CALL AAA(ALPHE,AP)
      WRITE(IP,77C)
      CALL AAA(CVAL,AP)
      WRITE(IP,78C)
      CALL AAA(DELTA,AP)
140  DC 16C K=1,AP
      IF(ABS(DELTA(K))-DISCR) 15C,15C,17C
150  IF(K=AP) 16C,24C,24C
160  CCNTINLE
170  DC 19C I=1,AP
      SLM=C.
      DC 18C J=1,AP
180  SLM=TRIX(I,J)*DELTA(J)+SLM
190  CBG(I)=CBG(I)+SLM
      CALL DATSW(3,JUNK)
      GC TC (20C,21C), JUNK
200  WRITE(IP,74C)
      CALL AAA(CBG,AP)
210  ITR=ITR+1

```

ITERATION CONTROL

```
IF(ITR=30) 8C,8C,22C
```

IF UNABLE TO CONVERGE, DUMP ALL

```

220  WRITE(IP,79C)
      WRITE(IP,78C)
      CALL AAA(DELTA,AP)
      WRITE(IP,73C)
      CALL AAA(CVAL,AP)
      DC 23C J=1,NLVL
      NR=MAXX(J)
      NC=MAXCCL(J)
      TALX=WHERE(2,J)
      WRITE(IP,80C) J,J,NR,NC,TALX
      DC 23C K=1,NR
230  WRITE(IP,81C) (ARRAY(J,K,L),L=1,NC)
      CALL EXIT

```

CONVERGENCE

```

240  WRITE(IP,82C) NAME
      WRITE(IP,83C) ITR,ALPB
      SLM=C.
      DC 25C I=1,AP
250  SLM=CLC(I)*ETA(I)+SUM
      Q=ASPEC*BWX**2

```

CALCULATE ADDITIONAL LIFT DISTRIBUTION,CL1

```

      CCLIF=Q*SLM
      DC 26C K=1,AP
260  CLACC(K)=CVAL(K)/CCLIF
      CLL=0.
      ALPHA=999.
      REYN=REY(ISTAR)
      TALX=TAL(ISTAR)

```

CALCULATE ZERO-LIFT ANGLES OUTBOARD AND INBOARD OF FLAP END

```

      REYCN=999.
      CALL ARC(ARRAY,TALX,MAXX,MAXCCL,IE,WHERE,NLVL)

```



```

A1=ALPHA
ALPHA=999.
C      LOAD FLAP CL TABLES INTO CORE
CALL CAGET(ARRAY,4,1W)
CALL ARC(ARRAY,TAUX,MAXW,MXCCL,IE,XHERE,NLVL)
A2=ALPHA
SDELT=A1-A2
ALPG(JP)=0.
ALPHA=ALPG(JP)
CLL=999.
REYN=REY(JP)
TALX=TAL(JP)
CC
      CALCULATE APPROXIMATE SPAN LOADING WITH FLAP
REYCN=999.
CALL ARC(ARRAY,TAUX,MAXW,MXCCL,IE,XHERE,NLVL)
CVAL(JP)=CLL
DC 29C K=1,JP
AK=K
STAR=ISTAR
IF(K-ISTAR) 28C,28C,27C
270 CBG(K)=C.5*CVAL(JP)*C(K)*CRB/BWX*(1.+SQRT(1.-(CCS(AK*PIER)/CCS(
  ISTAR*PIER))*2))
  GC TC 290
280 CBG(K)=C.5*CVAL(JP)*C(K)*CRB/BWX*(1.-SQRT(1.-((1.-CCS(AK*PIER))/
  1.(1.-CCS(ISTAR*PIER))*2)))
290 CCNTIME
  DC 30C K=1,JP
  IRI=R
  IRI=IRI-K
300 CBG(IRI)=CBG(K)
  IRI=R
  DC 31C K=1,JP
  ALPG(K)=0.
  CALL CATSW(3,I)
  GC TC (22C,33C), I
320 WRITE(IP,84C)
  CALL AAA(CLACC,JP)
  WRITE(IP,85C)
  CALL ZZZ(CLL)
  WRITE(IP,74C)
  CALL AAA(CBG,JP)
C      CALCULATE LIFT DISTRIBUTION WITH FLAP-UNCORRECTED FOR FLAP
C      END EFFECTS ON SECTION DATA
330 ITR=C
340 DC 40C K=1,JP
  SIG=0.
  DC 35C M=1,JP
350 SIG=CBG(M)*EETA(M,K)+SIG
  ALPHL(K)=SIG*(1.+IFAC*(TRANS(K)-1.))
  ALPH(K)=ALPG(K)-ALPHL(K)
  ALPC(K)=SDELT*FCPP(K)
  ALPH(K)=ALPH(K)-ALPC(K)
  CLL=C.
  ALPHA=999.
  REYN=KEY(K)
  REYCN=999.
  TAUX=TAL(K)
  IF(K-ISTAR) 38C,38C,36C
36C IF(K-IRI+ISTAR) 37C,38C,38C
37C CALL CAGET(ARRAY,4,1W)
  CALL ARC(ARRAY,TAUX,MAXW,MXCCL,IE,XHERE,NLVL)
  ALPHZ(K)=ALPHA
  ALPHA=(ALPH(K)-ALPHZ(K))*(1.-EDGE)/EDGE
  CLL=999.
  CALL ARC(ARRAY,TAUX,MAXW,MXCCL,IE,XHERE,NLVL)
  CVAL(K)=CLL
  GC TC 390
38C CALL CAGET(ARRAY,1,IY)
  CALL ARC(ARRAY,TAUX,MAXX,MXCCL,IE,WHERE,NLVL)
  ALPHZ(K)=ALPHA
  ALPHA=(ALPH(K)-ALPHZ(K))*(1.-EDGE)/EDGE
  CLL=999.
  CALL ARC(ARRAY,TAUX,MAXX,MXCCL,IE,WHERE,NLVL)
  CVAL(K)=CLL
390 CBG(K)=CVAL(K)*C(K)*CRB/BWX
400 DELTA(K)=CBG(K)-CBG(K)
  CALL CATSW(3,JUNK)
  GC TC (41C,42C), JUNK

```

```

410  WRITE(IP,75C)
      CALL AAA(ALFFL,NP)
      WRITE(IP,88C)
      CALL AAA(ALPC,NP)
      WRITE(IP,89C)
      CALL AAA(ALPF,NP)
      WRITE(IP,90C)
      CALL AAA(ALPFZ,NP)
      WRITE(IP,73C)
      CALL AAA(CVAL,NP)
      WRITE(IP,92C)
      CALL AAA(CBC,NP)
      WRITE(IP,78C)
      CALL AAA(DELTA,NP)
420  DC 44C K=1,NP
      IF(ABS(DELTA(K))-DISCR) 43C,43C,450
430  IF(K-NP) 44C,50C,50C
440  CONTINUE
450  DC 47C I=1,NP
      SUM=0.
      DC 46C J=1,NP
460  SUM=TRIX(I,J)*DELTA(J)+SUM
470  CBG(I)=CBG(I)+SUM
      CALL CATSW(3,JUNK)
      GC TC (48C,49C), JUNK
480  WRITE(IP,74C)
      CALL AAA(CBG,NP)
490  ITR=ITR+1
      IF(ITR-30) 34C,34C,22C
500  DC 51C K=1,NP
510  CLDEL(K)=CVAL(K)
      F1=CLDEL(JP)/CLACC(JP)
      F2=CLDEL(1)/CLACC(1)
      DC 52C K=1,ISTAR
520  CLACC(K)=F2*CLACC(K)
      DC 53C K=1,ISTAR,JP
530  CLAC1(K)=F1*CLACC(K)
      BDELT=CLAC1(ISTAR)-CLACC(ISTAR)
      DC 54C K=1,ISTAR
540  F(K)=(CLDEL(K)-CLACC(K))/BDELT
      FF=(CLDEL(ISTAR)-CLAC1(ISTAR))/BDELT
      ISTAR=ISTAR+1
      DC 55C K=1,JP
550  F(K)=(CLDEL(K)-CLAC1(K))/BDELT
      DC 56C K=1,JP
      IRI=R
      IRI=IRI-K
560  F(IRI)=F(K)
      CALL CATSW(3,JUNK)
      GC TC (57C,58C), JUNK
570  WRITE(IP,84C)
      CALL AAA(CLACC,NP)
      WRITE(IP,94C)
      CALL AAA(CLDEL,NP)
      WRITE(IP,97C)
      CALL ZZZ (F1)
      WRITE(IP,98C)
      CALL ZZZ (F2)
      WRITE(IP,99C)
      CALL AAA(CLACC2,NP)
      WRITE(IP,100C)
      CALL AAA(CLAC1,NP)
      WRITE(IP,101C)
      CALL AAA(F,NP)
      WRITE(IP,102C)
      CALL ZZZ(FF)
C
C
C      LCKK LP CL MAX FOR SECTION CN UNFLAPPED SIDE OF FLAP END
580  CALL CAGET(ARRAY,1,IY)
      REYN=999.
      XMAX=C.
      CLL=999.
      ALPFA=999.
      REYCN=REY(ISTAR)
      TALX=TAL(ISTAR)
      CALL ARC(ARRAY,TAUX,MAXX,MAXCL,IE,WHERE,NLVL)
      CLPFA=XMAX
      XMAX=C.
C

```

```

C      LOCK UP CL MAX FOR SECTION CN   FLAPPED SIDE OF FLAP END
C      CALL DGET (ARRAY,4, Iw)
C      CALL ARC (ARRAY,TAUX,MAHW,MWCCL,IE,XHERE,NLVL)
C      CLMF=XMAX
C      DCLMA=CLMF-CLMNF
C      CLL=999.
C      ALPFA=999.
C      REYN=999.
C      XMAX=0.
C      DC 63C K=1,AP
C      IRI=R
590  IF (K-ISTAR) 600,60C,590
600  IF (K-IRI+ISTAR) 610,60C,600
C      XMAX=C.
C      REYCN=REY(K)
C      TALX=TAL(K)
C
C      LOCK UP CLMAX FOR UNFLAPPED WING SECTIONS
C      CALL DGET (ARRAY,1,IY)
C      CALL ARC (ARRAY,TAUX,MAXX,MXCCL,IE,WHERE,NLVL)
610  GC TC 620
C      XMAX=C.
C      REYCN=REY(K)
C      TALX=TAL(K)
C
C      LOCK UP CLMAX FOR   FLAPPED WING SECTIONS
C      CALL DGET (ARRAY,4, Iw)
C      CALL ARC (ARRAY,TAUX,MAHW,MWCCL,IE,XHERE,NLVL)
620  F(K)=1.+F(K)*DCLMA/XMAX
630  CLMAX(K)=F(K)*XMAX
C      FF=1.+FF*DCLMA/CLMF
C      DC 67C K=1,AP
640  IF (K-ISTAR) 650,65C,64C
C      IF (K-IRI+ISTAR) 66C,650,65C
C
C      LOCK UP ALPHA AT CLMAX FOR UNFLAPPED WING SECTIONS
650  CALL DGET (ARRAY,1,IY)
C      ALPFA=999.
C      REYN=999.
C      CLL=999.
C      REYCN=REY(K)
C      TALX=TAL(K)
C      XMAX=1CC.
C      CALL ARC (ARRAY,TAUX,MAXX,MXCCL,IE,WHERE,NLVL)
C      GC TC 670
C
C      LOCK UP ALPHA AT CLMAX FOR   FLAPPED WING SECTIONS
660  CALL DGET (ARRAY,4, Iw)
C      XMAX=1CC.
C      REYCN=REY(K)
C      TALX=TAL(K)
C      REYN=999.
C      ALPFA=999.
C      CLL=999.
670  CALL ARC (ARRAY,TAUX,MAHW,MWCCL,IE,XHERE,NLVL)
C      ALPAX(K)=ALPFAZ(K)+(XMAX-ALPFAZ(K))*ELGE*F(K)
C      WRITE (IP,82C) NAME
C      WRITE (IP,1C3C)
C      CALL AAA (Y,AP)
C      WRITE (IP,1C4C)
C      CALL AAA (ALPAX,AP)
C      WRITE (IP,1C5C)
C      CALL AAA (CLMAX,AP)
C      WRITE (IP,1C6C)
C      CALL AAA (TAL,AP)
C      WRITE (IP,1C7C)
C      CALL AAA (REY,AP)
C      WRITE (IP,1C8C)
C      CALL AAA (C,AP)
C      WRITE (IP,1C9C)
C      CALL AAA (EPS,AP)
C      CALL DATSW (3,JUNK)
680  GC TC (68C,690), JUNK
C      WRITE (IP,11C0)
C      CALL ZZZ (DCLMA)

```

```

WRITE(IP,1010)
CALL AAA(F,AP)
WRITE(IP,1020)
CALL ZZ?(FF)
CALL MAIN5
690
C
720 FCRMAT(1X,10FERROR CODE,I2,1X,10FAT SECTION,I3,1X,32HIN PROGRAM, E
1XEXECUTION TERMINATED)
730 FCRMAT(10X,4FCVAL)
740 FCRMAT(10X,3FCBG)
750 FCRMAT(10X,5FALPHU)
760 FCRMAT(10X,5FALPHE)
770 FCRMAT(10X,3FCBC)
780 FCRMAT(10X,5FDelta)
790 FCRMAT(2X,40FUNABLE TO CONVERGE AFTER 30 ITERATIONS ABCRTEO)
800 FCRMAT(1HC/1FC.7H ARRAY(,I1,I1F 1, 1) TO (,I1,LP,,I2,IH,,I2,IH),F
110.5/1FC)
810 FCRMAT(12F10.4)
820 FCRMAT(1H1/1FC/35X,25A2/1X)
830 FCRMAT(1X,33F ITERATIONS REQUIRED TO CONVERGE ,I2,19H FOR ALPHB EQ
1VAL TC,F10.1/1FC)
840 FCRMAT(10X,5FCLADD)
850 FCRMAT(10X,2FCL)
880 FCRMAT(10X,4FALPC)
890 FCRMAT(10X,4FALPH)
900 FCRMAT(10X,5FALPHZ)
920 FCRMAT(10X,3FCBC)
960 FCRMAT(10X,5FCLDEL)
970 FCRMAT(10X,2FF1)
980 FCRMAT(10X,2FF2)
990 FCRMAT(10X,5FCLAD2)
1000 FCRMAT(10X,5FCLAD1)
1010 FCRMAT(10X,1FF)
1020 FCRMAT(10X,2FF)
1030 FCRMAT(1X/10X,'SPANWISE STATIONS-2Y/B')
1040 FCRMAT(10X,10F ALPHA MAX)
1050 FCRMAT(10X,7F CL MAX)
1060 FCRMAT(10X,31F THICKNESS / CHORD DISTRIBUTION)
1070 FCRMAT(10X,'SECTION REYNOLDS NUMBERS,MILLIONS')
1080 FCRMAT(10X,19F CHORD DISTRIBUTION)
1090 FCRMAT(10X,16F GEOMETRIC TWIST)
1100 FCRMAT(10X,6FDCCLMA)
ENC
SUBROUTINE MAIN5

```

```

C
C *****MAINS--CONTINUATION OF SUBROUTINE MAIN3 *****
DIMENSION ARRAY(5,25,8 ),C(19),EPS(19),TRANS(19),REY(19),ETA(19),
1HCPP(19),CLYAX(19),ZHERE(2,6),WHERE(2,6),Y(19),TAL(19),BETA(19,19)
2,TRIX(19,19),MAZZ(6),MZCCL(6),MAXX(6),MXCCL(6),XHERE(2,6),MWCCL(6)
3,MAXX(6),CM(19),CBG(19),CVAL(19),ALPG(19),CBC(19),ALPHU(19),ALPH(1
49),ALPHZ(19),ALPHE(19),DELTA(19),CL(19),YHERE(2,6),MYCCL
5(6),MAYY(6),CLADD(19),CLDEL(19),CLAD2(19),CLAD1(19),F(19),ALPC(19)
6,TCNY(19)
CCMYCN,KBR,KIR,KIL,KCL,VSA(19),SW(19),VSBAR,EYETL,CTS,XPB,YPB,JP,
11PRAB,ALPB,KSTAL,ISTAL,KCLNT,AB(3)
CCMYCN,NSLIP,VR(19),DA(19),AS(19),TL(19),SV(19),FUNC,YO,CUNAC,
1ALPHV(16)
COMMON INACT,ISKIT(3),ALPHA,REYN,CLL,REYN,XMAX,ALMAX(19),CLMAX,C,
1EPS,TRANS,REY,ETA,FCPP,ZHERE,WHERE,ARRAY,Y,BETA,TFAC,TRIX,TAL,MAXX
2,MAZZ,MYCCL,MZCCL,ASPEC,TAPER,BF,REYND,DISCK,PIEK,CRB,G,TSTAX,EDGE
3,SIC,ALPHR,NFLAP,NLVL,NP,IY,IZ,IR,IP,ISIS,ISTAR,A,B,H,TALT,TAUR,
4TWIST,R,BWX,YHERE,MYCCL,MAYY,FLAP,TLNY,TWISA,A,Z,CM,ACC,XHERE,
5MWCCL,MAXX,CAMB(19),CAMBR,CAMBT,DUMY1,DUMY2,NAME(25),AHERE(2,6),
6MAAA(6),MACCL(6),LHERE(2,6),MABS(6),MBCCL(6),CHERE(2,6),MACC(6),
7MCCCL(6),CHERE(2,6),MADC(6),MBCCL(6),STONY(19),SGENE(19),CVAL,
8ALPHU,CBC,CBG,DELTA,ALPHZ,ALPH,ALPHE,CLADD,CLDEL,CLAD2,CLAD1,
9F,IRI,FF,LCCER
3030 DC 6C K=1,NP
AK=K
ALPG(K)=ALPB+ALPHR+EPS(K)+ALPB*TFAC*(TRANS(K)-1.)
IF(K-ISTAR) 4C,4C,3C
3C IF(K-IRI+ISTAR) 5C,4C,4C
C
C FIND CL FROM FLAPS-UP DATA FOR UNFLAPPED SPAN STATIONS
C
40 ALPHA=ALPG(K)
CLL=999.
REYN=REY(K)
TALX=TAL(K)

```

```

REYCN=999.
CALL DGET (ARRAY,1,IY)
CALL ARC (ARRAY,TAUX,MAXX,MXCCL,IE,XHERE,NLVL)
CVAL(K)=CLL
GC TC 6C

```

C  
C  
C

FIND CL FROM FLAP DATA FOR UNFLAPPED SPAN STATIONS

```

50 ALPHA=ALPG(K)
   CLL=999.
   REYN=REY(K)
   TALX=TAL(K)
   REYCN=999.
   CALL DGET (ARRAY,4,IW)
   CALL ARC (ARRAY,TALX,MAHW,MWCCL,IE,XHERE,NLVL)
   CVAL(K)=CLL
60 CBG(K)=CVAL(K)*(ASPEC/(ASPEC+1.8))*C(K)*CRB*(0.5+(1.+TAPER)*SIN(AK
  1*PIER)/(3.14159*C(K)))

```

C  
C  
C

CHECK FOR DUMP

```

CALL DATSW(3,JUNK)
GC TC (70,81),JUNK
70 WRITE(IP,61C)
   CALL AAA(TRANS,NP)
   WRITE(IP,62C)
   CALL ZZZ(TFAC)
   WRITE(IP,62C)
   CALL AAA(ALFC,NP)
   WRITE(IP,63C)
   CALL AAA(CBG,NP)
81 ITR=C
   IF(NSLIP-1) 135,80,80
135 DC 136 K=1,NP
136 TCNY(K)=0.C
80 CLSTA=CBG(ISTAR)*BWX/(C(ISTAR)*CRB)

```

C  
C  
C

CHECK FOR DUMP

```

CALL DATSW(3,JUNK)
GC TC (90,100),JUNK
90 WRITE(IP,64C)
   CALL ZZZ(CLSTA)

```

C  
C  
C

LOOK UP ZERO LIFT ANGLES AT FLAP END-FLAPSIDE

```

100 IF(ITP.NE.C) GC TC 120
   CALL DGET (ARRAY,4,IW)
   ALPHA=999.
   CLL=C.
   REYN=REY(ISTAR)
   TALX=TAL(ISTAR)
   REYCN=999.
   CALL ARC (ARRAY,TALX,MAHW,MWCCL,IE,XHERE,NLVL)
   A3=ALPHA
   CALL DATSW(3,JUNK)
   GC TC (110,120),JUNK
110 WRITE(IP,65C)
   CALL ZZZ(A3)
120 A4=ALPHAZ(ISTAR)
   CLSTU=CLSTA/FF
   CALL DATSW(3,JUNK)
   GC TC (130,140),JUNK
130 WRITE(IP,66C)
   CALL ZZZ(CLSTU)
   WRITE(IP,67C)
   CALL ZZZ(A4)
140 CALL DGET (ARRAY,4,IW)
   ALPHA=999.
   CLL=CLSTU
   REYN=REY(ISTAR)
   TALX=TAL(ISTAR)
   REYCN=999.
   CALL ARC (ARRAY,TALX,MAHW,MWCCL,IE,XHERE,NLVL)
   ALPHX=ALPHA
   A1=ECGE*FF*(ALPHX-A3)+A3
   CALL DATSW(3,JUNK)
   GC TC (150,160),JUNK
150 WRITE(IP,68C)
   CALL ZZZ(A1)

```

160 CLSTL=CLSTA/F(ISTAR)

LCCK UP ALPHA CUBE 1

C  
C  
C

```
CALL CAGET(ARRAY,1,IY)
ALPHA=999.
CLL=CLSTU
REYN=REY(ISTAR)
TALX=TAL(ISTAR)
REYCN=999.
CALL ARC(ARRAY,TALX,MAXX,MAXCL,IE,WHERE,ALVL)
ALPHX=ALPHA
A2=EDGE*F(ISTAR)*(ALPHX-A4)+A4
CALL DATSW(3,JUNK)
GC TC(170,180), JUNK
170 WRITE(IP,69C)
CALL ZZZ(A2)
180 SCLT=A2-A1
IF(NSLIP.EC.0) GO TO 1802
CCLIFT=C.
DC 1801 K=1,NP
SV(K)=C.0
1801 CCLIFT=CBG(K)*ETA(K)+CCLIFT
CCLIFT=ASPEC*BWX**2*CCLIFT
VW=CCLIFT*FLNC/(9.87*ASPEC)
ALFPR=(ALPHX+EYETL)/57.293
ASBAR=ATAN((SIN(ALFPR)+VW)/VSBAR)-ALFPR
CALL DATSW(3,JUNK)
GC TC(57,51),JUNK
57 WRITE(IP,1009)
1009 FCRMAT(10X,2FVW)
CALL ZZZ(VW)
1010 WRITE(IP,1010)
FCRMAT(10X,5FALFPR)
CALL ZZZ(ALFPR)
1011 WRITE(IP,1011)
FCRMAT(10X,5FASBAR)
CALL ZZZ(ASBAR)
1 IF(ITR.NE.C) GO TO 519
DC 103 K=1,NP
ALPG(K)=ALPC(K)+TL(K)
ALPHZ(K)=ALPHZ(K)+CA(K)
103 ALPHE(K)=ALPG(K)-ALPHZ(K)
519 DC 107 K=KCK,KIK
AS(K)=ASBAR
VR(K)=VSA(K)/CCS(ALFPR+ASBAR)
ANG=AS(K)+ALPHE(K)/57.293
SYN=SIN(ANG)
CCZ=CCS(ANG)
107 SV(K)=VR(K)*SYN+VR(K)*SW(K)*CCZ-SIN(ALPHE(K)/57.293)
DC 108 K=KIL,KCL
AS(K)=ASBAR
VP(K)=VSA(K)/CCS(ALFPR+ASBAR)
ANG=AS(K)+ALPHE(K)/57.293
SYN=SIN(ANG)
CCZ=CCS(ANG)
108 SV(K)=VR(K)*SYN+VR(K)*SW(K)*CCZ-SIN(ALPHE(K)/57.293)
CALL DATSW(3,JUNK)
GC TC(52,53),JUNK
52 WRITE(IP,1071)
1071 FCRMAT(10X,2FSV)
CALL AAA(SV,NP)
WRITE(IP,1072)
1072 FCRMAT(10X,2FVR)
CALL AAA(VR,NP)
53 ANG=AS(ISTAR)+(ALPG(ISTAR)-A3)/57.293
SYN=SIN(ANG)
CCZ=CCS(ANG)
SVSRN=VSA(ISTAR)*SYN+VR(ISTAR)*SW(ISTAR)*CCZ-SIN(ANG-AS(ISTAR))
DELVR=SVSRN-SV(ISTAR)
KSTAR=IRI-ISTAR
SVSLP=VSA(KSTAR)*SYN+VR(KSTAR)*SW(KSTAR)*CCZ-SIN(ANG-AS(KSTAR))
DELVL=SVSLP-SV(KSTAR)
KGIN=ISTAR+1
KEND=KSTAR-1
DC 1700 K=KGIN,KEND
1700 SV(K)=SV(K)-DELVR
KGIN=KSTAR+1
DC 1710 K=KGIN,NP
1710 SV(K)=SV(K)-DELVR+DELVL
```

190

```

DC 126 K=1, NP
AK=K
SUM1=C.C
DC 121 N=1, NP
AN=N
SUM2=C.C
DC 122 M=1, NP
AM=M
122 SUM2=SUM2+SV(M)*SIN(AM*PIER)*SIN(AN*AM*PIER)
121 SUM1=SUM1+SUM2*SIN(AN*AK*PIER)/AN
126 TCNY(K)=VR(K)*(4.*SUM1/R+DELVR*STONY(K)-DELVL*SGENE(K))
1802 DC 240 K=1, NP
SIG=C.
DC 190 M=1, NP
190 SIG=(CBG(M)-TCNY(M))*BETA(M,K)+SIG
ALPHU(K)=SIG*(1.+TFAC*(TRANS(K)-1.))
ALPH(K)=ALPG(K)-ALPHU(K)
ALPC(K)=SCELT*FCPP(K)
ALPF(K)=ALPH(K)-ALPC(K)
REYN=REY(K)
TALX=TAU(K)
REYCN=999.
IF(K-1STAR) 220, 220, 200
200 IF(K-1RI+1STAR) 210, 220, 220
210 CALL CAGET(ARRAY, 4, 12)
ALPN=(ALPH(K)-ALPHZ(K))*(1.-F(K)*EDGE)/(EDGE*F(K))
CLL=999.
ALPHA=ALPN
CALL ARC(ARRAY, TAUX, MAXW, MXCCL, IE, XHERE, NLVL)
CVAL(K)=CLL*F(K)
GC TC 230
220 CALL CAGET(ARRAY, 1, 1Y)
ALPN=(ALPH(K)-ALPHZ(K))*(1.-F(K)*EDGE)/(EDGE*F(K))
ALPHA=ALPN
CLL=999.
CALL ARC(ARRAY, TAUX, MAXX, MXCCL, IE, WHERE, NLVL)
CVAL(K)=CLL*F(K)
230 CBC(K)=CVAL(K)*C(K)*CRB/BWX
240 DELTA(K)=CBC(K)-CBG(K)
CALL DATSW(3, JUNK)
GC TC (250, 260), JUNK
250 WRITE(IP, 720)
CALL AAA(ALPH, NP)
WRITE(IP, 700)
CALL AAA(ALPF, NP)
WRITE(IP, 710)
CALL AAA(ALPC, NP)
WRITE(IP, 730)
CALL AAA(CVAL, NP)
WRITE(IP, 740)
CALL AAA(DELTA, NP)
260 DC 280 K=1, NP
IF(ABS(DELTA(K))-DISCR) 270, 270, 290
270 IF(K-NP) 280, 360, 360
280 CONTINUE
290 DC 310 I=1, NP
SUM=C.
DC 300 J=1, NP
300 SUM=TRIX(I, J)*DELTA(J)+SUM
310 CBG(I)=CBG(I)+SUM
CALL DATSW(3, JUNK)
GC TC (320, 330), JUNK
320 WRITE(IP, 630)
CALL AAA(CBG, NP)
330 ITR=ITR+1
IF(ITR-30) 80, 80, 340

```

NCN CONVERGENCE DUMP

CCC

```

340 WRITE(IP, 750)
WRITE(IP, 740)
CALL AAA(DELTA, NP)
WRITE(IP, 730)
CALL AAA(CVAL, NP)
DC 350 J=1, NLVL
NR=MAXX(J)
NC=MXCCL(J)
TALX=WHERE(2, J)
WRITE(IP, 760) J, J, NR, NC, TAUX
DC 350 K=1, NR

```

```

350 WRITE(IP,77C) (ARRAY(J,K,L),L=1,NC)
    CALL EXIT
360 DC 38C K=1, NP
    IF (ALPH(K)-ALMAX(K)) 39C,37C,37D
370 WRITE(IP,78C) K,ALPH(K),ALMAX(K)
    KSTAL=1
380 CCNTIACE
    WRITE(IP,39C1)
3901 FCRMAT(10X,22) SPANWISE STATIONS,2Y/B)
    CALL AAA(Y,NP)
    CALL CATSW(3,JUNK)
    GC TC (39C,4CC),JUNK
390 WRITE(IP,79C)
    CALL AAA(CLMAX,NP)
400 WRITE(IP,80C)
    CALL AAA(CVAL,NP)
800 FCRMAT(10X,43) DISTRIBUTION OF SECTION LIFT COEFFICIENT-CL)
    IF (NSLIP.EC.C) CTS=0.C
    DC 201 K=1, NP
801 CL(K)=CVAL(K)*(1.-CTS)
    WRITE(IP,38C1)
    CALL AAA(CL,NP)
3801 FCRMAT(10X,44) DISTRIBUTION OF SECTION LIFT COEFFICIENT-CLS)
    SCV1=C.C
    DC 9CC I=1, NP
900 SUM1=CHC(I)*ETA(I)+SUM1
    Q=ASPEC*BX**2
    CLIFT=C*SUM1
    CLPP=CLIFT*(1.-CTS)
    WRITE(IP,34C1)
3401 FCRMAT(1X,4C(3H./.) /1FC/)
    WRITE(IP,341) ALPHB,CLIFT,CLPP
341 FCRMAT(10X,35) FUSELAGE ANGLE OF ATTACK,DEGREES. =,F9.5
1/1CX,35) LIFT COEFFICIENT,CL.....=,F9.5
2/1CX,35) LIFT COEFFICIENT,CLS.....=,F9.5)
    WRITE(IP,34C1)
    IF ((KSTAL.EC.C).AND.(KCOUNT.EC.C)) GO TO 2501
C
C      DEFINE EXACT SYALL ANGLE OF ATTACK
    IF ((IPRAB.EC.1).OR.(KCOUNT.EC.3)) GO TO 990C
    KCOUNT=KCOUNT+1
    GC TC (1000,2000,3000),KCOUNT
    AB(1)=(ALPHB+ALPHV(IPRAB-1))/2.
    ALPHB=AB(1)
    GC TC 990C
2000 IF (KSTAL.EC.0) GO TO 210C
    ISTALL=1
    AB(2)=(AB(1)+ALPHV(IPRAB-1))/2.
    ALPHB=AB(2)
    GC TC 990C
2100 ISTALL=C
    AB(2)=(AB(1)+ALPHV(IPRAB))/2.
    ALPHB=AB(2)
    GC TC 990C
3000 IF (KSTAL+ISTALL-1) 310C,320C,330C
3100 AB(3)=(AB(2)+ALPHV(IPRAB1))/2.
    ALPHB=AB(3)
    GC TC 990C
3200 AB(3)=(AB(2)+AB(1))/2.
    ALPHB=AB(3)
    GC TC 990C
3300 AB(3)=(AB(2)+ALPHV(IPRAB-1))/2.
    ALPHB=AB(3)
990C KSTAL=C
    DC 17C1 K=1, NP
1701 CL(K)=CLMAX(K)-CVAL(K)
    WRITE(IP,35C1)
3501 FCRMAT(10X,25) STALL MARGIN DISTRIBUTION /1X)
    CALL AAA(CL,NP)
    IF ((IPRAB.EC.1).OR.(KCOUNT.EC.3)) GO TO 171
    WRITE(IP,37C1) NAME
    WRITE(IP,38C1) ALPHB
3701 FCRMAT(1H1/1FC/35X,25) A2/1X)
3601 FCRMAT(1X,4C(3H./.) /1X/1CX,28) ADJUSTED ANGLE OF ATTACK TC,
1FB.3,32) SEARCHING FOR EXACT STALLPCINT,/1X/1X/,40(3H./.) /1X)
    IR=1CC
    GC TC 3030
2501 IR=C
    RETURN
171 IR=1C1

```



```

RETLRN
600 FCRMAT(10X,16FH THICKNESS FACTOR)
610 FCRMAT(10X,13FH CU BAR / CC)
620 FCRMAT(10X,4FH ALPG)
630 FCRMAT(10X,3FH CEG)
640 FCRMAT(10X,5FH CLSTA)
650 FCRMAT(10X,2FH A3)
660 FCRMAT(10X,5FH CLSTU)
670 FCRMAT(10X,2FH A4)
680 FCRMAT(10X,2FH A1)
690 FCRMAT(10X,2FH A2)
700 FCRMAT(10X,4FH ALPH)
710 FCRMAT(10X,4FH ALPC)
720 FCRMAT(10X,5FH ALPFU)
730 FCRMAT(10X,4FH CVAL)
740 FCRMAT(10X,5FH DELTA)
750 FCRMAT(1X,43FH UNABLE TO CONVERGE AFTER 30 ITERATIONS ABORTED)
760 FCRMAT(10X,7FH ARRAY(,11,11F 1, 1) TO (,11,11F,,12,11,,12,11),F
110.5/103)
770 FCRMAT(12F10.4)
780 FCRMAT(10X,19FH STALLED AT STATION ,12,18H ANGLE OF ATTACK =,F7.3,
110X,21FH SECTION STALL ANGLE =,F7.3)
790 FCRMAT(10X,5FH CLMAX)
END

```